Coordination Chemistry Reviews 255 (2011) 1733–1790

Contents lists available at ScienceDirect

Coordination Chemistry Reviews

journal homepage: www.elsevier.com/locate/ccr

Review

Penta-arylcyclopentadienyl complexes

Leslie D. Field[a,*], Charles M. Lindall[b], Anthony F. Masters[c,**], Guy K.B. Clentsmith[a]

[a] School of Chemistry, The University of New South Wales, Sydney, NSW 2052, Australia
[b] CSIRO Division of Molecular and Health Technologies, North Ryde, NSW 2113, Australia
[c] School of Chemistry, The University of Sydney, NSW 2006, Australia

Contents

---

* Corresponding author. Tel.: +61 293852700; fax: +61 293858008.
** Corresponding author. Tel.: +61 293513743; fax: +61 293513329.
E-mail addresses: L.Field@unsw.edu.au (L.D. Field), anthony.masters@sydney.edu.au (A.F. Masters).

doi:10.1016/j.ccr.2011.02.001

ARTICLE INFO

Article history:
Received 19 October 2010
Accepted 1 February 2011
Available online 21 February 2011

Keywords:
Cyclopentadiene derivatives
Pentaphenylcyclopentadiene
Decaphenylmetallocenes
Sandwich compounds
Penta-arylcyclopentadienyl compounds
Penta-arylcyclopentadiene

ABSTRACT

This review covers the coordination and general chemistry of the 1,2,3,4,5-penta-arylcyclopentadiene system, as anion, $C_5Ar_5^-$, radical, $C_5Ar_5^\bullet$, and cation, $C_5Ar_5^+$, as well as the neutral diene, C_5Ar_5H, and its derivatives. The structural rigidity and steric saturation offered by the penta-arylcyclopentadienyl ligand give rise to definite structural and geometric properties in its complexes that distinguish its chemistry from that of the parent cyclopentadiene.

1. Introduction

The cyclopentadienyl ligand has become one of the most widely used ligands in organometallic chemistry, since the discovery and characterization of ferrocene were reported in the early 1950s [1]. Cyclopentadienyl complexes are known for all of the transition metal and main group metals and metalloids, as well as all of the lanthanoid and the more common actinide metals. The properties and bonding types of cyclopentadienyl complexes are varied, with the ligand found in complexes of metals in low and high formal oxidation states. Both σ and π coordinations of the ligand are well established. In the latter case, the cyclopentadienyl anion can coordinate in η^5, η^3, η^2 and η^1 modes and neutral cyclopentadiene can coordinate in the η^4 and η^2 modes. The cyclopentadienyl ligand is generally very firmly bound to metals and metalloids, making the C_5H_5M unit a stable synthetic platform for the development of a wide range of chemistries for varied applications. The development of substituted cyclopentadienyl ligands, to combine the stability of the C_5R_5M moiety, with the flexibility to moderate the steric and/or electronic properties of the substituents, R, has been a natural extension of this field. In particular, the exploitation of bulky substituents, which influence the coordination sphere of the metal, has received considerable attention [2].

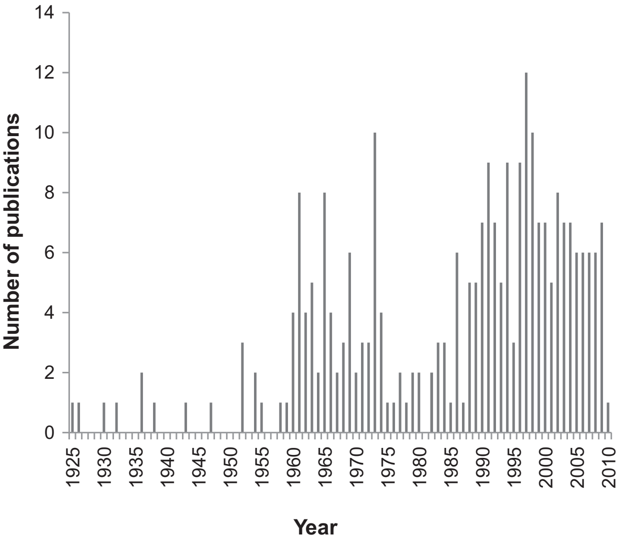

Fig. 1. Number of publications of C_5Ar_5H chemistry annually.

Penta-arylcyclopentadienyl ligands, and in particular, the pentaphenylcyclopentadienyl anion, form one class of bulky ligands formally derived from the cyclopentadienyl ligand. The ligand precursors were first prepared in 1925 [3], although the first metal complexes were not reported until 1964 [4], and the structure of the neutral pentaphenylcyclopentadiene (**1**) was not determined until 1992 [5]. A search of the literature to mid-2010 gives over 250 publications that feature the chemistry of penta-arylcyclopentadiene or penta-arylcyclopentadienyl species. The numbers of publications in this field are listed year by year in Fig. 1, whilst the elements, E, to which penta-arylcyclopentadiene/enyl species are known to coordinate, are illustrated in Fig. 2.

Given that (i) a previous literature survey was conducted some 20 years ago [2], and this also reviewed other sterically bulky cyclopentadiene derivatives, and (ii) a more recent review of ruthenium complexes incorporating pentaphenylcyclopentadienes was solely in the context of their potential as molecular motors [6], the chemistry of penta-arylcyclopentadienyl complexes is now sufficiently developed that a review of the chemistry is timely and warranted.

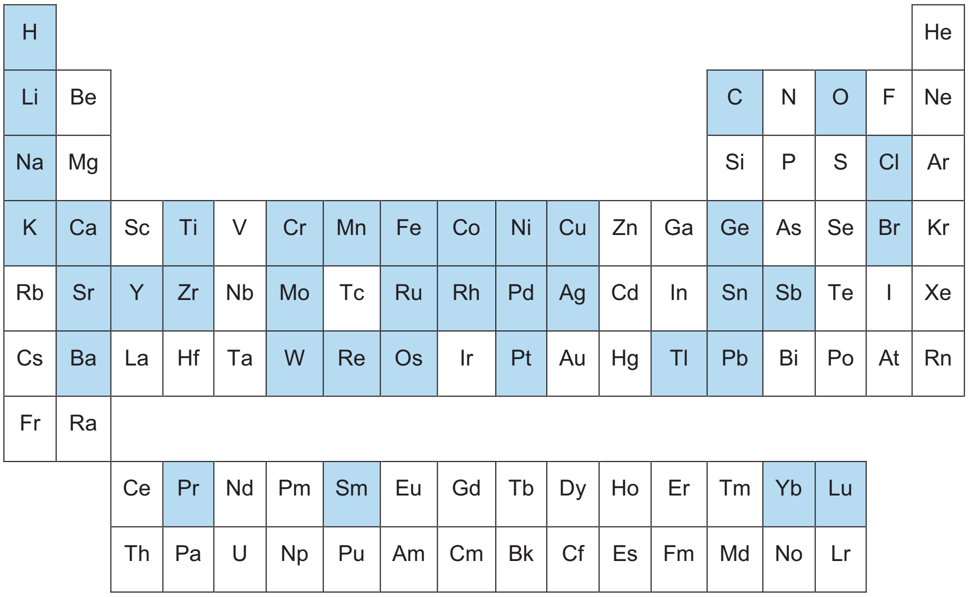

▨ H																	He
▨ Li	Be											▨ C	N	▨ O	F	Ne	
▨ Na	Mg											Si	P	S	▨ Cl	Ar	
▨ K	▨ Ca	Sc	▨ Ti	V	▨ Cr	▨ Mn	▨ Fe	▨ Co	▨ Ni	▨ Cu	Zn	Ga	▨ Ge	As	Se	▨ Br	Kr
Rb	▨ Sr	▨ Y	▨ Zr	Nb	▨ Mo	Tc	▨ Ru	▨ Rh	▨ Pd	▨ Ag	Cd	In	▨ Sn	▨ Sb	Te	I	Xe
Cs	▨ Ba	La	Hf	Ta	▨ W	▨ Re	▨ Os	Ir	▨ Pt	Au	Hg	▨ Tl	▨ Pb	Bi	Po	At	Rn
Fr	Ra																
		Ce	▨ Pr	Nd	Pm	▨ Sm	Eu	Gd	Tb	Dy	Ho	Er	Tm	▨ Yb	▨ Lu		
		Th	Pa	U	Np	Pu	Am	Cm	Bk	Cf	Es	Fm	Md	No	Lr		

Fig. 2. Elements for which C_5Ar_5E species are known.

Herein the physical and spectroscopic properties of, and synthetic routes to the penta-arylcyclopentadienyl moiety as an anion, $C_5Ar_5^-$, radical, $C_5Ar_5^\bullet$, or cation, $C_5Ar_5^+$, or as the neutral molecules, C_5Ar_5X (X = H, OH, halogen) are described. An attempt is also made to review the structures and chemistry of metal complexes incorporating the penta-arylcyclopentadiene/enyl ligand. Section 1 details the chemistry of the neutral diene itself, its physical and structural properties, and also synthetic routes to its derivatives and congeners, all of which themselves serve as ligand precursors. Penta-arylcyclopentadienyl derivatives of the alkali metals, which are formally anionic, appear in this section, as they are commonly used as transfer reagents by metathesis. Section 2 examines the chemistry of penta-arylcyclopentadienyl ligands bound to transition- and *f*-element metal centres, and also to main group metals, and proceeds systematically across the periodic table. In this section, extensive reference is made to cyclic voltammetry experiments, as they make possible a direct comparison with the voluminous experimental data collected for regular cyclopentadienyl complexes. Section 3 examines some miscellaneous applications of penta-arylcyclopentadienyl chemistry, including asymmetric synthesis. Section 4 provides a conclusion, and suggests directions for future research.

1.1. Ligand chemistry

1.1.1. Pentaphenylcyclopentadiene

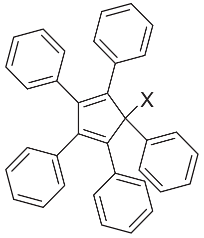

1, X = H; **2**, X = OH; **3**, X = Br

The penta-arylcyclopentadienyl moiety can exist as an anion, $C_5Ar_5^-$, radical, $C_5Ar_5^\bullet$, or cation, $C_5Ar_5^+$, or as the neutral molecules, C_5Ar_5X (X = OH (**2**), halogen, H (**1**), R, Ar). The pentaphenylcyclopentadienyl radical ($C_5Ph_5^\bullet$ (**4**)) and anion ($C_5Ph_5^-$) are stable at room temperature, whereas salts of the cation ($C_5Ph_5^+$) are stable at 0 °C as a solid, but only below −40 °C in solution. The most common route to C_5Ar_5X compounds for use in coordination/organometallic chemistry has been via the appropriate tetracyclone, $C_4Ar_4C(=O)$ (Scheme 1). This is due to (i) the tetracyclones can usually be prepared in high yields, and (ii) this route affords two useful synthetic intermediates C_5Ar_5Br (that may oxidatively add to low-valent transition metals), and C_5Ar_5H (from which alkali metal salts such as C_5Ar_5Li can be prepared). To date, the oxidative addition route to organometallic derivatives has been of relatively greater significance in penta-arylcyclopentadienyl chemistry, compared to the chemistry of the parent $C_5H_5^-$, despite the ready availability of C_5H_5Br [7].

1.1.2. Physical properties of pentaphenylcyclopentadiene

Pentaphenylcyclopentadiene (**1**) is a white crystalline solid, which melts at 259–260 °C [8] and sublimes at 194 °C (0.05 mm Hg) [8,9]; it has often been reported as a yellow solid with a sharp melting point between 244 and 254 °C. The infrared, ^1H, and ^{13}C NMR spectra have been extensively reported in the literature [8,10]. Spectroscopic data are collected in Table 1. Chloroform solutions of pentaphenylcyclopentadiene fluoresce strongly [11].

The ^{13}C NMR resonance position of the *para* C on the phenyl rings is a useful probe of the extent of charge delocalization onto the phenyl rings [10a]. Electron-withdrawing substituents on the phenyl rings shift this resonance to low field (higher ppm values). Thus, for example, the *para* C's in the $C_5Ph_5^-$ anion resonate at δ 119 ppm, upfield of the three corresponding resonances in C_5Ph_5H (**1**) [10a]. For the limited number of η^5-C_5Ph_5 complexes examined by ^{13}C NMR spectroscopy to date, this resonance is observed in the range δ 126–128 ppm [10a]. The ^{13}C NMR resonance of the sp^3 hybridized carbon in the cyclopentadiene ring is sensitive to the mode of coordination of the ligand. The lone sp^3 hybridized carbon is observed at δ 61 ppm in C_5Ph_5H (**1**) and this resonance shifts to $\sim\delta$ 142 ppm on formation of the aromatic anion. In η^5-C_5Ph_5 metal complexes, this resonance is typically observed in the range $\sim\delta$ 90–100 ppm. In $\{(\eta^6\text{-}C_6H_5)C_5Ph_4\}$ complexes, where a formally neutral phenyl ring bound to the cyclopentadienyl ring coordinates to a metal centre in an η^6 interaction [16], the resonance is observed at $\sim\delta$ 140 ppm, and in η^4-C_5Ph_5R complexes, it is observed at $\sim\delta$ 30 ppm [5,17]. The ^1H NMR resonance of the proton

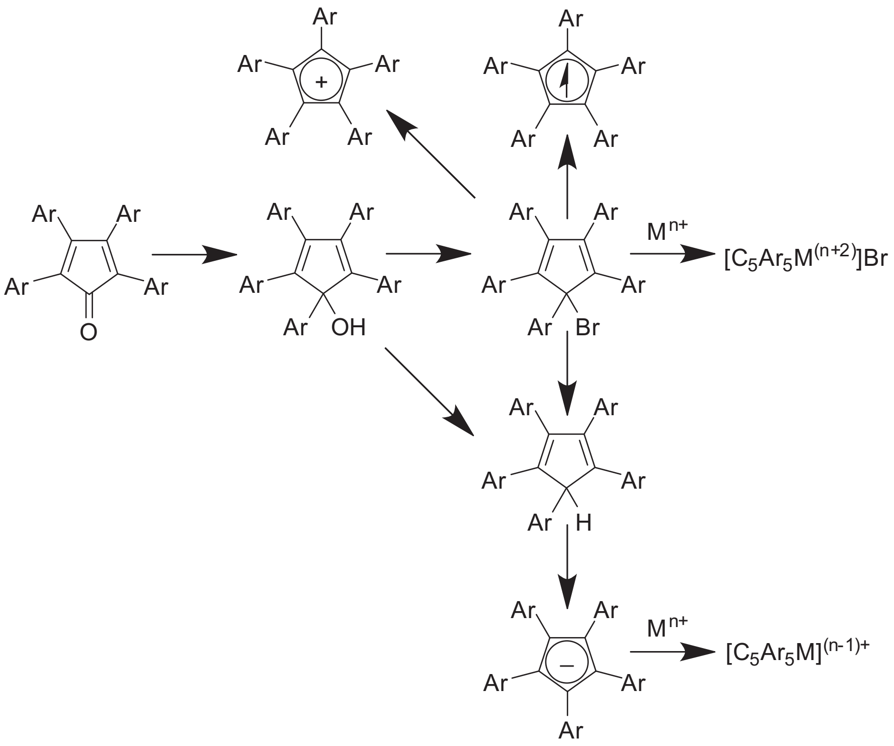

Scheme 1.

Table 1
Spectroscopic data for pentaphenylcyclopentadiene, C_5Ph_5H (**1**).

Infrared (cm^{-1})	^1H NMR (δ, ppm)	^{13}C NMR (δ, ppm)	Mass spectrum (m/z)	Refs.
–	5.00 (1 H), 6.82–7.30 (25 H, m) (chloroform-*d*)	–	–	[8b]
–	5.06 (s), 7.13–7.50 (m) (chloroform-*d*)	–	446, 119.58	[12]
3076w, 3022w, 1490m, 1483m, 1439w, 764s, 710s, 684s (KBr)	6.8–7.85 (m) (dimethyl sulfoxide-d_6)	126.0, 126.4, 126.9, 127.3, 127.5, 128.0, 128.4, 129.1, 129.5 (dimethyl sulfoxide-d_6)	447 (36%), 446 (100%), 291 (14%), 165 (14%), 91 (12%), 55 (10%), 44 (92%), 40 (48%)	[13]
	5.06 (s), 7.02–7.42 (m) (dimethyl sulfoxide-d_6)	61.3, 13 peaks in the region 124–132, 6 peaks in the region 134–148 (dimethyl sulfoxide-d_6)		[14]
	5.05 (1H), 6.8–7.2 (25 H) (chloroform-*d*)	–	446	[9]
2648, 2339, 2286, 2161, 1797, 1680, 1640, 1361, 1139, 837, 358	5.10 (s, 1H), 6.95–7.25 (m, 25H) (methylene-chloride-d_2)	62.7, 126.3, 126.5, 126.7, 127.7, 127.9, 128.5, 128.6, 129.0, 130.1, 135.6, 136.1, 138.1, 144.0, 141.5 (methylene-chloride-d_2)		[15]

Electronic absorption and emission spectra of (**1**) appear in Ref. [11].

on the sp^3 hybridized carbon is observed at δ 5.06 ppm in the spectrum of C_5Ph_5H (**1**) [10a]. This resonance disappears on formation of the anion, and is observed at $\sim\delta$ 5.15 ppm in η^4-C_5Ph_5H complexes [5,17a,18]. The major electronic spectroscopic absorptions of C_5Ph_5H (**1**) and of $C_5(p\text{-tol})_5H$ in methylene chloride are at λ_{max} 340 nm (ε log 4.1) and 346 nm (ε log 4.4), respectively [5,18]. In concentrated H_2SO_4 the major electronic spectroscopic absorptions of C_5Ph_5H (**1**) are at λ_{max} 520 nm (ε log 4.3) and 376 nm (ε log 4.1) [19].

1.1.2.1. Acidity of pentaphenylcyclopentadienyl derivatives. 1,2,3,4,5-Pentaphenylcyclopentadiene (**1**) (pK_{HA} 12.5) is a significantly stronger acid in dimethylsulfoxide than either cyclopentadiene (pK_{HA} 18.0) or pentamethylcyclopentadiene (pK_{HA} 26.1) [20]. There is an increase in the acidity of the ring proton as the cyclopentadienyl ring is substituted with phenyl groups (*e.g.*, (i) 2,5-diphenylcyclopentadiene, pK_{HA}14.3) and (ii) 2,3,4,5-tetraphenylcyclopentadiene, pK_{HA} 13.2) [21]. However, the increase in acidity is not proportional to the number of phenyl substituents. This effect has been attributed to steric crowding of the phenyl rings in the tetra- and pentaphenyl derivatives such that the phenyl rings are unable to attain coplanarity with the central C*p* ring and therefore restricting orbital overlap. The lack of effective π-overlap between the phenyl substituents and the cyclopentadienyl ring in the acid, C_5Ph_5H (**1**), is confirmed in the molecular structure of pentaphenylcyclopentadiene (**1**, Fig. 3) [22], is also observed in some of the structures of metal complexes of the $C_5Ph_5^-$ ligand [8a,17b,22,23], and is deduced from the ESR and ENDOR spectra of the $C_5Ph_5^\bullet$ radical (**4**) [24].[1] Thus, pentaphenyl-

---

[1] The earlier study [24b] suggested that the phenyl rings were nearly orthogonal to the C_5 ring, but the later studies concluded that the phenyl rings were at approximately 60° to the C_5 ring, [24c,d] consistent with the subsequently reported crystal structure [23aa].

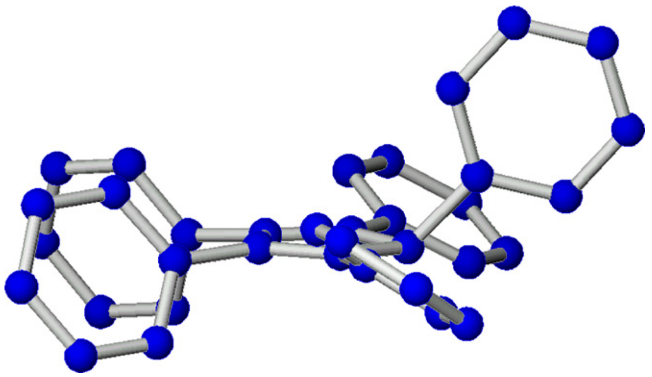

Fig. 3. Structure of C_5Ph_5H (**1**, hydrogen atoms omitted) [5].

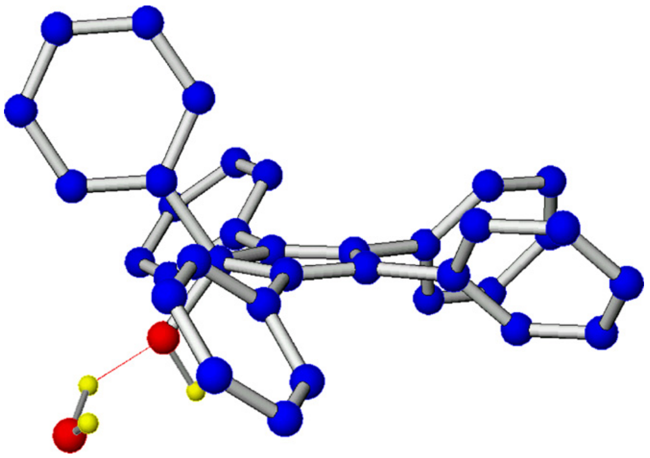

Fig. 4. Structure of $C_5Ph_5OH{\cdot}H_2O$ (**2**·H_2O) (only oxygen-bound hydrogen atoms are depicted) [33b].

cyclopentadiene (**1**) is not as acidic as simple substituent additions might suggest. The relatively low acidity of C_5Me_5H (pK_{HA} 26.1) has been attributed to a combination of methyl hyperconjugative stabilization in undissociated C_5Me_5H and steric inhibition of solvation of the $C_5Me_5^-$ anion [20,21]. These effects are proposed to lead to a significantly greater electron–donor ability of the $C_5Me_5^-$ ligand in comparison to the $C_5H_5^-$ ligand in metal complexes [20,25]. Since the steric inhibition of solvation should be at least as great for the $C_5Ph_5^-$ anion as for the $C_5Me_5^-$ anion, the major difference in the acidities of C_5Ph_5H (**1**) and C_5Me_5H is likely due to the methyl hyperconjugative stabilization that operates in the latter.

The acidity of the radical cation, $C_5Ph_5H^{\bullet +}$, has been estimated from electrochemical data according to Eq. (1) [21a]:

$$pK_{HA}^{\bullet +} = pK_{HA} + 16.83\,[E_{ox}(A^-) - E_{ox}(HA)] \qquad (1)$$

1.1.2.2. Electrochemistry of pentaphenylcyclopentadienyl derivatives. At room temperature in methylene chloride, pentaphenylcyclopentadiene (**1**) undergoes a reversible, one-electron oxidation at 0.765 V, and an irreversible oxidation at 1.300 V (*vs.* $Fc^{+/0}$) [26]. However, in acetonitrile or dimethylsulfoxide, only irreversible oxidations at 1.68 or 1.58 V (*vs.* $Fc^{+/0}$), respectively, are observed [21a]. The *reversible* oxidation of the $C_5Ph_5^-$ anion in dimethylsulfoxide (+0.208 V *vs.* the aqueous SHE; 0.333 V *vs.* $[Fe(C_5H_5)_2]^{+/0}$) occurs at more positive potentials than the *irreversible* oxidations of the $C_5H_5^-$ (by 0.236 V) and $C_5Me_5^-$ (by 0.837 V) anions in the same solvent. The $C_5Ph_5^{0/-}$ couple has also been attributed to a reversible electrode process at −0.29 V *vs.* $[Fe(C_5H_5)_2]^{+/0}$ in THF and methylene chloride [23k,27]. In these cases, the $C_5Ph_5^-$ ligand is assumed to be liberated following the irreversible reduction of a Pd-C_5Ph_5 complex at more negative potentials. After bulk electrochemical oxidation of the THF solution at −0.1 V, the solution becomes purple and a sharp ESR signal, assigned to a stable organic radical, is detected at $g = 2.044$ [28]. However, a benzene solution of the $C_5Ph_5^{\bullet}$ radical (**4**) exhibits a multi-line ESR spectrum at room temperature [29]. Confirmation of the assignment of the electrode process at −0.29 V is desirable. Similarly, the reversible reduction of the $C_5Ph_5^{\bullet}$ radical (**4**), produced after the irreversible bulk electrolytic oxidation of $[Ni(\eta^5\text{-}C_5Ph_5)\{OP(OMe)_2\}_3Co(\eta^5\text{-}C_5H_5)]$ (**5**), is assigned at −0.35 V *vs.* SCE in methylene chloride/Bu_4NPF_6/Pt, suggesting unusual stability of the radical in halogenated solvents [23m]. The *irreversible* oxidation of C_5Ph_5H (**1**) in acetonitrile or dimethylsulfoxide occurs at a more positive potential than those of 2,5-$Ph_2C_5H_4$, 1,2,3,4-$Ph_4C_5H_2$, or C_5Me_5H, but at a less positive potential than that of C_5H_6 [21b]. These data suggest a greater radical than anion stabilizing effect for both the $C_5Ph_5^-$ and $C_5Me_5^-$ anions, whereas the $C_5H_5^-$ anion has a greater anion stabilizing effect. The acidic C–H bond dissociation energy of $C_4Ph_4C(Ph)$–H is estimated to be 326 kJ mol^{-1}, approximately the same as that of acetonitrile [30].

Cyclic voltammetric data at Pt in 0.1 M Bu_4NPF_6/methylene chloride for the bromide derivatives $C_5Ar_4Ar'Br$ have been reported [29b]. These data are limited to a single scan rate and temperature, but have been interpreted in terms of a one-electron reduction to $C_5Ar_4Ar'Br^{\bullet -}$, which dissociates to give $C_5Ar_4Ar'^{\bullet}$ and Br^-. The radicals undergo a near reversible electron transfer at approximately −0.96 V *vs.* $Fc^{+/0}$. Recent cyclovoltammetric studies of C_5Ph_5R derivatives in acetonitrile at a platinum electrode report reduction to a radical anion, which decomposes to the stable $C_5Ph_5^{\bullet}$ radical (**4**) and the R^- anion, with oxidation of C_5Ph_5R giving a stable radical cation, $C_5Ph_5R^{\bullet +}$ [31].

*1.1.2.3. Structures of C_5Ph_5X (X = H (**1**), OH (**2**), Br (**3**)).* The crystal and molecular structures of C_5Ph_5X (X = H (**1**), Fig. 3) [5], OH (**2**) [15], Br (**3**, Fig. 6)) [32] establish that these species exist as discrete molecules in the solid state. C_5Ph_5OH (**2**) exists as inclusion compounds with DMSO, H_2O, MeOH and EtOH [33]. The interaction of C_5Ph_5OH (**2**) with H_2O is illustrated in Fig. 4, and the extended structure is shown in Fig. 5. The C_5Ph_5H molecule (**1**) was close to C_s molecular symmetry in the solid state. The C_5Ph_5H molecule consists of a planar C_5 ring, bisected by an approximate mirror plane which contains the CHPh fragment, with the unique proton and phenyl ring above and below the C_5 ring

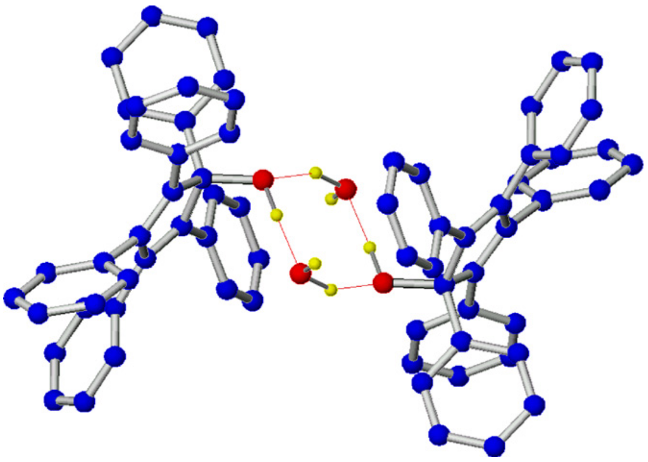

Fig. 5. Hydrogen-bond network of two molecules of $C_5Ph_5OH{\cdot}H_2O$ (**2**·H_2O), looking down the *a* axis (only oxygen-bound hydrogen atoms are depicted) [33b].

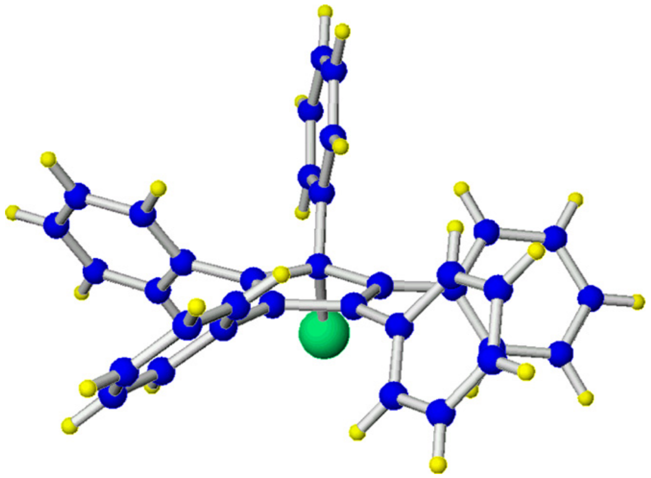

Fig. 6. Structure of C_5Ph_5Br (**3**) [32].

plane and the unique phenyl ring almost perpendicular to the C_5 ring. The remaining phenyl rings are canted with respect to the C_5 ring at an average angle of ~50°. The *ipso* carbons of these phenyl rings are slightly (0.04–0.16 Å) out of the C_5 plane. The bond lengths and angles of the conjugated system are similar to those of the coordinated pentaphenylcyclopentadienyl anion [8a,17b,22,23l–ab,23ad–as,34] and of tetraphenylcyclopentadiene [35]. The canting of the phenyl rings with respect to the plane of the cyclopentadiene ring, in order to relieve their steric interaction, is clearly evident in this and other structures.

The structural parameters of C_5Ph_5X (X = OH (**2**), Br (**3**)) are, in general, similar to those of C_5Ph_5H (**1**). However, the C_5Ph_5OH molecule (**2**) is less symmetric in the solid state, as there is no mirror symmetry perpendicular to the C_5 ring. A water of crystallization is hydrogen-bound to the OH group, and makes short intermolecular contacts with the 2- and 5-phenyl rings. These contacts may be sufficient to lower the symmetry in the solid state.

1.1.2.4. Structures of other ligand precursors. The intensely violet pentaphenylcyclopentadienyl radical (**4**) was first reported in 1925 from the reaction of pentaphenylcyclopentadienyl bromide (**3**) with silver [3]. Subsequently, it was established that zinc, triethylamine, potassium hydroxide and stannous halides react similarly to produce the radical from the parent halide [13,23aa,36]. The radical is reasonably stable in air and the intense violet transient colour observed in many reactions suggests it may be an intermediate in the syntheses of many pentaphenylcyclopentadienyl metal complexes. After the penta-isopropylcyclopentadienyl radical [37], the $C_5Ph_5^{\bullet}$ radical was only the second cyclopentadienyl radical to be structurally characterized, following its high yield (84%) synthesis by the reaction between SnX_2 (X = Cl, Br) and C_5Ph_5Br (**3**) (Eq. (2)) [23aa]:

$$C_5Ph_5Br + SnX_2 \xrightarrow[\text{RT, 5 days}]{Et_2O/THF} C_5Ph_5^{\bullet} + SnX_2 \cdot 2THF + SnX_4 \tag{2}$$

The structure of the radical (Fig. 7) is similar to those of the C_5Ar_5X series, except that the *ipso* carbons of all phenyl groups are in (or very close to) the C_5 plane. Unfortunately, because of disorder consequent upon slight canting of the molecule with respect to a mirror plane, the structure was of insufficient quality to obtain reliable metric data, although the central C_5 ring appears planar and the familiar canting of the phenyl rings is apparent.

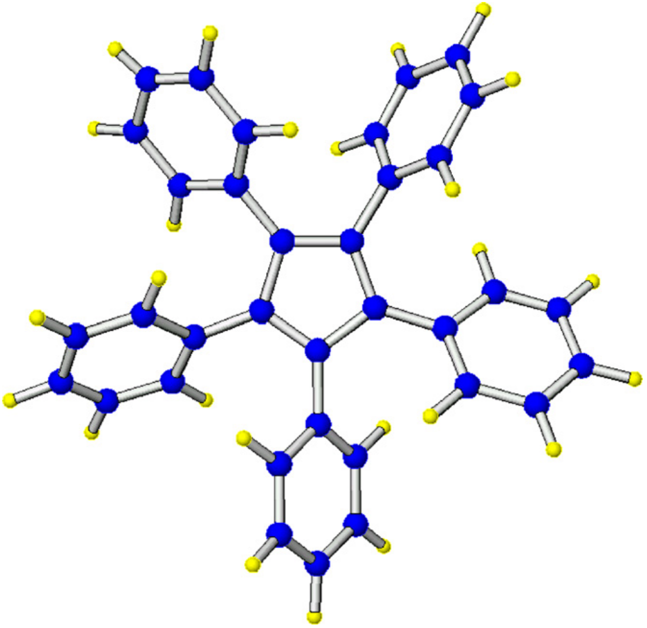

Fig. 7. Structure of the $C_5Ph_5^{\bullet}$ radical (**4**) [23aa].

Group 1 salts of the pentaphenylcyclopentadienyl anion have long been accessible as poorly soluble, non-crystalline solids. The anion has been structurally characterized as its $[Na(DME)_3]^+$ (**6**, Fig. 8) and $[Yb(THF)_6]^{2+}$ salts (**7**, Fig. 9) and exhibits a similar planarity of the central C_5 ring and canting of the phenyl groups to the radical and the ligated anions [38].

The additional alkyl substitution on the penta-(*p*-tolyl)-cyclopentadienyl ligand has proven useful in conferring increased solubility on metal complexes, in simplifying the interpretation of ^1H NMR spectroscopy, and in stabilizing higher metal oxidation states. The structure of the ligand precursor, $[C_5(p\text{-tol})_5Br]$ (**8**, Fig. 10), is similar to that of the analogous C_5Ph_5Br (**3**) [32]. More recent chemistry that substitutes the cyclopentadienyl ring with alkyl-substituted aryl groups that increase solubility (*i.e.* C_5Ar_5H, Ar = 3,5-$Bu_2{}^tC_6H_3$ (**9**) [39], 3,5-$Me_2C_6H_3$ (**10**) [40], 4-$Bu^nC_6H_4$ (**11**)) [41] allows for insight into solution structures and solution dynamics, especially those pertaining to the alkali metal salts of penta-arylcyclopentadiene [39,42]. C_5Ar_5H (Ar = 3,5-

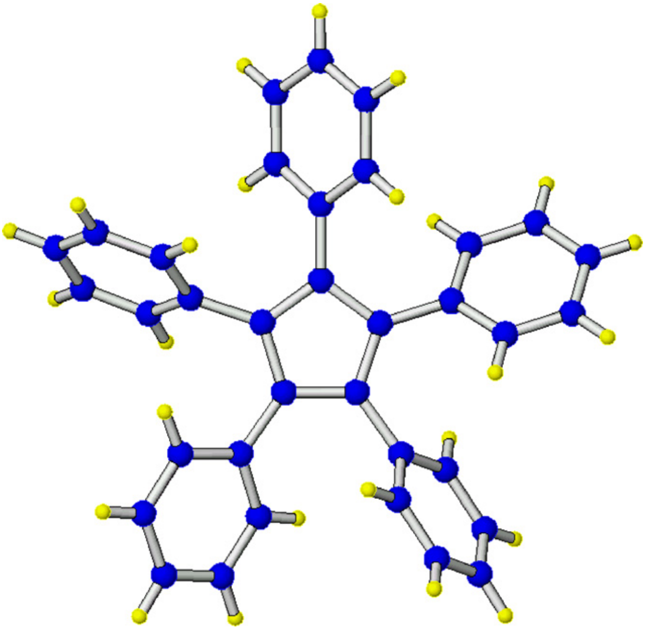

Fig. 8. Structure of $C_5Ph_5^-$ anion as its $[Na(DME)_3]^+$ salt (**6**) [38a].

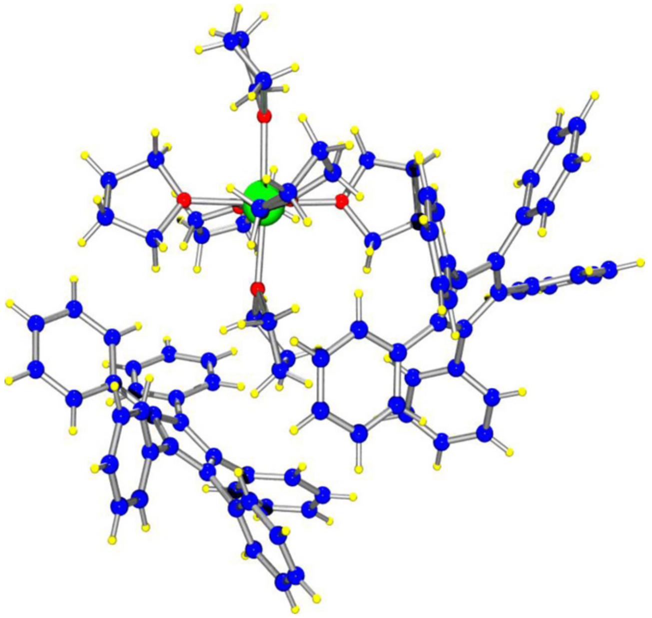

Fig. 9. Structure of the $C_5Ph_5^-$ anion of $[Yb(THF)_6][C_5Ph_5]_2$ (**7**) [38b].

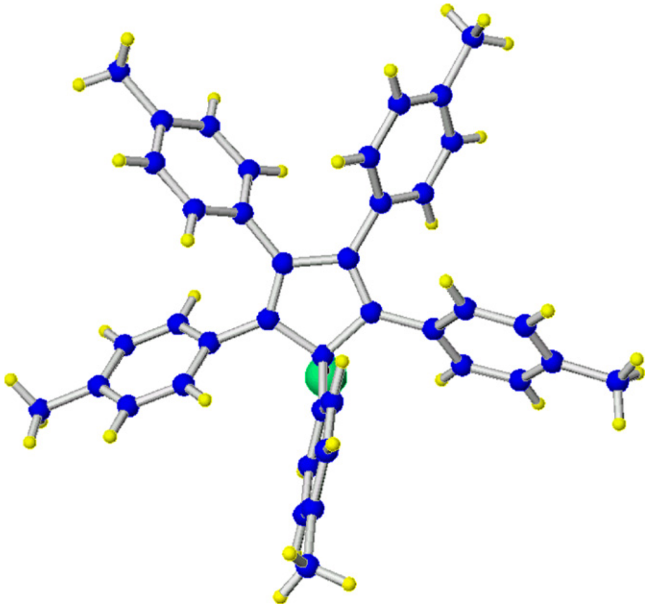

Fig. 10. Structure of C_5(*p*-tol)$_5$Br (**8**) [32].

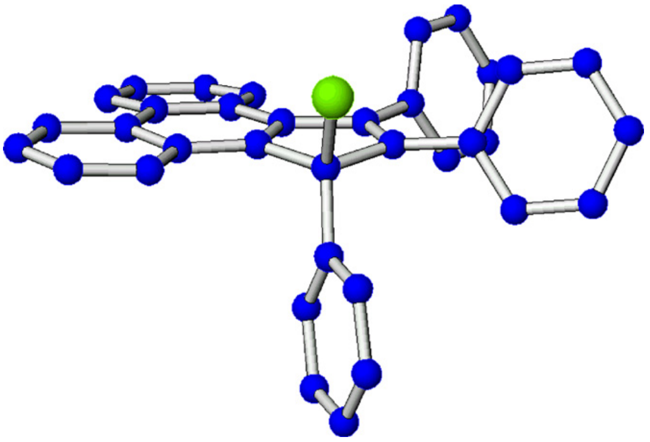

Fig. 11. Structure of 1-bromo-1,2,3-triphenylcyclopenta[*l*]phenanthrene (hydrogen atoms omitted) (**15**) [32].

$\mathrm{Bu_2{}^tC_6H_3}$ (**9**), 3,5-$Me_2C_6H_3$ (**10**)) may be easily deprotonated by $\mathrm{Bu^nLi}$ in Et_2O or THF, and multinuclear NMR spectroscopy performed upon the resultant $[LiC_5Ar_5]$ species (Ar = 3,5-$\mathrm{Bu_2{}^tC_6H_3}$ (**12**), 3,5-$Me_2C_6H_3$ (**13**)) salts suggested free rotation of the aryl groups in solution. The ^{7}Li NMR spectra of **12**/**13** suggested an equilibrium between the monomer, $[C_5Ar_5Li(THF)_n]$, and the metallate, $[(C_5Ar_5)_2Li]Li(THF)_n$, and provided evidence that the solution structure was the same as the solid state structures [39]. Likewise, the bulky, *per*-arylated $C_5(4\text{-}\mathrm{Bu^n}C_6H_4)_5H$ (**11**), may be conveniently prepared in the one pot by palladium catalyzed reaction of the aryl bromide with cyclopentadiene (Section 1.1.3.7) [40]. The potassium salt, $[\{C_5(4\text{-}\mathrm{Bu^n}C_6H_4)_5\}K]$ (**14**), crystallized as a solvent-donor free, one-dimensional coordination polymer that was almost linear in the solid state, and was represented as $[\{C_5(4\text{-}\mathrm{Bu^n}C_6H_4)_5\}K]_\infty$ [41]. The structure of $[\{C_5(4\text{-}\mathrm{Bu^n}C_6H_4)_5\}K]$ (**14**) was marked by a series of attractive *ortho*-C–H. . .*ortho*-aryl-C(π) interactions between the phenyl substituents on alternate carbocycles; these extended intermolecularly along the metallocene chain. These non-classical interactions will be discussed in relation to the alkaline-earth and *f*-element metal complexes that derive from C_5Ph_5H (**1**), and from $C_5(4\text{-}\mathrm{Bu^n}C_6H_4)_5H$ (**11**) [43].

Condensation or bridging of the phenyl substituents yields ligand precursors with extended planar aromatic systems. The structure of 1-bromo-1,2,3-triphenylcyclopenta[*l*]phenanthrene (**15**, Fig. 11) has the same canting of the non-condensed phenyl groups as in other C_5Ar_5Br molecules [32], with the distinctive phenanthrene residue on one side of the molecule.

1.1.3. Syntheses of ligands and ligand precursors

Photolysis of $C_5Ph_5(OMe)$ (**16**) affords CH_2O and C_5Ph_5H (**1**). Irradiation of any of the three C_5Ph_4(*p*-tol)(OMe) (**17**) isomers affords the same mixture of C_5Ph_4(*p*-tol)H (**18**) isomeric products, a result interpreted in terms of a delocalized free radical intermediate [44].

1.1.3.1. From tetra-arylcyclopentadienones. 1,2,3,4,5-Pentaphenylcyclopentadiene (**1**) was first reported in 1925 [3], as a result of the reaction of 1-chloro-1,2,3,4,5-pentaphenylcyclopenta-

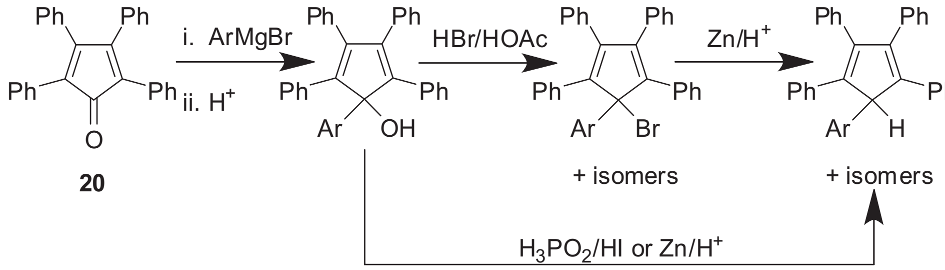

Scheme 2.

2,4-diene (**19**) with an excess of zinc dust in glacial acetic acid. 1-Halo-1,2,3,4,5-pentaphenylcyclopenta-2,4-diene derivatives have been prepared by the reactions of HCl or HBr with 1,2,3,4,5-pentaphenylcyclopenta-2,4-dien-1-ol (**2**) in glacial acetic acid. 1,2,3,4,5-Pentaphenylcyclopenta-2,4-dien-1-ol (**2**) has in turn been prepared by the reaction between tetraphenylcyclopentadienone (tetracyclone) (**20**) with the appropriate phenyl Grignard reagent (Scheme 2).

This method has undergone several modifications [13,23c,e,45], but remains a convenient route to pentaphenylcyclopentadiene (**1**) by way of pentaphenylcyclopentadien-1-ol (**2**) and 1-bromopentaphenylcyclopentadiene (**3**) from commercially available tetracyclone (**20**). It also allows the preparation of 1-aryl-2,3,4,5-tetraphenylcyclopentadienyl precursors, for example, (4-alkylphenyl)-2,3,4,5-tetraphenylcyclopentadien-1-ol, by the selection of an appropriate Grignard reagent. Conversion of the penta-arylcyclopentadien-1-ols into the corresponding 1-bromopenta-arylcyclopentadienes can be effected with HBr in glacial acetic acid. Isolation of the intermediate 1-bromopenta-arylcyclopentadiene is not necessary, since the penta-arylcyclopentadiene can be produced from the penta-arylcyclopentadien-1-ol in a single step by reduction of the alcohol in glacial acetic acid with H_3PO_2/HI, zinc/HBr or zinc/HCl, although the preparation using hypophosphorous acid generally results in higher yields (Scheme 2).

This route from tetracyclone to the aryl-tetraphenylcyclopentadienol to the bromide or hydride permits the easy introduction of a single different aryl substituent to form C_5Ph_4ArX (X = Br, H) from commercially available tetracyclone (**20**). These materials are routinely obtained as a mixture of isomers, consistent with the formation of delocalized cationic intermediates in the reaction of the alcohol with acid. Separation of the isomers is usually unnecessary, since the presence of isomers does not affect the subsequent organometallic and coordination chemistry [13]. The syntheses of less symmetrical $C_5Ar^1Ar^2Ar^3Ar^4Ar^5X$ derivatives require the syntheses of the appropriately substituted tetracyclone analogue (*vide infra*).

At least in the case of 1,2,3,4,5-pentaphenyl-2,4-cyclopentadien-1-ol (**2**), the yield is independent of the order of addition of the Grignard reagent to the tetracyclone [13,46]. If the reaction temperature is less than about 90 °C, the 1,2,3,4,5-pentaphenyl-2,4-cyclopentadien-1-ol (**2**) is obtained as the major product. However, at 173 °C, 1,2,3,4,5-pentaphenyl-2,4-cyclopentadien-1-ol (**2**) isomerizes by a symmetry-allowed suprafacial [1,5] sigmatropic phenyl shift to produce 2,2,3,4,5-pentaphenyl-3-cyclopenten-1-one (Scheme 3) [46,47]. This product had earlier been incorrectly formulated as 2,3,3,4,5-pentaphenyl-1,4-cyclopentadien-1-ol [48].

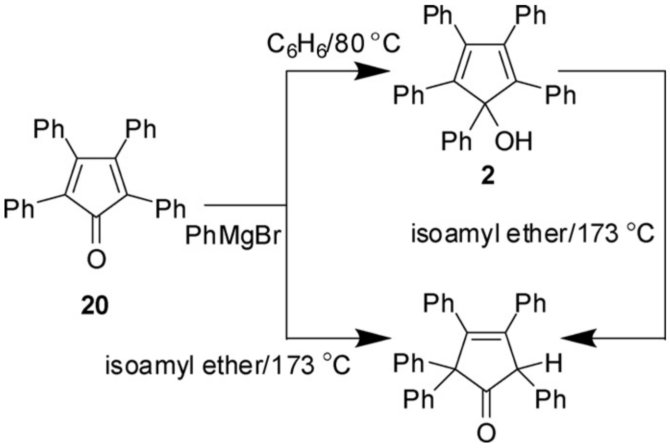

Scheme 3.

Alternatively, 2,3,4,5-tetraphenyl-2,4-cyclopentadien-1-ol can be prepared by $LiAlH_4$ reduction of tetracyclone (**20**) in 90% yield and converted to 2,3,4,5-tetraphenyl-2,4-cyclopentadienyl-1-tosylate in 75% yield by reaction with *p*-toluenesulfonyl chloride and pyridine in benzene. The tosylate ester reacts with a methyl Grignard reagent to produce 5-methyl-1,2,3,4-tetraphenyl-1,3-cyclopentadiene (**21**) in 16% yield (Scheme 4) [49].

Higher yielding routes to 5-methyl-1,2,3,4-tetraphenyl-1,3-cyclopentadiene have been reported, but the method is of potential interest in the syntheses of derivatives with substituents that react with H_3PO_2/HI, zinc/HBr or zinc/HCl or that may have limited solubility or stability in glacial acetic acid at reflux. The reduction of 1-bromopentaphenylcyclopentadiene (**3**) by $NaBH_4$ has also been reported to produce pentaphenylcyclopentadiene (**1**) [50].

Tetracyclone (**20**) also reacts with phenyl-lithium in ether to produce 1,2,3,4,5-pentaphenylcyclopenta-2,4-diene (**1**) in 70% yield after hydrolysis [51]. Similarly, addition of **20** to phenyl-lithium followed by acidic hydrolysis produces 1,2,3,4,5-pentaphenylcyclopenta-2,4-diene (**1**) in 33% yield (Scheme 5) [8b].

1.1.3.2. From 1,4-dilithio-1,2,3,4-tetraphenylbutadiene. The dimerization of diphenylacetylene by lithium has been investigated in several laboratories [52]. The reaction proceeds readily at room temperature to produce 1,4-dilithio-1,2,3,4-tetraphenylbutadiene as a red solid which reacts with reagents XBr_2 to produce C_4Ph_4X (Scheme 6).

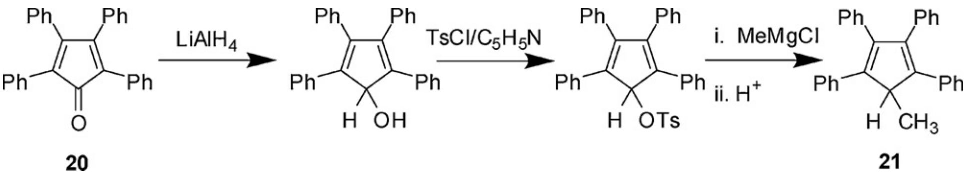

Scheme 4.

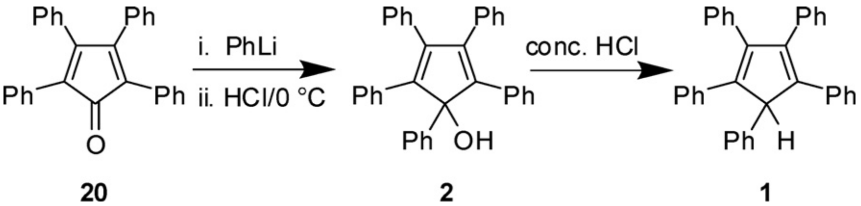

Scheme 5.

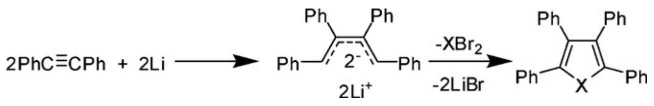

Scheme 6.

Thus, for example, reactions with CBr_4 or α,α-dichlorotoluene yield 1,1-dibromo-2,3,4,5-tetraphenylcyclopentadiene (**22**, 39%, $X = CBr_2$) or pentaphenylcyclopentadiene (**1**) (51%, X = PhCH), respectively. The reaction is somewhat complicated by the presumed, slow isomerization of 1,4-dilithio-1,2,3,4-tetraphenylbutadiene to a material that produces 1,2,3-triphenylnaphthalene on hydrolysis. Yields of 1,4-dilithio-1,2,3,4-tetraphenylbutadiene are therefore limited to some 66%. In an interesting variation, zirconocene dichloride reacts with 1,4-dilithio-1,2,3,4-tetraphenylbutadiene to produce *bis*cyclopentadienyltetraphenylzirconacyclopentadiene [52g].

*1.1.3.3. From the pentaphenylcyclopentadienyl radical (**4**).* Hydrolysis of a toluene solution of the pentaphenylcyclopentadienyl radical (**4**) yields 1,2,3,4,5-pentaphenylcyclopentadien-1-ol (**2**) (22%) and 1,2,3,4,5-pentaphenylcyclopentadiene (**1**) (28%) [53].

1.1.3.4. From the heptaphenyltropylium cation. Treatment of heptaphenyltropylium bromide with excess potassium in dimethoxyethane for 4 h, followed by hydrolysis, generated *cis*-stilbene and pentaphenylcyclopentadiene (**1**) (94%) (Scheme 7) [49,54]. Heptaphenylcycloheptatriene is produced in 52% yield from the Diels–Alder condensation of tetracyclone (**20**) and triphenylcyclopropene in the melt (∼200 °C) [55] and forms heptaphenyltropylium bromide on reaction with excess bromine [56].

1.1.3.5. From tricyclo-octenone carbonyl compounds. Tricyclo-octenone carbonyl derivatives react with Bu^tOK in dimethylsulfoxide at 70 °C over 72 h to produce aryl- or alkyl-substituted tetraphenylcyclopentadiene and cinnamic acid derivatives (Scheme 8). 1,2,3,4,5-pentaphenylcyclopentadiene (**1**) was prepared in 78% yield and 5-methyl-1,2,3,4-tetraphenyl-1,3-cyclopentadiene (**21**) in 75% yield [49].

The *endo*-1,2,3,4,5,6,7-heptaphenyltricyclo[3.2.1.0]-6-octen-8-one precursor to pentaphenylcyclopentadiene (**1**) in Scheme 8 was obtained in 85% yield from the room temperature Diels–Alder condensation of tetracyclone (**20**) with triphenylcyclopropene [56,57].

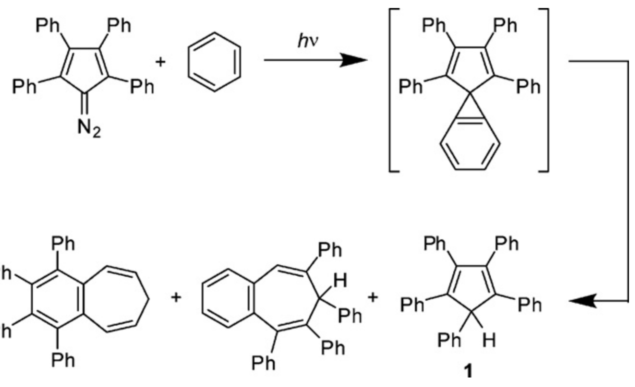

Scheme 9.

1.1.3.6. From diazotetraphenylcyclopentadiene. Photolysis of diazotetraphenylcyclopentadiene in benzene at 100 °C, followed by thermolysis of the product tetraphenylspirocaradiene (Scheme 9) produces a mixture of 1,2,3,4,5-pentaphenylcyclopentadiene (**1**) (47%), benzotetraphenylcycloheptatriene (43%) and tetraphenylbenzocycloheptatriene (10%) [58]. At lower temperatures, the yield of 1,2,3,4,5-pentaphenylcyclopentadiene (**1**) is considerably reduced [58c].

The thermal reaction of diazotetraphenylcyclopentadiene in benzene produces spiroindazoles, which may be later photolyzed in benzene to produce 1H-cyclopenta(1)phenanthrenes (Scheme 10) [59].

The method can be generalized to the reaction of olefins with diazotetraphenylcyclopentadiene and so this route is of potential interest as a means of introducing a single substituent to the tetraphenylcyclopentadienyl ring. At higher reaction temperatures, cyclization onto an adjacent phenyl ring can complicate the chemistry (Scheme 11) [58a].

Diazotetraphenylcyclopentadiene can be prepared in yields of 60–90% from the reaction of tetraphenylcyclopentadiene with *p*-toluenesulfonyl azide or from the reaction of tetracyclone (**20**) with *p*-toluenesulfonyl hydrazine [60].

1.1.3.7. Metal-assisted formation of coordinated penta-arylcyclopentadienyl ligands. Examples of the metal-assisted formations of coordinated penta-arylcyclopentadienyl ligands are relatively rare. The reactions often proceed in low yield and the reactions commonly involve the condensation of diarylacetylenes in the presence of an organometallic

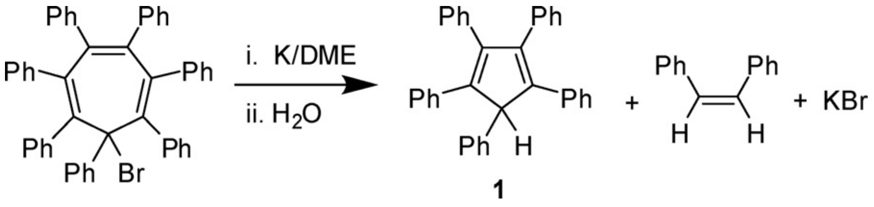

Scheme 7.

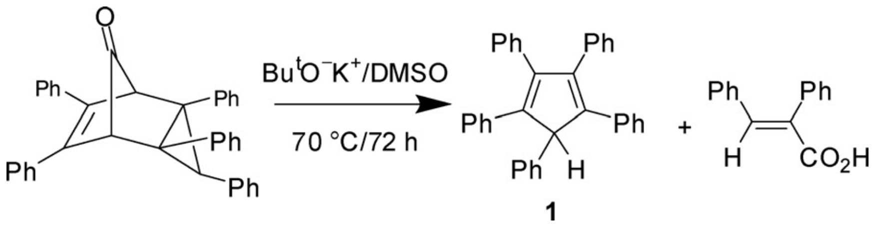

Scheme 8.

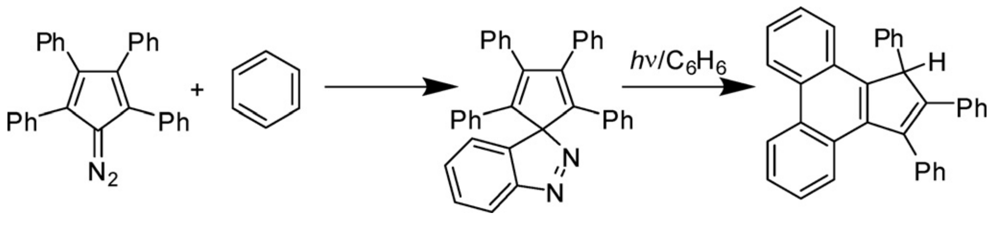

Scheme 10.

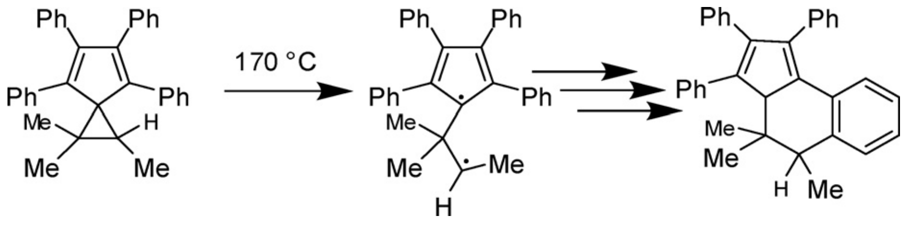

Scheme 11.

$$[\mathrm{Mo(CO)_6}] \xrightarrow[\mathrm{C_6H_6/160\ °C}]{\mathrm{Ph{-}C{\equiv}C{-}Ph}} \begin{array}{l} [\mathrm{Mo_2(C_2Ph_2)(C_4Ph_4)_2(CO)_4}]\ + \\ [\mathrm{Mo(C_2Ph_2)_2(C_4Ph_4)(CO)}]\ + \\ [\mathrm{Mo(C_4Ph_4)(C_5Ph_4O)(CO)_2}]\ + \\ [\mathrm{Mo(C_4Ph_4)_2(CO)_2}]\ + \\ [\mathrm{Mo(C_5Ph_5)_2}]\ + \\ \mathrm{(PhC_2Ph)_3(CO)_2} \end{array}$$

Scheme 12.

reagent to produce the coordinated penta-arylcyclopentadienyl ligands.

The reaction of approximately 1.5 equivalents of diphenylacetylene with $[Mo(CO)_6]$ under pressure produced decaphenylmolybdenocene (**23**) in only low yield (3.5%) as an insoluble, relatively stable, red powder, from which C_5Ph_5H (**1**) could be liberated in 42% yield using 1-methylnaphthalene as a solvent at prolonged reflux [4]. A range of other products were also formed (Scheme 12).

The major inorganic products were formulated as green $[Mo(\eta^4\text{-}C_4Ph_4)(CO)_2]_2(\mu\text{-}PhC{\equiv}CPh)$ (45% yield) and violet $[Mo(PhC{\equiv}CPh)_2(\eta^4\text{-}C_4Ph_4)(CO)]$ (40% yield). The structure of $[Mo(\eta^4\text{-}C_4Ph_4)_2(CO)_2]$ was later confirmed crystallographically [61], although the major product, originally formulated as $[Mo(\eta^4\text{-}C_4Ph_4)(CO)_2]_2(\mu\text{-}PhC{\equiv}CPh)$, was structurally characterized as $[Mo(CO)_2(\eta^4\text{-}Ph_4C_5O)Mo(\eta^4\text{-}C_4Ph_4)(CO)](\mu\text{-}PhC{\equiv}CPh)$ [62]. The reaction between $[Mo(diglyme)(CO)_3]$ and diphenylacetylene in benzene at reflux forms $[Mo(\eta^5\text{-}C_5Ph_5)_2]$ (**23**) and $[Mo(PhC{\equiv}CPh)_2(C_4Ph_4)(CO)]$ in 3.5% and 35% yields, respectively [4].

A similar reaction between five equivalents of diphenylacetylene and $[Mo(\eta^6\text{-}C_5H_5Me)(CO)_3]$ produced several products, including decaphenylmolybdenocene (**23**) [63]. The reaction between molten diphenylacetylene and $[W(PhC{\equiv}CPh)_3(CO)]$ (or $[W(CO)_3(N{\equiv}CMe)_3]$) gives dark-red crystalline, air-stable $[W(CO)(PhC{\equiv}CPh)\{\eta^5\text{-}C_3Ph_3(C_5Ph_5)\}]$, purple $[W(CO)(PhC{\equiv}CPh)\{\eta^6\text{-}C_3Ph_3(C_5Ph_5)\}]$ and orange-red $[W(\eta^5\text{-}C_5Ph_5)_2]$ (**24**) in 14%, 6% and 32% yields, respectively (Scheme 13) [17].

The η^4-coordinated C_5Ph_4R ring differs from the C_5 ring of C_5Ph_5H (**1**) inasmuch as the formally sp^3 hybridized carbon is bent out of the plane of the diene carbon atoms. A mixture of $[W(CO)(PhC{\equiv}CPh)\{\eta^5\text{-}C_3Ph_3(C_5Ph_5)\}]$ (70%) and $[W(CO)(PhC{\equiv}CPh)\{\eta^6\text{-}C_3Ph_3(C_5Ph_5)\}]$ (22%) was also formed when a THF solution of $[W(PhC{\equiv}CPh)(\eta^8\text{-}C_8Ph_8)]$ (produced from the reaction of $[W(N{\equiv}CMe)(PhC{\equiv}CPh)_2(\eta^4\text{-}C_4Ph_4)]$ with diphenylacetylene) was treated with 1 atm CO at 50 °C [17b]. The alkyne coupling is promoted by replacement of the CO ligand of $[W(PhC_2Ph)_3(CO)]$ with MeC≡N, to give $[W(PhC{\equiv}CPh)_3(N{\equiv}CMe)]$, which, when subjected to brief reflux in toluene under nitrogen with 5 equivalents of diphenylacetylene, affords a 7% yield of $[W(C_5Ph_5)_2]$ (**24**), $[W(N{\equiv}CMe)(PhC{\equiv}CPh)(\eta^4\text{-}C_4Ph_4)]$

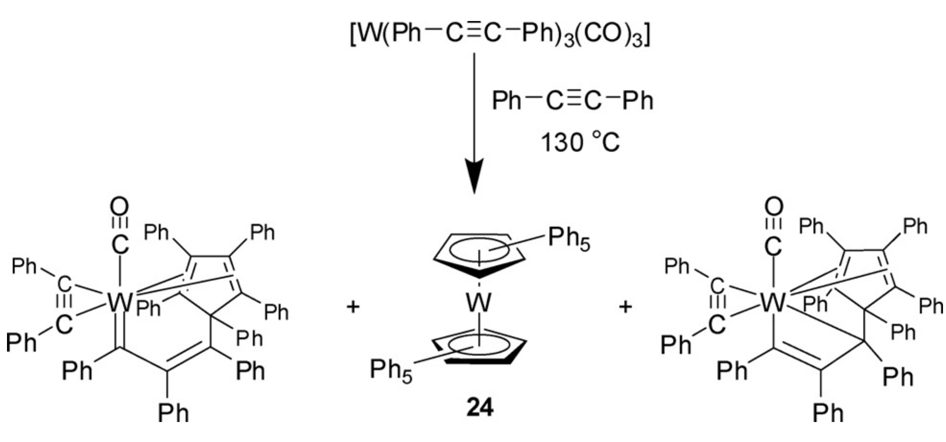

Scheme 13.

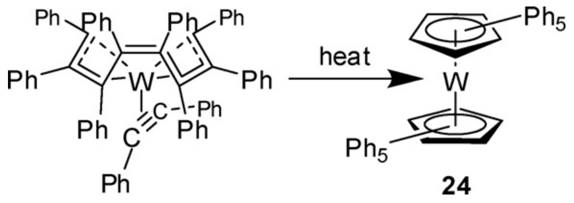

Scheme 14.

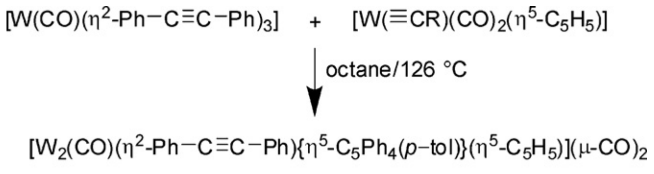

26

Scheme 15.

(19%) and [W(PhC≡CPh)(η^8-C_8Ph_8)] (42%). A mixture of [W(N≡CMe)(PhC≡CPh)(η^4-C_4Ph_4)] with diphenylacetylene in toluene at reflux also produces [W(PhC≡CPh)(η^8-C_8Ph_8)], which, after the same treatment, gives in turn [W(C_5Ph_5)$_2$] (**24**) in 87% yield (Scheme 14) [17b,23ao].

Interestingly, irradiation of a benzene solution of diphenylacetylene and [Fe(CO)$_5$] produced a 45% yield of [Fe(η^4-C_5Ph_4O)(CO)$_3$], from which tetracyclone (**20**) can be quantitatively liberated on heating. Additionally, phenylacetylene reacts with [Fe(CO)$_5$] to produce [Fe(η^4-2,5-$Ph_2C_5H_2O$)(CO)$_3$] [64]. [C_4(*p*-tol)$_4$C(=O)] (**25**) can also be synthesized by this route [36].

The preformed diphenylacetylene complex, [W(CO)(PhC≡CPh)$_3$], reacts with [W(≡CR)(CO)$_2$(η^5-C_5H_5)] to produce red-brown crystals of binuclear, [W(CO){η^5-C_5Ph_4(*p*-tol)}W(η^2-PhC≡CPh)(η^5-C_5H_5)](μ-CO)$_2$ (**26**) in 20% yield (Scheme 15) [65].

The penta-arylcyclopentadienyl complex, [W(CO){η^5-C_5Ph_4(*p*-tol)}W(η^2-PhC≡CPh)(η^5-C_5H_5)](μ-CO)$_2$ (**26**), has been structurally characterized (Fig. 12) [65].

In another curious reaction, a mixture of $Os_3(CO)_{12}$ and C_5Ph_5Br in toluene at reflux produces a range of products all in relatively poor yield. One of these products is 1-benzyl-1,2,3,4,5-pentaphenylcyclopenta-2,4-diene (**27**, Fig. 13) [32], which has been prepared more conveniently by the reaction between [C_5Ph_5Li] (**28**) and benzyl chloride [66]. This material is not obtained from C_5Ph_5Br (**3**) in toluene at reflux, and appears to result from an osmium-assisted coupling of C_5Ph_5Br (**3**) with the toluene solvent. The corresponding reaction in chlorobenzene produces [Os(η^5-C_5Ph_5)(CO)$_2$Br] (**29**) in good yield [23af].

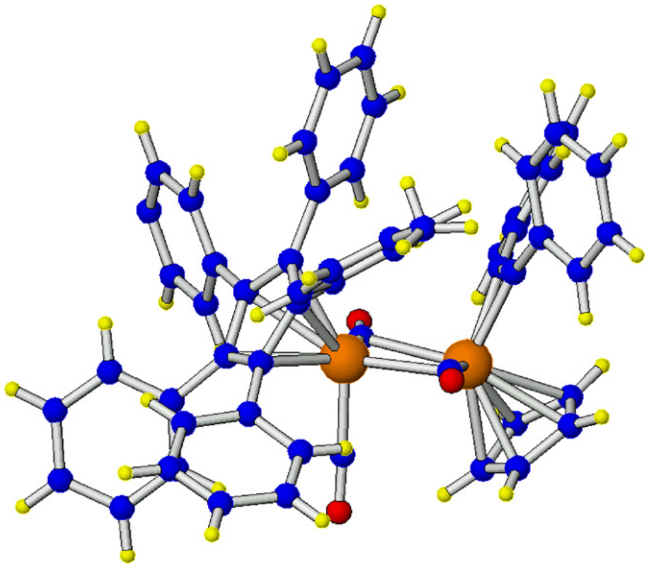

Fig. 12. Structure of [W(CO{η^5-C_5Ph_4(*p*-tol)}W(η^2-PhC_2Ph)(η^5-C_5H_5)](μ-CO)$_2$ (**26**) [65].

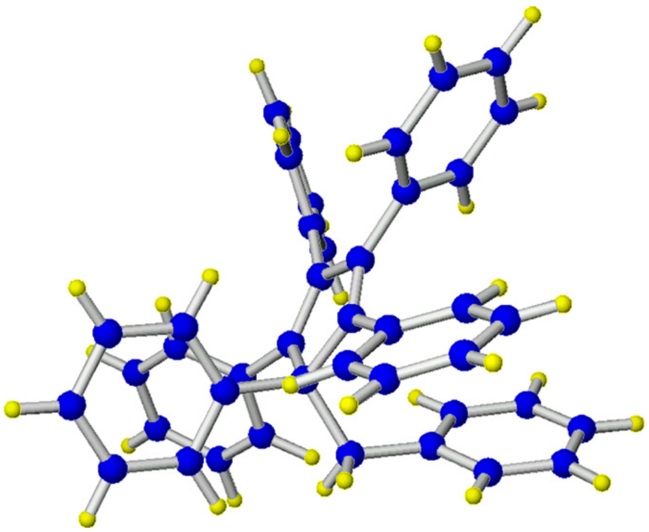

Fig. 13. Structure of $C_5Ph_5(CH_2C_6H_5)$ (**27**) [32].

Substituted pentaphenylcyclopentadienes are prepared in good yield by the copper-mediated reaction of zirconacylopentadienyls with iodopropenoates in THF at room temperature [67]. Thus the general reaction of Scheme 16 in which $R^1 = R^2 = R^3 = R^4 = R^5$ = Ph, and R = Me (**30**) proceeds in 78% isolated yield over 1 h. The structure of the product has been established unequivocally by X-ray diffraction.

The authors propose that the reaction involves the production of an organocuprate intermediate in a *trans*-metallation step. In a related reaction, pentaphenylcyclopentadiene (**1**) has been prepared in 47% yield by the formal coupled deoxygenation of the product of [2 + 2 + 2] cycloaddition of benzaldehyde to two equivalents of diphenylacetylene, mediated by zirconocene and $AlCl_3$ (Scheme 17) [67b].

When diphenylacetylene is stirred for 24 h in a methanolic suspension of [Pd(OAc)$_2$]$_3$, [Pd(η^5-C_5Ph_5)]$_2$(μ-PhC≡CPh) (**31**), is produced. This compound represents one of the few stable, formally Pd(I) species, and a rare example of an alkyne bridge across two palladium centres [9,23a,68]. The compound is soluble in benzene and chloroform.

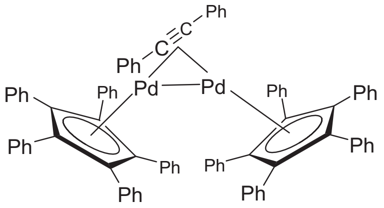

31

The following stoichiometry (Eq. (3)) was suggested on the basis of quantitative product identification (this is complicated by the concomitant decomposition of [Pd(OAc)$_2$]$_3$ to Pd(0) in alcohols) [69]:

$$[Pd(OAc)_2]_3 + 7PhC \equiv CPh + 6MeOH \rightarrow [Pd(\eta^5 - C_5Ph_5)]_2$$
$$(\mu - PhC \equiv CPh)(\mathbf{31}) + Ph(0) + 2PhC(OMe)_3 + 6HOAc \qquad (3)$$

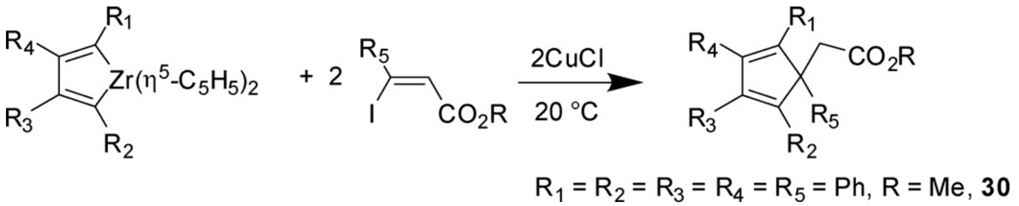

Scheme 16.

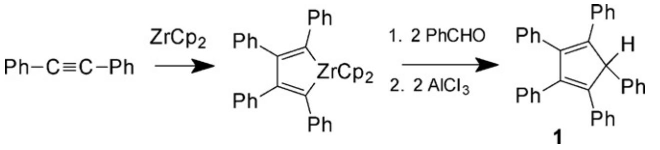

Scheme 17.

The reaction could also be performed with $Pd(NO_3)_2 \cdot xH_2O$, $[Pd(O_2CCF_3)_2]$ or $[Pd(O_2CCF_3)_2(acetone)_2]$, or with ethanol as solvent, although the best yields (70–85%) were obtained with $[Pd(OAc)_2]_3$ in methanol.

The reaction involves a remarkable room temperature cleavage of a carbon–carbon triple bond and was proposed to occur in an analogous fashion to the palladium(II) chloride induced cyclotrimerization of acetylenes to benzenes in organic solvents (Scheme 18) [70].

Thus, diphenylacetylene π-bound to Pd(II) undergoes nucleophilic attack by MeOH to form a σ-vinylic species. The palladium and methoxy groups of the intermediate **A** (Scheme 18) are suggested to be mutually *trans* because this leads to a structure that is analogous to the structure of a 4-ethoxytetraphenylbuta-1,3-dien-1-yl ligand, trapped on a $[Pd(acac)PMe_2Ph]$ moiety as an intermediate (**32**) in the synthesis of $[Pd(\eta^5\text{-}C_5Ph_5)]_2(\mu\text{-}PhC{\equiv}CPh)$ (**31**) [68].

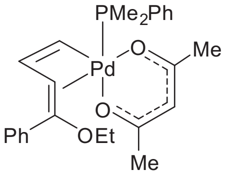

32

Insertion of a second diphenylacetylene, rearrangement of the triene, reductive ring closure and oxidative alcoholysis to remove $PhC(OMe)_3$ generates the univalent $[Pd(\eta^5\text{-}C_5Ph_5)]$ intermediate that dimerizes and coordinates a bridging alkyne. The steps leading to intermediate **B** (Scheme 18) parallel those suggested by Maitlis for the formation of hexaphenylbenzene from diphenylacetylene and "$PdCl_2$" [70,71].

Although $[Pd(endo\text{-}C_4Ph_4OMe)Cl]_2$ does not react directly with diphenylacetylene [72], it does react in methylene chloride with MOAc (M = Ag, Tl) to generate the incompletely characterized "$[Pd(endo\text{-}C_4Ph_4OMe)(OAc)]_n$", which in turn reacts with diphenylacetylene in methanol to produce $[Pd(\eta^5\text{-}C_5Ph_5)]_2(\mu\text{-}PhC{\equiv}CPh)$ (**31**). Alternatively, $[Pd(\eta^5\text{-}C_5Ph_5)]_2(\mu\text{-}PhC{\equiv}CPh)$ (**31**) is readily produced from $[Pd(endo\text{-}C_4Ph_4OMe)(OAc)Cl]_2$ by reaction with diphenylacetylene and excess sodium acetate in warm methanol. This sequence, with the intermediacy of "(*endo*-methoxytetra(*p*-tolyl)cyclobutenyl)palladium acetate", is the preferred route to the penta(*p*-tolyl)cyclopentadienyl analogue of **31** since it proceeds in higher yield (50%) compared to the alternative reaction of di(*p*-tolyl)acetylene with palladium acetate in methanol (yield ~5%).

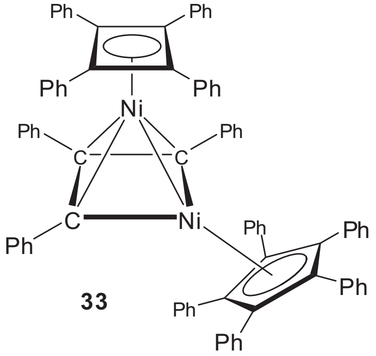

33

Complexes with mixed penta-arylcyclopentadienyl ligands can be produced by treating "$[Pd(endo\text{-}C_4Ph_4OMe)(OAc)]_n$" with other diarylacetylenes, for example $(Cp\text{-}X\text{-}C_6H_4)_2$ (X = OMe, Br, Me) or PhC≡C-naphthyl.

The (palladium acetate/palladium chloride)/diarylacetylene/methanol route to $[Pd(\eta^5\text{-}C_5Ar_5)]_2(\mu\text{-}ArC{\equiv}CAr)$ is apparently general. The penta-arylcyclopentadiene is liberated by reaction of $[Pd(\eta^5\text{-}C_5Ar_5)]_2(\mu\text{-}ArC{\equiv}CAr)$ with excess HCl in $CHCl_3$. These reactions have synthetic utility as a route to mixed penta-arylcyclopentadienes of the type 1-Ar^1-2-Ar^2-3,4,5-$Ar_3{}^3$-cyclopentadienes. However, this is the only substitution pattern that is accessible by this approach. This substitution pattern is also readily achieved by the tetracyclone route (Section 1.1.3.1) and the preferred synthesis would depend on the availability of the requisite starting materials.

Hexaphenylbenzene is produced from palladium(II) chloride and diphenylacetylene in alcohol [73]. No hexaphenylbenzene is detected in the palladium acetate/diphenylacetylene/methanol reactions so the acetate ligand clearly has a product directing effect in this chemistry.

Treatment of $Al(C_4Ph_4)Ph$ with lithium gives $[Al(C_4Ph_4)Ph](Li)_2$, which reacts with molar equivalents of $Al(C_4Ph_4)Ph$ and $NiBr_2$ to form aluminum-free, deep violet $[Ni(\eta^4\text{-}C_4Ph_4)Ni(\eta^5\text{-}C_5Ph_5)](\mu\text{-}C_3Ph_3)$ (**33**), in 7% yield, along with blue $[Ni(\eta^4\text{-}C_4Ph_4)_2]$ in 4% yield [23b].

The reaction of diphenylacetylene with 1,2,3-triphenylcyclopropene is catalyzed by Ni(0) species generated from $[Ni(acac)_2]$ and EtMgCl producing C_5Ph_5H (**1**) (Scheme 19) [12,74].

In the presence of [Ni(bipy)(COD)], it is suggested that 1,2,3-triphenylcyclopropene forms a carbene, which reacts to form C_5Ph_5H (**1**) via the intermediacy of a nickelacyclohexadienyl complex. The nickel-catalyzed reaction of α-lithiobenzylphenyl sulfone in the presence of diphenylacetylene produces C_5Ph_5H (**1**) by way of the nickel–carbene complex in Scheme 19 [12].

The $C_5Ph_4(p\text{-}tol)^-$ ligand has also been generated in the reaction between $[W(CO)(PhC{\equiv}CPh)_3]$ and $[W({\equiv}C\text{-}(4\text{-}MeC_6H_5))(\eta^5\text{-}C_5H_5)(CO)_2)]$ (Scheme 15) [65].

In reactions that are metal-assisted, at least those in which palladium-catalyzed reactions of pre-formed metallocenes are involved, penta-arylcyclopentadienyls can be produced in 30–80% yield by the reaction of aryl halides with metallocenes, or met-

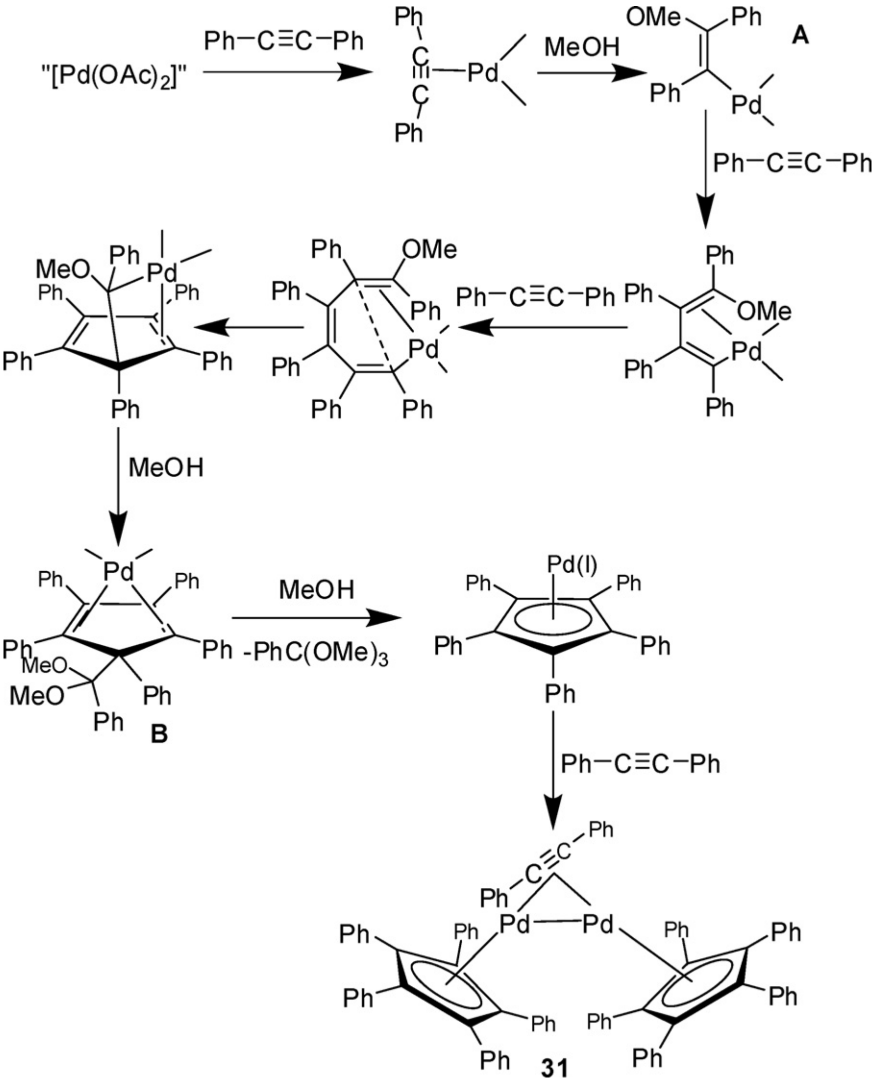

Scheme 18.

allocene dihalides, in the presence of a $[Pd(OAc)_2]/PR_3/Cs_2CO_3$ catalyst (Scheme 20) [40,75].

Suitable metallocenes include $M(\eta^5\text{-}C_5H_5)_2$ (M = Fe, Co, Ni), $M'(\eta^5\text{-}C_5H_5)_2Cl_2$ (M′ = Ti, Zr); $Tl(\eta^5\text{-}C_5H_5)$ or cyclopentadiene itself may also be used as a substrate in place of the metallocene. The most effective complexes for the synthesis of pentaphenylcyclopentadiene are the metallocene dihalides; cobaltocene and nickelocene proved far less effective. Intermediates isolated during the reaction of zirconocene dichloride suggest that the arylation occurs sequentially, although it was not established that all arylations occurred on the metallocene. Scrambling of aryl rings was observed when 4-fluorobromobenzene underwent reaction in the presence of PPh_3. In general, the best yields were obtained with the more basic and bulkier $PBu_3{}^t$. A variant on this reaction, in which $C_5(p\text{-tol})_5H$ (**34**) is produced in 65% yield (Scheme 21), is disclosed in the patent literature [75b]. This multifold, palladium-catalyzed arylation of cyclopentadiene appears to be the most convenient and general route to *per*-arylated cyclopentadienes with increasing steric bulk, which have possible applications in supramolecular chemistry [39,41,76].

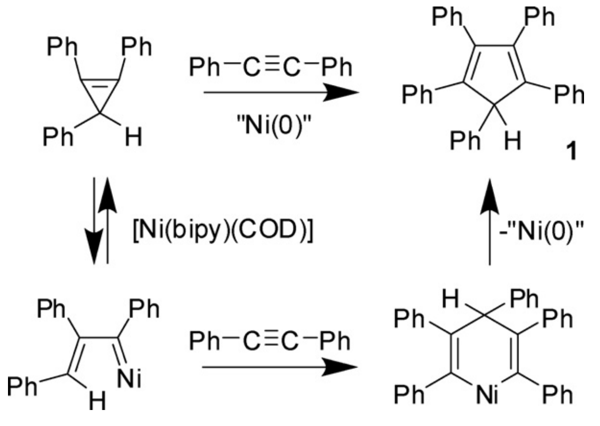

Scheme 19.

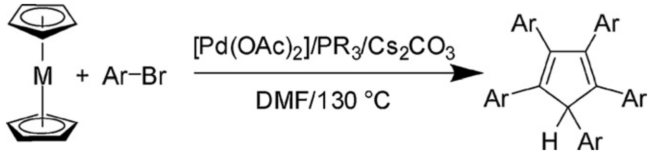

Scheme 20.

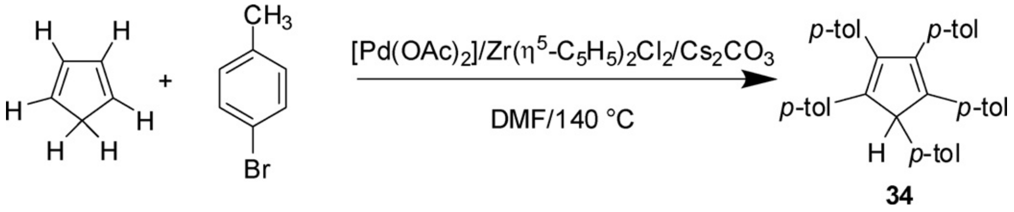

Scheme 21.

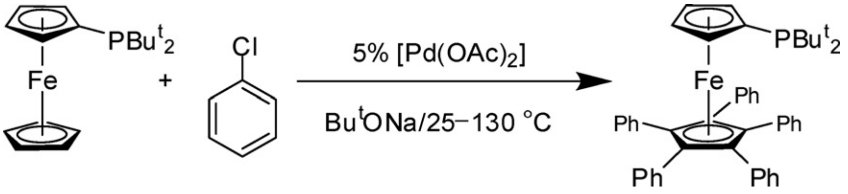

Scheme 22.

Similarly, palladium-mediated reactions of aryl halides with ferrocene derivatives produce iron penta-arylcyclopentadienyl complexes in high yield (Scheme 22) [77].

An unusual metal-assisted reaction of the pentaphenylcyclopentadienyl ligand is the light-induced reaction of coordinated $C_5Ph_5^-$ in the $[Fe(\eta^5-C_5Ph_5)(C_6H_6)]^+$ cation, in the presence of $P(OEt)_3$, to produce $C_{35}H_{26}$, 4,8-diphenyltribenzo[*b,f,i*]tricyclo[6.2.1.0]undecane (**35**, Fig. 14), an isomer of pentaphenylcyclopentadiene (**1**), in low yield [5].

When $[Pd(8\text{-methylquinoline})]_2(\mu\text{-}Cl)_2$ is heated with diphenylacetylene in chlorobenzene at reflux, a 25% yield of yellow-orange crystals of the cyclopalladated, $[Pd\{C(Ph)=C(Ph)CH(Ph)C(Ph)=CHC_9H_6N\}Cl]$ is generated [78]. This complex can be depalladated with PPh_3 in boiling methanol, to produce yellow crystals of structurally characterized $C_5Ph_4(C_9H_7N)\cdot HCl$ (**36**, Fig. 15) in 72% yield (Scheme 23) [79].

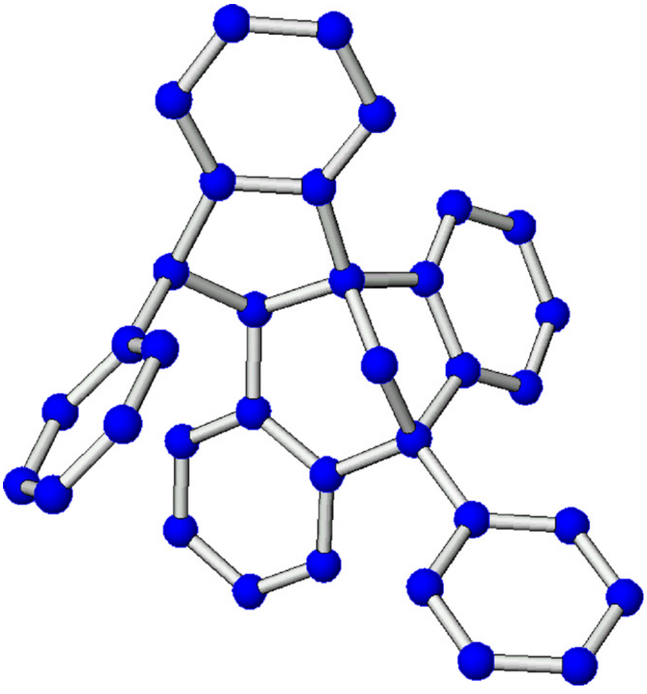

Fig. 14. Structure of 4,8-diphenyltribenzo[*b,f,i*]tricyclo[6.2.1.0]undecane, $C_{35}H_{26}$ (**35**) (hydrogen atoms omitted) [5].

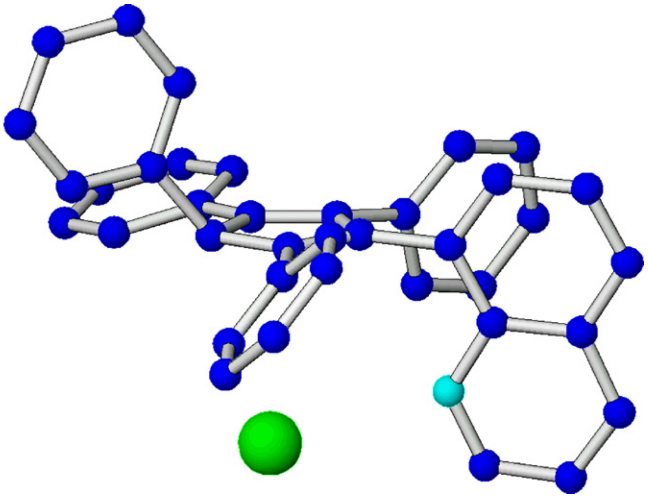

Fig. 15. Structure of $C_5Ph_4(C_9H_7N)\cdot HCl$ (**36**) (hydrogen atoms omitted) [79].

1.2. The pentaphenylcyclopentadiene cation and related species

The pentaphenylcyclopentadienyl cation, $C_5Ph_5^+$, attracted significant interest as an early example of an anti-aromatic system with a thermally accessible triplet state. However, some confusion has existed over its characterization. The purple product obtained by dissolution of C_5Ph_5OH (**2**) in concentrated H_2SO_4 at room temperature was originally formulated as $C_5Ph_5^+$ [3,80]. However, $C_5Ph_5^+$ exists for only a few seconds under these conditions [19,54,66a,81]. The major products identified from this reaction are C_5Ph_5H (**1**) and 1,2,3-triphenyl-1-H-cyclopenta[1]-phenanthrene (**15**, Scheme 24).

A later report indicated that boiling C_5Ph_5OH (**2**) in acetic acid/1% H_2SO_4 produced 45% 1,2,3,4,5-pentaphenyl-2,4-

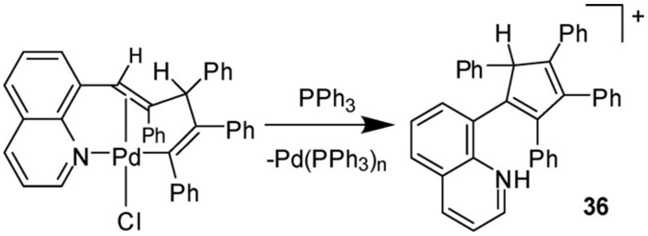

Scheme 23.

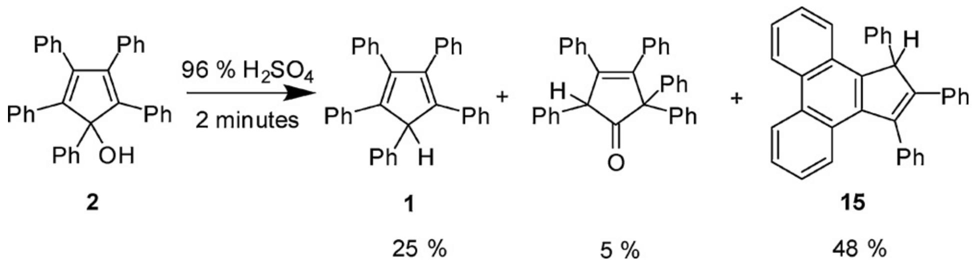

Scheme 24.

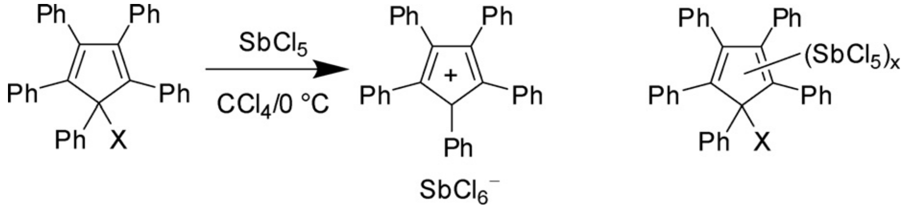

Scheme 25.

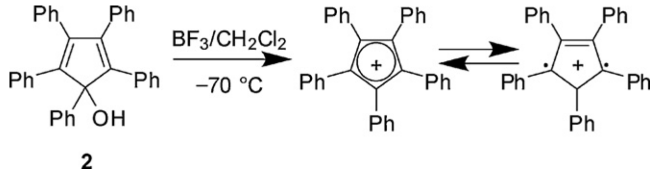

Scheme 26.

cyclopentadiene (**1**) and 35% of a compound believed to be 2,2,3,4,5-pentaphenyl-3-hydroxy-4-cyclopenten-1-one [47]. Low yields of C_5Ph_5H (**1**) are also obtained from the thermal reaction of stilbene with sulfur [82].

The intense purple colour (λ_{max} 516 nm, ε log 4.3) which had been attributed to $C_5Ph_5^+$ is actually a composite spectrum of a mixture of C_5Ph_5H (**1**) (λ_{max} 520 nm, ε log 4.3; 376 nm, ε log 4.1) and the triphenylcyclopentadienophenanthrene (λ_{max} 502 nm, ε log 4.5). In concentrated H_2SO_4, C_5Ph_5H (**1**) forms a bright orange solution with a strong ESR signal (λ_{max} 520 nm, ε log 4.3; 376 nm, ε log 4.1). C_5Ph_5H (**1**) can be quantitatively recovered on dilution [19].

However, $C_5Ph_5^+$ can be produced at low temperature. The intensely blue cation can be generated (along with an uncharacterized $SbCl_5/C_5Ph_5X$ adduct) [83] in ~20% yield by treatment of C_5Ph_5X (X = Cl (**19**), Br (**3**)) with three equivalents of $SbCl_5$ at 0 °C in CCl_4 (Scheme 25), or by treatment of C_5Ph_5OH (**2**) with BF_3 or $AlCl_3$ at −70 °C (Scheme 26).[2] Crystalline $[C_5Ph_5]^+[SbCl_6]^-$ (**37**) has a strong ESR signal (presumably at room temperature) at $g \sim 2$, attributed to a triplet state, a multiplicity consistent with recent theoretical calculations [84]. However, the cation generated from BF_3 (λ_{max} 650 nm, ε log 4.7), presumably $[C_5Ph_5]^+[BF_3OH]^-$ (**38**), although quite stable at −70 °C, decomposes irreversibly above −40 °C [85]. The frozen solution ESR spectrum is that of a triplet with some monoradical impurities. A combination of frozen solution ESR, variable temperature ESR, and NMR spectra established that the $C_5Ph_5^+$ cation exists in a ground-state singlet state in equilibrium with a thermally accessible, low-lying triplet excited state at ~2 kJ mol^{-1} higher energy (Scheme 26) [7,85a]. The energy difference between the ground and excited states is dependent upon the presence of substituents on the phenyl rings. The energy difference is approximately 0.8 kJ mol^{-1} greater in the $C_5Ph_4(p\text{-tol})^+$ cation than in the $C_5Ph_5^+$ cation [36,85b]. The substitution of additional phenyl rings by *p*-tolyl moieties has little effect on the relative energies of the singlet and triplet states; the $[C_5(p\text{-tol})_5]^+$ cation appears to be more stable than $C_5Ph_5^+$ [36].

By contrast, the $C_5Cl_5^+$ and $C_5H_5^+$ cations exist as ground state triplets [7]. The $C_5Ph_5^+$ cation does not appear to react with dioxygen [85a].

Other routes to penta-arylcyclopentadienyl cations include reactions of C_5Ar_5OH or C_5Ar_5Br with SbF_5, or $AlCl_3$, reaction of C_5Ph_5Br with $AgBF_4$, and of *p*-NMe_2-substituted C_5Ph_5Br and $C_5Ph_5Br{\cdot}HBr$ derivatives with RN_3 at −50 °C [29a,36]. In addition, electrolysis of a methylene chloride solution of C_5Ph_5Br (**3**) at +0.7 V (*vs.* $Fc^{+/0}$) generates a blue solution (λ_{max} 626 nm) of the cation radical, $C_5Ph_5^{\bullet +}$ [86].

1.3. *The pentaphenylcyclopentadienyl anion*

The pentaphenylcyclopentadienyl anion, $C_5Ph_5^-$, is a very useful synthetic intermediate and can be conveniently prepared in high (80–95%) yield as its alkali metal salts [14,23e]. Consistent with the acidity of C_5Ph_5H (**1**), the ring proton is readily removed by several routes (Eqs. (4)–(7)):

$$C_5Ph_5H\,(\mathbf{1}) + Bu^nLi \xrightarrow[100\,^\circ C]{C_7H_8} C_5Ph_5Li\,(\mathbf{28}) + Bu^nH \tag{4}$$

$$C_5Ph_5H(\mathbf{1}) + M \xrightarrow[100^\circ C]{C_7H_8} C_5Ph_5M + \tfrac{1}{2}H_2, \quad M = Na,\ K,\ Cs \tag{5}$$

$$C_5Ph_5H\,(\mathbf{1}) + NaH \xrightarrow[110\,^\circ C]{C_7H_8} C_5Ph_5Na\,(\mathbf{39}) + H_2 \tag{6}$$

$$C_5Ph_5H\,(\mathbf{1}) + NaNH_2 \xrightarrow[110\,^\circ C]{C_7H_8} C_5Ph_5Na\,(\mathbf{39}) + NH_3 \tag{7}$$

The sodium salt of the pentaphenylcyclopentadienyl anion is most satisfactorily produced by the reaction of C_5Ph_5H (**1**) with sodium or sodium amide in toluene at reflux, to give $[NaC_5Ph_5]$ (**39**) [23e]. The $C_5Ph_5^-$ salts are more easily isolated than the corresponding $C_5H_5^-$ salts and they can even be handled briefly in air. The enhanced stability of the MC_5Ph_5 salts is attributed in part to electron withdrawal by the aryl substituents, although the ^{13}C NMR spectra are inconsistent with resonance delocalization of partial negative charge onto the phenyl carbons. The phenyl rings and

---

[2] The antimony adduct may be produced exclusively if the reaction is performed at −22 °C with only the one equivalent of $SbCl_5$; see [83].

the cyclopentadienyl rings are unable to achieve the coplanarity required for efficient resonance stabilization of this type.

The ^{13}C NMR spectra of $C_5Ph_5^-$ exhibit only five resonances (δ (ppm) $\sim$ 142 (**C**$_5$), 131, 126, 121, 120 (*ipso*-C of C_6H_5 rings)). The $\delta \sim 142$ and 120 ppm resonances were assigned to quaternary carbons from the ^{1}H coupled spectra. ^{13}C NMR resonances at $\delta \sim 140$ ppm were subsequently assigned to the ring carbons of the non-bound cyclopentadienyl ring of zwitterionic [Fe(η^5-C_5Ph_5){(η^6-C_6H_5)C_5Ph_4}] (**40**) [16]. The observation of only five ^{13}C NMR resonances for $C_5Ph_5^-$ salts suggests that the $C_5Ph_5^-$ anion has D_{5h} symmetry. By contrast, twenty of the twenty-one possible ^{13}C NMR resonances of C_5Ph_5H (**1**) can be resolved, consistent with the local C_s symmetry of the crystal structure, and restricted rotation of three, non-symmetry related phenyl rings [5]. In THF, the $C_5Ph_5^-$ anion undergoes a reversible one-electron cyclic voltammetric oxidation at $E_{1/2}$ −0.84 V (*vs.* Fc$^{+/0}$; −0.28 V *vs.* SCE) [87].

1.4. The pentaphenylcyclopentadienyl radical

Zeigler and Schnell first reported that the pentaphenylcyclopentadienyl radical, $C_5Ph_5^\bullet$ (**4**), could be produced by treatment of C_5Ph_5Br (**3**) with silver in benzene [3]. The radical is relatively stable towards oxygen and also with respect to dimerization, characteristics attributed in an early theoretical study to a resonance energy of $\sim$15.5 kJ mol^{-1} [88]. Heeg et al. noted that a purple solid and a lead mirror were obtained on the attempted sublimation of [Pb(C_5Ph_5)$_2$] (**41**) [23f], a process by which Lamansky subsequently generated the $C_5Ph_5^\bullet$ radical (**4**) [11]. The radical is highly coloured (λ_{max} 585 nm, 584 nm (CH_2Cl_2))[86] and like C_5Ph_5H (**1**) fluoresces strongly (but at shorter wavelength: λ_{max} 390 nm *vs.* 454 nm for (**1**)) [11], and can be isolated and recrystallized as an air-sensitive powder [29a,36]. An absorption at 463 nm in the electronic spectrum (λ_{max} 350, 463, 575 nm) of the $C_5Ph_5^\bullet$ radical (**4**), distinguishes the radical from neutral C_5Ph_5H (**1**) and the $C_5Ph_5^-$ anion [11]. The electronic spectrum is sensitive to substituent variation on the phenyl rings. Thus, for example, λ_{max} shifts as phenyl groups are successively replaced by *p*-tolyl groups (no *p*-tolyl, λ_{max} 585 nm; 1 × *p*-tolyl, λ_{max} 593 nm; 2 × *p*-tolyl, λ_{max} 598–601 nm; 3 × *p*-tolyl, λ_{max} 604–608 nm, 4 × *p*-tolyl, λ_{max} 609 nm, 5 × *p*-tolyl, λ_{max} 613 nm in benzene) [36].

The *g* value of the $C_5Ph_5^\bullet$ radical (**4**) initially reported as 1.95 in the ESR experiment, was corrected to 2.0025 [89]. At room temperature in dry toluene, the spectrum has been reported as a multi-line (>28) absorption centred at *g* 2.0030, whilst a broad resonance centred at *g* 2.0028 is observed when the solution is cooled to 60 K. A broad ESR signal centred at *g* 2.0028 is observed from solid samples. At 60 K, the signal from the solid is not significantly narrower than the room temperature resonance, but some slight anisotropy is reported [11]. An extensive series of symmetrically and non-symmetrically substituted $C_5Ar_5^\bullet$ radicals has been prepared and examined by ESR, ENDOR, and electronic spectroscopies [24a,d,29a,36,90]. At room temperature, the $C_5Ar_5^\bullet$ radicals exhibit multi-line spectra at $g \sim 2.00$ [24a,d,29a]. When a pentane solution of the radical is cooled to ~ -80 °C the observed line-width is reduced from 150 mG to 50 mG [24d]. The spectroscopic width is $\sim$20 G at room temperature and $\sim$9 G at ~ -80 °C [19,24d,29a]. The ESR and ENDOR spectra of the $C_5Ar_5^\bullet$ radicals indicate a twist angle between the C_5 and phenyl rings of $\sim 40°$. The symmetrically (D_5) substituted radicals have been assigned a ground-state with twofold degeneracy, which is lifted as the symmetry is lowered (*e.g.* in C_5Ph_4(*p*-tol)$^\bullet$ (**42**), C_2 symmetry) [24d].

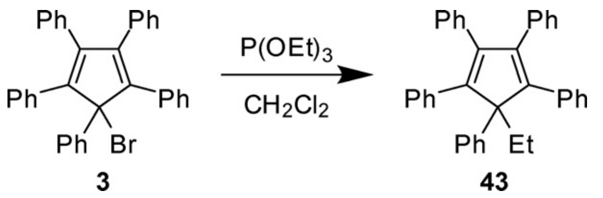

Scheme 27.

Penta-arylcyclopentadienyl radicals can also be prepared by reactions of *p*-NMe$_2$-substituted C_5Ph_5Br (**3**) and $C_5Ph_5Br \cdot HBr$ derivatives with R_3N or KOH at room temperature [29a,36]. The $C_5Ph_5^\bullet$ radical (**4**) was only the second cyclopentadienyl radical to be structurally characterized [23aa].

1.5. Reactions of C_5Ph_5X derivatives

Few reactions of coordinated C_5Ar_5 ligands have been explored [5,91]. Some of the reactions of C_5Ph_5X derivatives that may be of relevance to reactions of the coordinated ligand are collected in the following sub-sections.

1.5.1. Reactions with dioxygen

C_5Ph_5H (**1**) reacts photochemically with dioxygen in the presence of a sensitizer such as methylene blue to produce an isolable *endo*-peroxide, which can be thermally or photochemically rearranged to the *bis*epoxide in 70% yield. The *bis*epoxide can be reduced to C_5Ph_5H (**1**) with zinc [92].

1.5.2. Reactions with phosphites

In methylene chloride, C_5Ph_5Br (**3**) reacts with triethylphosphite at room temperature to produce 1-ethyl-1,2,3,4,5-pentaphenylcyclopenta-2,4-diene (**43**) in 57% yield (Scheme 27); triphenylphosphine does not react in this fashion [15].

1.5.3. Diels–Alder condensations

Hexaphenylbenzene can be produced by Diels–Alder condensation of diphenylacetylene with tetracyclone (**20**), followed by elimination of CO [36].

1.6. Syntheses of tetra-arylcyclopentadienones

Cyclopentadienes substituted with different groups at positions 2, 3, 4 and 5 can be synthesized by initial formation of the appropriate aryl-substituted tetracyclones. The early liter-

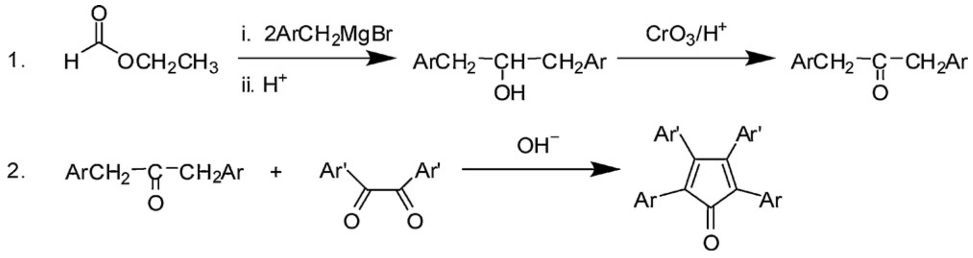

Scheme 28.

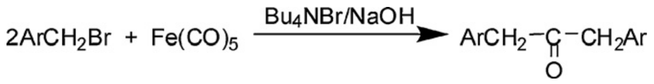

$$2ArCH_2Br + Fe(CO)_5 \xrightarrow{Bu_4NBr/NaOH} ArCH_2-\underset{\displaystyle O}{\overset{}{\underset{\|}{C}}}-CH_2Ar$$

Scheme 29.

ature detailing the chemistry of cyclopentadienones has been reviewed [93]. A most convenient route to tetracyclones is by base-catalyzed condensation of disubstituted benzyl and disubstituted 1,3-diphenylacetone in absolute alcohol [90b,c,94]. The requisite diphenylacetone derivatives can be prepared by chromic acid oxidations of the corresponding alcohols which are available from the condensation of the appropriately substituted benzyl Grignard reagent with ethyl formate (Scheme 28) [95]. Substituted tetracyclones formed in this way can be converted from the alcohol and bromide to the substituted penta-arylcyclopentadiene.

Although the method works well in general, it can be complicated by a lack of selectivity in the synthesis of the dibenzylketones from the Grignard and ethyl formate, and has been reported to give poor yields in some cases.

The substituted dibenzylketones are more conveniently prepared by the phase-transfer catalyzed reaction between the aryl halide and $[Fe(CO)_5]$ (Scheme 29) [96]. The reaction is performed between immiscible aqueous and benzene phases with a tetrabutylammonium salt acting as the phase-transfer catalyst.

High yields of the substituted dibenzylketones are possible by this route, which can be extended to the syntheses of mixed ketones [96]. The base condensation to the substituted tetracyclone is routine and can be performed in high yield. This is the route of choice to penta(*p*-tolyl)cyclopentadiene derivatives [18,97].

1.7. Aryl-substituted pentaphenylcyclopentadiene derivatives

A wide variety of tetracyclone derivatives are available by a range of synthetic methods as discussed previously [91,93,98]. These include derivatives with halo-, carboxylato-, and amino-substituents on the phenyl rings, and with phenyl rings substituted in *ortho*, *meta* and *para* positions. Bridged *bis*tetracyclones have also been reported in reasonable yield, and some of these bridged derivatives have been converted to the corresponding bromides and bridged *bis*pentaphenylcyclopentadienes in acceptable yields, as in, for example, Scheme 30 [99].

Few of these derivatives have been utilized in the context of coordination or organometallic chemistry, but the scope of such applications is considerable [18,91,97].

2. Metal chemistry

2.1. Complexes of Group 2

Attempts at alkaline earth penta-arylcyclopentadienyl complexes have been sporadic [100], and the general insolubility of C_5Ph_5 complexes has hindered the isolation of species such as $[M(C_5Ph_5)_2]$ (M = Mg, Ca, *etc.*). In an extension to the ytterbium chemistry briefly discussed in Section 1.1.2.4, $[Ca(\eta^5\text{-}C_5Ph_5)_2]$ (**44**) may be isolated from the solvent-separated ion-pair, $[Ca(THF)_6][C_5Ph_5]_2$, by addition of toluene, and the amorphous solid was characterized by MALDI-TOF mass spectroscopy in an inert C_{60}/C_{70} matrix. $[Ba(\eta^5\text{-}C_5Ph_5)_2]$ (**45**) has also been accessed by this route, and this material has been structurally characterized [38b]. Significantly, the Ba–(C_5-ring centroid) distance of 2.670 Å was 0.1 Å less than that of comparable Ba sandwich compounds, and the bond shortening was attributed to non-classical C–H. . .C(π) interactions between interplanar *ortho*-C–H bonds and the *ortho*-phenyl carbon atom on the adjoining ring. As with the alkali-metal derivatives [39,41], problems of solubility may be overcome by use of penta-arylcyclopentadienes with solubilizing groups incorporated on the aryl rings. The alkaline-earth series $[M\{C_5(4\text{-}Bu^nC_6H_4)_5\}_2]$ (M = Ca (**46**), Sr (**47**), Ba (**48**)) is isolated in straightforward fashion, by σ-bond metathesis between the appropriate alkaline-earth dibenzyl derivative and varying equivalents of C_5Ar_5H (Ar = 4-$Bu^nC_6H_4$ (**11**)) [101]. All of these materials are soluble in the least polar solvents, such as pentane and hexanes, and structural characterization has been performed, with the structure of $[Ba\{C_5(4\text{-}Bu^nC_6H_4)_5\}_2]$ (**48**), shown in Fig. 16 as a representative. The structure of $[Sr\{C_5(4\text{-}Bu^nC_6H_4)_5\}_2]$ (**47**), is isomorphous. Group 2 metallocenes, and likewise sandwich compounds of bivalent *f*-element metals, in general are known to present equivocal structures that are hard to rationalize even with resort to theoretical treatment [102], and the simplest such metallocene, $Be(C_5H_5)_2$, has been structurally characterized as a η^5/η^1 non-sandwich structure [103]. Heavier Group 2 metallocenes show distinctly bent geometries [102a,104], and by way of example the $[M\{\eta^5\text{-}1,2,4\text{-}(Me_3Si)_3C_5H_2\}_2]$ (M = Ca, Sr, Ba) series has pronounced bent geometry (∠(C_5-ring centroid)–M–(C_5-ring centroid), M = Ba 162.2°, Sr 159.4°, Ca 166.7°), and long M–(C_5-ring centroid) distances (M = Ba 3.01(2) Å, Sr 2.812(9) Å, Ca 2.63(2) Å) [102b].

In striking contrast, the $[M\{C_5(4\text{-}Bu^nC_6H_4)_5\}_2]$ (M = Ca (**46**), Sr (**47**), Ba (**48**)) series displays (i) the perfect S_{10} molecular symmetry of the sandwich structures in the solid state, (ii) relatively short M–(C_5-ring centroid) distances (M–(C_5-ring centroid) M = Ba 2.667(1) Å, Sr 2.513(1) Å, Ca 2.3561(4) Å), (iii) the perceptible out of plane bending of the aryl substituents on alternate ligands *towards* or away from each other depending on the transannular distance, and (iv) short distances between the *ortho*-aryl hydrogen atoms and the *ortho*-aryl carbons on the alternate ring. Such structural features, which are also observed in part in transition metal and main-group metal decaphenylmetallocene species, $[M(\eta^5\text{-}C_5Ph_5)_2]$ (M = Mo (**23**), W (**24**), Sn (**235**)), have been interpreted as a result of attractive C–H. . .C(π) interactions, which operate between the *ortho*-aryl hydrogen atoms and the *ortho*-aryl carbons of the aryl substituents on alternate cyclopentadienyl planes. That bulky hydrocarbyl substituents on the cyclopentadienyl rings would bend out of plane (*i.e.* $\alpha > 0°$, Fig. 16) is a facile expectation for such bulky sandwich complexes, and in fact values of α exceed 5° for $[Ba(C_5Pr^i_5)_2]$ (Ba–(C_5-ring centroid) = 2.748(2) Å) [37b], which presents another example of a linear metallocene. In fact, the aryl substituents of this alkaline-earth series (**46**–**48**) bend in towards each other ($-\alpha$ = 5.3(2), 3.4(2), and 1.2(1)° for $[M\{\eta^5\text{-}C_5(4\text{-}Bu^nC_6H_4)_5\}_2]$, M = Ba (**48**), Sr (**47**), Ca (**46**), respectively), facilitated by the $H(\delta^+)$–$C(\delta^-)$ interaction that propagates through the interwoven aryl network between the cyclopentadienyl planes; inward bending is rendered all the more noteworthy in that the M–(C_5-ring centroid) distance is significantly shorter for the penta-arylcyclopentadienyl derivatives with respect to comparable, bulky sandwich complexes [101a]. The values of α correlate linearly with the size of the M–(C_5-ring centroid) distance, and the smaller metal centres exhibit *outward* bending from the cyclopentadienyl plane [101a]. For $[Ba\{\eta^5\text{-}C_5(4\text{-}Bu^nC_6H_4)_5\}_2]$ (**48**), this interaction results in interplanar *ortho*-aryl-H-*ortho*-C(π) distances of 2.74–2.89 Å, which is smaller than the sum of the van der Waals radii for carbon and hydrogen (2.90 Å); even smaller interplanar distances are observed for homologous $[Sr\{\eta^5\text{-}C_5(4\text{-}Bu^nC_6H_4)_5\}_2]$ (**47**), and $[Ca\{\eta^5\text{-}C_5(4\text{-}Bu^nC_6H_4)_5\}_2]$ (**46**), and sandwich complexes of the transition and main-group metals. Whilst individual C–H. . .C(π) contacts are energetically trifling (8–21 kJ), the fact that the S_{10} molecular symmetry allows for ten such contacts strongly argues that this geometry is preferred on this basis, whereas the alternative D_5 symmetry for the sandwich structure, in which the aryl substituents of both cyclopentadienyl planes are canted at the same angle, and would therefore give rise to a pair of enan-

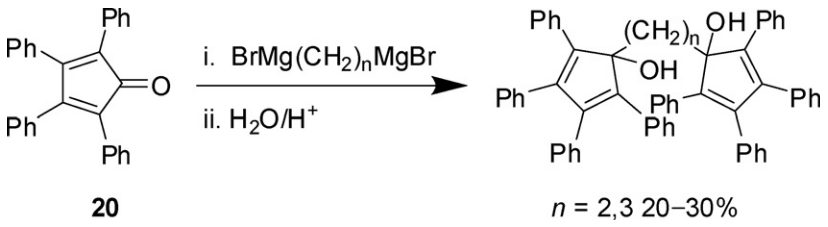

Scheme 30.

tiomers, cannot support interaction of the same type [41,43,101a]. This is arguably the reason why all known sandwich complexes of penta-arylcyclopentadienyl ligands across the periodic table, including their metallocenium cations, $[M(C_5Ar_5)_2]^+$, adopt S_{10} molecular symmetry, and that sandwich complexes incorporating the penta-arylcyclopentadienyl rings are more closely bound to the cyclopentadienyl core with respect to the metal centre than in similarly bulky, non-arylated cyclopentadienyl ligands.

2.2. Complexes of Group 4

2.2.1. Titanium complexes

The synthesis of red-violet $[M(C_5Ph_5)_2Cl_2]$ (M = Ti (**49**), Zr (**50**)) in 27% (**49**) or 40% (**50**) yields (Scheme 31) was reported without characterization data in 1983 [45a,105].

The titanium complex was obtainable in 70% yield as the extremely hygroscopic $[Ti(C_5Ph_5)_2Cl_2]\cdot 3H_2O$ (**49**$\cdot 3H_2O$), the synthesis of which was confirmed by the preparation of the analytically pure yellow crystalline silsesquioxane derivative, $[Ti(\eta^5\text{-}C_5Ph_5)\{Si_7O_{12}(C_6H_{11})_7\}]$ (**51**, Scheme 32) [106]. $[Ti(C_5Ph_5)_2Cl_2]\cdot 3H_2O$ (**49**$\cdot 3H_2O$) undergoes a reversible one-electron reduction at −0.78 V and a quasi-reversible reduction at −2.47 V (both *vs.* $Fc^{+/0}$), with the one-electron reduction product, $[Ti(C_5Ph_5)_2Cl_2]^-$ being relatively stable on the cyclic voltammetric time-scale. The *tris-iso*propoxide analogue of $[Ti(\eta^5\text{-}C_5Ph_5)(Si_7O_{12}(C_6H_{11})_7)]$ (**51**), crystalline $[Ti(\eta^5\text{-}C_5Ph_5)(OPr^i)_3]$ (**52**), is produced in 67% yield by the reaction of $[TiCl(OPr^i)_3]$ with NaC_5Ph_5 (**39**) under nitrogen. Yellow $[Ti(\eta^5\text{-}C_5Ph_5)(OPr^i)_3]$ (**52**) is quantitatively converted to air-stable, purple $[Ti(\eta^5\text{-}C_5Ph_5)Cl_3]$ (**53**) by reaction with gaseous HCl in toluene at reflux under nitrogen (Scheme 33) [107].

The mixed-ligand species, pentaphenylcyclopentadienyltitanocene dichloride, $[Ti(\eta^5\text{-}C_5Ph_5)(\eta^5\text{-}C_5H_5)Cl_2]$ (**54**), is obtained as a brown crystalline solid in 60% yield by the reaction of $[KC_5Ph_5]$ (**55**) and $[Ti(C_5H_5)Cl_3]$ at room temperature [23n]. In the solid state, the planes of the two C_5 rings are at 131° with respect to each other, and the phenyl rings are canted at between 41° and 65° to the C_5 ring (Fig. 17). The $C_5Ph_5^-$ ring centroid is significantly farther (2.22 Å) from the titanium atom than is the corresponding centroid on the $C_5H_5^-$ ligand (2.07 Å).

2.2.2. Zirconium complexes

In contrast to the 1983 report of red-orange $[Zr(C_5Ph_5)_2Cl_2]$ (**50**, Scheme 31) [45a,105], the reaction of $ZrCl_4$ with LiC_5Ph_5 (**28**) in toluene at reflux produces analytically pure, yellow, crystalline $[Zr(C_5Ph_5)Cl_3]$ (**56**) in 88% yield (Scheme 34). The formulation of the solid has been confirmed crystallographically (Fig. 18). Subsequent reaction with LiC_5H_5 (**28**) at room temperature generates pale-yellow crystals of the diamagnetic sandwich, $[Zr(\eta^5\text{-}C_5Ph_5)(\eta^5\text{-}C_5H_5)Cl_2]$ (**57**) in 95% yield. The “bent” structure of pentaphenylcyclopentadienyl zirconocenedichloride has been confirmed crystallographically (Fig. 19) [23ah].

The steric demands of the pentaphenylcyclopentadienyl ligand may stabilize the monomeric piano-stool structure of $[Zr(C_5Ph_5)Cl_3]$ (**56**) against the oligomerization commonly observed in less bulky $[Zr(C_5R_5)Cl_3]$ derivatives. Perhaps significantly, the $C_5Ph_5^-$ ligand is about 0.1 Å closer to the zirconium in the 12-electron trichloride (Zr–(C_5-ring centroid) = 2.222 Å), than in the 16-electron pentaphenylzirconocene dichloride (Zr–(C_5Ph_5-ring centroid) = 2.302(5); Zr–(C_5H_5-ring centroid) = 2.211 Å). Normals from the planes of the two carbocycles bound to the zirconium centre intersect at 133°, similar to the correspond-

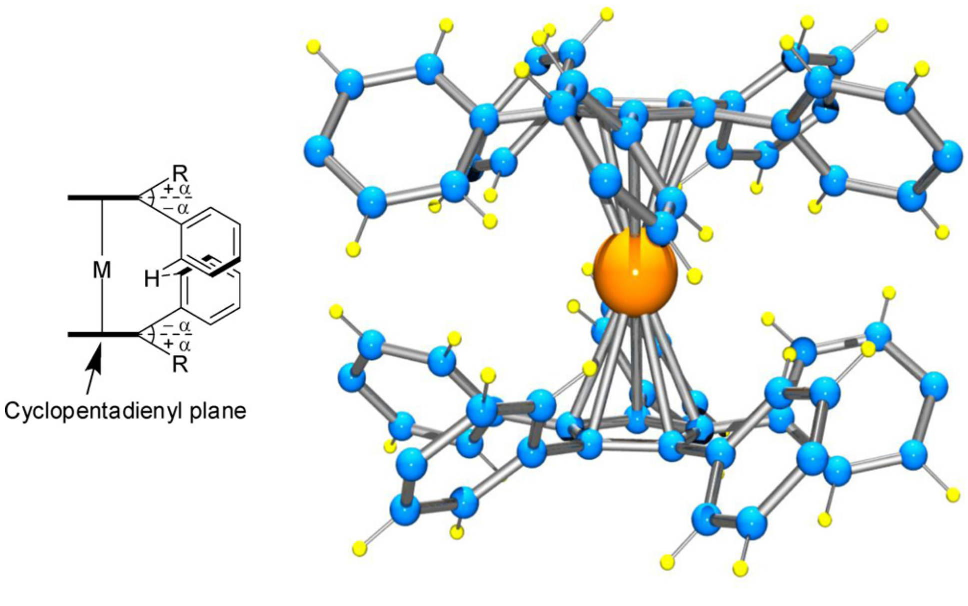

Fig. 16. Structure of $[Ba\{\eta^5\text{-}C_5(4\text{-}Bu^nC_6H_4)_5\}_2]$ (**48**), with Bu^n groups removed for clarity; legend defines parameters used in the text [101].

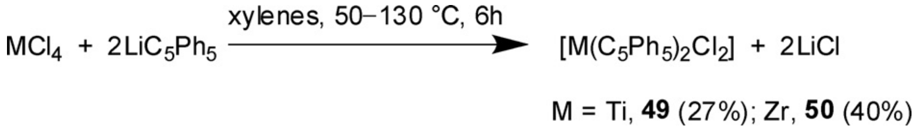

$$MCl_4 + 2LiC_5Ph_5 \xrightarrow{\text{xylenes, 50–130 °C, 6h}} [M(C_5Ph_5)_2Cl_2] + 2LiCl$$

M = Ti, **49** (27%); Zr, **50** (40%)

Scheme 31.

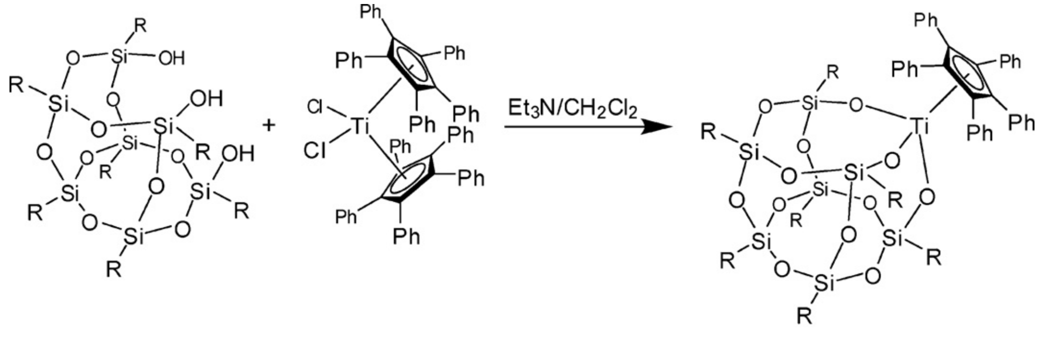

49 R = cyclohexyl **51**

Scheme 32.

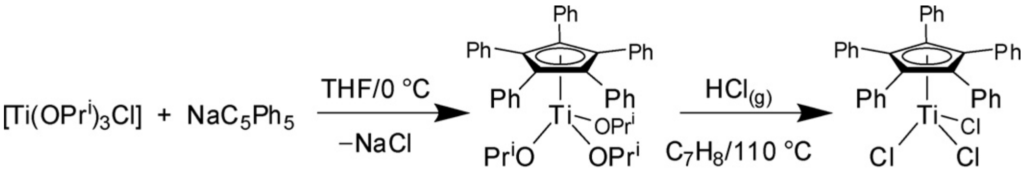

39 **52** **53**

Scheme 33.

ing angle in [Ti(C_5Ph_5)(C_5H_5)Cl_2] (**54**). The zirconium complexes were prepared because of their potential as stereoselective catalysts for [4+2] cycloadditions. Pentaphenylcyclopentadienyl zirconium trichloride (**56**) catalyzes the addition of acrolein or of methyl acrylate to cyclopentadiene with significantly different *endo*:*exo* selectivities to those of the control reaction [23as].

2.3. Complexes of Group 5

No compounds of vanadium, niobium, nor tantalum have been reported.

2.4. Complexes of Group 6

2.4.1. Chromium complexes

Chromium compounds of $C_5Ph_5^-$ have been isolated in oxidation states 0, I, II and III. A feature of chromium pentaphenylcyclopentadienyl chemistry is the number of stable, monomeric radical species reported. Decaphenylchromocene (**58**) is prepared in 12% yield as an insoluble, purple, air-stable solid by the addition of C_5Ph_5Br (**3**) and zinc dust to [Cr$(CO)_3$(N≡CMe)$_3$] in THF [23w]. It is oxidized by either bromine or nitrosonium tetrafluoroborate to produce [Cr$(C_5Ph_5)_2$]X (X = Br_3^- (**59**), BF_4^- (**60**)) as an air-stable red-brown crystalline solid in high (~80%) yield [23w,z]. The stability of [Cr$(C_5Ph_5)_2$] (**58**) and [Cr$(C_5Ph_5)_2$]X (**59**–**60**) contrasts markedly with the high reactivity of chromocene and the chromocenium cation. Solid [Cr$(C_5Ph_5)_2$]X has parallel, staggered C_5 rings, and idealized S_{10} molecular symmetry, with phenyl groups canted at approximately 50° to the C_5 core (Fig. 20, Cr–(C_5-ring centroid) = 1.836(8) Å).

Decaphenylchromocene (**58**) undergoes a reversible, one-electron oxidation at −0.95 V (*vs.* $Fc^{+/0}$). This is almost identical to the potential of the [Cr$(C_5H_5)_2$]$^{+/0}$ couple (Table 2).

Chromium hexacarbonyl reacts with MC_5Ph_5 (M = Na (**39**), Li (**28**)) in diglyme to give good yields of bright yellow salts of the [Cr(C_5Ph_5)$(CO)_3$]$^-$ anion [23p,45a,105], which can be oxidized chemically (64% yield) or electrochemically (quasi-reversible, one-electron, −0.69 V *vs.* $Fc^{+/0}$ in methylene chloride) to the paramagnetic, deep blue-green, thermally stable [Cr(C_5Ph_5)$(CO)_3$]$^\bullet$ (**61**, Scheme 35) [23p]. The radical is irreversibly oxidized at ~0.9 V (100 mV s^{-1}) [23x].

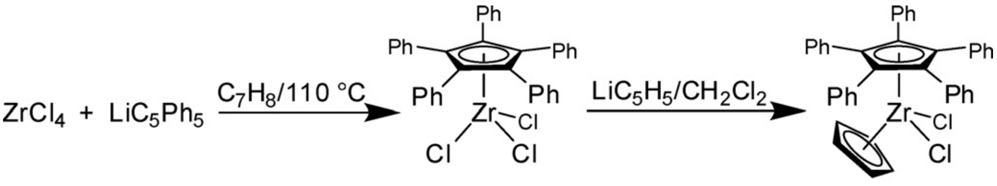

56 **57**

Scheme 34.

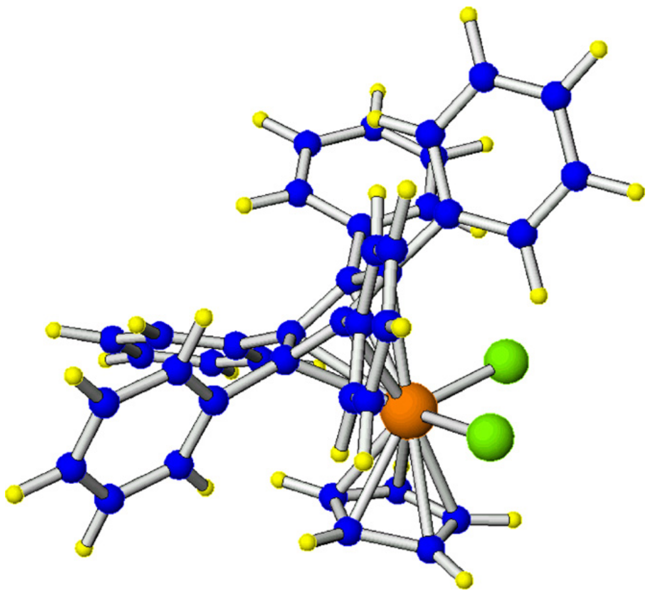

Fig. 17. Structure of [Ti(η^5-C_5Ph_5)(η^5-C_5H_5)Cl_2] (**54**) [23n].

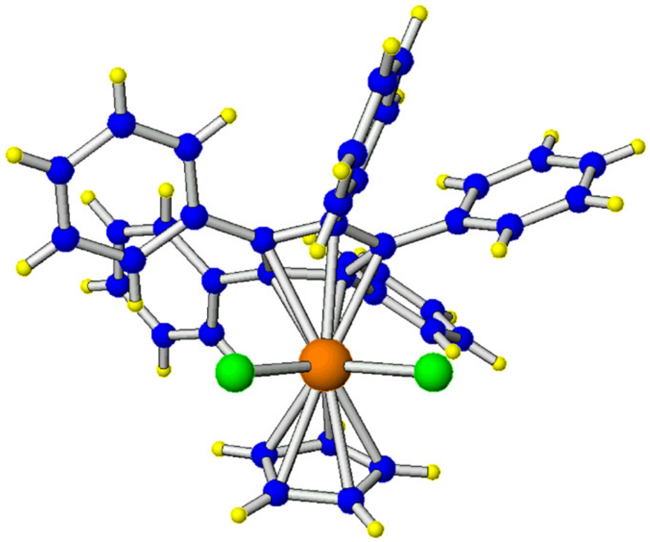

Fig. 19. Structure of [Zr(η^5-C_5Ph_5)(η^5-C_5H_5)Cl_2] (**57**) [23ah].

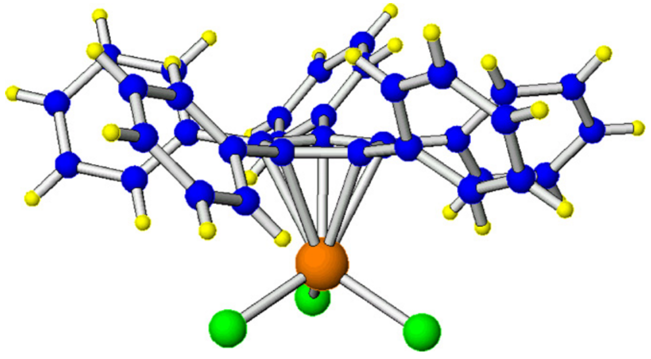

Fig. 18. Structure of [Zr(η^5-C_5Ph_5)Cl_3] (**56**) [23ah].

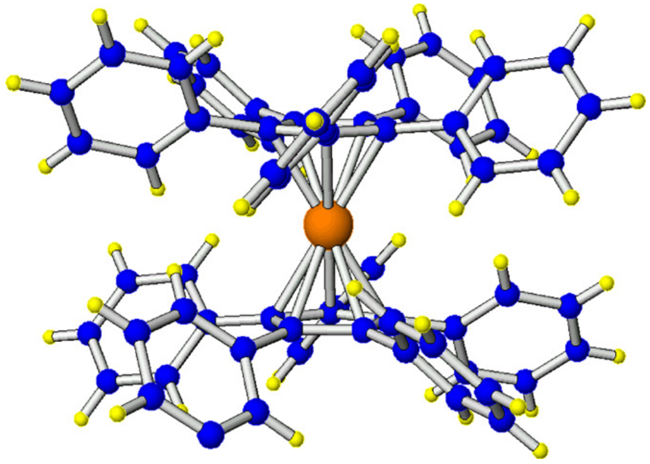

Fig. 20. Structure of the [Cr(η^5-C_5Ph_5)$_2$]$^+$ cation in [Cr(η^5-C_5Ph_5)$_2$]X (X = Br_3^- (**59**), BF_4^- (**60**)) [23z].

Table 2

Cyclic voltammetric half wave potentials (V *vs.* $Fc^{+/0}$ as zero) for +/0 redox couples of [M(η^5-C_5Ph_5)$_2$]BF_4 complexes and their metallocene analogues.

M	[M(C_5H_5)$_2$][a]	[M(C_5Ph_5)$_2$]BF_4	Refs.[b]
Cr	−0.96	−0.95[d]	[23z]
Mo	"−1.57"[c]	−0.46[d]	[23ar]
W		−0.583[e]	[23ao]
Fe	0.00	−0.04[d]	[26]
Co	−1.25	−0.88[d]	[23z]
Ni	−0.50	−0.08[d]	[23w]

[a] [M(C_5H_5)$_2$] data from [108].

[b] References for [M(C_5Ph_5)$_2$] data.

[c] Estimated in Ref. [109].

[d] Measured in methylene chloride, scan rate 100 mV s^{-1}, glassy carbon working electrode, Ag/AgCl (3 M NaCl) reference electrode, 0.1 M tetrabutylammonium tetrafluoroborate, 100% *iR* compensation.

[e] Measured in methylene chloride, scan rate 100 mV s^{-1}, Pt working electrode, Ag/AgCl reference electrode, 0.1 M tetrabutylammonium hexafluorophosphate.

There is no evidence for any dimerization of the [Cr(C_5Ph_5)(CO)$_3$]$^\bullet$ (**61**) radical in the solid state (Fig. 21) or in solution. This behaviour contrasts markedly with those of other [Cr(C_5R_5)(CO)$_3$]$_2$ species, which, although they exhibit long Cr–Cr distances, are predominantly dimeric. Thus, for example, the cyclopentadienyl (R = H) and pentamethylcyclopentadienyl (R = Me) complexes are 10% and 90% dissociated in solution [110], respectively, although both are dimeric in the solid state. The behaviour of [Cr(C_5Ph_5)(CO)$_3$]$^\bullet$ (**61**) also contrasts with that of [Mo(C_5Ph_5)(CO)$_3$]$^\bullet$ (**62**), which, although significantly monomeric in solution, is dimeric in the solid state [111]. The chromium and molybdenum complexes illustrate the interplay of the steric bulk of the ligand and the size of the metal.

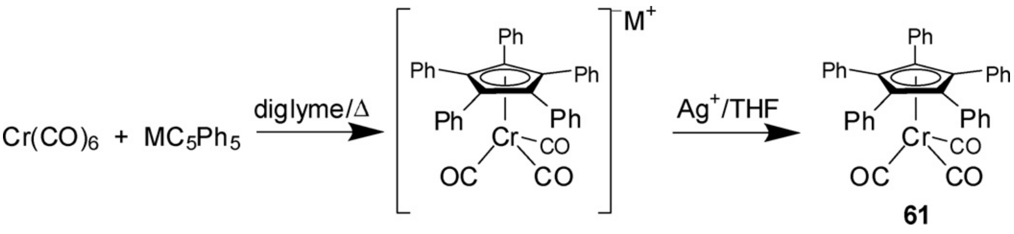

Scheme 35.

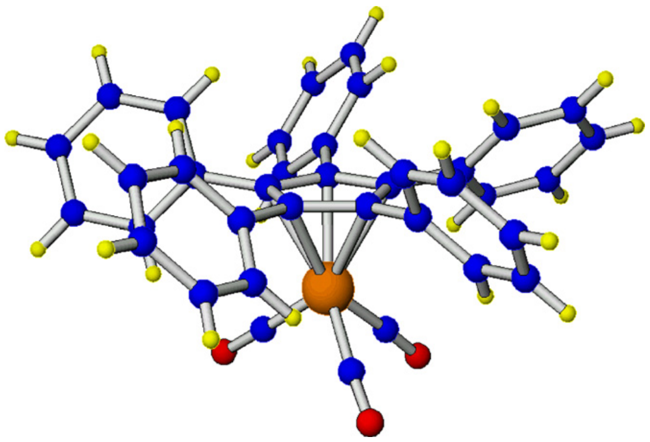

Fig. 21. Structure of $[Cr(C_5Ph_5)(CO)_3]^{\bullet}$ (**61**) [23p].

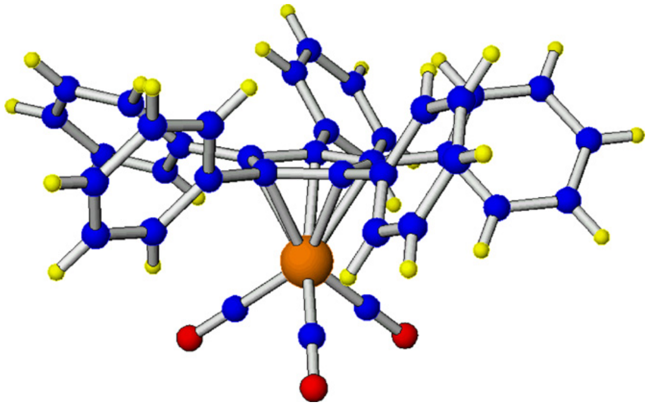

Fig. 22. Structure of $[Cr(C_5Ph_5)(CO)_3]^-$ (**63**) as its PPN$^+$ salt [23p].

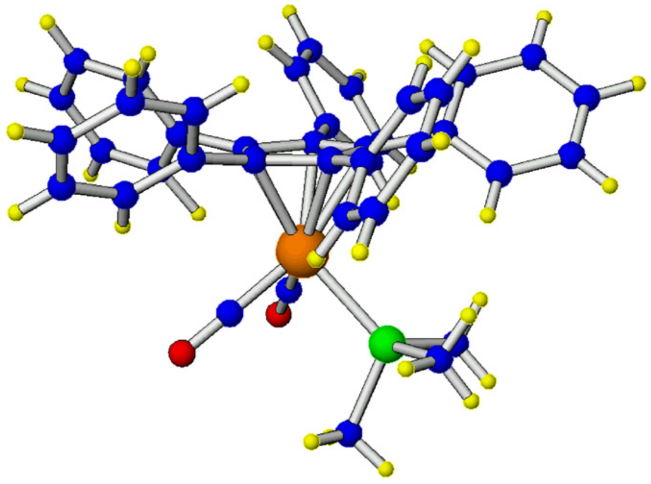

Fig. 23. Structure of $[Cr(C_5Ph_5)(CO)_2PMe_3]^{\bullet}$ (**64**) [23x].

A comparison between the structures of the anion $[Cr(C_5Ph_5)(CO)_3]^-$ (**63**) (Fig. 22, Cr–(C_5-ring centroid) = 1.867(1) Å) and the radical (**61**, Fig. 21, Cr–(C_5-ring centroid) = 1.860(3) Å), show that the significant changes on oxidation are a lengthening of the Cr–CO (but not the Cr-ring centroid) bond distances and a compression of two of the OC–Cr–CO angles, consistent with the existence of two near equi-energetic ground-state electronic configurations, a possibility also suggested by the frozen solution ESR spectra, which indicate a low-spin d^5 system. The symmetry lowering in these $[Cr(C_5Ph_5)(CO)_2L]^{\bullet}$ piano stool, radical species has been ascribed to Jahn–Teller effects and gives rise to very low energy ligand-field electronic transitions in the near- to mid-IR [112]. The radical (**61**) undergoes ready carbonyl monosubstitution by small, soft Lewis bases (*e.g.* PMe_3 or $P(OMe)_3$) to give dark red/magenta, air-sensitive compounds of the type $[Cr(C_5Ph_5)(CO)_2L]^{\bullet}$ (Scheme 36). The yields are near quantitative for small Lewis bases [23x].

The crystal structure of $[Cr(C_5Ph_5)(CO)_2PMe_3]^{\bullet}$ (**64**, Fig. 23, Cr–(C_5-ring centroid) = 1.881(3) Å) shows a similar compression of two of the OC–Cr–CO and OC–Cr–P angles to that observed in the tricarbonyl radical. Like the tricarbonyl radical, the $[Cr(C_5Ph_5)(CO)_2L]^{\bullet}$ complexes undergo reversible, one-electron reductions at between −1.26 and −1.56 V (*vs.* $Fc^{+/0}$ in methylene chloride), and also undergo an irreversible oxidation near 0 V (100 mV s^{-1}) [23x].

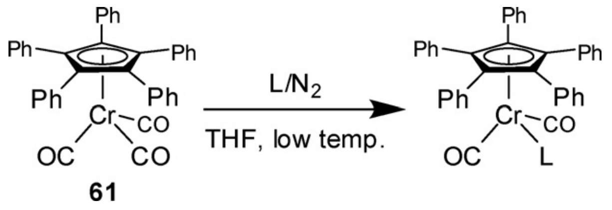

Scheme 36.

The radical, $[Cr(C_5Ph_5)(CO)_3]^{\bullet}$ (**61**), also reacts with halogens to give, initially, $[Cr(C_5Ph_5)(CO)_3X]$ complexes, which decompose (X = I (**65**), decomposition within days; X = Br (**66**), decomposition within minutes; X = Cl (**67**) decomposition within seconds) to the antiferromagnetically coupled, olive-green dimers, $[Cr(C_5Ph_5)X]_2(\mu\text{-}X)_2$, of which the chloride (**68**) has been crystallographically characterized (Fig. 24, Cr–(C_5-ring centroid) = 1.911(3) Å). The poorly soluble dimers are cleaved by THF to give more soluble $[Cr(C_5Ph_5)X_2(THF)]$ derivatives [23an].

$[Cr(C_5Ph_5)(CO)_3]^{\bullet}$ (**61**) is an effective chain transfer catalyst in the AIBN-initiated polymerization of methyl methacrylate [113]. Metallo-radical hydrides are believed to be key intermediates in these chain transfer catalytic reactions, in which they function to add H$^{\bullet}$ to monomers to start a new chain, rather than acting as hydrogenation catalysts. The light green hydride, $[Cr(C_5Ph_5)(CO)_3H]$ (**69**), has been isolated from the reaction of the

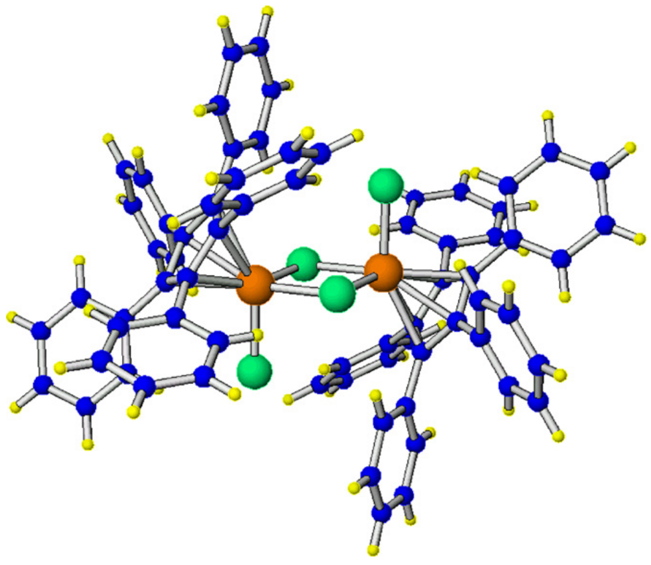

Fig. 24. Structure of $[Cr(C_5Ph_5)Cl]_2(\mu\text{-}Cl)_2$ (**68**) [23an].

$[Cr(C_5Ph_5)(CO)_3]^-$ (**63**) anion with HCl in ether at 0 °C [113a], and the hydride initiates methyl methacrylate polymerization, without hydrogenation of the monomer. Some competition between polymerization and hydrogenation has been observed with styrene as substrate [113]. This is reportedly the first isolable hydride that catalyzes chain transfer. In the ^1H NMR spectrum, the hydride resonates at $\delta\ ^1H\ -3.94$ ppm.

A combination of chromium(III) *tris*(2-ethylhexanoate), hexachloroethane, triethylaluminum, and C_5Ph_5H (**1**) catalyzes the trimerization and oligomerization of ethylene [113b,114]. Although catalysis occurs in the absence of C_5Ph_5H (**1**), the activity and selectivity with respect to trimers were both higher in the presence of added diene although it is not clear whether or how the C_5Ph_5H (**1**) was coordinated and/or deprotonated.

Chromium hexacarbonyl also reacts with C_5Ph_5H (**1**) in diglyme, to give zerovalent $[Cr\{(\eta^6\text{-}C_6H_5)C_4Ph_4H\}(CO)_3]$ (**70**) [45a,105].

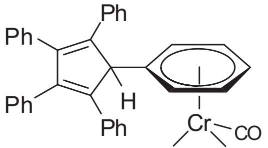

70

2.4.2. Molybdenum complexes

Molybdenum pentaphenylcyclopentadienyl complexes have been isolated in oxidation states 0, I, II and III. Decaphenylmolybdenocene (**23**) is a bright-red, air stable, paramagnetic solid first isolated in low yield by the reaction of $Mo(CO)_6$, $[Mo(diglyme)(CO)_3]$ or $[Mo(toluene)(CO)_3]$ with diphenylacetylene (Eqs. (8) and (9)) [4,63]:

$$[Mo(CO)_6] \text{ or } [Mo(CO)_3diglyme] + \text{excess } Ph-C \equiv C-Ph \xrightarrow[160\,^{\circ}C/C_6H_6]{16\,atm} \underset{\mathbf{23}}{[Mo(C_5Ph_5)_2]} \tag{8}$$

$$[Mo(CO)_3(toluene)] + [5Ph-C\equiv C-Ph \xrightarrow[98\,^{\circ}C/heptane]{1\,atm} \underset{\mathbf{23}}{[Mo(C_5Ph_5)_2]} \tag{9}$$

The reactions, with the initial product formulations, are depicted in Scheme 37.

Other products reported from these reactions are hexaphenyl-Dewar-benzene, the trinuclear complex, triangulo-trimolybdenumdicarbonyl-*bis*[μ-[1,1′-(η^2:η^2-1,2-ethynediyl)*bis*-[benzene]]*tris*[(1,2,3,4,5,6-η^6)-methylbenzene] (**71**) as shown below, and a yellow product, initially formulated as *bis*tetraphenylcyclobutadiene(diphenylacetylene)tetracarbonyldimolybdenum, $[Mo(CO)_2(C_4Ph_4)]_2(\mu\text{-}PhC{\equiv}CPh)_2$ (Scheme 37), but which was later structurally characterized as $[Mo_2(CO)_3(\eta^4\text{-}C_4Ph_4)](\mu\text{-}PhC{\equiv}CPh)(\mu\text{-}C_4Ph_4C(=O))$ (**72**), which contains a coordinated, bridging tetracyclone ligand (Fig. 25) [62].

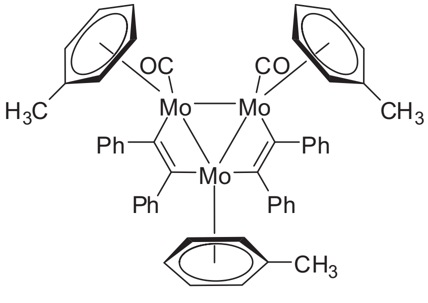

71

The identity of bright yellow $[Mo(\eta^4\text{-}C_4Ph_4)_2(CO)_2]$ was later confirmed by X-ray crystallography [61]. A violet compound, formulated as $[Mo(C_4Ph_4)(PhC{\equiv}CPh)(CO)]$, was produced in the reactions of diphenylacetylene with either $Mo(CO)_6$ or $[Mo(C_6H_5Me)(CO)_3]$ [4,63].

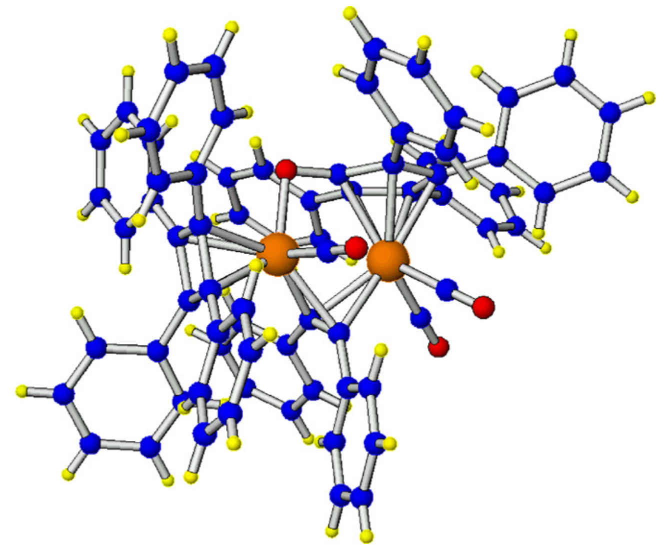

Fig. 25. Structure of $[Mo_2(\eta^4\text{-}C_4Ph_4)(CO)_3](\mu\text{-}PhC{\equiv}CPh)(\mu\text{-}C_4Ph_4C(=O))$ (**72**) [62,115].

Decaphenylmolybdenocene (**23**) can also be produced by the reaction of $[Mo(\eta^4\text{-}C_4Ph_4)(\eta^2\text{-}PhC{\equiv}CPh)_2(N{\equiv}CMe)]$ with diphenylacetylene (Scheme 38) [116].

Decaphenylmolybdenocene (**23**) is quantitatively converted to green, air-stable, crystalline $[Mo(C_5Ph_5)_2]^+$ salts by oxidation with halogens or $NOBF_4$. The $[Mo(C_5Ph_5)_2]^+$ cation is reduced reversibly to $[Mo(C_5Ph_5)_2]$ (**23**) by magnesium turnings or by $NaBH_4$ in a mixture of methanol and methylene chloride [4,23ao,ar].

Molybdenum hexacarbonyl reacts with LiC_5Ph_5 (**28**) in glyme at reflux or THF under nitrogen to give the yellow-brown $[Mo(C_5Ph_5)(CO)_3]^-$ anion (Scheme 38), which in turn reacts with CH_3I, PCl_3, PBr_3 or I_2 to give $[Mo(C_5Ph_5)(CO)_3X]$ (X = CH_3 (**73**), Cl (**74**, 14%), Br (**75**, 28%), I (**76**, 46%)), of which $[Mo(C_5Ph_5)(CO)_3I]$ (**76**) has been crystallographically characterized as the typical “four-legged piano stool” derivative (Fig. 26) [23y,45a,105].

Oxidation of the $[Mo(C_5Ph_5)(CO)_3]^-$ anion produces purple $[Mo(C_5Ph_5)(CO)_2]_2(\mu\text{-}CO)_2$ (**77**, 90% yield), which is much less air-sensitive in the solid state than in solution (Scheme 39) [111,117]. In solution, the dimer (**77**) exists in equilibrium with the radical monomer (**62**) [111,117]. Because of the very low solubility of the dimer, it cannot be recrystallized, and, although prepared as a relatively pure compound, the product often contains small amounts of the $C_5Ph_5^\bullet$ radical (**4**), which can be detected by ESR spectroscopy by its characteristic 33-line spectrum [111].

The dimer reacts thermally with chelating *bis*phosphines, P_2, to produce the 19-electron $[Mo(C_5Ph_5)(CO)_2(P_2)]$ (**78**), which exists in solution in equilibrium with the 17-electron complex with only one phosphorus of the P_2 species coordinated [111].

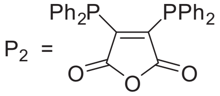

As noted above, the molybdenum chemistry, in which the dimer, $[Mo(C_5Ph_5)(CO)_2]_2(\mu\text{-}CO)_2$ (**77**), is the predominant $[M(C_5Ph_5)(CO)_3]$ species, contrasts with the chromium chemistry, in which the radical, $[Cr(C_5Ph_5)(CO)_3]^\bullet$ (**61**), is the predominant solution species.

The molybdenum arene complex, $[Fe(\eta^5\text{-}C_5H_5)\{\eta^5\text{-}C_5Ph_4(\eta^6\text{-}C_6H_5)Mo(CO)_3\}]$ (**79**), has been produced from the reaction of

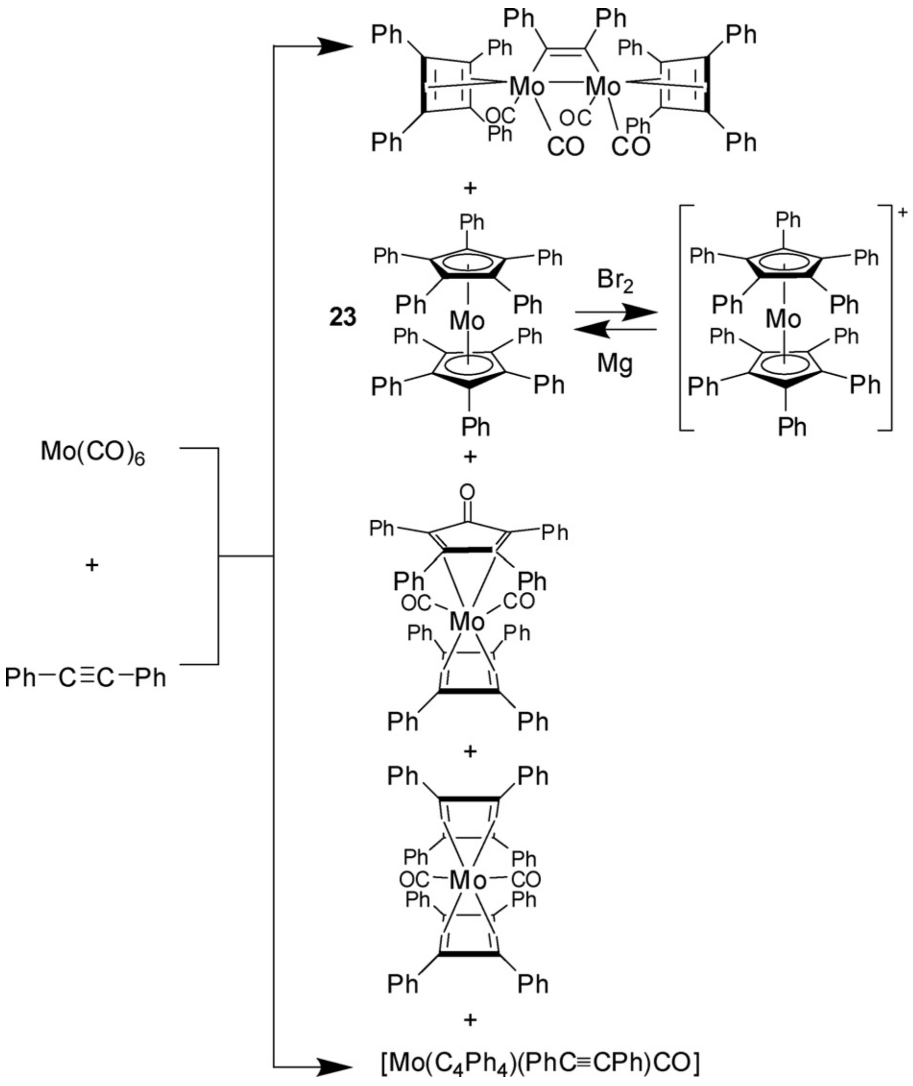

Scheme 37.

$[Fe(C_5Ph_5)(C_5H_5)]$ (**80**) with $[Mo(CO)_3(N{\equiv}CMe)_3]$ in DME at reflux [45a,105].

2.4.3. Tungsten complexes

Decaphenyltungstenocene (**24**) can be produced in 87% yield by thermolysis of the tungstenocyclic carbene, $[W(PhC{\equiv}CPh)(\eta^8\text{-}C_8Ph_8)]$, or in 30% yield by thermolysis of $[W(PhC{\equiv}CPh)_3(CO)]$ (Scheme 40) [17,23am,ao,118].

As are most other decaphenylmetallocenes, decaphenyltungstenocene is poorly soluble in most solvents. However, it can be oxidized by either I_2 or Ag^+ to the more soluble, structurally characterized, decaphenyltungstenocenium cation (**81**, Fig. 27), which can be reduced back to decaphenyltungstenocene (**24**) by cobaltocene. The metallocenium cation exhibits S_{10} molecular symmetry as anticipated, and the W–(C_5-ring centroid) distance (2.018(2) Å) correlates linearly with the out of plane bending angle of the

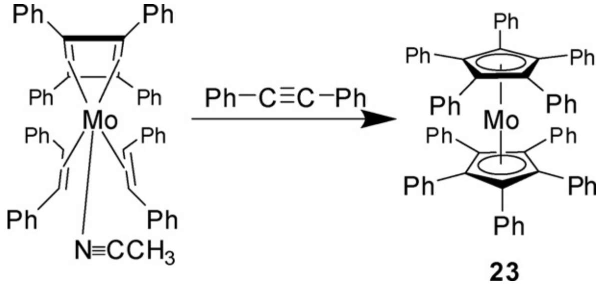

Scheme 38.

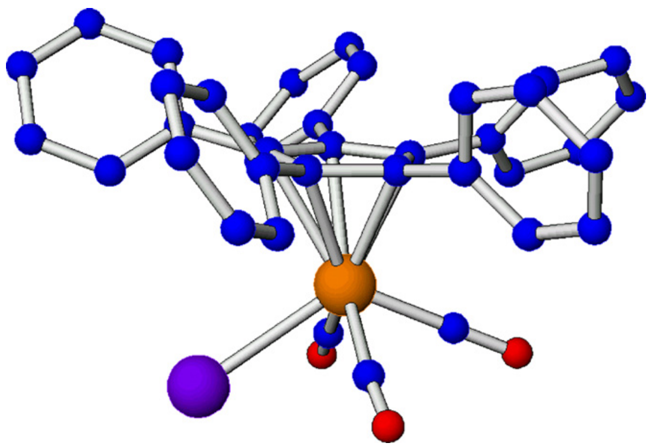

Fig. 26. Structure of $[Mo(C_5Ph_5)(CO)_3I]$ (**76**) (hydrogen atoms omitted); (Mo–(C_5-ring centroid) = 2.042(6) Å) [23y].

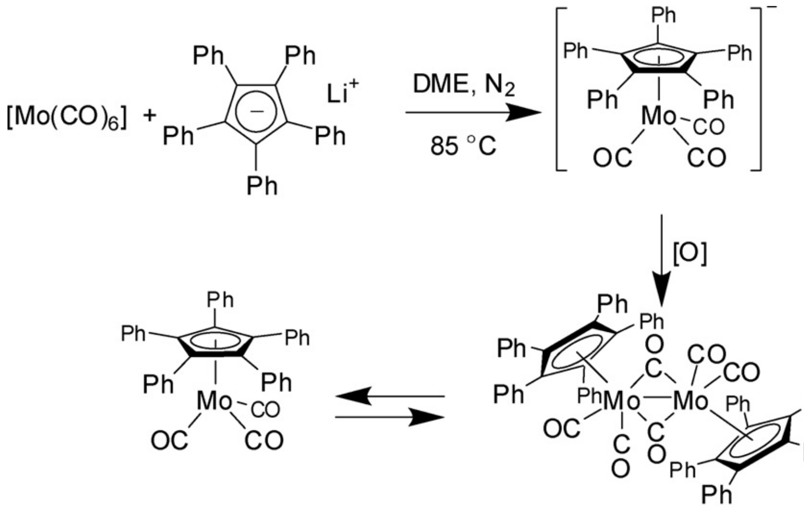

62 **77**

Scheme 39.

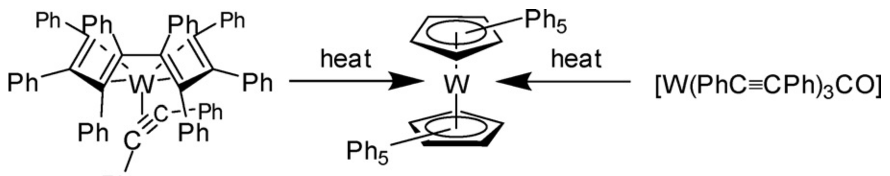

24

Scheme 40.

phenyl rings ($\alpha = 6.2°$); even for this third-row transition metal, the trans-annular distance is too short to enforce inward bending [101a].

Reaction of the decaphenyltungstacenium triiodide (**81**) with Ag^+ in water/methylene chloride results in oxidation of the tungsten and formation of air-stable, dark green $[W(=O)(C_5Ph_5)_2]$ (**82**) in 56% yield [17b]. The C_5 rings of the C_5Ph_5 ligands of solid $[W(=O)(C_5Ph_5)_2]$ (**82**) are not parallel, and the W–C bond lengths are not uniform. The binding of the ligand has accordingly been described as η^3-allyl/η^2-olefin, rather than the more common, *bis*(η^5)-cyclopentadienyl mode (Fig. 28). The central phenyl substituent of the allyl portion is eclipsed by the W=O bond.

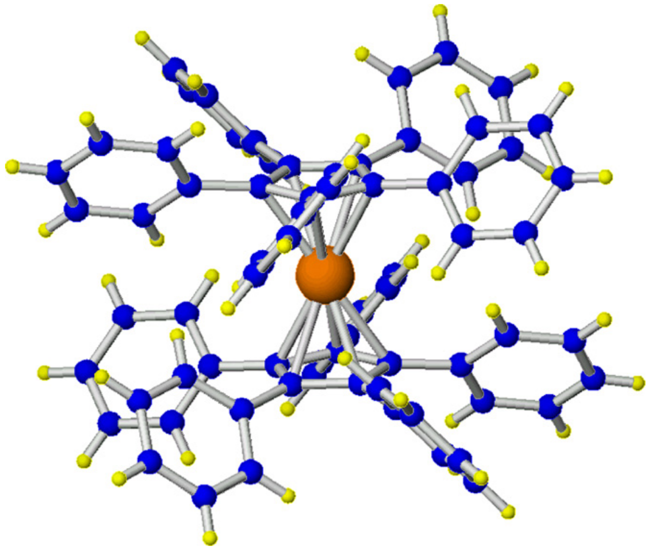

Fig. 27. Structure of the $[W(C_5Ph_5)_2]^+$ cation in $[W(C_5Ph_5)_2]I_3$ (**81**) [23am].

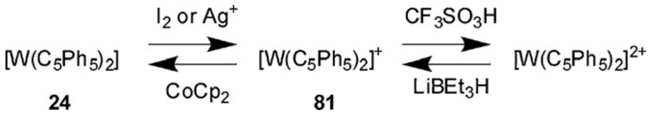

Scheme 41.

The decaphenyltungstenocenium cation (**81**) reacts with CF_3SO_3H to produce the decaphenyltungstenocenium dication (Scheme 41), which reacts with $LiBEt_3H$ to regenerate decaphenyltungstenocene (**24**).

Consistent with these reactions, $[W(C_5Ph_5)_2]^+$ (**81**) in methylene chloride/0.1 M TBHP exhibits a cyclic voltammetric oxidation at +53 mV,[3] a reversible, one-electron reduction at −583 mV, and a further, quasi-reversible reduction at −1890 mV (all *vs.* $Fc^{+/0}$). The existence of the formally $W(IV) \rightleftarrows W(III) \rightleftarrows W(II) \rightleftarrows W(I)$ electron transfer series is a reflection of the ability of the $C_5Ph_5^-$ ligand to stabilize multiple and unusual oxidation states. Decaphenyltungstenocene (**24**) obeys the Curie Law (Weiss constant 0) between 5 and 300 K, and the magnetic behaviour is interpreted in terms of an orbitally degenerate $^3E_{2g}$ ground state, similar to those postulated for the "unknown" tungstenocene [119]. The EPR spectrum of powdered $[W(C_5Ph_5)_2]$ (**24**) at 77 K contains absorptions assigned as $g_\parallel$ (1.91, 1.98) and $g_\perp$ (3.85). The reaction of decaphenyltungstenocene (**24**) with dihydrogen (5 atm) for 7 days produces slightly air sensitive, orange-yellow crystals of $[W(C_5Ph_5)_2H_2]$ (**83**, 73%), or orange $[W(C_5Ph_5)_2HCl]$ (**84**, 84%) in THF or 1,2-dichloroethane, respec-

---

[3] The scan rate, reversibility criteria, and the reversibility of the process at +53 mV are not reported.

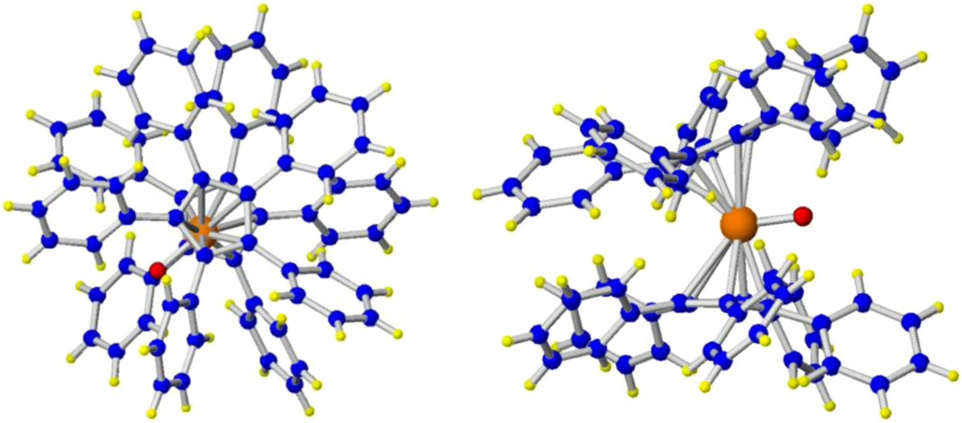

Fig. 28. Two views of the structure of [W(=O)(C_5Ph_5)$_2$] (**82**) [17b].

tively. The hydrochloride (**84**) is reasonably presumed to result from reaction of the dihydride (**83**) with chlorinated solvents (Eq. (10)) [23ao]:

$$\underset{\mathbf{83}}{[W(C_5Ph_5)H_2]}\xleftarrow[110\,^\circ C/THF]{H_2,\,5\,atm}\underset{\mathbf{24}}{[W(C_5Ph_5)_2]}\xrightarrow[110^\circ C/C_2H_4Cl_2]{H_2,\,5\,atm}\underset{\mathbf{84}}{[W(C_5Ph_5)(H)(Cl)]}\quad(10)$$

$$\underset{\mathbf{24}}{[W(C_5Ph_5)_2]}\xrightarrow[110\,^\circ C/C_2H_4Cl_2]{CO,\,5\,atm}\underset{\mathbf{85}}{[W(C_5Ph_5)(CO)]}\quad(11)$$

Pale yellow [W(C_5Ph_5)$_2$(CO)] (**85**) is obtained in 80% yield by heating decaphenyltungstenocene (**24**) under 5 atm of CO in 1,2-dichloroethane (Eq. (11)) [23ao].

Reaction of W(CO)$_6$ with LiC_5Ph_5 (**28**) in diglyme at reflux for 6 h generates the salt, Li[W(C_5Ph_5)(CO)$_3$] (**86**). The salt was not isolated, but reacts with PX_3 or I_2 to give [W(η^5-C_5Ph_5)(CO)$_3$X] in 3% (X = Cl, **87**), 19% (X = Br, **88**) or 37% (X = I, **89**) yields. All compounds were characterized by infrared (ν_{CO}), ^{1}H NMR and mass spectroscopy [23y].

The tungsten derivative of the penta-arylcyclopentadienyl ligand, C_5Ph_4(2,5-(MeO)$_2C_6H_3$)$^-$, [W{C_5Ph_4(2,5-(MeO)$_2C_6H_3$)}(CO)$_3$Br] (**90**), has been briefly reported [120]. It can be reduced coulometrically to the anion, [W{C_5Ph_4(2,5-(MeO)$_2C_6H_3$)}(CO)$_3$]$^-$, which can be quasi-reversibly oxidized to the radical, [W{C_5Ph_4(2,5-(MeO)$_2C_6H_3$)}(CO)$_3$]$^\bullet$, neither of which has been isolated. The molybdenum analogue, [Mo{C_5Ph_4(2,5-(MeO)$_2C_6H_3$)}(CO)$_3$Br] (**91**) behaved similarly.

2.5. Complexes of Group 7

2.5.1. Manganese complexes

The only manganese derivatives reported to date are [Mn(η^5-C_5Ar_5)(CO)$_3$] (Ar = Ph (**92**), *p*-tol (**93**)) and [Mn(η^5-C_5Ph_5)(CO)$_2$L] (L = PMe_2Ph (**94**), PBu_3 (**95**), C≡NBu^t (**96**)) [121]. Yellow crystals of [Mn(η^5-C_5Ar_5)(CO)$_3$] are prepared by the reaction of LiC_5Ph_5 (**28**) with Mn(I) sources such as any of [Mn(CO)$_3$(N≡CCH$_3$)$_3$]Br, [Mn(CO)$_5$Br] or [Mn(CO)$_3$(N≡CCH$_3$)$_2$Br]/Zn in THF at reflux, and react with donors such as phosphines or isonitriles, L, in the presence of Me_3NO to produce yellow crystalline [Mn(η^5-C_5Ph_5)(CO)$_2$L] (Scheme 42).

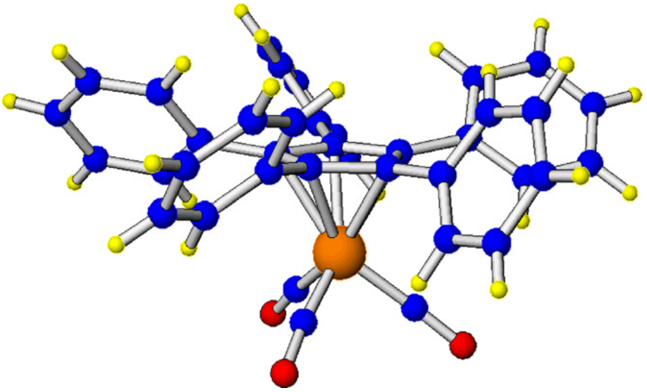

Fig. 29. Structure of [Mn(η^5-C_5Ph_5)(CO)$_3$] (**92**) [23ai,121].

The compounds, [Mn(η^5-C_5Ar_5)(CO)$_3$], undergo reversible, one-electron oxidations at +0.98 V and +0.89 V (*vs.* Fc$^{+/0}$, Eq. (12)). These potentials are significantly more positive than those measured in the oxidation of the analogous [Mn(η^5-C_5H_5)(CO)$_3$] [27a,28]:

$$[Mn(\eta^5\text{-}C_5Ar_5)(CO)_3] \rightleftarrows [Mn(\eta^5 - C_5Ar_5)(CO)_2]^+ + e^- \quad (12)$$

The structures of [Mn(η^5-C_5Ph_5)(CO)$_3$] (**92**) and [Mn(η^5-C_5Ph_5)(CO)$_2PMe_2Ph$] (**94**) (Figs. 29 and 30) illustrate the typical paddle wheel orientations of the C_5Ph_5 phenyl rings.

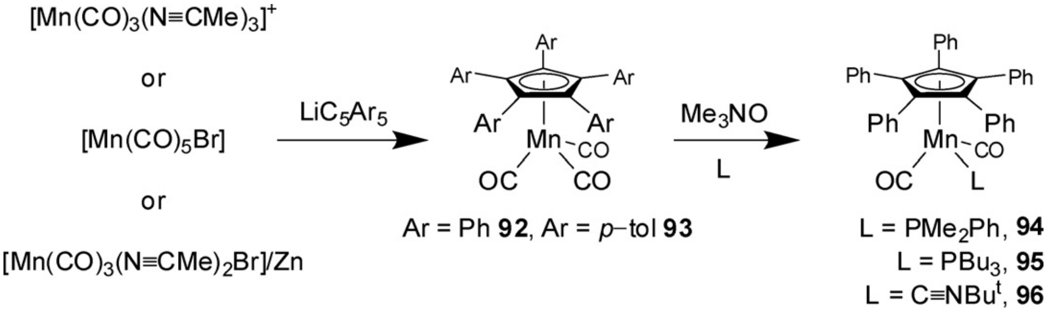

Scheme 42.

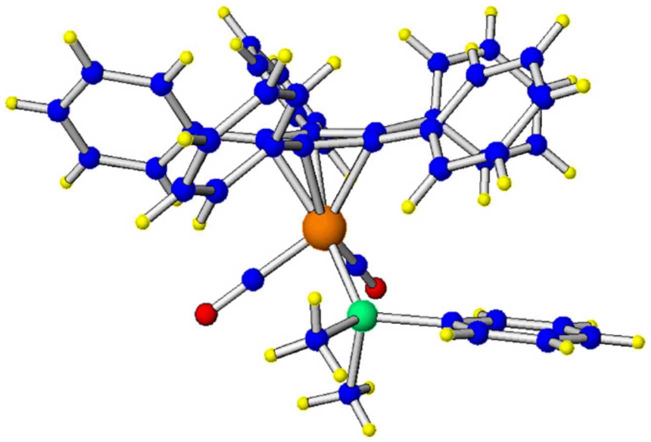

Fig. 30. Structure of [Mn(η^5-C_5Ph_5)$(CO)_2PMe_2Ph$] (**94**) [23ai,121].

However, whilst substitution of a carbonyl of [Mn(η^5-C_5R_5)$(CO)_3$] by a phosphine or isonitrile results in a decrease in the Mn–(C_5-ring centroid) distance on average [121], this distance has increased for [Mn(η^5-C_5Ph_5)$(CO)_2PMe_2Ph$] (**94**) (Fig. 30, Mn–(C_5-ring centroid) = 1.809 Å) relative to [Mn(η^5-C_5Ph_5)$(CO)_3$] (Mn–(C_5-ring centroid) 1.784 Å), and is significantly longer than in other [Mn(η^5-C_5R_5)$(CO)_2L$] compounds reported to date. This lengthening of the Mn–(C_5-ring centroid) bond is probably due to the minimization of steric interactions between the phenyl groups of the phosphine and $C_5Ph_5^-$ ligands, although there appears to be free rotation in solution. Similarly, the phenyl *ipso* carbons of [Mn(η^5-C_5Ph_5)$(CO)_3$] (**92**) are on average 0.161 Å (range 0.089–0.198 Å) from the C_5 plane, on the side opposite to the manganese atom; those of [Mn(η^5-C_5Ph_5)$(CO)_2PMe_2Ph$] (**94**) are 0.202 Å (range 0.162–0.268 Å) from the C_5 plane, with the greatest deviation from the plane observed for the *ipso* carbon of the ring that eclipses the PPh ring (Fig. 31).

2.5.2. Rhenium complexes

White, crystalline [Re(η^5-C_5Ph_5)$(CO)_3$] (**97**) was obtained in 72% yield by the thermolysis of tetracarbonyl(triphenylpropenetriyl)rhenium in hexanes at reflux (Scheme 43), and was characterized by infrared, ^1H and ^{13}C NMR, and mass spectroscopies. Mixed arene cyclopentadienyls can be produced by incorporating different substituents on the propenetriyl ligand and the alkyne [111,122].

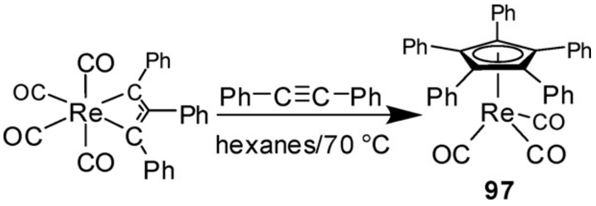

Scheme 43.

An alternative synthesis of [Re(C_5Ph_5)$(CO)_3$] (**97**) involves addition of MC_5Ph_5 to [Re$(CO)_5$Br] [123]. Irradiation of the cyclopentadienyl congener in heptane or pentane results in complexes of the type [Re(η^5-C_5H_5)$(CO)_2$(alkane)] [124]. The failure to isolate similar derivatives of the C_5R_5 (R = Me, Ph) complexes was attributed to destabilization due to interactions between the coordinated alkane and the C_5 ring substituents [123].

2.6. Complexes of Group 8

2.6.1. Iron complexes

[Fe$(CO)_5$] reacts directly with C_5Ph_5H at 175 °C to produce orange-yellow [Fe(η^4-C_5Ph_5H)$(CO)_3$] (**98**) in 6% yield. The complex was characterized spectroscopically (ν_{CO} 2037, 1972, 1961 cm^{-1}) and by elemental analysis [4]. Nevertheless, [Fe(η^5-C_5Ph_5)$(CO)_2$Br] (**99**), first reported in 1965 [125], and structurally characterized in 1989 (Fe-(C_5-ring centroid) = 1.738(5) Å) [23g], remains the centrepiece of iron penta-arylcyclopentadienyl chemistry. It is easily synthesized from Fe$(CO)_5$ and C_5Ph_5X in the presence of zinc (Scheme 44) [13].

The reaction also proceeds in the absence of zinc and has been exemplified for a series of halopenta-arylcyclopentadienes, C_5Ph_4ArBr, and $C_5(3,5\text{-}Me_2C_6H_3)_4ArBr$ (Ar = Ph, 3-MeC_6H_4, 3,5-$Me_2C_6H_3$, 2,3-$Me_2C_6H_3$, 2,4,6-$Me_3C_6H_2$, 3-C_6H_4F, 3,5-$C_6H_3F_2$, 2,6-$C_6H_3F_2$) [29b]. In this case, reaction occurs by a two-step process, which involves firstly, the reaction of the Fe$(CO)_5$ and C_5Ar_5X to generate the $C_5Ar_5^{\bullet}$ radical, which can be detected in the intensely purple solution by its characteristic multi-line ESR spectrum [29b]; this reaction occurs at 20 °C. The second step, which occurs at higher temperatures, is suggested to involve reaction between a $C_5Ar_5^{\bullet}$ radical and a bromoironcarbonyl intermediate, "[Fe$(CO)_n$Br]" identified by means of Fe–Br absorptions in the far IR spectrum [29b].

Simple reactions reported for complexes of this type are summarized in Schemes 45 and 47 [16,23l,o,w,ac,aq,34a,97,126]. The

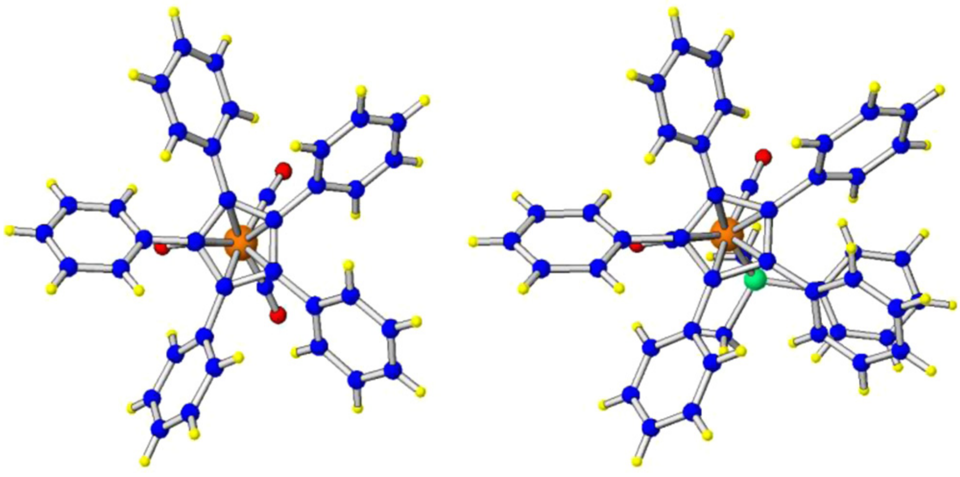

Fig. 31. Comparison of structures of [Mn(η^5-C_5Ph_5)$(CO)_3$] (**92**)) and [Mn(η^5-C_5Ph_5)$(CO)_2PMe_2Ph$] (**94**)).

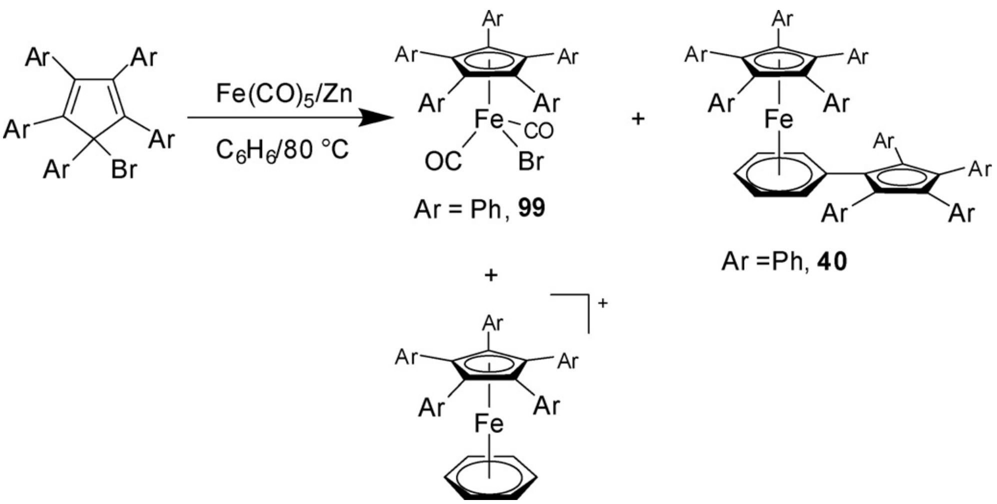

Scheme 44.

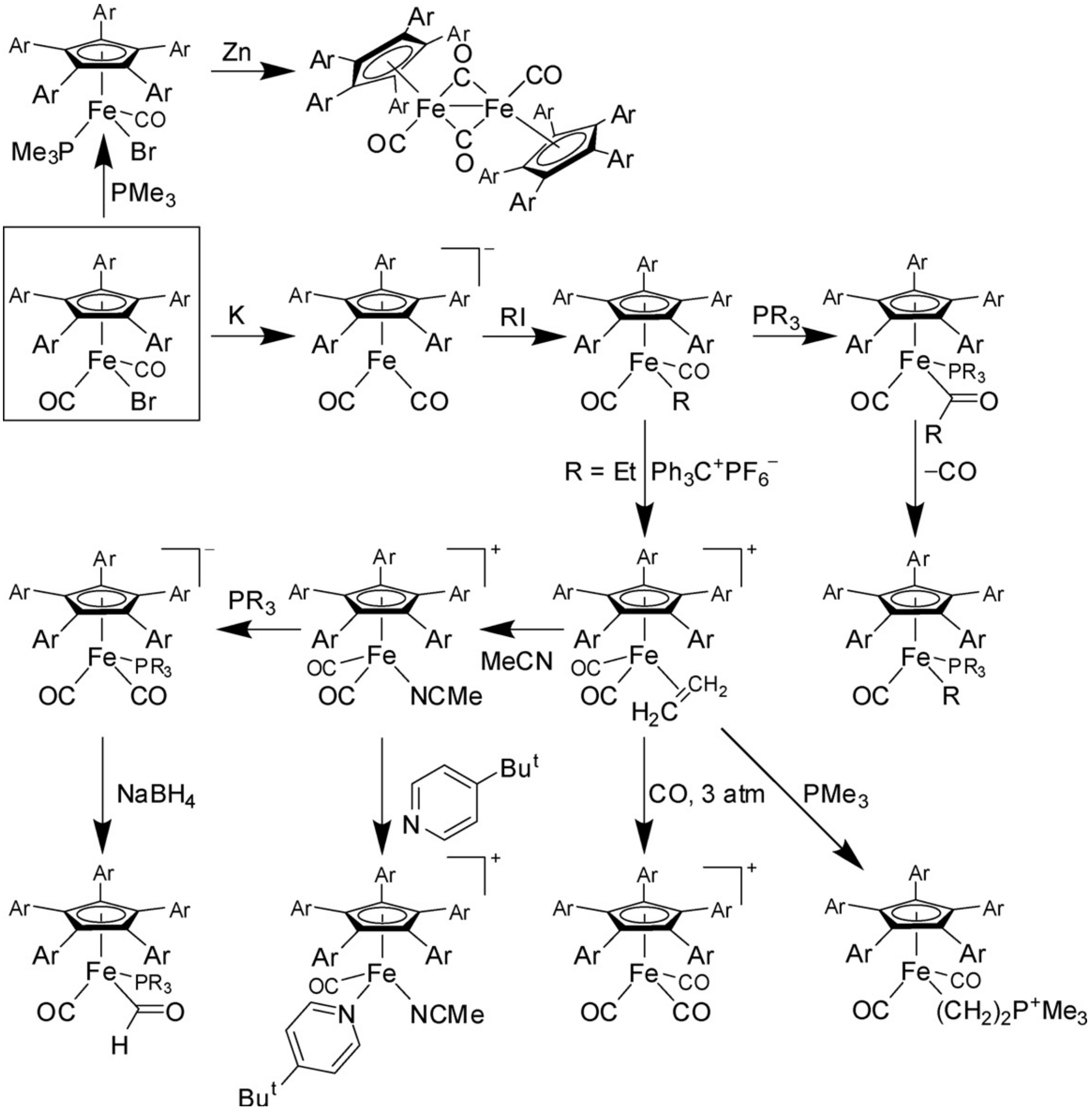

Scheme 45.

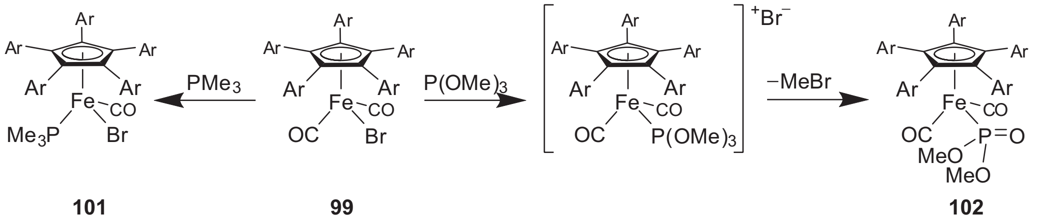

Scheme 46.

stability of the formyl complex, [Fe(η^5-C_5Ph_5)(CO){C(=O)H}PMe_3] (**100**) contrasts with the thermal instability of the $C_5Me_5^-$ congener, [Fe(η^5-C_5Me_5)(CO){C(=O)H}$PMePh_2$] [127].

Although [Fe(η^5-C_5Ph_5)$(CO)_2$Br] (**99**) reacts with PMe_3 to form [Fe(η^5-C_5Ph_5)(CO)(Br)PMe_3] (**101**) as illustrated in Scheme 45, the reaction with $P(OMe)_3$ is more complicated, producing [Fe(η^5-C_5Ph_5)$(CO)_2${P(=O)$(OMe)_2$}] (**102**), probably by an Arbusov-type dealkylation, resulting from attack of liberated Br^- on initially formed {[Fe(η^5-C_5Ph_5)$(CO)_2$$P(OMe)_3$]}$^+$ (Scheme 46) [23r].

A radical-promoted Arbusov reaction has been postulated in the case of phosphite reactions with [Fe(η^5-C_5Ar_5)$(CO)_2$]$_2$ (*vide infra*) [128].

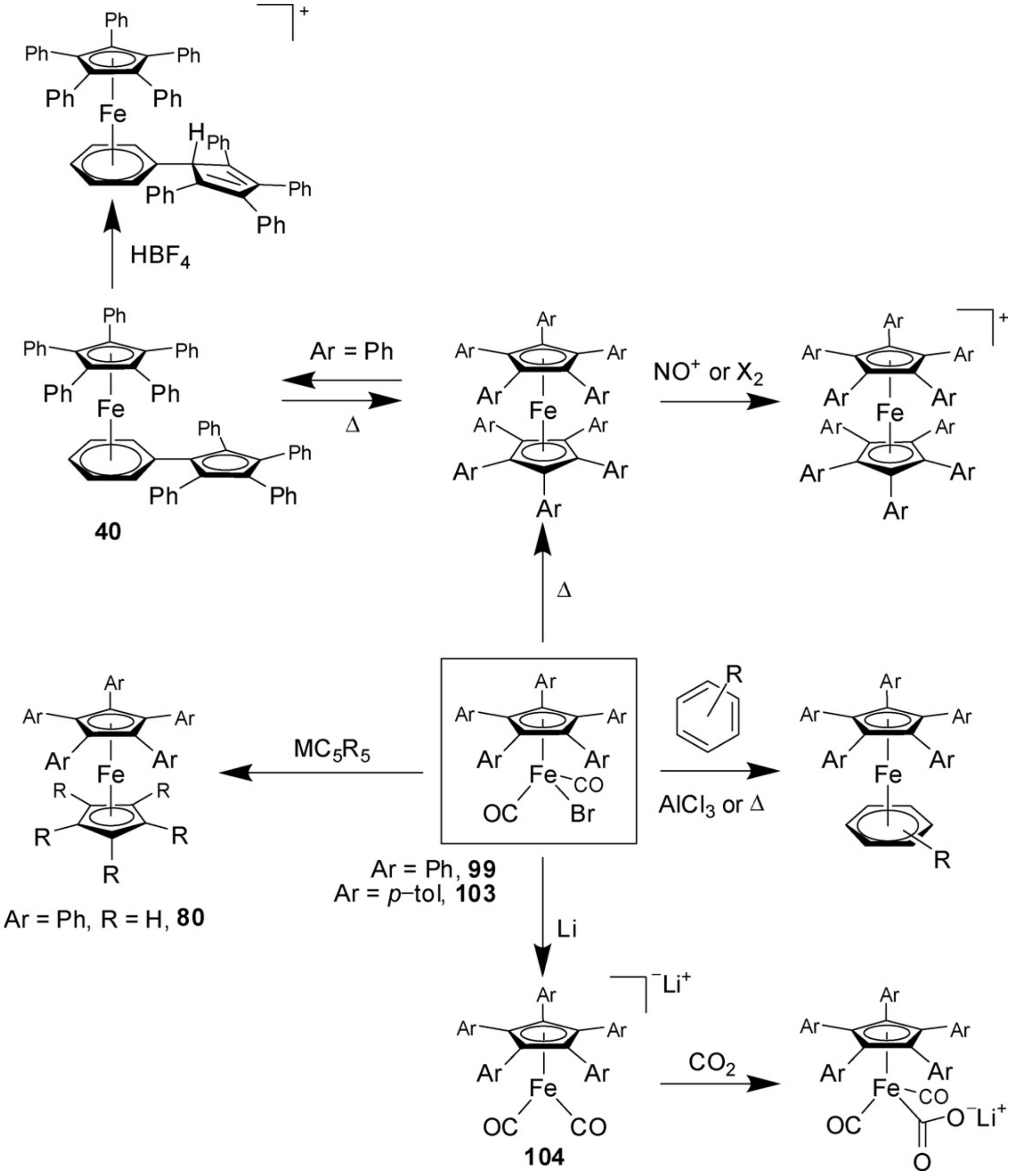

Scheme 47.

$$[\mathrm{Fe}(\eta^5\text{-}\mathrm{C_5Ar_5})(\mathrm{CO})_2\mathrm{Br}] \underset{-\,e^-}{\overset{+\,e^-}{\rightleftharpoons}} [\mathrm{Fe}(\eta^5\text{-}\mathrm{C_5Ar_5})(\mathrm{CO})_2\mathrm{Br}]^{\bullet-}$$

$$[\mathrm{Fe}(\eta^5\text{-}\mathrm{C_5Ar_5})(\mathrm{CO})_2\mathrm{Br}]^{\bullet-} \underset{-\,e^-}{\overset{+\,e^-}{\rightleftharpoons}} [\mathrm{Fe}(\eta^5\text{-}\mathrm{C_5Ar_5})(\mathrm{CO})_2]^{\bullet} + \mathrm{Br}^-$$

$$[\mathrm{Fe}(\eta^5\text{-}\mathrm{C_5Ar_5})(\mathrm{CO})_2]^{\bullet} \underset{-\,e^-}{\overset{+\,e^-}{\rightleftharpoons}} [\mathrm{Fe}(\eta^5\text{-}\mathrm{C_5Ar_5})(\mathrm{CO})_2]^-$$

Scheme 48.

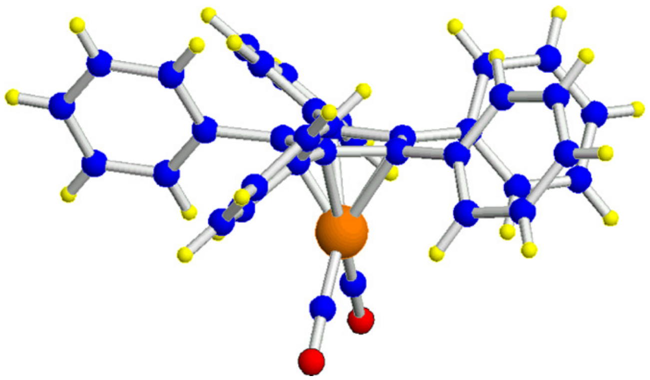

Fig. 32. Structure of the $[\mathrm{Fe}(\eta^5\text{-}\mathrm{C_5Ph_5})(\mathrm{CO})_2]^-$ anion (**104**) [23aq].

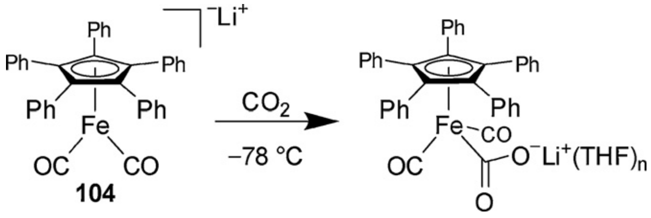

Scheme 49.

The pivotal complexes $[\mathrm{Fe}(\eta^5\text{-}\mathrm{C_5Ar_5})(\mathrm{CO})_2\mathrm{Br}]$ (Ar = Ph (**99**), *p*-tol (**103**)) undergo reversible 1-electron cyclic voltammetric oxidations, and the resultant $[\mathrm{Fe}(\eta^5\text{-}\mathrm{C_5Ar_5})(\mathrm{CO})_2\mathrm{Br}]^+$ cations react relatively rapidly on the cyclic voltammetric time-scale [129]. They also undergo an apparent 2-electron cyclic voltammetric reduction. The reductive behaviour is interpreted as a reversible 1-electron reduction to the anion radical, which rapidly loses Br^-, producing the $[\mathrm{Fe}(\eta^5\text{-}\mathrm{C_5Ar_5})(\mathrm{CO})_2]^{\bullet}$ radical at a potential at which it is immediately and reversibly reduced to the anion, $[\mathrm{Fe}(\eta^5\text{-}\mathrm{C_5Ar_5})(\mathrm{CO})_2]^-$ (**104**) (Scheme 48) [129].

Subsequent reactions of the radical and anion, which generate species such as the dimer, $[\mathrm{Fe}(\eta^5\text{-}\mathrm{C_5Ph_5})(\mathrm{CO})]_2(\mu\text{-}\mathrm{CO})_2$ (**105**), and tetramer, $[\mathrm{Fe}(\eta^5\text{-}\mathrm{C_5Ar_5})]_4(\mu\text{-}\mathrm{CO})_4$, are evident in the cyclic voltammetry. Red crystals of salts of the anion, $[\mathrm{Fe}(\eta^5\text{-}\mathrm{C_5Ph_5})(\mathrm{CO})_2]^-$ (**104**), can be produced chemically in 53% yield by sodium reduction of $[\mathrm{Fe}(\eta^5\text{-}\mathrm{C_5Ph_5})(\mathrm{CO})_2\mathrm{Br}]$ (**99**), or of the dimer, $[\mathrm{Fe}(\eta^5\text{-}\mathrm{C_5Ph_5})(\mathrm{CO})]_2(\mu\text{-}\mathrm{CO})_2$ (**105**), and this complex is sufficiently stable to be isolated and structurally characterized (Fig. 32) [23aq]. The compound has the usual "paddle-wheel" orientation of the phenyl rings and has dimensions similar to those of the isoelectronic $[\mathrm{Co}(\eta^5\text{-}\mathrm{C_5Ph_5})(\mathrm{CO})_2]$ (**106**); the Fe-($\mathrm{C_5}$-ring centroid) distance is 1.75(3) Å [23e].

The Li^+, but not the Na^+ nor the K^+, salt of $[\mathrm{Fe}(\eta^5\text{-}\mathrm{C_5Ph_5})(\mathrm{CO})_2]^-$ reacts with $\mathrm{CO_2}$ at low temperature to form a metallocarboxylate ion (Scheme 49), which appears to owe its stability to tight ion binding with the Li^+ (solvent) cation. This contrasts to the chemistry of the analogous cyclopentadienyl complexes.

The metallocarboxylate anion is thermally unstable and it and the alkali metal salts of $[\mathrm{Fe}(\eta^5\text{-}\mathrm{C_5Ph_5})(\mathrm{CO})_2]^-$ are converted to the hydride, $[\mathrm{Fe}(\eta^5\text{-}\mathrm{C_5Ph_5})(\mathrm{CO})_2\mathrm{H}]$ (**107**), upon warming [23aq].

The formyl complex, $[\mathrm{Fe}(\eta^5\text{-}\mathrm{C_5Ph_5})(\mathrm{CO})\{\mathrm{C}(=\mathrm{O})\mathrm{H}\}\mathrm{PMe_3}]$ (**100**), of Scheme 46 was the first, neutral, first row transition metal formyl complex that was stable at room temperature [126b]. The enhanced stability of **100** (at least with respect to the $\mathrm{C_5H_5}^-$ and $\mathrm{C_5Me_5}^-$ analogues) was attributed to both steric protection of the formyl group by the $\mathrm{C_5Ph_5}^-$ ligand, and the decreased electron density on the formyl carbon as a consequence of electron withdrawal by the $\mathrm{C_5Ph_5}^-$ phenyl rings. The compound exists as a mixture of diastereomers resulting from the chirality of the $\mathrm{C_5Ph_5}^-$ ligand and the metal centre. Thus, the ν_{CO} stretching absorptions are doubled up in the solid state IR spectrum and the single $^{13}\mathrm{C}$ NMR resonance of the $\mathrm{C_5}$ ring observed at room temperature is split into a 1:2:1:1 multiplet at low temperatures, consistent with slow rotation of the $[\mathrm{Fe}(\eta^5\text{-}\mathrm{C_5Ph_5})(\mathrm{CO})\{\mathrm{C}(=\mathrm{O})\mathrm{H}\}\mathrm{PMe_3}]$ tripod on the NMR timescale [23r]. Similarly, a 1:1:2:1:1:1:1:2 multiplet, observed for the $\mathrm{C_5}$ ring carbon atoms in the solid state $^{13}\mathrm{C}$ NMR spectrum of $[\mathrm{Fe}(\eta^5\text{-}\mathrm{C_5Ph_5})(\mathrm{CO})(\mathrm{C_2H_5})\mathrm{PMe_3}]$ (**108**), was attributed to the presence of two diastereomers in the solid state [126b].

In addition to the synthetic pathway depicted in Scheme 44, an alternative route to iron-arene pentaphenylcyclopentadienyl complexes is by way of the reaction of $\mathrm{Li}[\mathrm{C_5Ph_5}]$ (**28**), iron chloride, and the lithium salt of 2,3-cyclopenteno-4-dimethylaminopyridine (Scheme 50) [130].

When the heterocycle is η^5-bound to the iron centre, coordination to the other face by either $\mathrm{C_5Ph_5}^-$ or $\mathrm{C_5Me_5}^-$ results in a planar, chiral iron species whose pendant $\mathrm{NMe_2}$ nucleophile, in an enantiopure form achieved by resolution of the metal complex, can catalyze the enantioselective acylation of racemic alcohols without the use of enzymes [130a]; enantioselective rearrangement of *O*-acylated enolates [130b,c], and kinetic resolution of allylic alcohols [131], are also feasible. Likewise, the *N*-oxide derivative (**109**), which has been structurally characterized (Fig. 33) [23ap], may

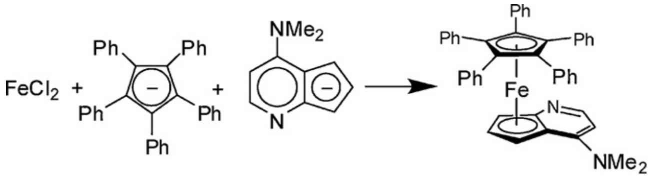

Scheme 50.

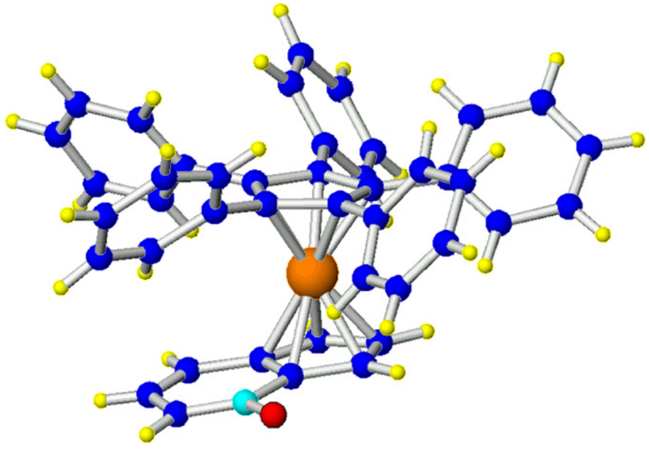

Fig. 33. Structure of [Fe(η^5-C_5Ph_5)(η^5-C_8H_6NO)] (**109**) [23ap].

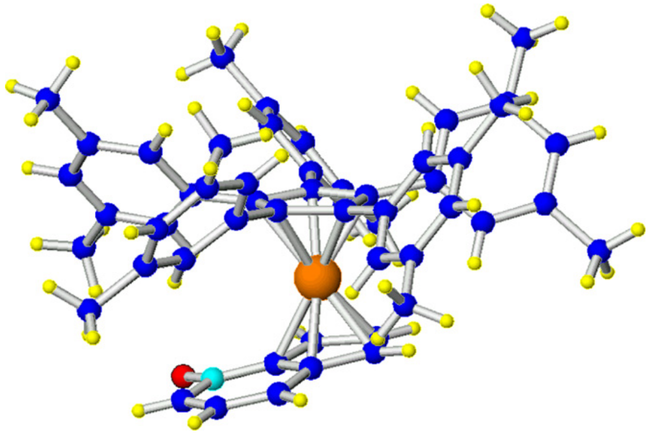

Fig. 34. Structure of [Fe{η^5-C_5(3,5-$Me_2C_6H_3$)$_5$}(η^5-C_8H_6NO)] (**110**) [23ap].

be derived by dimethyldioxirane oxidation of [Fe(η^5-C_5Ph_5)(η^5-C_8H_6N)] [23ap].

Planar, chiral complexes of these types have proven to be very effective stereoselective catalysts [23aj–al,ap,130a,132]. These species are effective in a variety of catalytic enantioselective acylations involving acylation at the indenyl nitrogen or *N*-oxide. The function of the [Fe(η^5-C_5Ph_5)] unit is firstly to induce planar chirality to the indenyl ligand, which carries the nucleophilic catalytic site, and, secondly, to provide steric bulk in the vicinity of the catalytic site [23ap]. Even greater bulk (and improved catalytic effectiveness) is provided by the deployment of [Fe{η^5-C_5(3,5-$Me_2C_6H_3$)$_5$}(η^5-C_8H_6NO)] (**110**), which provides a structurally characterized example of a complex incorporating the bulky C_5(3,5-$Me_2C_6H_3$)$_5^-$ ligand, and illustrates the steric demands of this aryl group (Fig. 34) [23ap]. The steric loading on the pentaarylcyclopentadienyl group has the result here that the carbocycle and the heterocycle are distinctly non-parallel. Complex **110** achieves catalytic desymmetrization of *meso*-epoxides with $SiCl_4$ with excellent enantioselectivity [23ap].

[Fe(η^5-C_5Ph_5){η^5-4-$NMe_2C_8H_4N$(OAc)}] (**111**) provides a structurally characterized example of the acylated indenyl as its SbF_6^- salt (Fig. 35), and illustrates a key step in these syntheses, the addition of an acyl group to the planar, chiral [Fe(η^5-C_5Ph_5)(η^5-4-$Me_2NC_8H_5N$)] species [23ap].

A poorly resolved (R = 0.25) structure has been reported for another postulated catalytic intermediate: the ion pair formed between a deacylated substrate and the N-acylated [Fe(η^5-C_5Ph_5){η^5-C_8H_5N(R)}] (R = pyrrolidino) catalyst (Fig. 36) [132a].

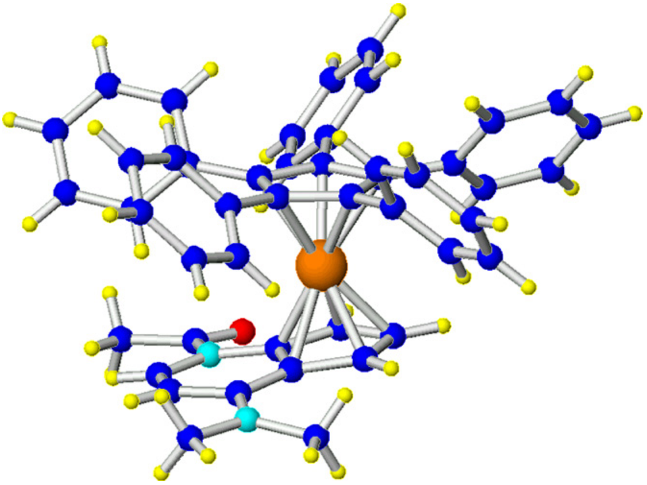

Fig. 35. Structure of the [Fe(η^5-C_5Ph_5){η^5-4-$NMe_2C_8H_5N$(OAc)}]$^+$ cation (**111**) [23al].

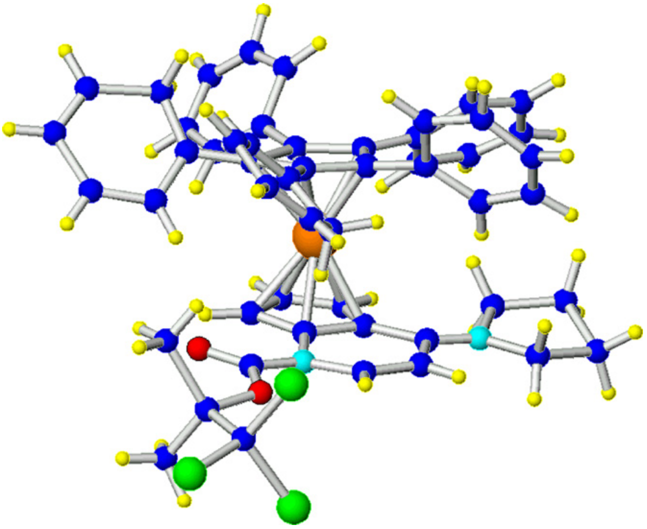

Fig. 36. Structure of the [Fe(η^5-C_5Ph_5){η^5-4-(NC_4H_8)C_8H_5N(C(=O)OCMe_2CCl_3)}]$^+$ cation [132a].

Decaphenylferrocene (**112**) is a lilac-coloured, insoluble solid, which was first reported in 1983 [10b,45a,105,133]. The complex can be prepared by reaction of $Fe(CO)_5$ with C_5Ph_5Br (**3**) and zinc, or by thermolysis of [Fe(η^5-C_5Ph_5)$(CO)_2$Br] (**99**). Although the crystal structure has been reported [23s], the data are of insufficient quality ($R \sim 17\%$) to provide useful metric details. The compounds [M$(C_5Ph_5)_2$] (M = Fe (**112**), Ni (**113**)) are isostructural. Mössbauer and photoelectron spectroscopies are consistent with the anticipated Fe(II) oxidation state [126d]. Decaphenylferrocene (**112**) is slightly easier to oxidize than ferrocene, and undergoes a reversible, one-electron oxidation at −0.040 V (*vs.* $Fc^{+/0}$) to the decaphenylferrocenium cation [26], which undergoes a further, electrochemically reversible, one-electron oxidation to the unstable dication at +0.745 V (*vs.* $Fc^{+/0}$, Eq. (13)):

$$\underset{\mathbf{112}}{[Fe(\eta^5\text{-}C_5Ph_5)_2]} \overset{-40\,\text{mV}}{\rightleftarrows} \underset{\mathbf{114}}{[Fe(\eta^5\text{-}C_5Ph_5)_2]^+} \overset{+745\,\text{mV}}{\rightleftarrows} [Fe(\eta^5\text{-}C_5Ph_5)_2]^{2+} \tag{13}$$

Reaction of decaphenylferrocene (**112**) with a slight excess of dilute triflic acid produces the formally Fe(IV) hydride, $[Fe(C_5Ph_5)_2H]^+$, detectable by its ^1H NMR resonance at δ

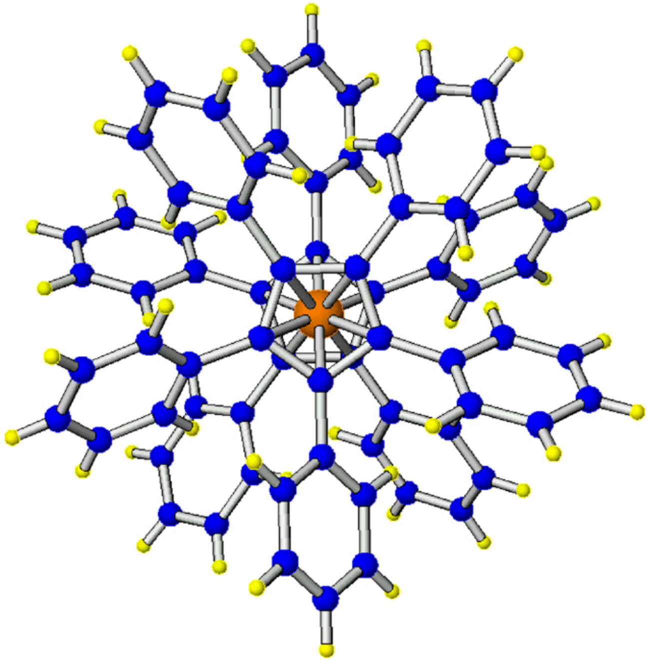

Fig. 37. Structure of the $[Fe(\eta^5\text{-}C_5Ph_5)_2]^+$ (**114**) cation [23s,23w,126d].

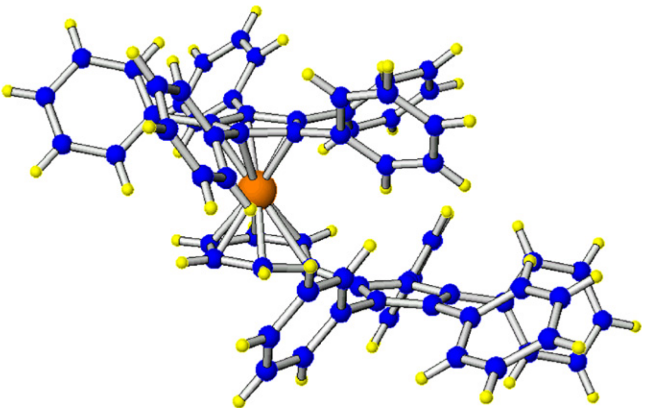

Fig. 38. Structure of $[Fe(\eta^5\text{-}C_5Ph_5)\{(\eta^6\text{-}C_6H_5)C_5Ph_4\}]$ (**40**) [23ar].

−0.77 ppm. The hydride, $[Fe(C_5Ph_5)_2H]^+$, isomerizes to the protonated linkage isomer, $[Fe(\eta^5\text{-}C_5Ph_5)\{(\eta^6\text{-}C_6H_5)C_5Ph_4H\}]^+$, and undergoes an electrochemically reversible, one-electron reduction at −0.220 V (*vs.* $Fc^{+/0}$) to what is presumed to be the formally Fe(III) hydride.

The decaphenylferrocenium cation, $[Fe(C_5Ph_5)_2]^+$ (**114**), can be produced chemically in high yield (> 80%), by oxidation of decaphenylferrocene (**112**) with, *e.g.*, $NOBF_4$, X_2, or excess triflic acid [23s,w,26,126d]. It exists in the solid state with the familiar S_{10} molecular configuration with parallel C_5 rings and canted phenyl groups (Fig. 37); the Fe-(C_5-ring centroid) distance is 1.807(5) Å [23s,w,126d]. Its highly anisotropic solid state ESR spectrum at 4 K is characteristic of low-spin Fe(III) d^5 sandwich complexes [26].

$[Fe(\eta^5\text{-}C_5Ph_5)_2]$ (**112**) exists in equilibrium with its more soluble linkage isomer, $[Fe(\eta^5\text{-}C_5Ph_5)\{(\eta^6\text{-}C_6H_5)C_5Ph_4\}]$ (**40**), obtainable as one of the products from the reaction of $Fe(CO)_5$ with C_5Ph_5Br (**3**) in the presence of zinc (Scheme 44) [16]. In the solid state (Fig. 38), one C_5Ph_5 ligand is η^5-coordinated (Fe-(C_5-ring centroid) = 1.6933(10) Å), whilst the other has a phenyl group η^6-bound to the iron centre (Fe-(C_6-ring centroid) = 1.6988(10) Å) [23ar]. The NMR spectra indicate that this structure is preserved in solution [16]. Whereas $[Fe(C_5Ph_5)_2]$ (**112**) is slightly easier to oxidize than ferrocene, the zwitterionic, linkage isomer (**40**) is much easier to oxidize than either $[Fe(C_5Ph_5)_2]$ (**112**) or $[Fe(C_5H_5)_2]$, and undergoes a reversible, one-electron oxidation at −0.170 V (*vs.* $Fc^{+/0}$) [16,26]. Furthermore, the oxidations of $[Fe(C_5Ph_5)_2]$ (**112**) and $[Fe(C_5H_5)_2]$ are metal-based, whilst ESR spectroscopy suggests that oxidation of the linkage isomer is ligand-based [26].

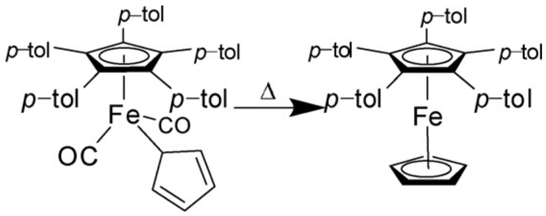

115 **116**

Scheme 51.

Sym-pentaphenylferrocene, $[Fe(\eta^5\text{-}C_5Ph_5)(\eta^5\text{-}C_5H_5)]$ (**80**), is much more soluble than decaphenylferrocene (**112**). It is prepared by thermolysis of the product of the reaction between $Na(C_5H_5)$ and $[Fe(\eta^5\text{-}C_5Ph_5)(CO)_2Br]$ (**99**) [125]. Since $[Fe\{C_5(p\text{-}tol)_5\}(\eta^1\text{-}C_5H_5)(CO)_2]$ (**115**) can be isolated as a deep red air-stable solid from the reaction between $[Fe\{C_5(p\text{-}tol)_5\}(CO)_2Br]$ (**103**) and $Na(C_5H_5)$, and is thermally converted to $[Fe\{C_5(p\text{-}tol)_5\}(\eta^5\text{-}C_5H_5)]$ (**116**) (Scheme 51), the synthesis of $[Fe(\eta^5\text{-}C_5Ph_5)(\eta^5\text{-}C_5H_5)]$ (**80**) probably proceeds in an analogous fashion, although $[Fe(\eta^5\text{-}C_5Ph_5)(\eta^1\text{-}C_5H_5)(CO)_2]$ (**117**) was not isolated [23o,97].

$[Fe(C_5Ph_5)(C_5H_5)]$ (**80**) undergoes a reversible oxidation at E^0 = +0.240 V (*vs.* $Fc^{+/0}$) and a quasi-reversible reduction at $E_{1/2}$ = −1.491 V. The stabilization of $[Fe(C_5Ph_5)(C_5H_5)]^-$ is unusual for ferrocene and its substituted derivatives (reduction of $[Fe(\eta^5\text{-}C_5H_5)_2]$ complexes typically occurs at *ca.* −3 V) [134], and the ease of reduction has been ascribed to a square scheme, involving rapid equilibria favouring the parent complex, $[Fe(C_5Ph_5)(C_5H_5)]$ (**80**), in the Fe(II) oxidation state and the linkage isomer, $[Fe(C_5H_5)\{(\eta^6\text{-}C_6H_5)(C_5Ph_4)\}]^-$ in the Fe(I) oxidation state (Scheme 52) [23o].

The bulky $C_5Ph_5{}^-$ ligand has proven useful in protecting the metal–C link in the formation of coordinated "carbyne" chains with redox-active end groups, in which the $[Fe(\eta^5\text{-}C_5Ph_5)(CO)_2]$ moiety functions as an electron-withdrawing acceptor group (Scheme 53) [135].

$$\begin{tikzcd}
{[Fe(\eta^5\text{–}C_5Ph_5)(\eta^5\text{–}C_5H_5)]} \arrow[r, shift left, harpoon] \arrow[d, shift left, "E^0 \approx -3\ V"] & {[Fe((\eta^6\text{–}C_6H_5)(C_5Ph_4))(\eta^5\text{–}C_5H_5)]} \arrow[l, shift left, harpoon] \arrow[d, shift left, "E^0 = -1.49\ V"] \\
{[Fe(\eta^5\text{–}C_5Ph_5)(\eta^5\text{–}C_5H_5)]^-} \arrow[u, shift left] \arrow[r, shift left, harpoon] & {[Fe((\eta^6\text{–}C_6H_5)(C_5Ph_4))(\eta^5\text{–}C_5H_5)]^-} \arrow[u, shift left] \arrow[l, shift left, harpoon]
\end{tikzcd}$$

Scheme 52.

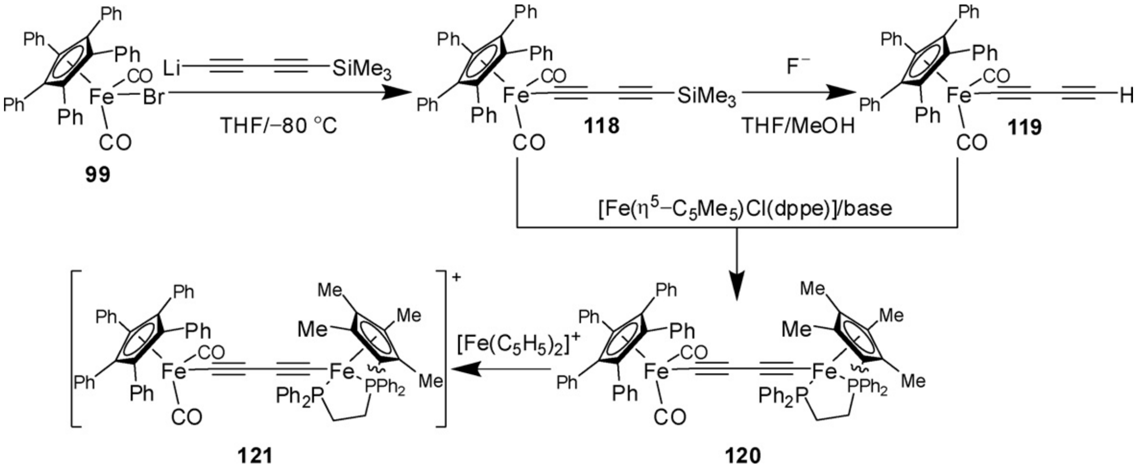

Scheme 53.

Thus, $[Fe(\eta^5\text{-}C_5Ph_5)(CO)_2Br]$ (**99**) reacts with one equivalent of $Li\text{-}(C{\equiv}C)_2SiMe_3$ in THF at −80 °C to produce $[Fe(\eta^5\text{-}C_5Ph_5)(CO)_2\{(C{\equiv}C)_2SiMe_3\}]$ (**118**) as a yellow powder in 70–75% yield. $[Fe(\eta^5\text{-}C_5Ph_5)(CO)_2\{(C{\equiv}C)_2H\}]$ (**119**) is obtained as a brown solid from the trimethylsilyl precursor in 85% yield by reaction with fluoride ion in methanol/THF. The compounds were characterized by infrared, Mössbauer, ^1H, ^{13}C and ^{31}P NMR spectroscopies, and cyclic voltammetry. Both butadiyne compounds, $[Fe(\eta^5\text{-}C_5Ph_5)(CO)_2\{(C{\equiv}C)_2X\}]$ (X = $SiMe_3$ (**118**), H (**119**)), undergo irreversible reductions (at −1.43 and −1.33 V *vs.* $Fc^{+/0}$, respectively) [136]. The redox potentials and those of the $C_5Me_5^-$ analogues are interpreted to argue that the $C_5Ph_5^-$ and $C_5Me_5^-$ ligands stabilize low and high oxidations states, respectively.

The grey-green binuclear complex, $[Fe(\eta^5\text{-}C_5Ph_5)(CO)_2Fe(\eta^5\text{-}C_5Me_5)(dppe)]\{\mu\text{-}(C{\equiv}C)_2\}$ (**120**), was prepared in 59% yield by treatment of either of the mononuclear butadiynes with $[Fe(\eta^5\text{-}C_5Me_5)(\eta^2\text{-}dppe)Cl]$ with strong base. Chemical oxidation of the product with ferrocenium, $[Fe(\eta^5\text{-}C_5H_5)_2]PF_6$, produces $[Fe(\eta^5\text{-}C_5Ph_5)(CO)_2Fe(\eta^5\text{-}C_5Me_5)(dppe)]\{\mu\text{-}(C{\equiv}C)_2\}PF_6]$ (**121**) as a green solid in 86% yield. Accordingly, the neutral binuclear species (**120**) undergoes one reversible (−0.74 V *vs.* $Fc^{+/0}$) and one quasi-reversible oxidation (+0.47 V *vs.* $Fc^{+/0}$) to the mono- and dication, respectively. The contrast with the behaviour of the mononuclear precursors indicates effective electronic communication between the two iron centres, presumably through the intermediacy of the conjugated $(C{\equiv}C)_2$ spacer. The Mössbauer spectrum argues that **121** exists as a trapped Fe(II)–Fe(III) mixed-valence species.

Dimeric $[Fe(\eta^5\text{-}C_5Ph_5)(CO)]_2(\mu\text{-}CO)_2$ (**105**) can also be isolated as a reactive green solid during the preparation of *sym*-pentaphenylcyclopentadienylferrocene (**80**) [23o], and the analogous $[Fe\{\eta^5\text{-}C_5(p\text{-}tol)_5\}(CO)]_2(\mu\text{-}CO)_2$ (**122**) by the reduction of $[Fe\{\eta^5\text{-}C_5(p\text{-}tol)_5\}(CO)_2Br]$ (**103**) with zinc (Scheme 45). The exclusively *trans*-configuration assigned to both dimers on the basis of their infrared spectra [137], is presumably a consequence of the steric constraints exerted by the penta-arylcyclopentadienyl ligands. An alternative route to $[Fe(\eta^5\text{-}C_5Ar_5)(CO)]_2(\mu\text{-}CO)_2$ is by means of hydrogen abstraction from $[Fe(\eta^5\text{-}C_5Ar_5)(CO)_2H]$ by long-lived triarylmethyl radicals, such as the trityl radical (Scheme 54) [138]. The more soluble $[Fe\{\eta^5\text{-}C_5Ph_4(p\text{-}tol)\}(CO)]_2(\mu\text{-}CO)_2$ (**123**) is prepared in a similar fashion.

Infrared spectroscopic data argued that the dimers, $[Fe(\eta^5\text{-}C_5Ar_5)(CO)]_2(\mu\text{-}CO)_2$, existed in solution in equilibrium with the monomeric 17-electron radicals, which react with RX (R = Me, Et, Pr^i, allyl, Bu^t, Bz, X = Br, I) to generate $[Fe(\eta^5\text{-}C_5Ar_5)(CO)_2R]$ and $[Fe(\eta^5\text{-}C_5Ar_5)(CO)_2X]$ (Scheme 54). The $C_5Ar_5^-$ ligand is (unusually) displaced on reaction with PMe_3 with the slow formation of small amounts of $[Fe(CO)_3PMe_3]$ and $[Fe(\eta^5\text{-}C_5Ar_5)(CO)_2H]$, whilst *tert*-butyl isocyanide reacts to give the salt,

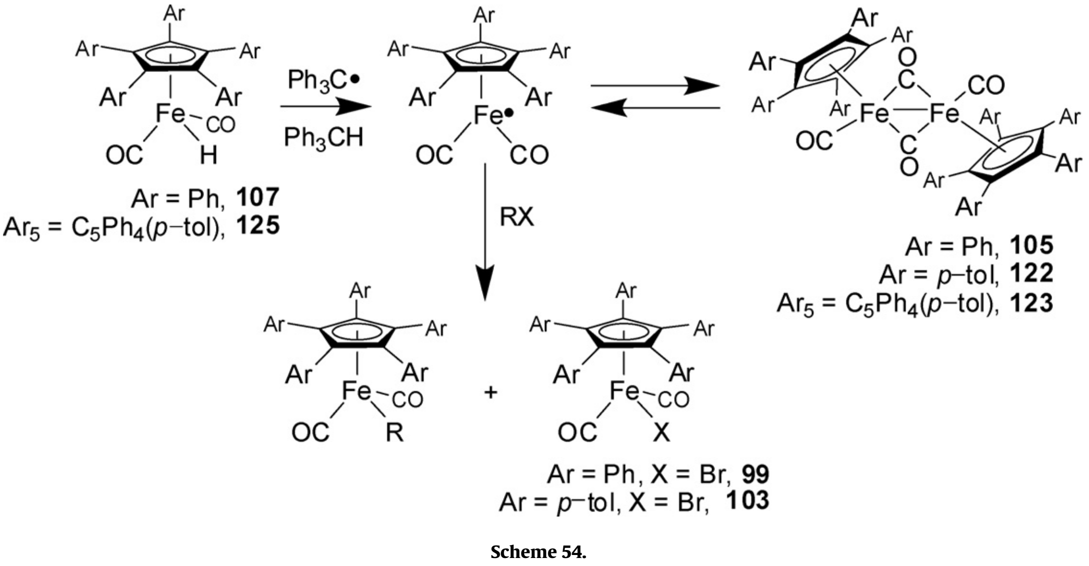

Scheme 54.

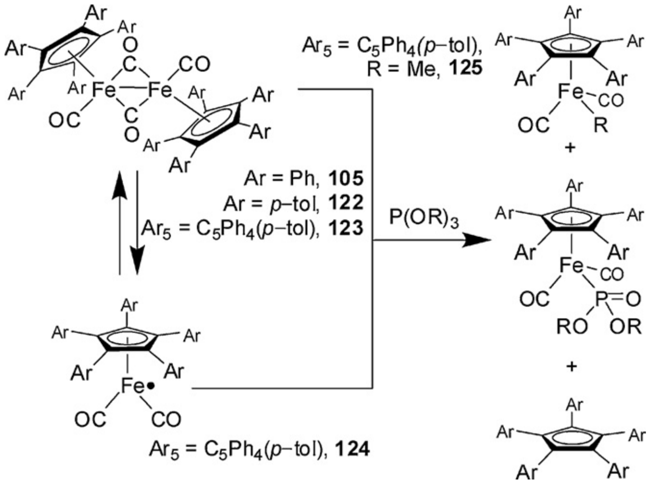

Scheme 55.

$[\mathrm{Fe}(\eta^5\text{-}\mathrm{C_5Ar_5})(\mathrm{C{\equiv}NBu^t})_3][\mathrm{Fe}(\eta^5\text{-}\mathrm{C_5Ar_5})(\mathrm{CO})_2]$. ^{13}CO labels can be incorporated into the dimer as bridging and terminal ligands by means of the dimer–monomer equilibrium. The equilibrium constant for dimer dissociation was estimated as 10^{-3} [128b,138]. The bulky $\mathrm{C_5Ar_5}^-$ ligands obviously play an important role in stabilizing the radicals, since recombination of photogenerated $[\mathrm{Fe}(\mathrm{C_5H_5})(\mathrm{CO})_2]^\bullet$ to form the dimer is extremely rapid at room temperature ($k_{20\,^\circ\mathrm{C}} \sim 10^9\,\mathrm{mol\,L^{-1}\,s^{-1}}$) [139]. The reactivity of the dimers, $[\mathrm{Fe}(\eta^5\text{-}\mathrm{C_5Ar_5})(\mathrm{CO})]_2(\mu\text{-}\mathrm{CO})_2$, is exemplified by the reaction of $[\mathrm{Fe}\{\eta^5\text{-}\mathrm{C_5}(p\text{-tol})_5\}(\mathrm{CO})]_2(\mu\text{-}\mathrm{CO})_2$ (**122**) with KBr in the solid state, which generates $[\mathrm{Fe}\{\eta^5\text{-}\mathrm{C_5}(p\text{-tol})_5\}(\mathrm{CO})_2\mathrm{Br}]$ (**103**) [97].

Dimeric $[\mathrm{Fe}\{\eta^5\text{-}\mathrm{C_5Ph_4}(p\text{-tol})\}(\mathrm{CO})]_2(\mu\text{-}\mathrm{CO})_2$ (**123**) reacts slowly with the bulky phosphites, $\mathrm{P(OPr^i)_3}$ or $\mathrm{P(OPh)_3}$, to produce the expected carbonyl/phosphite 17-electron radicals, $[\mathrm{Fe}\{\eta^5\text{-}\mathrm{C_5Ph_4}(p\text{-tol})\}(\mathrm{CO})\mathrm{P(OR)_3}]^\bullet$. However, smaller phosphites, $\mathrm{P(OR)_3}$ (R = Me, Et), react faster, presumably with the radical intermediate, $[\mathrm{Fe}\{\eta^5\text{-}\mathrm{C_5Ph_4}(p\text{-tol})\}(\mathrm{CO})\}\mathrm{P(OR)_3}]^\bullet$. The coordinated phosphite is also attacked by excess dicarbonyl radical, $[\mathrm{Fe}\{\eta^5\text{-}\mathrm{C_5Ph_4}(p\text{-tol})\}(\mathrm{CO})_2]^\bullet$ (**124**), to generate $[\mathrm{Fe}\{\eta^5\text{-}\mathrm{C_5Ph_4}(p\text{-tol})\}(\mathrm{CO})_2\mathrm{Me}]$ (**125**) and Arbusov rearrangement products, which react with CO or excess $\mathrm{P(OR)_3}$, to give phosphonate complexes that were identified spectroscopically, but not isolated (Scheme 55) [128].

Preparation of the dimer (**105**) from $[\mathrm{Fe}(\eta^5\text{-}\mathrm{C_5Ph_5})(\mathrm{CO})_2\mathrm{H}]$ (**107**) can be followed by infrared spectroscopy. The hydride carbonyl absorptions at 2009 and 1954 cm^{-1}, were replaced by absorptions at 1956 and 1781 cm^{-1}, as expected for the terminal and bridging carbonyl absorptions of *trans*-$[\mathrm{Fe}(\eta^5\text{-}\mathrm{C_5Ph_5})(\mathrm{CO})]_2(\mu\text{-}\mathrm{CO})_2$ (**105**). Rapid replacement of the absorption at 1781 cm^{-1} by one at 1788 cm^{-1} was attributed to the interconversion of diastereomers of the dimer arising from the chirality of the pentaphenylcyclopentadienyl ligands, because of the helical canting of the phenyl rings [128b,138]. Interestingly, two forms of *trans*-$[\mathrm{Fe}\{\eta^5\text{-}\mathrm{C_5Ph_4}(p\text{-tol})\}(\mathrm{CO})]_2(\mu\text{-}\mathrm{CO})_2$ (**123**) are isolable. One of these compounds is more soluble in benzene than the other (the less soluble form is generally the major product in the synthesis). The differing solubilities are ascribed to the presence of diastereomers, in which the relative canting of the phenyl substituents of the $\{\mathrm{C_5Ph_4}(p\text{-tol})\}^-$ ligands differentiates the product, however, this has not yet been established unequivocally.

Photochemical reaction of $[\mathrm{Fe}\{\eta^5\text{-}\mathrm{C_5Ph_4}(p\text{-tol})\}(\mathrm{CO})_2\mathrm{H}]$ (**126**) with phosphines, L = $\mathrm{PMe_3}$, $\mathrm{PMe_2Ph}$, $\mathrm{PMePh_2}$, or $\mathrm{PPh_3}$, generates orange $[\mathrm{Fe}\{\eta^5\text{-}\mathrm{C_5Ph_4}(p\text{-tol})\}(\mathrm{CO})(\mathrm{H})\mathrm{L}]$ in 18–53% yields. Two ν_{CO} stretches are observed at 1920 and 1890 cm^{-1}, consistent with the existence of diastereomers as a consequence of the chirality engendered by the canting of the $\mathrm{C_5Ar_5}^-$ ligand and the chirality at iron [140].

Several *aza*-ferrocenyl and *aza*-*bis*ferrocenyl ligands incorporating the $\mathrm{C_5Ph_5}^-$ moiety (Scheme 56) have been prepared and bound to palladium centres through the nitrogen donors [141]. When activated by methylaluminoxane, the cationic palladium complex of the *trans*-*aza*-*bis*ferrocenyl ligand, catalyzes ethylene oligomerization, with turnover frequencies of between 13 and 54 mol of ethylene per mole of catalyst per hour [141].

The bulky ferrocenyl groups were introduced with the aim of blocking associative chain transfer of ethylene from the axial faces of the metal at the catalytic site. A target *aza*-*bis*(pentaphenylferrocenyl) ligand could not be prepared. The low reactivity of the complex derived from the *trans*-*aza*-*bis*ferrocenyl ligand was attributed to the lower nucleophilicity of the alkyl group *trans* to the $\mathrm{C_5Ph_5}^-$ in the catalyst resting state (Fig. 39) resulting in a slower addition to ethylene.

In related work, a patent describes the synthesis of the penta-aryl-*aza*-ferrocenyl derivative, $\mathrm{Fe}(\eta^5\text{-}\mathrm{C_5Ar_5})\{\eta^5\text{-}2\text{-}$

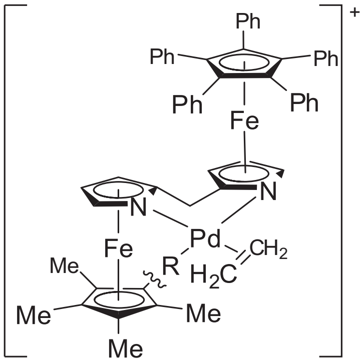

Fig. 39. Proposed catalyst resting state for ethylene oligomerization by Pd coordinated to an *aza*-*bis*ferrocenyl ligand [141].

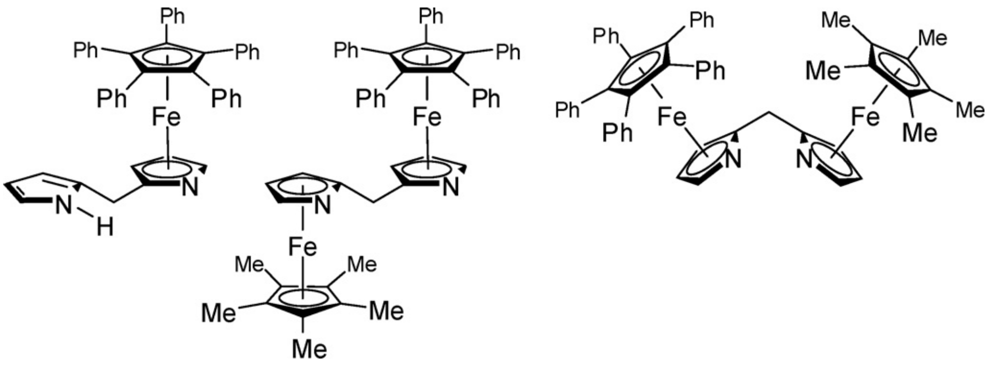

Scheme 56.

(C(=O)H)C_4H_3N} (**127**) (Ar = Ph (**127a**), Ar = 4-FC_6H_4 (**127b**), Ar = 4-$MeOC_6H_4$ (**127c**)), as orange solids prepared in 87% yield from the reaction of LiC_5Ar_5 with $FeCl_2$, followed by potassium pyrrolide [142]. The bidentate, nitrogen ligands (**128**) (R = H (**128a**), Me (**128b**), Pr^i (**128c**)), were prepared as red solids in ~70% yield by condensation with the appropriate amine.

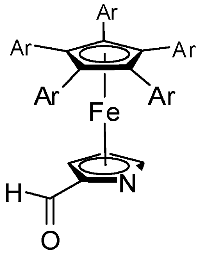

Ar = Ph, **127a**
Ar = 4−FC_6H_4, **127b**
Ar = 4−$MeOC_6H_4$, **127c**

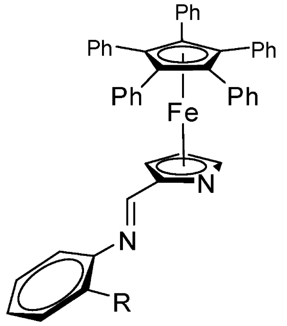

R = H, **128a**
R = Me, **128b**
R = Pr^i, **128c**

Coordination of **128** to $NiBr_2$ or [Pd(COD)MeCl] produced the Pd(II) and Ni(II) complexes (**129**) as illustrated (Ar = Ph; $n = 0$; $L^1 = L^2$ = Br, M = Ni, R = H (**129a**); R = Me (**129b**); Pr^i (**129c**); M = Pd, L^1 = Cl, L^2 = Me, R = Pr^i (**129d**); $n = +1$, M = Pd, L^1 = OEt_2, L^2 = Me, R = Pr^i (**129e**)) in 80–90% yield as orange to red solids. These materials were characterized only by ^1H NMR spectroscopy in the original patent [142]; a fuller description was made available in the literature [143].

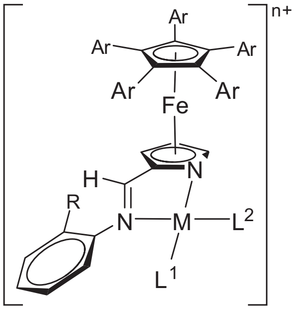

$n = 0$
M = Ni, R = H, $L^1 = L^2$ = Br, **129a**
R = Me, **129b**
R = Pr^i, **129c**
M = Pd, R = Pr^i, L^1 = Cl, L^2 = Me, **129d**
$n = +1$
M = Pd, R = Pr^i, L^1 = OEt_2, L^2 = Me, **129e**

When treated with methylaluminoxane, this series (**129a**–**e**) was active as ethylene polymerization catalysts and as ethylene/methylmethacrylate copolymerization catalysts.

A simple synthesis of novel, enantiopure *aza*-ferrocenyl and *aza*-ruthenocenyl derivatives, via the addition of a removable chiral auxiliary to the pyrrolide ring and separation of the resulting diastereomers has also been reported [144].

2.6.2. Ruthenium complexes

The starting point for much of ruthenium pentaphenylcyclopentadienyl chemistry is yellow, crystalline [Ru(η^5-C_5Ph_5)$(CO)_2$Br] (**130**), which is prepared in 68% yield by the reaction of $Ru_3(CO)_{12}$ with C_5Ph_5Br (**3**) in toluene at reflux under nitrogen (Scheme 57). As in other syntheses that employ this route, a deep purple colour, characteristic of the $C_5Ph_5^\bullet$ radical (**4**), is observed [45a,145]. In contrast, the major product obtained from the reaction between $Ru_3(CO)_{12}$ and C_5Ph_5Br (**3**) in the presence of zinc in xylenes at reflux is the arene cation, $[Ru(\eta^5\text{-}C_5Ph_5)(\eta^6\text{-}Me_2C_6H_4)]^+$ (**131**), isolated as its BPh_4^- salt (Scheme 57) [23ae].

Carbonyl substitution in [Ru(η^5-C_5Ph_5)$(CO)_2$Br] (**130**) occurs dissociatively [8a]. Limited kinetic studies indicate a significant reorganization in the transition state, which is stabilized (at least with respect to other cyclopentadienyl ligands) by the bulk of the $C_5Ph_5^-$ ligand. The reaction is reversible (CO will displace PPh_3 from [Ru(η^5-C_5Ph_5)$(CO)_2$Br] (**130**)) and the CO must be removed, either by oxidation with, *e.g.*, Me_3NO, or, if the reaction is induced thermally, by purging of the CO.

The ruthenium compounds [Ru(η^5-C_5Ph_5)$(CO)_2$Br] (**130**), [Ru(η^5-C_5Ph_5)(CO)(Br)PEt_3] (**132**), [Ru(η^5-C_5Ph_5)(CO)(Br)PPh_3] (**133**), [Ru(η^5-C_5Ph_5)(CO)(Br)$P(OMe)_3$] (**134**), [Ru(η^5-C_5Ph_5)(CO)(Br)$P(OPh)_3$] (**135**), [Ru(η^5-C_5Ph_5)$(CO)_2$Me] (**136**), [Ru(η^5-C_5Ph_5)(CO)(PEt_3)Me] (**137**), [Ru(η^5-C_5Ph_5)(CO)(PEt_3)Et] (**138**), [Ru(η^5-C_5Ph_5)(CO)(PEt_3){C(=O)Me}] (**139**), [Ru(η^5-C_5Ph_5)(CO)(PEt_3)(η^1-MeC=CMe_2)] (**140**), $[Ru(\eta^5\text{-}C_5Ph_5)(CO)(PEt_3)_2]^+$ (**141**), $[Ru(\eta^5\text{-}C_5Ph_5)(CO)_2PEt_3]^+$ (**142**), $[Ru(\eta^5\text{-}C_5Ph_5)(CO)(H_2C{=}CH_2)PEt_3]^+$ (**143**), $[Ru(\eta^5\text{-}C_5Ph_5)(CO)(MeC{\equiv}CMe)PEt_3]^+$ (**144**), $[Ru(\eta^5\text{-}C_5Ph_5)(CO)\{P(OMe)_3\}_2]^+$ (**145**), $[Ru(\eta^5\text{-}C_5Ph_5)(CO)_2P(OMe)_3]^+$ (**146**), and the dimeric $[Ru(\eta^5\text{-}C_5Ph_5)(CO)]_2(\mu\text{-}CO)_2$ (**147**), have been adequately characterized (Scheme 58) [8a,145,146], with structural characterization reported for the compounds [Ru(η^5-C_5Ph_5)$(CO)_2$Br] (**130**, Ru-(C_5-ring centroid) = 1.95(5) Å), and [Ru(η^5-C_5Ph_5)(CO)(Br)PPh_3] (**133**, Ru-(C_5-ring centroid) = 1.93(5) Å) [8a,23j]. The structure of [Ru(η^5-C_5Ph_5)$(CO)_2$Br] (**130**) is similar to those of the iron (**99**) and osmium analogues (**29**) [23j], and appears to be maintained in solution. However, ^{13}C and ^{31}P NMR spectroscopies indicate that in solution, the related [Ru(η^5-C_5Ph_5)(CO)(PEt_3)(η^1-MeC=CMe_2)] (**140**) exists as two rotamers in a 1:1 ratio [145]. The ^{31}P and ^{13}C NMR spectra of [Ru(η^5-C_5Ph_5)(CO)(Br)PPh_3] (**133**) also indicate the presence of two isomers in solution, a phenomenon not observed for the $P(OMe)_3$ (**134**) and $P(OPh)_3$ (**135**) analogues [8a]. In contrast to most $C_5Ph_5^-$ compounds, in which the angles between the C_5 ring and the phenyl planes average approximately 56°, these angles in [Ru(η^5-C_5Ph_5)(CO)(Br)PPh_3] (**133**) are 56°, 53°, 53°, 66° and 26°, as a consequence of interference between the phenyl rings of the $C_5Ph_5^-$ and PPh_3 ligands. The C_5 carbocycle and a phenyl ring of the phosphine ligand are near parallel; the two ligands approach to within the van der Waals diameter of carbon, and an *ortho*-H of the $C_5Ph_5^-$ ligand is only 2.83 Å from each of two PPh_3 carbons; this is possibly a consequence of C–H···C(π) interactions discussed earlier [43]. The result is restricted rotation of the phenyl rings of both ligands and the generation of a mixture of diastereomers (the phenyl rings of the two ligands form chiral arrays and the ruthenium itself is a stereogenic centre), at least on the NMR time-scale [8a] (Figs. 40 and 41).

With the exception of [Ru(η^5-C_5Ph_5)(CO)(PEt_3)(η^1-MeC=CMe_2)] (**140**), compounds of formula [Ru(η^5-C_5Ph_5)(CO)(X)PR_3] (X = Br, R = Et (**132**); R = Ph (**133**); R = OMe (**134**)), [Ru(η^5-C_5Ph_5)(CO)(PEt_3)Me] (**137**), [Ru(η^5-C_5Ph_5)(CO)(PEt_3)Et] (**138**), and [Ru(η^5-C_5Ph_5)(CO)(PEt_3){C(=O)Me}] (**139**) each undergo a reversible one-electron cyclic voltammetric oxidation in 0.1 M Bu_4NPF_6/methylene chloride in the potential range −0.47 to 1.33 V (*vs.* $Fc^{+/0}$). The compounds could be oxidized chemically and studied in solution, but no Ru(III) derivatives were isolated. However, oxidation of $[Ru(\eta^5\text{-}C_5Ph_5)(CO)_2P(OMe)_3]^+$ (**142**) with cobaltocene generated a mixture of [Ru(η^5-C_5Ph_5)$(CO)_2$Me] (**136**), [Ru(η^5-C_5Ph_5)(CO)(Cl)$P(OMe)_3$] (**148**) and [Ru(η^5-C_5Ph_5)$(CO)_2${P(=O)$(OMe)_2$}] (**149**); the postulated route to

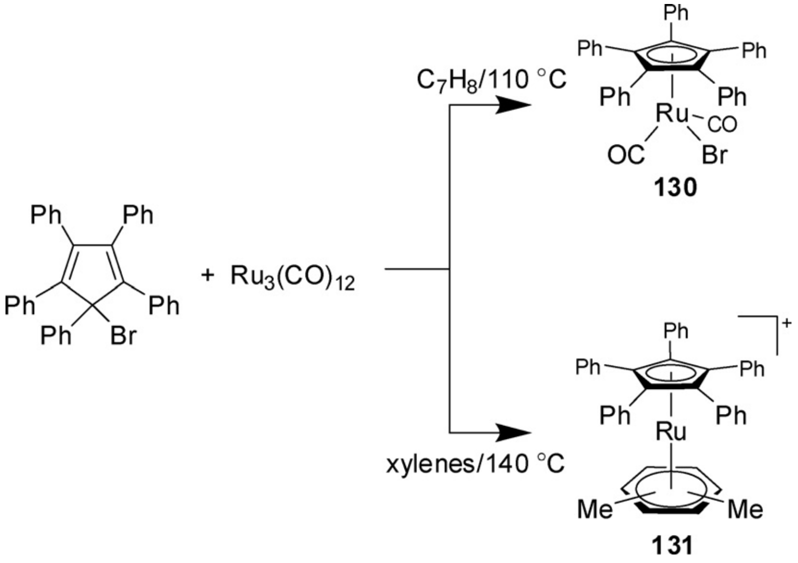

Scheme 57.

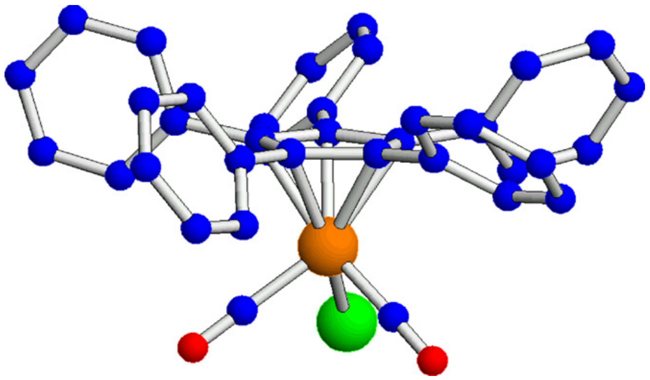

Fig. 40. Structure of $[Ru(\eta^5\text{-}C_5Ph_5)(CO)_2Br]$ (hydrogen atoms omitted) (**130**) [23j].

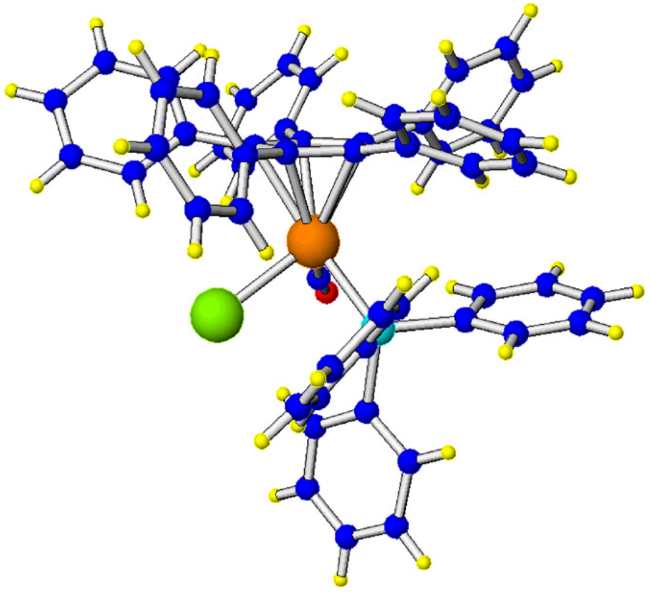

Fig. 41. Structure of $[Ru(\eta^5\text{-}C_5Ph_5)(CO)(Br)PPh_3]$ (**133**) [8a].

the dicarbonyls was a Michaelis–Arbusov rearrangement, possibly through the intermediacy of $[Ru(\eta^5\text{-}C_5Ph_5)(CO)P(OMe)_3]^{\bullet}$ (**150**), although the original paper favoured a nucleophilic $[Ru(\eta^5\text{-}C_5Ph_5)(CO)_2]^-$ anion [145].

The chemistry and electrochemistry of nitrosyl-substitution products of $[Ru(\eta^5\text{-}C_5Ph_5)(CO)_2Br]$ (**130**), $[Ru(\eta^5\text{-}C_5Ph_5)(CO)(Br)L]$ (L = PR_3 (**132**, **133**), $P(OR)_3$ (**134**, **135**), and $[Ru(\eta^5\text{-}C_5Ph_5)(CO)(C{\equiv}NBu^t)Br]$ (**151**)) are summarized in Scheme 59 [146]. These reactions exemplify four pathways for the interaction of NO^+ with metal carbonyls: (i) one-electron oxidation, (ii) CO-substitution, (iii) halide displacement, and (iv) NO^+-induced migratory insertion (the migratory insertion to give $[Ru(\eta^5\text{-}C_5Ph_5)(NO)\{C({=}O)Me\}L]^+$ from $[Ru(\eta^5\text{-}C_5Ph_5)(CO)(Me)L]$ does not occur when $[Ru(\eta^5\text{-}C_5Ph_5)(CO)(Me)L]$ is treated with Ag^+ under CO). A common intermediate, $[Ru(\eta^5\text{-}C_5Ph_5)(CO)(NO)(X)L]$, in which the NO ligand can be linear or bent, a one- or a three-electron donor, was postulated.

Whereas most of the compounds of Scheme 59 undergo irreversible cyclic voltammetric electron transfers, the cyclic voltammetric oxidations of $[Ru(\eta^5\text{-}C_5Ph_5)(NO)L]$ and reductions of $[Ru(\eta^5\text{-}C_5Ph_5)(NO)\{C({=}O)Me\}L]^+$ are reversible.

Whilst decaphenylcyclopentadienyl ruthenium, the ruthenium analogue of the iron sandwich **112**, has not been reported, the mixed ligand ruthenocenes, $[Ru(\eta^5\text{-}C_5Ar_5)(\eta^5\text{-}C_5H_5)]$ (Ar = Ph (**152**), (*p*-tol) (**153**), and $Ar_5 = Ph_4H$ (**154**)), and $[Ru(\eta^5\text{-}C_5Ph_5)(\eta^5\text{-}C_5Me_5)]$ (**155**), have been prepared and structurally characterized [23ae]. They are conveniently prepared from the reaction of $[Ru(\eta^5\text{-}C_5Ar_5)(CO)_2Br]$ (Ar = Ph, **130**) with MC_5R_5, to give the η^1-cyclopentadienyl species, $[Ru(\eta^5\text{-}C_5Ar_5)(CO)_2(\eta^1\text{-}C_5R_5)]$, which is thermalized to $[Ru(\eta^5\text{-}C_5R_5)(\eta^5\text{-}C_5H_5)]$ (Scheme 58). Alternatively, these complexes are available by the reaction of $[Ru(\eta^5\text{-}C_5R_5)(\eta^4\text{-}1,5\text{-}COD)Cl]$ with LiC_5Ar_5 (Scheme 60).

The mixed ligand metallocenes, $[Ru(\eta^5\text{-}C_5Ar_5)(\eta^5\text{-}C_5R_5)]$ (Ar = Ph, R = H (**152**); (*p*-tol) (**153**); $Ar_5 = Ph_4H$ (**154**); Ar = Ph, R = Me (**155**)), in contrast to the apparently irreversible, two-electron cyclic voltammetric oxidation of ruthenocene, undergo two consecutive, one-electron oxidations. The difference in behaviour is possibly due to the stability of the higher oxidation state when the ruthenium centre is bound to the bulky $C_5Ar_5^-$ ligand, and the inhibition of formation of *bis*ruthenocene analogues, which are implicated in the oxidative electrochemistry of ruthenocene [23ae,129].

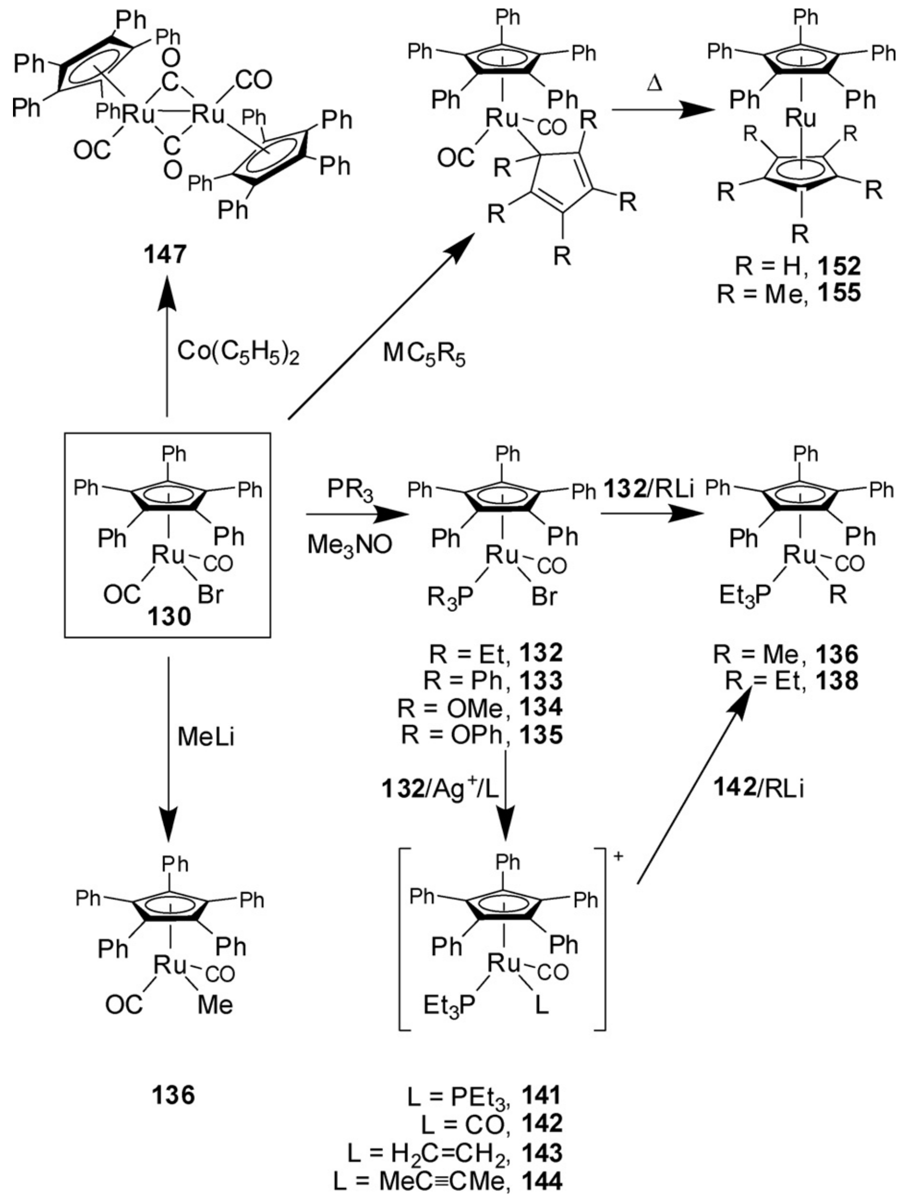

Scheme 58.

The cyclic voltammetric and non-linear optical properties of the alkenyl complexes, [Ru(η^5-C$_5$Ph$_5$)(CO)$_2${(*Z*)-HC=CHR}] (R = Ph (**156**), 4-C$_6$H$_4$NO$_2$ (**157**)) and [Ru(η^5-C$_5$Ph$_5$)(CO){(*Z*)-HC=CH(4-C$_6$H$_4$NO$_2$)}PMe$_2$Ph] (**158**) have been examined [147]. The yellow-green complexes [Ru(η^5-C$_5$Ph$_5$)(CO)$_2${(*Z*)-HC=CHPh}] (**156**), and [Ru(η^5-C$_5$Ph$_5$)(CO)$_2${(*Z*)-HC=CH(4-C$_6$H$_4$NO$_2$)}] (**157**), were prepared in 30% yield by treatment of either H$_2$C=CHPh or H$_2$C=CH(4-C$_6$H$_4$NO$_2$) with the (unisolated) intermediate product of the reaction between [Ru(η^5-C$_5$Ph$_5$)(CO)$_2$Br] (**130**) and NaBH$_4$, which is presumably a metal hydride. Further reaction of [Ru(η^5-C$_5$Ph$_5$)(CO)$_2${(*Z*)-HC=CH(4-C$_6$H$_4$NO$_2$)}] (**157**) with PMe$_2$Ph and Me$_3$NO gives orange [Ru(η^5-C$_5$Ph$_5$)(CO){(*Z*)-HC=CH(4-C$_6$H$_4$NO$_2$)}PMe$_2$Ph] (**158**) in 64% yield. Compounds [Ru(η^5-C$_5$Ph$_5$)(CO)$_2${(*Z*)-HC=CHR}] (R = Ph (**156**) (Fig. 43), R = 4-C$_6$H$_4$NO$_2$ (**157**) (Fig. 42)) have typical "piano-stool" structures; the Ru-(C$_5$-ring centroid) distance is 1.93(5) Å in both instances. However, inclusion of an electron-withdrawing nitro group in **157** results in a marked shortening of the Ru–CO distance that is approximately normal to the vinyl group (1.786(13) Å *vs.* 1.864(14) Å for the remaining carbonyl). The reversible oxidation of [Ru(η^5-C$_5$Ph$_5$)(CO){(*Z*)-HC=CH(4-C$_6$H$_4$NO$_2$)}PMe$_2$Ph] (**158**) contrasts with the irreversible oxidations at more positive potentials of the dicarbonyls **156** and **157**. A large quadratic non-linearity is observed for [Ru(η^5-C$_5$Ph$_5$)(CO){(*Z*)-HC=CH(4-C$_6$H$_4$NO$_2$)}PMe$_2$Ph] (**158**), significantly greater than those observed for **156** and **157**.

A similar reaction between [Ru(η^5-C$_5$Ph$_5$)(CO)$_2$Br] (**130**), NaBH$_4$, and phenyl acetylene, gave [Ru(η^5-C$_5$Ph$_5$)(CO)$_2$C≡CPh] (**159**), which was structurally characterized (Fig. 44) [148].

The complexes [Ru{η^5-C$_5$Ph$_4$(2,5-(MeO)$_2$C$_6$H$_3$)}(CO)$_2$Br] (**160**) and [Ru{η^5-C$_5$Ph$_4$(2,5-(MeO)$_2$C$_6$H$_3$)}(CO)]$_2$(μ-CO)$_2$ (**161**) have also been prepared [120].

In contrast to the syntheses of the pentaphenylcyclopentadienyl-*aza*-ferrocenes described above, the ruthenium analogue, [Ru(η^5-C$_5$Ph$_5$)(η^5-C$_4$H$_4$N)] (**162**), was prepared as a tan solid in 45% yield by a variant on the synthesis of pentaphenylruthenocenes (**152**–**155**) (Scheme 61) [144].

Introduction of the sulfoxide by lithiation of the heterocycle (Scheme 62) gave only one diastereomer. Cleavage of the sulfoxide

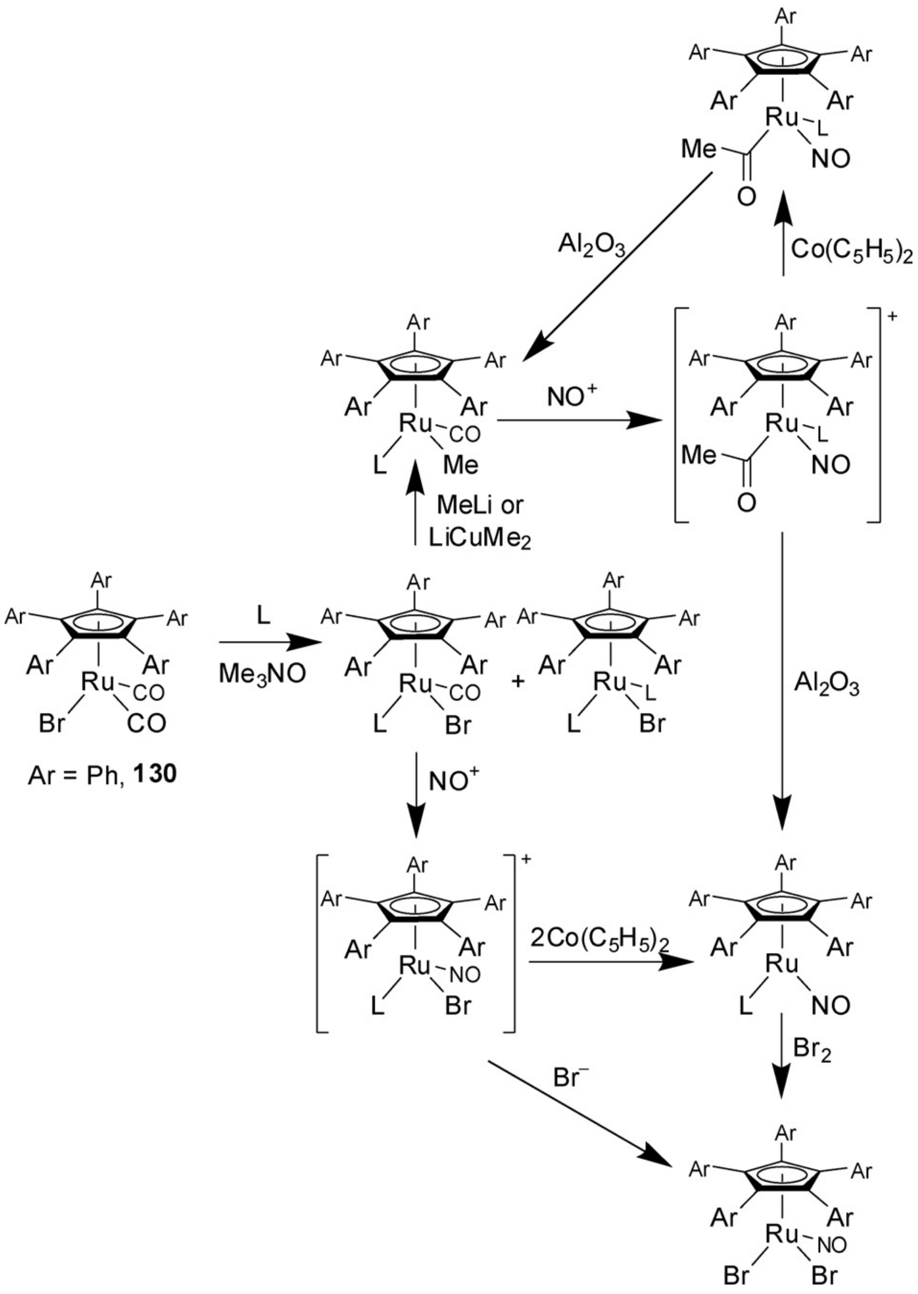

Scheme 59.

and trapping of the chiral anion with I_2 or paraformaldehyde, produced the chiral pentaphenylcyclopentadienyl-*aza*-ruthenocenes, R = I (**163**), CH_2OH (**164**), with *ee* values of 99 and 85%, respectively, the latter attributed to a combination of the steric demands of the $C_5Ph_5^-$ ligand, and the electrophilicity of the paraformaldehyde [144].

2.6.3. Osmium complexes

Cyclopentadienyl and substituted cyclopentadienyl complexes of osmium are relatively rare. Most have been prepared from Os(II) or Os(IV) precursors, either directly, or prepared *in situ*. The first reported osmium pentaphenylcyclopentadienyl complexes were $[Os(\eta^5\text{-}C_5Ph_5)(CO)_2Br]$ (**29**), and the

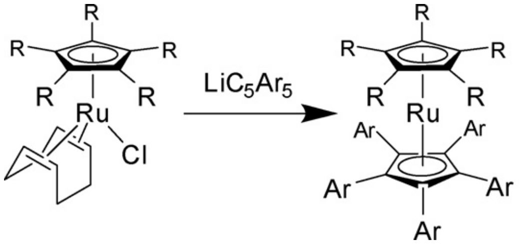

Ar = Ph, R = H, **152**
Ar = *p*-tolyl, R = H, **153**
Ar_5 = Ph_4H, R = H, **154**
Ar = Ph, R = Me, **155**

Scheme 60.

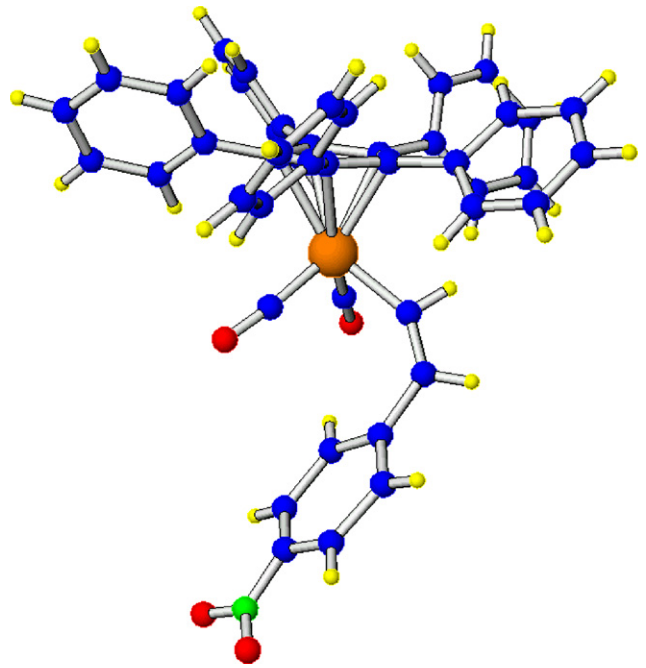

Fig. 42. Structure of $[Ru(\eta^5\text{-}C_5Ph_5)(CO)_2\{(Z)\text{-}HC{=}CH(4\text{-}C_6H_4NO_2)\}]$ (**157**) [147].

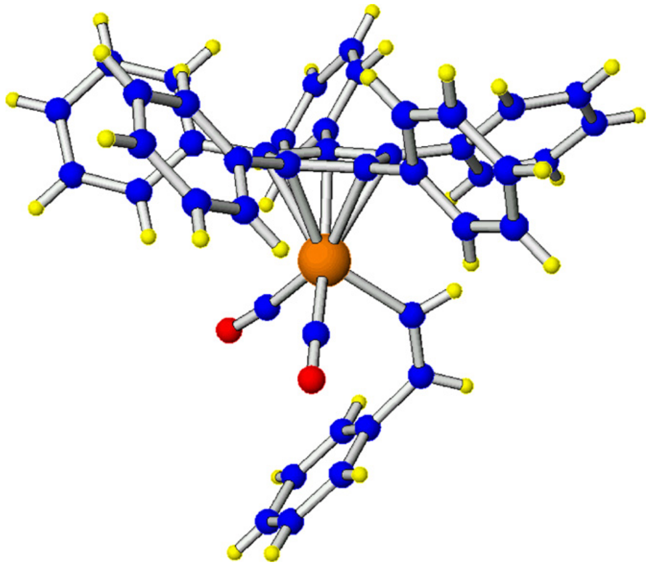

Fig. 43. Structure of $[Ru(\eta^5\text{-}C_5Ph_5)(CO)_2\{(Z)\text{-}HC{=}CHPh\}]$ (**156**) [147].

related, $[Os\{\eta^5\text{-}C_5Ph_4(4\text{-}Bu^tC_6H_4)\}(CO)_2Br]$ (**165**), $[Os\{\eta^5\text{-}C_5(p\text{-}tol)_5\}(CO)_2Br]$ (**166**) (Scheme 63) and $[Os(\eta^5\text{-}C_5Ph_5)(CO)(Br)L]$ (L = PMe_2Ph (**167**), $P(OEt)_3$ (**168**), $P(OCH_2)_3CCH_3$ (**169**) and $C{\equiv}NBu^t$ (**170**)), prepared by Me_3NO-mediated CO substitution of the dicarbonyl (Scheme 64). The archetypal $[Os(\eta^5\text{-}C_5Ph_5)(CO)_2Br]$ (**29**) was obtained in 65% yield as an air-stable, pale yellow solid from the formal oxidative addition of C_5Ph_5Br (**3**) to $Os_3(CO)_{12}$ in chlorobenzene at reflux [23af]. The use of chlorobenzene as solvent is crucial in that the reaction in toluene leads to low yields and a novel reaction between the ligand (or a radical generated *in situ*) and the solvent, to generate 1-benzyl-1,2,3,4,5-pentaphenylcyclopenta-2,4-diene (**27**) (*vide supra*, Section 1.1.3.7).

As does the isostructural $[M(\eta^5\text{-}C_5Ph_5)(CO)_2Br]$ (M = Fe (**99**), Ru (**130**)), $[Os(\eta^5\text{-}C_5Ph_5)(CO)_2Br]$ (**29**) crystallizes as discrete molecules (Fig. 45) with a planar C_5 ring, a "paddle-wheel" configuration of the phenyl groups, and no unusually close intermolecular contacts; the Os-(C_5-ring centroid) distance is 1.90(5) Å.

A small amount of $[Os(\eta^5\text{-}C_5Ph_5)(CO)_2H]$ (**171**) was obtained from the synthesis of $[Os(\eta^5\text{-}C_5Ph_5)(CO)_2Br]$ (**29**). White crystals of the hydride were produced in 69% yield from the reaction of $[Os(\eta^5\text{-}C_5Ph_5)(CO)_2Br]$ (**29**) with $NaBH_4$, or from the synthesis of, *e.g.*, $[Os(\eta^5\text{-}C_5Ph_5)(CO)_2Bu]$ (**172**). The metal hydride reacts with CHX_3, to give $[Os(\eta^5\text{-}C_5Ph_5)(CO)_2X]$ (X = Cl (**173**), Br (**29**), I (**174**), Scheme 65).

2.7. *Complexes of Group 9*

2.7.1. *Cobalt complexes*

By comparison with that of iron, the penta-arylcyclopentadienyl chemistry of cobalt is relatively unexplored. Diamagnetic, crystalline $[Co(C_5Ph_5)(CO)_2]$ (**106**), the first $C_5Ph_5^-$ complex of cobalt, was reported briefly in 1983 [45a,105], and in more detail by several groups in 1986 [23e,27b,87a,149]. It is described variously as

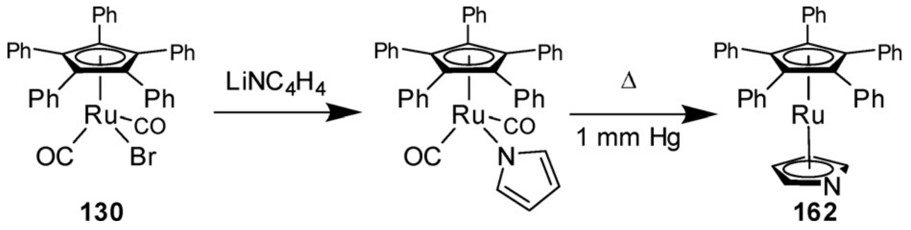

Scheme 61.

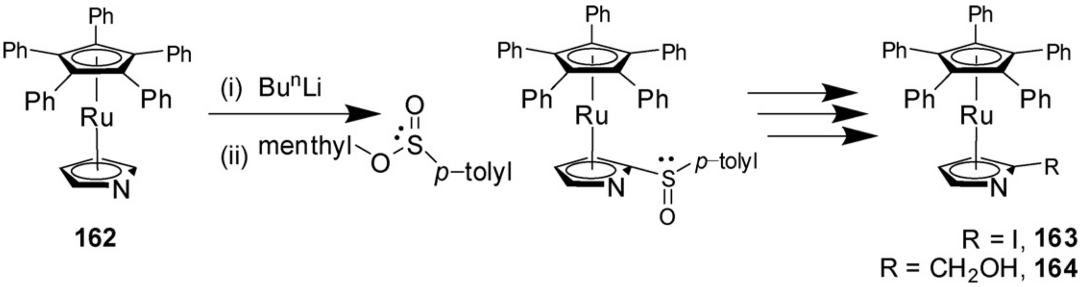

Scheme 62.

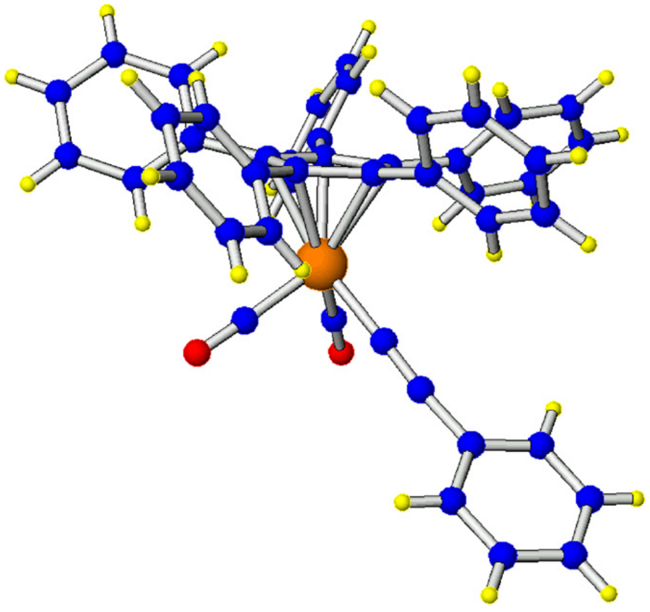

Fig. 44. Structure of [Ru(η^5-C_5Ph_5)$(CO)_2C{\equiv}CPh$] (**159**) [148].

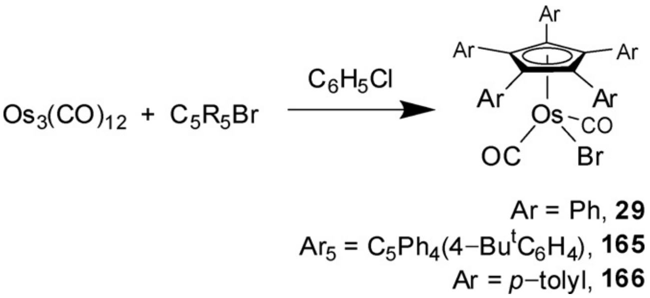

Scheme 63.

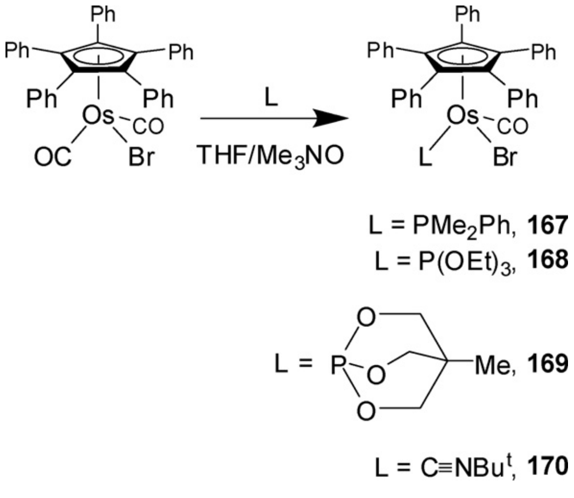

Scheme 64.

purple [23e],[4] orange [45a], or brown [87a], and can be prepared from C_5Ph_5H (**1**) and $[Co_2(CO)_8]$ in 9% yield [23e] or, in the presence of zinc dust, 65% yield [28], or from $KCo(CO)_4$ and C_5Ph_5Br (**3**) in 81% yield [45a,149]. Solid $[Co(C_5Ph_5)(CO)_2]$ (**106**) decomposes slowly in air. The solid state structure (Fig. 46) illustrates the common "paddle-wheel" orientation of the phenyl groups, which are disposed slightly to the opposite side of the C_5 ring from the cobalt atom, and are canted with respect to this ring at an average angle of 55.8°; the Co–(C_5-ring centroid) distance is 1.686(6) Å [23e].

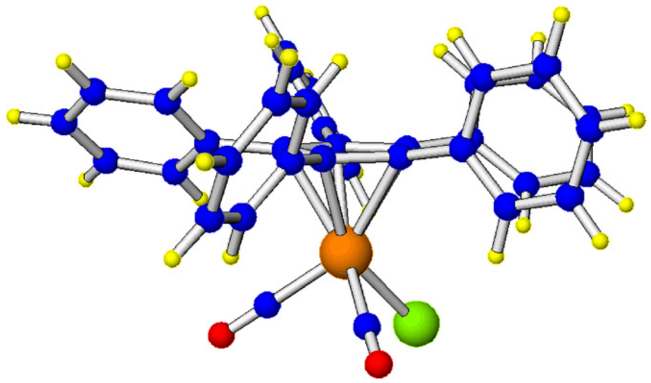

Fig. 45. Structure of [Os(η^5-C_5Ph_5)$(CO)_2$Br] (**29**) [23af].

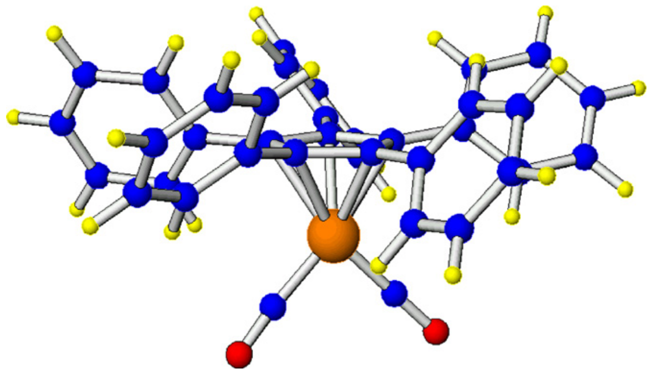

Fig. 46. Structure of $[Co(C_5Ph_5)(CO)_2]$ (**106**) [23e].

$[Co(C_5Ph_5)(CO)_2]$ (**106**) is oxidized by iodine, to produce black crystalline $[Co(C_5Ph_5)(CO)I_2]$ (**175**) in 80% yield. This can be reduced in turn by $[Co(C_5H_5)_2]$ in the presence of phosphites, to generate light brown $[Co(C_5Ph_5)(CO)P(OR)_3]$ in moderate yield (Scheme 66). Green, crystalline $[Co(C_5Ph_5)(NO)P(OR)_3]^+$ is formed in 80% yield by oxidation of $[Co(C_5Ph_5)(CO)P(OR)_3]$ with NO^+. The nitrosyl cation is reduced by $[Co(C_5H_5)_2]$ to the metal–metal bonded dimer, $[Co(C_5Ph_5)]_2(\mu\text{-}NO)_2$ (**176**), which is obtained in 94% yield as a green-brown solid, which can be oxidized by $[p\text{-}N_2C_6H_4F]PF_6$ in 75% yield to the dimeric cation, $\{[Co(C_5Ph_5)]_2(\mu\text{-}NO)_2\}^+$ (**177**), obtainable as a dark green solid (Scheme 66) [150]. The cyclic voltammetric behaviour of these compounds is consistent with these chemical electron transfers. Thus, $[Co(C_5Ph_5)(NO)P(OR)_3]^+$ is irreversibly reduced and $[Co(C_5Ph_5)]_2(\mu\text{-}NO)_2$ (**176**) undergoes two successive, reversible, one-electron oxidations (and an irreversible one-electron reduction). In marked contrast to $[Co(C_5Ph_5)_2]^{+/0}$ (*vide infra*), the replacement of H by Ph on the cyclopentadienyl ring has almost no effect on the potential of the reversible, formally Co(III/II) couple.

The thermal or photochemical reaction of $[Co(C_5Ph_5)(CO)_2]$ (**106**) with PR_3 was not observed, even in the presence of Me_3NO [27b]. However, $[Co(C_5Ph_5)(CO)_2]$ (**106**) reacts photochemically with white phosphorus and $[Cr(CO)_5(THF)]$ to form $[Co(C_5Ph_5)(\eta^4\text{-}P_4\{Cr(CO)_5\}_3)]$ (**178**) (Scheme 66) [23ab]. The crystal structure establishes the η^4-coordination of the *cyclo*-P_4 ligand to the cobalt atom and the coordination of each $Cr(CO)_5$ unit to a single phosphorus centre (Fig. 47). The angle between the P_4 and cyclopentadienyl

---

[4] The crystal used for X-ray diffraction is described as "purple", but the other reports describe $[Co(C_5Ph_5)(CO)_2]$ (**106**) as orange or brown.

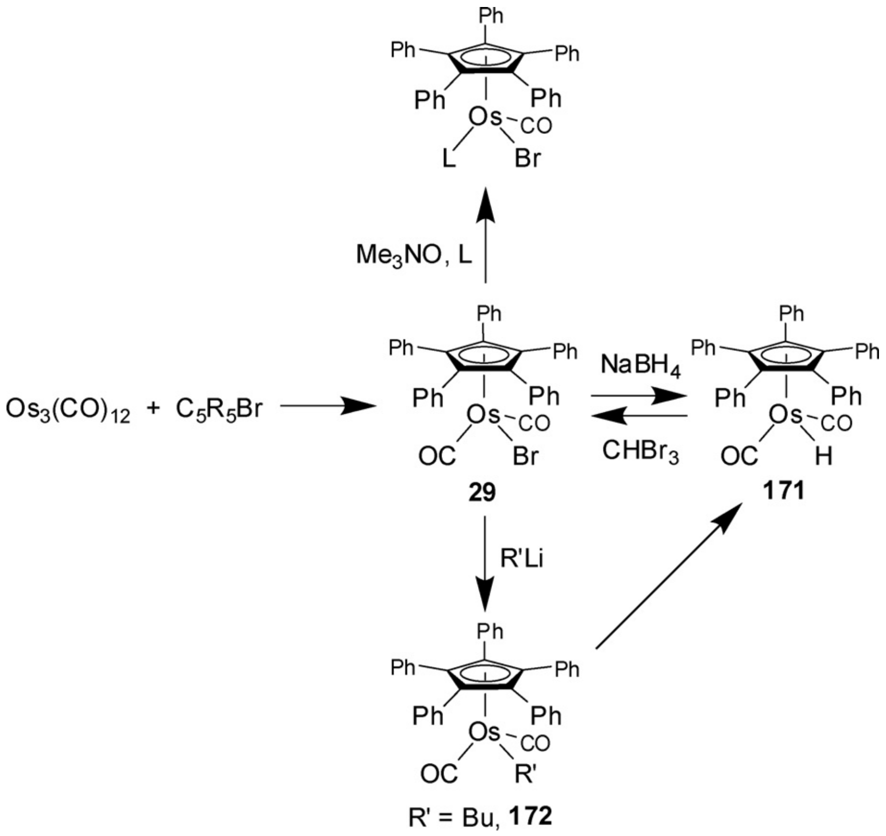

Scheme 65.

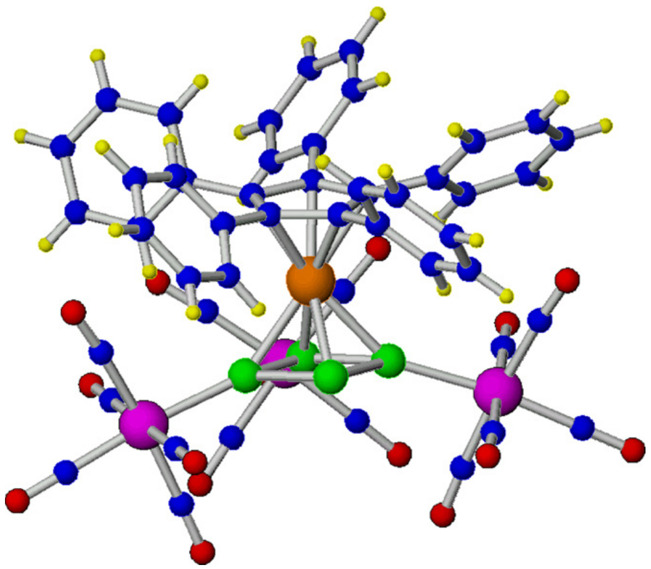

Fig. 47. Structure of $[Co(C_5Ph_5)(\eta^4-P_4\{Cr(CO)_5\}_3)]$ (**178**) [23ab].

C_5 planes (9°) is greater than that with less crowded cyclopentadienyl ligands (*e.g.*, 4° in the C_5H_5 analogue), and by contrast with less bulky cyclopentadienyl analogues, which form $[Co(C_5R_5)(\eta^4-P_4\{Cr(CO)_5\}_4)]$ through the intermediacy of the bicyclotetraphosphane complexes, $[Co(C_5R_5)(CO)(\eta^{1:1}-P_4)\{Cr(CO)_5\}_4]$, the $C_5Ph_5^-$ compound loses $Cr(CO)_5$ units in solution, to form $[Co(C_5Ph_5)(\eta^4-P_4\{Cr(CO)_5\}_2)]$ (**179**).

$[Co(C_5Ph_5)(CO)_2]$ (**106**) undergoes an electrochemically irreversible oxidation, but is reversibly reduced to the anion, $[Co(C_5Ph_5)(CO)_2]^-$, at −2.04 V (*vs.* $Fc^{+/0}$). The anion is reasonably long-lived (slowly liberating $C_5Ph_5^-$) and can be generated electrolytically or chemically with sodium naphthalenide [87a]. This behaviour contrasts significantly with that of $[Co(C_5H_5)(CO)_2]$, which undergoes a one-electron reduction to $\{[Co(C_5H_5)]_2(\mu-CO)_2\}^-$, which reacts readily with electrophiles. The radical anion, $[Co(C_5H_5)(CO)_2]^{\bullet -}$, is significantly less stable than $[Co(C_5Ph_5)(CO)_2]^{\bullet -}$, the former is only isolated in a frozen matrix [151]. DFT calculations on $[Co(C_5Ph_5)(CO)_2]^{\bullet -}$ have been discussed briefly in the context of an extensive evaluation of the differences between the calculated and observed ESR hyperfine coupling constants for the $[Co(C_5H_5)(CO)_2]^{\bullet -}$ anion [152]. The complexes $[Co(C_5Ph_5)(CO)P(OR)_3]$ undergo reversible one-electron oxidations to the cations, $[Co(C_5Ph_5)(CO)P(OR)_3]^+$ [27b].

Solid, air-stable, insoluble, deep-red decaphenylcobaltocene (**180**) is obtained in 39% (or 50%) yield by the reaction of anhydrous cobalt(II) bromide and two equivalents of $Li(C_5Ph_5)$ (**28**) in THF (or toluene) at reflux under nitrogen [23z,153]. Alternatively, activated cobalt can be treated with C_5Ph_5H (**1**) [153]. The stability of $[Co(C_5Ph_5)_2]$ (**180**) is in marked contrast to $[Co(C_5RR'_4)_2]$ (R = H, R′ = H, Ph; R = R′ = Me), which are sensitive to air and moisture. In the absence of structural or solution data, the *bis*(η^5) sandwich structure can be differentiated from the potential "linkage isomer" structure, by the presence of infrared absorptions at 1500, 741, 713 and 699 cm^{-1}, observed in the IR spectra of $[M'(C_5Ph_5)_2]$ (M′ = Fe (**112**), Ni (**113**)), but not in that of the linkage isomer, $[Fe(\eta^5-C_5Ph_5)\{(\eta^6-C_6H_5)(C_5Ph_4)\}]$ (**40**). Oxidation with $NOBF_4$ in methylene chloride produces air-stable, dark orange, crystalline $[Co(C_5Ph_5)_2]BF_4$ (**181**) in 92% yield [23w]. The crystal structure (Fig. 48) confirms the decaphenylmetallocene conformation, expected from the infrared spectroscopic absorptions at 1501, 744, 712, and 699 cm^{-1} (*vide supra*), and possesses the familiar S_{10}

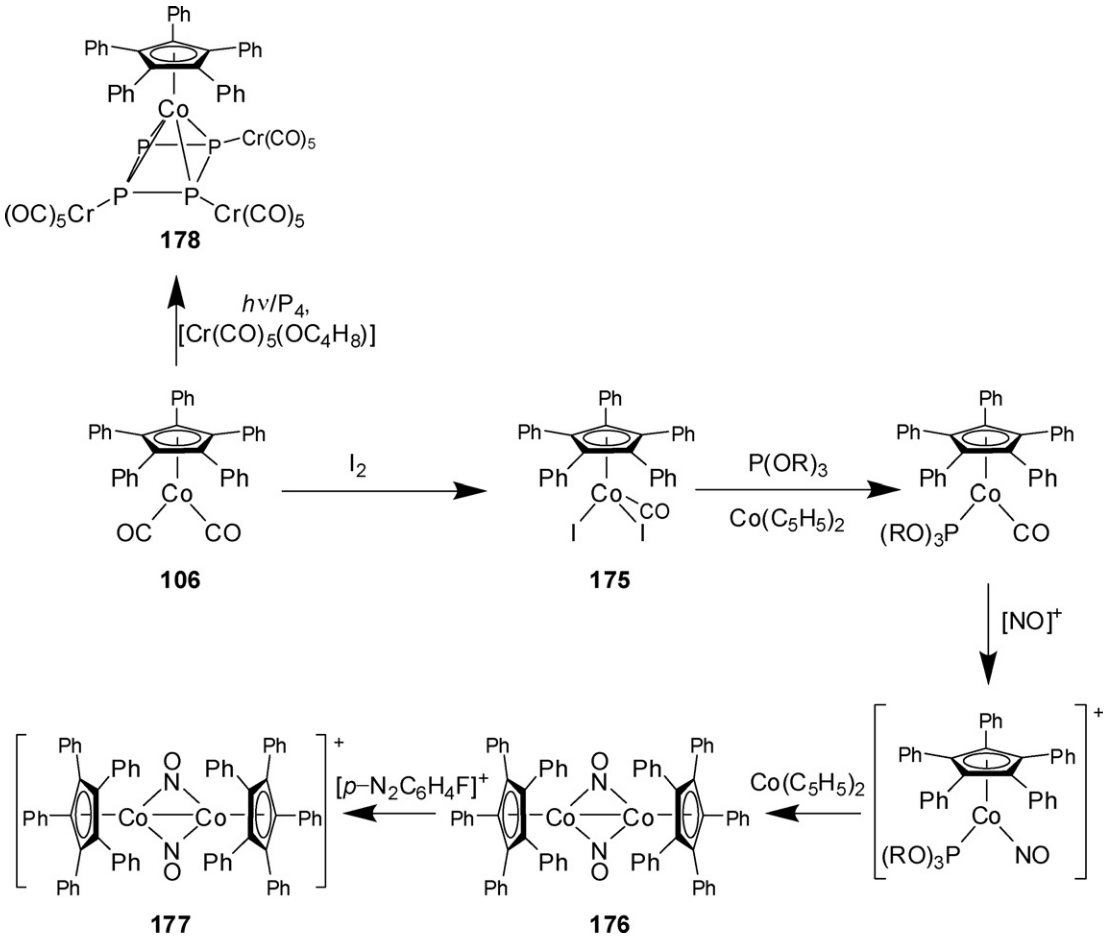

Scheme 66.

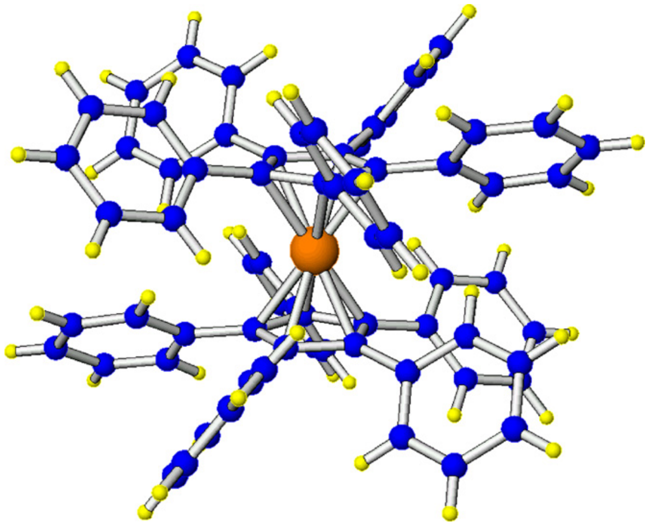

Fig. 48. Structure of $[Co(C_5Ph_5)_2]^+$ as its BF_4^- salt (**181**) [23z].

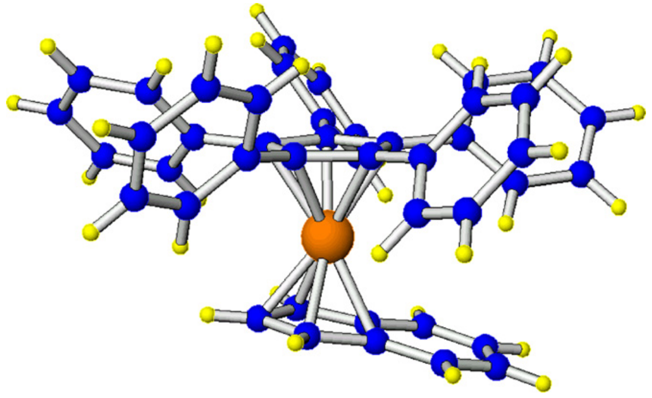

Fig. 49. Structure of $[Co(\eta^5\text{-}C_5Ph_5)(\eta^5\text{-}C_9H_7)]^+$ as its BF_4^- salt (**182**) [23ai].

molecular symmetry [23z]. The Co–(C_5-ring centroid) distance of 1.750(5) Å is significantly longer than the Fe–(C_5-ring centroid) distance of the isoelectronic $[Fe(C_5H_5)_2]$ (1.654 Å) [154], possibly a consequence of significant inter-ligand phenyl/phenyl interactions in the former. Confirmation of this effect is found in the 1.664 Å Co–(C_5-ring centroid) distance of $[Co(\eta^5\text{-}C_5Ph_5)(\eta^5\text{-}C_9H_7)]BF_4$ (**182**) and the 11° angle between the $C_5Ph_5^-$ and indenyl planes (Fig. 49) [23ai]; the Fe-(C_5-ring centroid) distance observed for d^5 $[Fe(\eta^5\text{-}C_5Ph_5)_2]Br_3$ (**114**) (1.807(5) Å) also illustrates the steric effect [126d]. Decaphenylcobaltocene (**180**) undergoes a reversible one-electron oxidation at −0.88 V (*vs.* $Fc^{+/0}$), and is therefore much harder to oxidize than cobaltocene or decamethylcobatocene (−1.25 V and −1.88 V, respectively, *vs.* $Fc^{+/0}$) [108]. An additional reversible electrode process, formally the $[Co(C_5Ph_5)_2]^{0/-}$ couple, is observed at −1.74 V (*vs.* $Fc^{+/0}$). This can be compared with the analogous reversible $[Co(C_5H_5)_2]^{0/-}$ couple at −2.19 V (*vs.* $Fc^{+/0}$) (Eq. (14)) [155]. The following reversible electron transfer series is

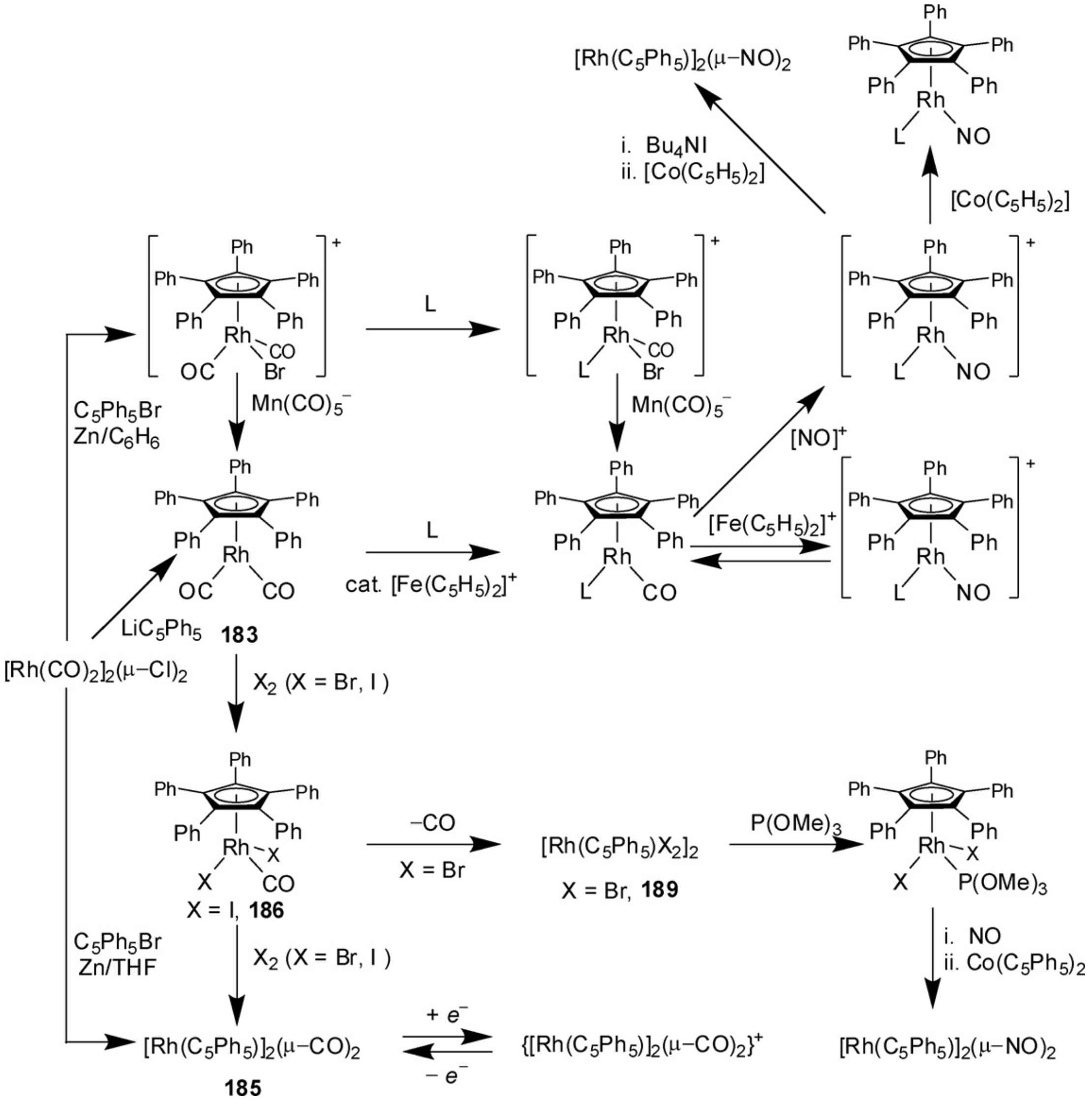

Scheme 67.

therefore observed:

$$\underset{\mathbf{181}}{[\mathrm{Co}(\eta^5\text{-}\mathrm{C}_5\mathrm{Ph}_5)_2]^+} \overset{-880\,\mathrm{mV}}{\rightleftarrows} \underset{\mathbf{180}}{[\mathrm{Co}(\eta^5\text{-}\mathrm{C}_5\mathrm{Ph}_5)_2]} \overset{-1740\,\mathrm{mV}}{\rightleftarrows} [\mathrm{Co}(\eta^5\text{-}\mathrm{C}_5\mathrm{Ph}_5)_2]^- \qquad (14)$$

2.7.2. Rhodium complexes

Although decaphenylcyclopentadienyl complexes of rhodium have not been reported, orange crystals of [Rh(η^5-C_5Ph_5)$(CO)_2$] (**183**) are prepared in 13–30% yields by the reaction of $C_5Ph_5^-$ salts with $[Rh(CO)_2]_2(\mu\text{-}Cl_2)_2$ in THF (Scheme 67) [23d,e]. Alternatively, a 30% yield is obtained from the reaction of $[Rh(CO)]_2(\mu\text{-}Cl_2)_2$ with C_5Ph_5Br (**3**) and zinc dust in THF. If this latter reaction is conducted in benzene, brick-red crystals of incompletely characterized [Rh(η^5-C_5Ph_5)$(CO)_2$Br][$ZnCl_3$] (**184**) are isolated in 50% yield [27b]. This salt is converted to [Rh(η^5-C_5Ph_5)$(CO)_2$] (**183**) by treatment with [N$(PPh_3)_2$][Mn$(CO)_5$]. The structure of [Rh(η^5-C_5Ph_5)$(CO)_2$] (**183**) is a typical "two-legged piano stool" (Fig. 50) [23d]. A second, blue, material was obtained from the MC_5Ph_5/[Rh(η^5-C_5Ph_5)$(CO)_2$] reaction [23e]. This is arguably [Rh(η^5-C_5Ph_5)$]_2(\mu\text{-}CO)_2$ (**185**), which is also a side product of the C_5Ph_5Br/[Rh(η^5-C_5Ph_5)$(CO)_2$]/Zn reaction, but which is best prepared as an impure dark green solid (in 19% yield) by cobaltocene reduction of [Rh(η^5-C_5Ph_5)(CO)I_2] ((**186**), prepared in 85% yield as a black crystalline solid by the oxidation of [Rh(η^5-C_5Ph_5)$(CO)_2$] (**183**) with I_2 in hexane/toluene) [27b].

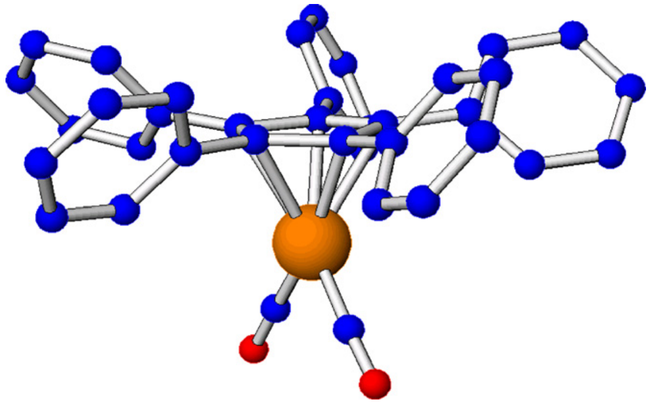

Fig. 50. Structure of [Rh(η^5-C_5Ph_5)$(CO)_2$] (hydrogen atoms omitted) (**183**) [23d].

The complex, [Rh(η^5-C_5Ph_5)$(CO)_2$] (**183**), undergoes two irreversible, one-electron oxidations [27b]. In the presence

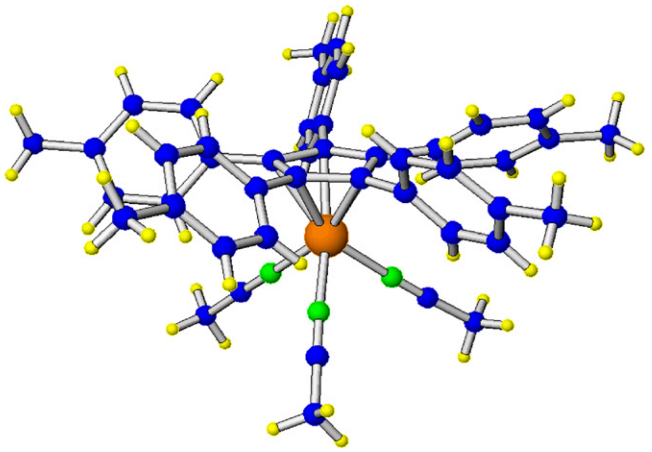

Fig. 51. Structure of the [Rh{η^5-C_5(*p*-tol)$_5$}(N≡CMe)$_3$]$^+$ (**188**) cation [23ai].

of phosphine or phosphite ligands, L, the radical cations, [Rh(η^5-C_5Ph_5)(CO)L]$^{\bullet +}$, are generated, and undergo reversible, one-electron reductions to [Rh(η^5-C_5Ph_5)(CO)L], which can be prepared from the dicarbonyl by an oxidative substitution, catalyzed by the $Fc^{+/0}$ couple (Scheme 67). The radical cations, [Rh(η^5-C_5Ph_5)(CO)L]$^{\bullet +}$, were studied *in situ*, and are significantly more stable than their $C_5R_5^-$ (R = H, Me) analogues. The analogous nitrosyl radical cations, [Rh(η^5-C_5Ph_5)(NO)L]$^{\bullet +}$, can be isolated in ~90% yield as their red PF_6^- salts (Scheme 67), which undergo reversible, one-electron reductions or chemical reduction to [Rh(η^5-C_5Ph_5)(NO)L] [150]. One-electron reduction, either chemically or electrochemically, of the “parent”, [Rh(η^5-C_5Ph_5)(CO)$_2$] (**183**), yields anion radicals, [Rh(η^5-C_5Ph_5)(CO)$_2$]$^{\bullet -}$, which are also of considerably greater stability than their $C_5R_5^-$ (R = H, Me) analogues [27b].

Yellow crystals of the useful synthetic intermediates, [Rh(η^5-C_5Ar_5)(N≡CMe)$_3$]$^+$ (Ar = Ph (**187**), *p*-tol (**188**)) have been prepared in 80–90% yield by the reactions of Ag^+ with [Rh(η^5-C_5Ar_5)(CO)I_2] (**186**) (90% yield) or [Rh(η^5-C_5Ph_5)Br_2]$_2$ (**189**) in acetonitrile (Scheme 68) [23ai].

Crystalline [Rh(η^5-C_5Ar_5)(N≡CMe)$_3$]$^+$ has the typical “three-legged piano stool” structure, with the phenyl rings canted in a propeller fashion around the C_5 ring (Fig. 51) [23ai].

Reaction of the [Rh(η^5-C_5Ar_5)(N≡CMe)$_3$]$^+$ complexes with $C_5R_5^-$ salts generates salts of the metallocenium cations, [Rh(η^5-C_5Ar_5)(η^5-C_5R_5)]$^+$ (Ar = Ph, *p*-tol; R = H, Me) in high yield as white solids [23ai].

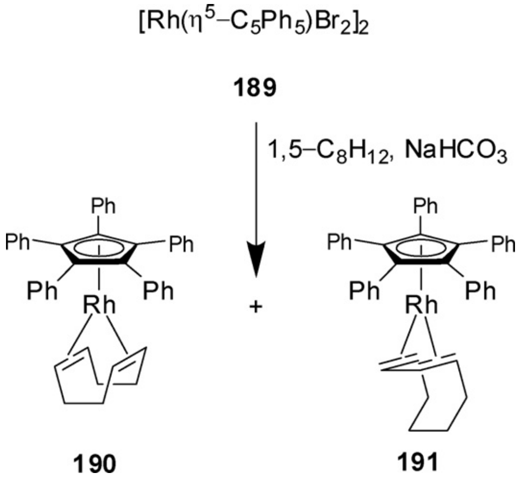

Scheme 69.

The rhodium cyclo-octadiene complexes, orange-yellow [Rh(η^5-C_5Ph_5)(η^4-1,5-C_8H_{12})] (**190**), and orange [Rh(η^5-C_5Ph_5)(η^4-1,3-C_8H_{12})] (**191**, a rare example of Rh-ligated 1,3-COD) were prepared in 71% yield as a 1:4 mixture from the reaction of [Rh(η^5-C_5Ph_5)Br_2]$_2$ (**189**) with 1,5-C_8H_{12} and base at room temperature (Scheme 69); they can be separated by fractional crystallization. Alternatively, the reaction of C_5Ph_5H (**1**) with [Rh(1,5-COD)]$_2$(μ-Cl)$_2$ gives [Rh(η^5-C_5Ph_5)(η^4-1,5-C_8H_{12})] (**190**) exclusively in 8.5% yield [22,87c].

The two compounds exist as discrete molecules with the typical “propeller” orientation of the phenyl groups (**191**, Fig. 52, Rh–(C_5-ring centroid) = 1.894(5) Å, and **190**, Fig. 53, Rh–(C_5-ring centroid) = 1.928(5) Å) [22]. The series supports oxidation states of Rh(0), (I), (II) and (III).

[Rh(η^5-C_5Ph_5)(η^4-1,5-C_8H_{12})] (**190**) undergoes two reversible one-electron oxidations at +0.09 V and +0.72 V (*vs.* $Fc^{+/0}$). The isomeric [Rh(η^5-C_5Ph_5)(η^4-1,3-C_8H_{12})] (**191**), is easier to oxidize, and undergoes two reversible one-electron oxidations at −0.01 V and +0.25 V (*vs.* $Fc^{+/0}$). The thermodynamic stabilization of the higher oxidation state complexes of the1,3-COD isomer is attributed to the formation of an agostic Rh–(C–H) interaction that is facilitated in the higher oxidation states both by the depopulation of the metal

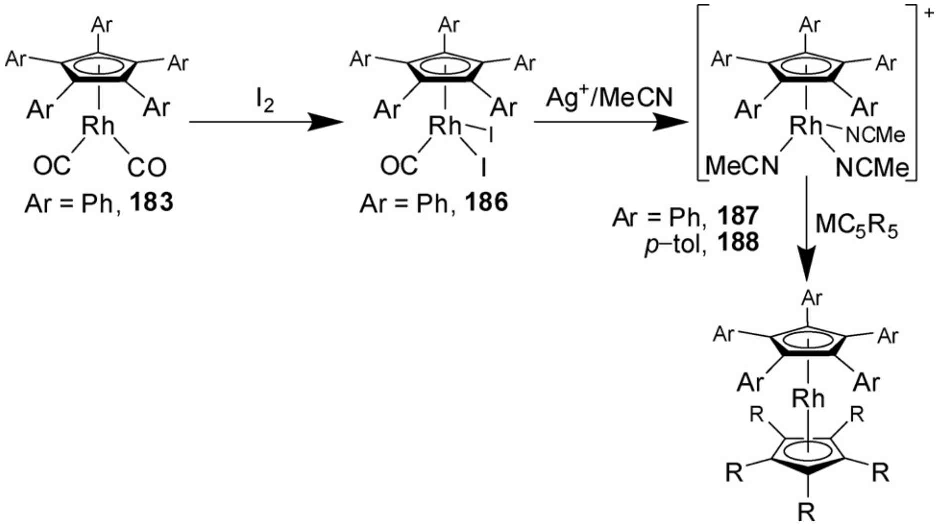

Scheme 68.

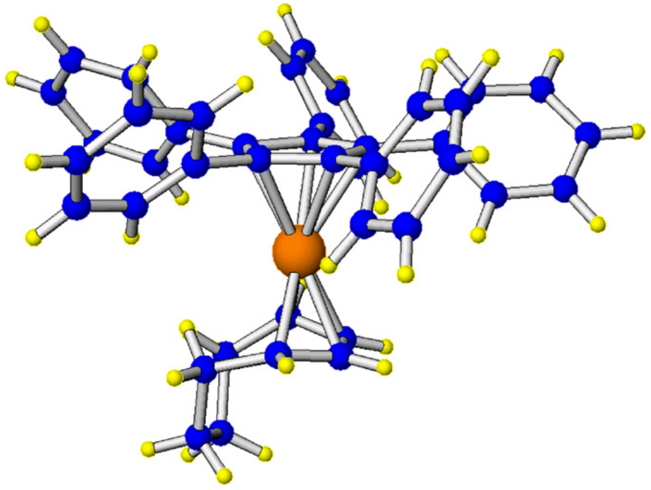

Fig. 52. Structure of [Rh(η^5-C_5Ph_5)(η^4-1,3-C_8H_{12})] (**191**) [22].

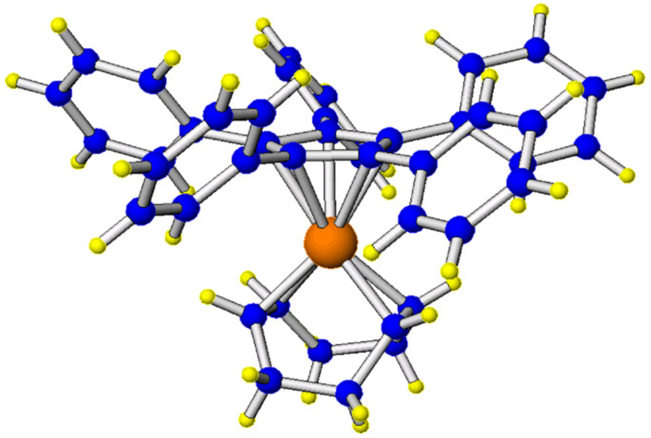

Fig. 53. Structure of [Rh(η^5-C_5Ph_5)(η^4-1,5-C_8H_{12})] (**190**) [22].

acceptor orbital, and by the orientation of the C(5)–H ring hydrogen at a distance suitable for M–H agostic interaction; there is no equivalent orientation in the 1,5-COD isomer. Both compounds are reduced (at −3.17 V and −3.08 V, respectively), to unstable anions that lose $C_5Ph_5^-$ upon reduction.

The 17-electron species, purple [Rh(η^5-C_5Ph_5)(η^4-1,5-C_8H_{12})]$^{\bullet+}$, and green [Rh(η^5-C_5Ph_5)(1,3-η^4-C_8H_{12})]$^{\bullet+}$, and the 16-electron dications, green [Rh(η^5-C_5Ph_5)(η^4-1,5-C_8H_{12})]$^{2+}$ and [Rh(η^5-C_5Ph_5)(η^4-1,3-C_8H_{12})]$^{2+}$, were prepared by bulk electrolysis or chemical oxidation, and, although sufficiently stable for UV-spectroscopic and ESR experiments, were not isolated. The very considerable kinetic stabilization of the oxidized products by comparison with less highly substituted cyclopentadienyl analogues was attributed to the steric influence of the $C_5Ph_5^-$ ligands.

The coordinated COD ligand isomerizes from the 1,3- to the 1,5-isomer in the higher oxidation states (Scheme 70).

2.7.3. Iridium complexes

No iridium penta-arylcyclopentadienyl complexes have been reported.

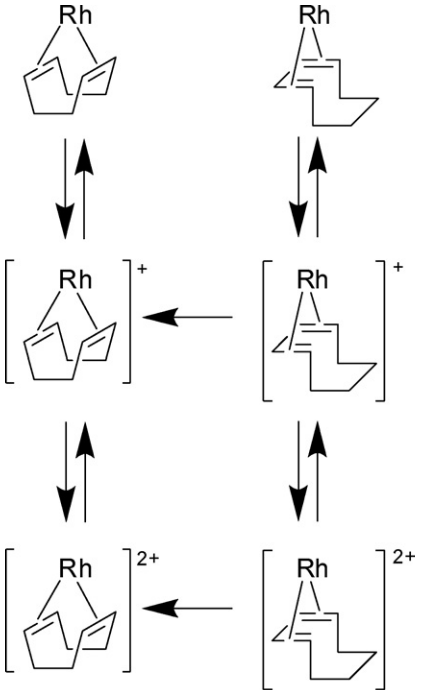

Scheme 70.

2.8. Complexes of Group 10

2.8.1. Nickel complexes

Air-stable, brown, decaphenylnickelocene (**113**) was first prepared in 85% yield by reaction of the 1,2,3,4,5-pentaphenylcyclopentadienyl radical (**4**) with [Ni(COD)$_2$] [156]. It can also be conveniently prepared in 40% yield by treatment of [Ni(CO)$_2$(PPh$_3$)$_2$] with 5-bromo-1,2,3,4,5-pentaphenylcyclopenta-1,3-diene (**3**) in THF in the presence of zinc dust [23w,126d]. The apparent diamagnetism of the nickel complex [156], which contrasts with the paramagnetism of nickelocene [157], is a consequence of the large diamagnetic correction of the ligands [23w]. Black-purple crystals of the decaphenylnickelocenium cation, [Ni(η^5-C_5Ph_5)$_2$]$^+$ (**192**), are produced in 87 or 79% yield, by oxidation of decaphenylnickelocene (**113**) with bromine or NOBF$_4$, respectively. The air-stability of salts of the [Ni(C_5Ph_5)$_2$]$^+$ cation again contrasts markedly with the sensitivity and reactivity of [Ni(η^5-C_5H_5)$_2$] or [Ni(η^5-C_5Ph_4H)$_2$]. In the solid state, the [Ni(C_5Ph_5)$_2$]$^+$ cation displays the typical S_{10} molecular geometry, with "paddle-wheel" configuration of the phenyl rings, where the phenyl rings are canted at an average of 48.6° with respect to the C_5 rings (Fig. 54). The Ni–(C_5-ring centroid) distance is 1.836(8) Å [23w].

In THF, [Ni(C_5Ph_5)$_2$]$^+$ (**192**) undergoes two electrochemically near reversible, one-electron transfers at +0.45 and −0.08 V (*vs.* Fc$^{+/0}$), assigned to the [Ni(C_5Ph_5)$_2$]$^{2+/+}$ and [Ni(C_5Ph_5)$_2$]$^{+/0}$ processes, respectively. These values compare with +0.36 and −0.44 V *vs.* Fc$^{+/0}$ for [Ni(C_5H_5)$_2$] in THF [158], suggesting that the $C_5Ph_5^-$ ligand stabilizes lower oxidation states better than does the $C_5H_5^-$ ligand. The [Ni(C_5Ph_5)$_2$]$^+$ cation is readily reduced to decaphenylnickelocene (**113**) with magnesium [23w].

Pentaphenylcyclopentadienylnickelocene (**193**) can be prepared in 88% yield by reaction of [Ni(C_5Ph_5)(CO)Br] (**194**) with TlC$_5$H$_5$ [149]. The half-sandwich, [Ni(C_5Ph_5)(CO)Br] (**194**), is prepared by the reaction of nickel tetracarbonyl with 5-bromo-1,2,3,4,5-pentaphenylcyclopenta-1,3-diene (**3**) [149]. It reacts with NaI to give [Ni(C_5Ph_5)(CO)I] (**195**) in 83% yield [149], or with

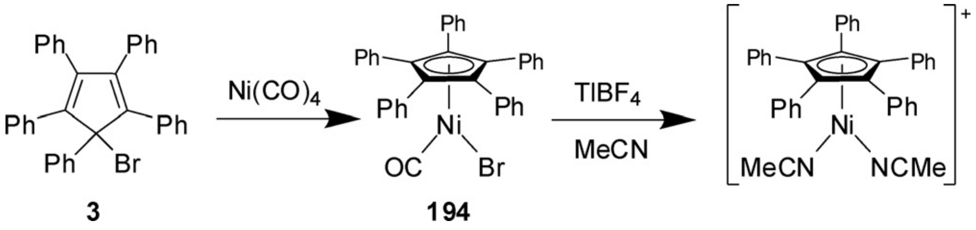

Scheme 71.

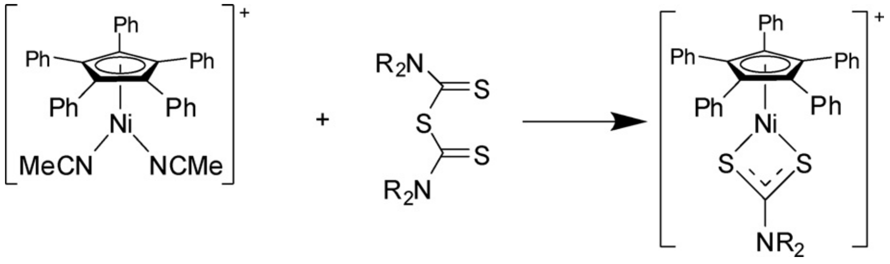

Scheme 72.

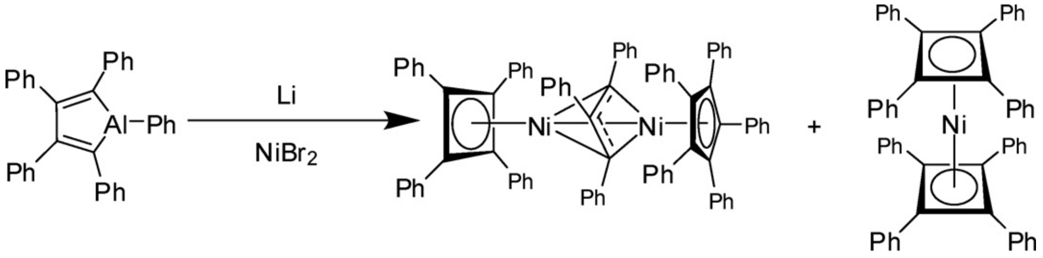

33

Scheme 73.

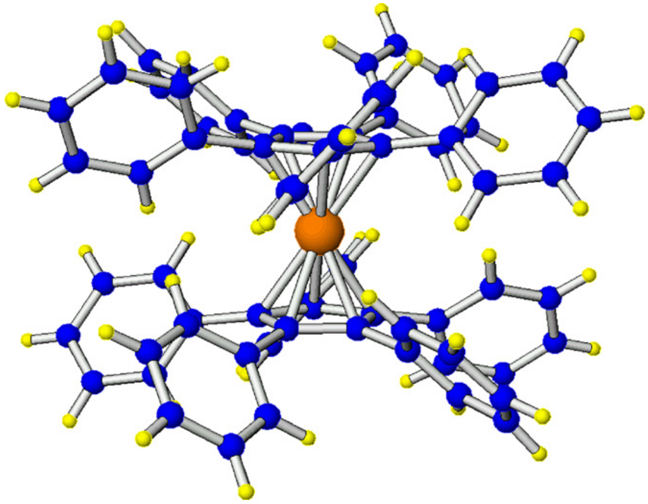

Fig. 54. Structure of $[Ni(C_5Ph_5)_2]^+$ (**192**) cation [23w].

TlBF$_4$ in acetonitrile to produce the dark red acetonitrile cation, $[Ni(C_5Ph_5)(N{\equiv}CMe)_2]^+$ (Scheme 71).

In turn, this reacts with thiuram disulfide or monosulfide to produce black crystals of the formally 17-electron, Ni(III) dithiocarbamate complex, $[Ni(C_5Ph_5)(S_2CNR_2)]^+$ in 50% yield (Scheme 72) [23i].

The red Ni(II) dithiocarbamate, $[Ni(C_5Ph_5)(S_2CNR_2)]$, is produced by reaction of $[Ni(\eta^5\text{-}C_5Ph_5)(CO)Br]$ (**194**) with NaS_2CNR_2 [23i]. The Ni(II) and Ni(III) dithiocarbamate complexes can be quantitatively interconverted by reaction with $[Fe(\eta^5\text{-}C_5H_5)_2]^+$ or $(Me_2N)_2C{=}C(NMe_2)_2$, respectively, consistent with the observation of a reversible, formally $Ni^{III/II}$ one-electron transfer process at +0.265 V *vs*. SCE. A reversible, one-electron, $Ni^{II/I}$ electron transfer is also observed at −1.43 V *vs*. SCE, although the formally Ni(I) species has not been isolated.

Reaction of a suspension of $[Ni(\eta^5\text{-}C_5Ph_5)(CO)Br]$ (**194**) and $AgClO_4$ in methylene chloride in an ultrasonic bath in an inert atmosphere produces “especially reactive”, red $[Ni(\eta^5\text{-}C_5Ph_5)(CO)]ClO_4$ (**196**) in 92% yield [23m]. The shift in the ν_{CO} absorption of $[Ni(\eta^5\text{-}C_5Ph_5)(CO)Br]$ (**194**) from 2070 to 2083 cm^{-1} provides a convenient means to monitor the reaction. The infrared absorptions at 1599 and 1443 cm^{-1}, typical of an η^5-bound C_5Ph_5 ligand, are observable in the product, which is soluble in methylene chloride, insoluble in hexanes, and reacts with donors such as diethyl ether or THF (Eq. (15)):

$$\underset{\mathbf{194}}{[Ni(C_5Ph_5)(CO)Br]} + Ag^+ \xrightarrow{CH_2Cl_2/N_2} \underset{\mathbf{196}}{[Ni(C_5Ph_5)(CO)]^+} + AgBr\downarrow \quad (15)$$

$[Ni(\eta^5\text{-}C_5Ph_5)(CO)]ClO_4$ (**196**) reacts with $Na[Co(C_5H_5)\{OP(OR)_2\}_3]$ (R = Me, Et, Pr) in methylene chloride to generate formally 20-electron, paramagnetic, air-stable, yellow crystals of $[Ni(C_5Ph_5)\{OP(OR)_2\}_3Co(C_5H_5)]$ (**5**) in *ca.* 70–80% yield. Solid $[Ni(C_5Ph_5)\{OP(OMe)_2\}_3Co(C_5H_5)]$ (**5**) has two unpaired electrons, consistent with the pseudooctahedral nickel centre established crystallographically (Fig. 55).

The synthesis of [Ni(η^4-C_4Ph_4)Ni(η^5-C_5Ph_5)](μ-C_3Ph_3) (**33**) by reaction of [(C_4Ph_4)AlPh]$^{2-}$$Li_2$, Al($C_4Ph_4$)Ph, and $NiBr_2$ (Scheme 73) was discussed earlier [23b].

Complexes of the type [Ni(η^5-C_5Ph_5)(η^3-allyl)] and [Ni(η^5-C_5Ph_5)(η^2-$H_2C{=}CH_2$)Me] (**197**) have been reported [159]. The olefin complex (**197**) is more thermally and kinetically stable than is the $C_5H_5^-$ analogue.

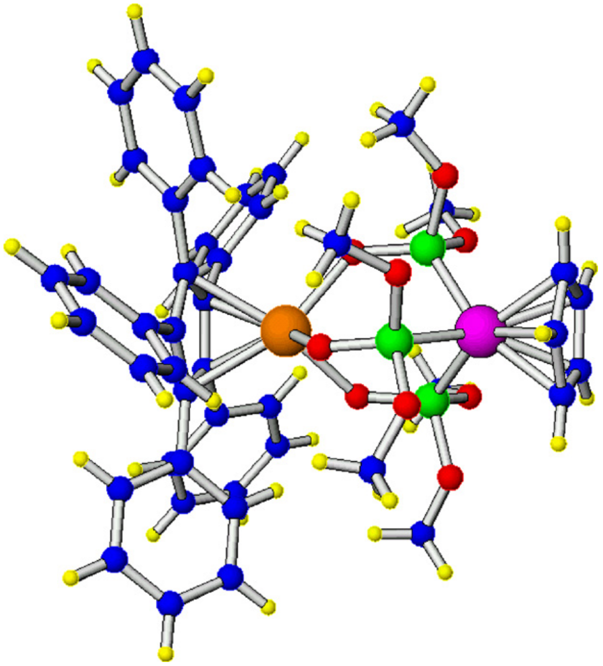

Fig. 55. Structure of one molecule of [Ni(C_5Ph_5){OP(OMe)$_2$}$_3$Co(C_5H_5)] (**5**) [23m].

The dark red/red-purple complexes, **198**, **199**, **200**, and **201**, as shown, were prepared in 70–80% yield by the reactions of [Ni(η^5-C_5Ph_5)(CO)Br] (**194**) with $Ph_2PCH_2C({=}O)R$ in the presence of 1,8-*bis*(dimethylamino)naphthalene, or with Na{$Ph_2PC{=}C(O)N(Ph)N{=}C(Me)$}under argon [23q,u].

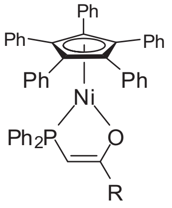

198

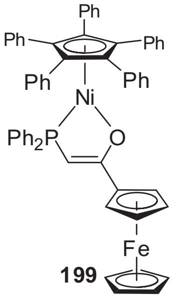

199

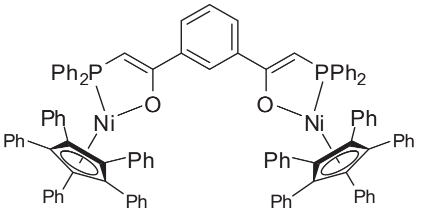

200

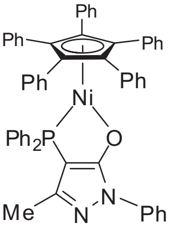

201

When activated with $NaBH_4$, **199** proved to be an effective olefin polymerization and oligomerization catalyst [160]. At 130 °C and 38 bar ethylene pressure, 40% of the olefin conversion was to polyethylene, with the remaining 60% of the substrate oligomerized with 98% selectivity to linear α-olefins. The average turnover frequency was 13 mol of ethylene per mole of catalyst per minute. Under similar conditions, with **201** as the catalyst precursor, 91% of the ethylene was oligomerized, mainly to linear olefins, of which 87% were α-olefins (turnover frequency 32 mole of ethylene per mole of catalyst per minute) [23u]. By comparison, the cyclopentadienyl analogue was active as a polymerization catalyst [23q]. Black-red crystals of the protonated derivative, [Ni(C_5Ph_5){$Ph_2PCH_2C({=}O)$}{Fe(η^5-C_5H_4)(η^5-C_5H_5)}]BF_4 (**202**), were structurally characterized (Fig. 56, Ni–(C_5-ring centroid) = 1.770(1) Å), as were crystals of Ni(η^5-C_5Ph_5) pyrazololato derivative (**201**) (Fig. 57) [23u].

In both compounds, the $C_5Ph_5^-$ and O, Ni, P planes are approximately perpendicular. Although the typical propeller arrangement of the five phenyl rings was observed in both cases, one Ni–C distance is significantly shorter than the others. The shortening of this bond was attributed to the influence of the chelating oxygen atom, which is *trans* to that carbon atom. The bonding of the ligand to the nickel is described as a σ, η^4 diene-alkyl bonding mode [23q], although the authors comment that an allyl-ene mode cannot be discounted [23u].

The nickel complexes, **198** and **199**, both undergo a quasi-reversible, apparently one-electron reduction at *ca.* −1.8 V (*vs.* $Fc^{+/0}$) [86]. They also undergo electrochemically quasi-reversible, one-electron oxidations at +0.02 and +0.18 V, respectively, assigned to the formation of a cationic Ni(III) radical [23q,86]. An additional, quasi-reversible, one-electron oxidation at −0.04 V (*vs.* $Fc^{+/0}$) for [Ni(C_5Ph_5){$Ph_2PCH{=}C(O)$}{Fe(η^5-C_5H_4)(η^5-C_5H_5)}] (**199**) is attributed to electron transfer at the ferrocenyl substituent. This process is followed by an intramolecular electron transfer, to generate a Ni(III) species. The radical that derives from **198**,

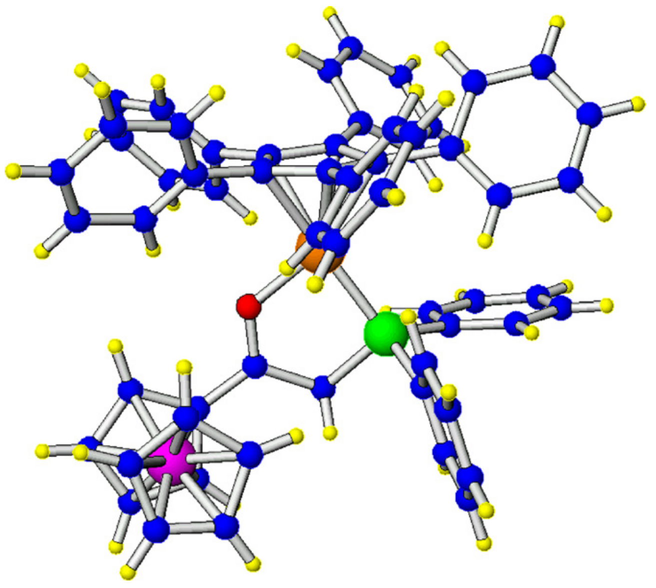

Fig. 56. Structure of the cation of [Ni(η^5-C_5Ph_5){$Ph_2PCH_2C(=O)$}{Fe(η^5-C_5H_4)(η^5-C_5H_5)}]BF_4 (**202**) [23q].

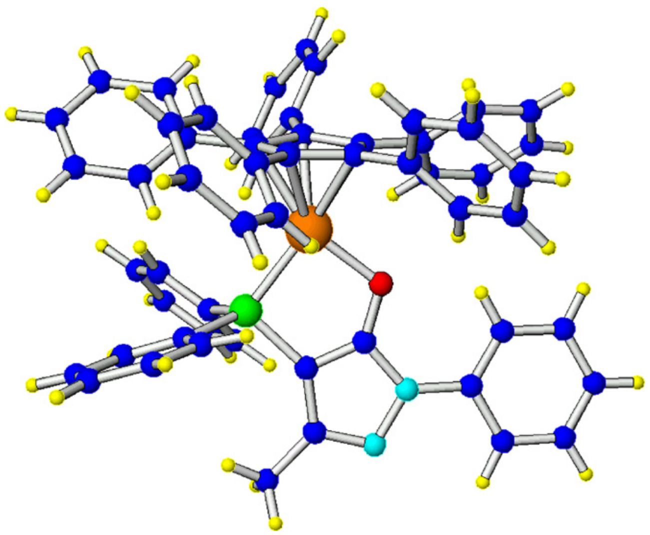

Fig. 57. Structure of the Ni(η^5-C_5Ph_5) pyrazololato derivative (**201**) [23u].

[Ni(C_5Ph_5){$Ph_2PCH{=}C(O)Ph$}]$^{\bullet+}$, is stable for at least 6 h in solution, but both radicals react irreversibly by means of electron transfer from the electron-rich enolate oxygen, to generate a cationic Ni(II) radical. Attempted chemical oxidation of **199** produces **202** [23q].

In a variant of this synthesis, reaction of [Ni(C_5Ph_5)(CO)X] (X = Br (**194**), I (**195**)) with the ylide, $Ph_3P{=}CHC(O)CH_2PPh_2$, produces red crystals of [Ni(C_5Ph_5)($Ph_2PCH_2C(O)CH{=}PPh_3$)]X in 71% (X = I (**203**)) and 85% (X = Br, (**204**)) yield [161].

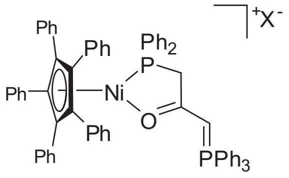

X = I, **203**
X = Br, **204**

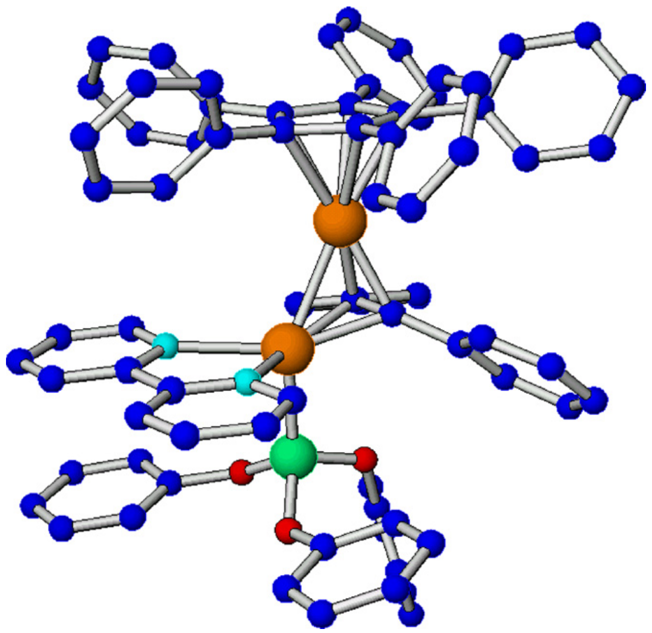

Fig. 58. Structure of the cation of {[$Pd_2(C_5Ph_5)$(bipy)$P(OPh)_3$](μ–PhC≡CPh)}(PF_6) (**206**) (hydrogen atoms omitted) [23k].

2.8.2. *Palladium complexes*

The first palladium pentaphenylcyclopentadienyl compound reported was [Pd(C_5Ph_5)]$_2$(μ-PhC≡CPh) (**31**), isolated in 33% yield (from starting palladium) as a dark green, diamagnetic solid from the reaction of PhC≡CPh with [$Pd(OAc)_2$]$_3$ in methanol (Section 1.1.3.7) [9,23a,162]. Although the structure has been determined, the structural parameters are unavailable. The Pd–Pd distance is 2.639 Å and the C–C distance of the bridging acetylene is 1.33 Å, with the Pd–(C_5 carbon) distances in the range, 2.27–2.46 Å. The complex, an example of the rare Pd(I) oxidation state, undergoes three reversible, one-electron redox processes in methylene chloride at −1.55, +0.09 and +0.70 V (*vs.* $Fc^{+/0}$) [27a,28,163], corresponding to the electron-transfer series (Eq. (16)):

$$[Pd_2]^- \overset{-1550\,\mathrm{mV}}{\rightleftarrows} [Pd_2] \overset{+90\,\mathrm{mV}}{\rightleftarrows} [Pd_2]^+ \overset{+700\,\mathrm{mV}}{\rightleftarrows} [Pd_2]^{2+} \tag{16}$$

The reduction to the monoanion is followed by a slow chemical reaction, to generate the $C_5Ph_5^-$ anion which was identified by ESR experiments and by observation of the reversible $C_5Ph_5^{0/-}$ couple at −0.73 V (*vs.* $Fc^{+/0}$). The monocation is more stable in THF. The dication, although stable on the cyclic voltammetric time-scale, decomposes on the coulometric time-scale. Chemical oxidation of neutral [Pd(C_5Ph_5)]$_2$(μ-PhC≡CPh) (**31**) by $AgPF_6$ in toluene yields dark green-black, air-stable crystals of paramagnetic {[Pd(C_5Ph_5)]$_2$(μ-PhC≡CPh)}PF_6 (**205**) in 54% yield [27a,28]. The frozen-solution ESR spectrum exhibits a single line at g = 2.044. Although neutral [Pd(C_5Ph_5)]$_2$(μ-PhC≡CPh)$^\bullet$ is unreactive, the daughter cation, {[Pd(C_5Ph_5)]$_2$(μ-PhC≡CPh)}$^+$ (**205**), undergoes a series of solvent-dependent reactions. In methylene chloride it forms green Pd(II) cleavage products, [Pd(C_5Ph_5)L_2]$^+$ (L_2 = dppe, η^4-COD, η^4-COT, η^4-dibenzocyclo-octatetraene, η^4-norbornadiene), in 27–90% yield [27a,28,87b,163,164], and, in donor solvents, purple to dark violet, asymmetric, binuclear cations, {[$Pd_2(C_5Ph_5)(L^1)(L^2)$](μ-PhC≡CPh)}$^+$ (L^1 = Me_2CO, PPh_3, $P(OPh)_3$, L^2 = bipy; L^1 = Me_2CO, PPh_3, L^2 = Me_2bipy; L^1 = Me_2CO, L^2 = phen; L^1 = N≡CMe, L^2 = PPh_3) in 40–85% yield, presumably with the intermediacy of solvato species, {[$Pd_2(solvent)_3(C_5Ph_5)_2$](μ-PhC≡CPh)}$^+$ [23k]. The structures of {[$Pd_2(C_5Ph_5)$(bipy)$P(OPh)_3$](μ-PhC≡CPh)}(PF_6) ((**206**), Fig. 58) and {[$Pd_2(C_5Ph_5)$bipy](μ-PhC≡CPh)}{[$Pd_2(C_5Ph_5)$(N≡CMe)bipy](μ-

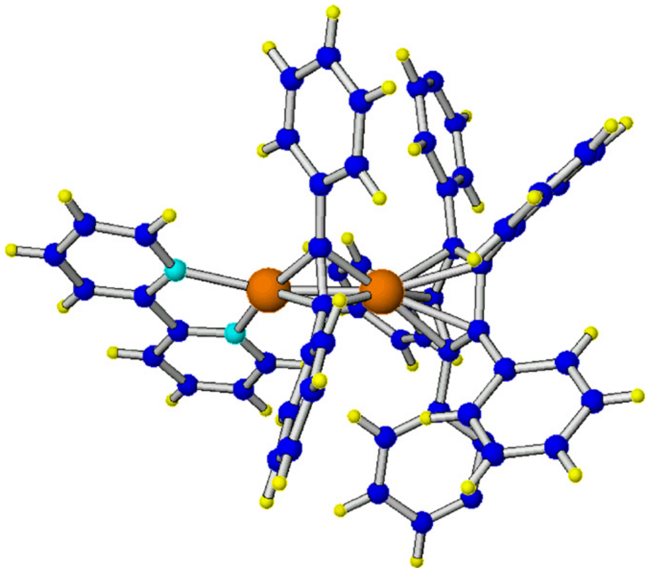

Fig. 59. Structure of the $\{[Pd_2(C_5Ph_5)bipy](\mu\text{-}PhC{\equiv}CPh)\}^+$ cation of **207** [23k].

$PhC{\equiv}CPh)\}(PF_6)_2$ ((**207**), Figs. 59 and 60) have been determined. The phenyl rings adopt the usual propeller arrangement, and are unexceptional, other than for the one phenyl ring of the $\{[Pd_2(C_5Ph_5)bipy](\mu\text{-}PhC{\equiv}CPh)\}^+$ cation that is almost perpendicular to the C_5 ring, possibly to avoid a steric clash with the bipy ligand on the other palladium atom. There is some suggestion that the $C_5Ph_5^-$ ligand may be bound in an "allyl-ene" fashion in this cation, and that the Pd–Pd interaction consists of a single bond joining a 16 valence electron Pd atom to an 18-electron Pd atom.

The cleavage reaction of the cation in poorly coordinating solvents has the following stoichiometry (Eq. (17)), in which half an equivalent of the starting neutral dimer is regenerated:

$$2\{[Pd(C_5Ph_5)]_2(\mu - PhC \equiv CPh)\}^+ + 4L \rightarrow 2[Pd(C_5Ph_5)L_2]^+$$
$$+ [Pd(C_5Ph_5)]_2(\mu - PhC \equiv CPh) + PhC \equiv CPh \qquad (17)$$

The mononuclear cations, $[Pd(C_5Ph_5)L_2]^+$, undergo electrochemically reversible, one-electron oxidations and reductions (*ca.* -0.8 V *vs.* $Fc^{+/0}$), to generate novel Pd(III) and Pd(I) $^*\pi$-complexes [27a,163]. The mononuclear Pd(I) species contrast with the more typical binuclear Pd(I) compounds, and have been prepared coulometrically. Quantitative, coulometric reduction of $[Pd(C_5Ph_5)COD]^+$ generated the neutral, formally univalent, $[Pd(C_5Ph_5)COD]$ (**208**), which was characterized in solution as a red-orange species with a solution ESR spectroscopic absorption at $g = 2.0706$ ($\langle a \rangle_{Pd}$ 25 G) [27a,87b]. Frozen solution spectra of $[Pd(C_5Ph_5)(\eta^4\text{-}C_{16}H_{12})]$ (**209**) allow the assignment of the anisotropic ESR parameters, and argue that the coordinated diene has a significant amount of radical character, with the SOMO assigned 70% metal character [163,164]. Although the complexes, $[Pd(C_5Ph_5)diene]$, have significant stability in solution, once generated, their isolation was difficult as they undergo rapid radical reactions with H, OH and OR donors, which add to one of the coordinated double bonds, to generate diamagnetic $[Pd(C_5Ph_5)(\sigma, \pi\text{-}L_2)]$ complexes (*e.g.*, Scheme 74) [87b].

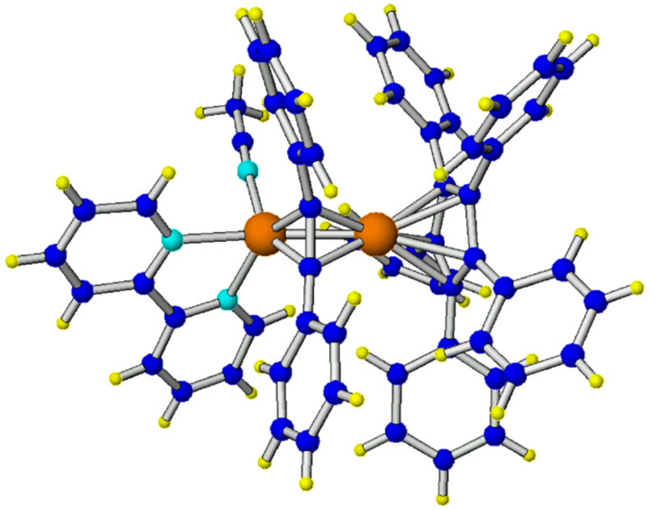

Fig. 60. Structure of the $\{[Pd_2(C_5Ph_5)(N{\equiv}CMe)bipy](\mu\text{-}PhC{\equiv}CPh)\}^+$ cation of **207** [23k].

The stability of the Pd(I) π-complexes is in marked contrast to the cyclopentadienyl analogues, a reflection of both the stabilization of lower oxidation states as a consequence of the electron-withdrawing effects of the phenyl substituents, and the greater kinetic stability of the π-complexes of the $C_5Ph_5^-$ ligand; this effect is also manifest for the Pd(III) species. The cyclooctatetraene ligand in the complexes, $[Pd(C_5Ph_5)COT]^{+/0}$, was determined to be in the 1,5-(tub-like) conformation in both oxidation states [163].

Reaction of the cleavage product, $[Pd(C_5Ph_5)COD]BF_4$ (**210**), with tri(1-cyclohepta-2,4,6-trienyl)phosphine, $P(C_7H_7)_3$, in methylene chloride at reflux, generates $[Pd(C_5Ph_5)\{P(C_7H_7)_2(\eta^2\text{-}C_7H_7)\}]BF_4$ (**211**) as a diamagnetic, dark-green powder in 74% yield [165].

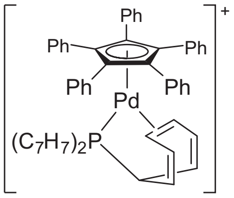

211

A range of Pd-allyl monomeric derivatives, $[Pd(C_5Ph_5)(\eta^3\text{-}allyl)]$, was obtained in ~80% yield, generally reported as red-purple crystalline solids, by the reaction of $[Pd(\eta^3\text{-}allyl)]_2(\mu\text{-}Cl)_2$ with NaC_5Ph_5 (**39**) in THF [166]. The proximity of the $C_5Ph_5^-$ phenyl groups results in a deshielding and shielding of the ^1H NMR resonances of the allyl *anti* and *syn* protons, respectively. In general, the complexes, $[Pd(C_5Ph_5)(\eta^3\text{-}allyl)]$, react with excess of the Lewis base, $P(OPh)_3$, to yield coupled products, $C_5Ph_5(allyl)$, and PdL_4. However, $[Pd(C_5Ph_5)(\eta^3\text{-}Me_2CCHCH_2)]$ (**212**) produces isoprene and C_5Ph_5H (**1**) as the organic products, and $[Pd(C_5Ph_5)(\eta^3\text{-}2\text{-}ClC_3H_4)]$ (**213**) reacts with $P(OPh)_3$, to produce allene and $[Pd(C_5Ph_5)(Cl)P(OPh)_3]$ (**214**). Thermolysis of $[Pd(C_5Ph_5)(\eta^3\text{-}2\text{-}ClC_3H_4)]$ (**213**) either in the solid state or in chloroform at reflux, or reaction of $[PdCl_2(CNR)_2]$ with NaC_5Ph_5 (**39**) in THF afforded the first example of a halo-bridged palladium cyclopentadienyl complex, $[Pd(C_5Ph_5)]_2(\mu\text{-}Cl)_2$ (**215**), which reacts reversibly with π-acid ligands, CO, $H_2C{=}CH_2$, and allene to form kinetically labile green mono-adducts, $[Pd(C_5Ph_5)(\pi\text{-}acid)Cl]$, identified spectroscopically in solution. Reduction of the chloro-bridged dimer in the presence of CO or acetylenes gives the Pd(I) dimers, $[Pd(C_5Ph_5)]_2(\mu\text{-}CO)_2$ (**216**) and $[Pd(C_5Ph_5)]_2(\mu\text{-}RC{\equiv}CR)$, respectively. These reactions are summarized in Scheme 75.

The reactions of $Li[C_5Ph_{5-n}H_n]$ with $[PdCl_2(C{\equiv}NAr)_2]$ (Ar = 2,6-$Me_2C_6H_3$; 2,4,6-$Me_3C_6H_2$, 2,4,6-$Bu_3{}^tC_6H_2$) illustrate the effects of varying the number of phenyl substituents on the cyclopentadienyl ring [23t]. With $Li[C_9H_7]$ as the reagent, mixed yields

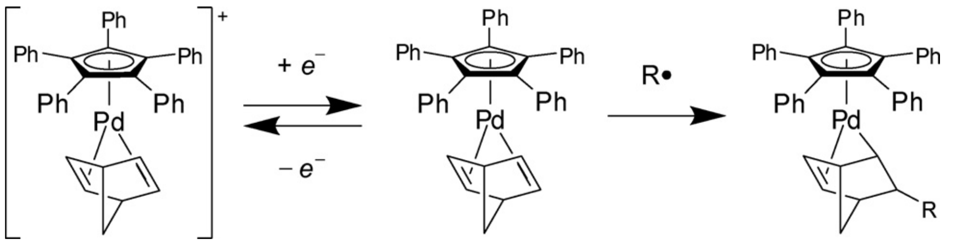

Scheme 74.

of dark red *syn*-[Pd(C≡NAr)]$_2$(μ-η^3-C$_9$H$_7$)$_2$ are obtained [167], and likewise the use of K[C$_5$Ph$_3$H$_2$] resulted in a 25–55% yield of [Pd(C≡NAr)]$_2$(μ-η^3-C$_5$H$_3$Ph$_3$)$_2$, in which η^3-bound cyclopentadienyl ligands bridge the palladium–palladium bond in a *syn* fashion, similar to the configuration observed in [Pd(PEt$_3$)]$_2$(μ-η^3-C$_5$H$_5$)$_2$ [168]. Use of the bulkier C$_5$Ph$_5$$^-$ and C$_5$Ph$_4$H$^-$ ligands, however, results in the formation of violet crystals of [Pd(η^5-C$_5$Ph$_{5-n}$H$_n$)]$_2$(μ-C≡NRAr)$_2$ in 51 (n = 0) and 21 (n = 1)% yields. The lower yield of the tetraphenylcyclopentadienyl compound is due in part to its decomposition to a 22% yield of the ketenimine, Ph$_4$C$_4$C═C═NR (**217**).

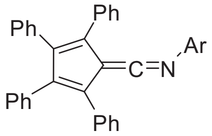

217

Purple [Pd(η^5-C$_5$Ph$_5$){η^3-CH$_2$C(CH$_2$Cl)CH$_2$}] (**218**) can be prepared in 77% yield from [Pd{η^3-CH$_2$C(CH$_2$Cl)CH$_2$}Cl]$_2$ and LiC$_5$Ph$_5$ (**28**) [23ag]. It reacts with the sulfinate anion, PhSO$_2$$^-$, to give a near quantitative yield of purple crystals of the *O*-alkylated, [Pd(η^5-C$_5$Ph$_5$){η^3-CH$_2$C(CH$_2$OS(═O)Ph)CH$_2$}] (**219**) exclusively,

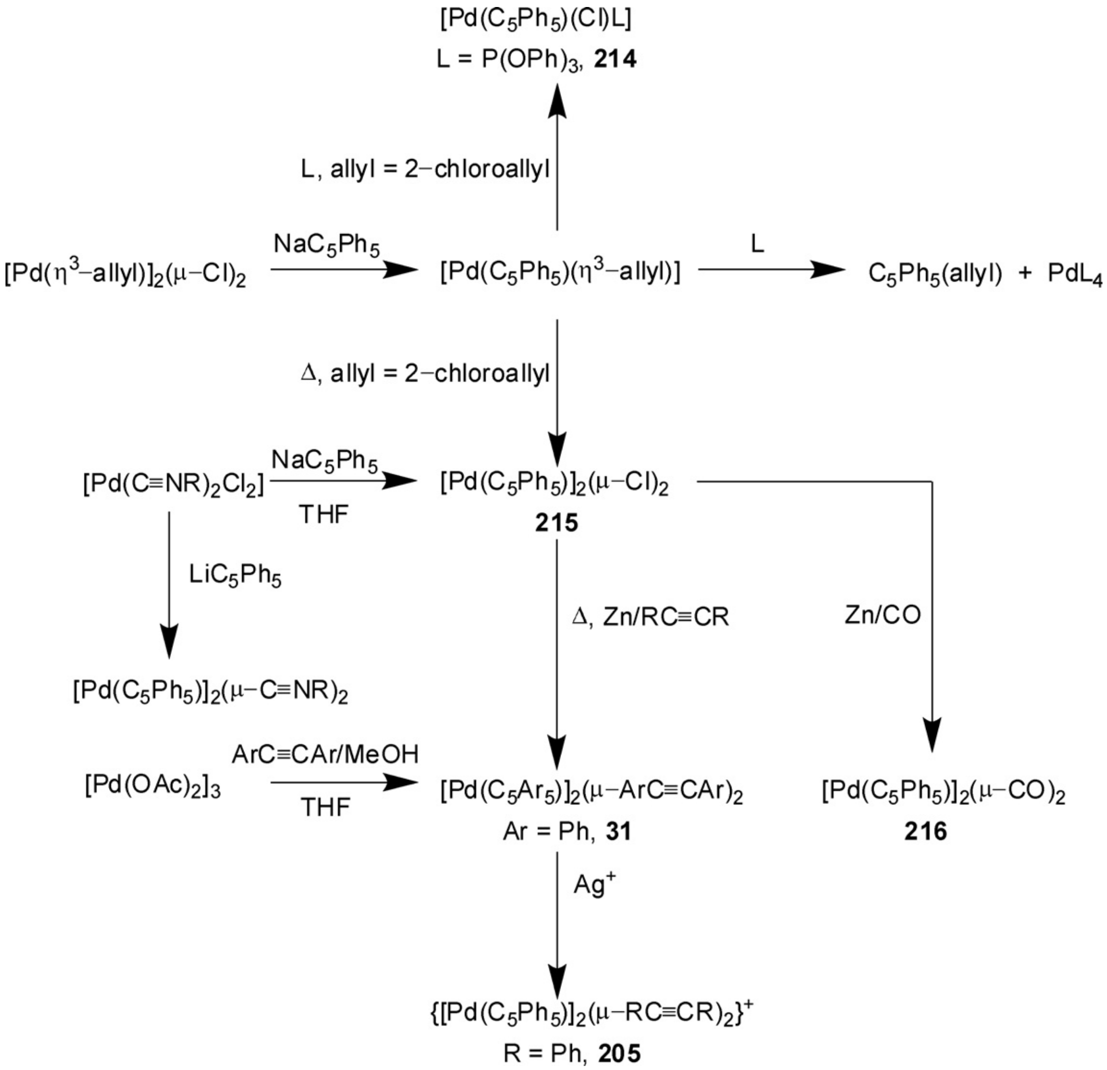

Scheme 75.

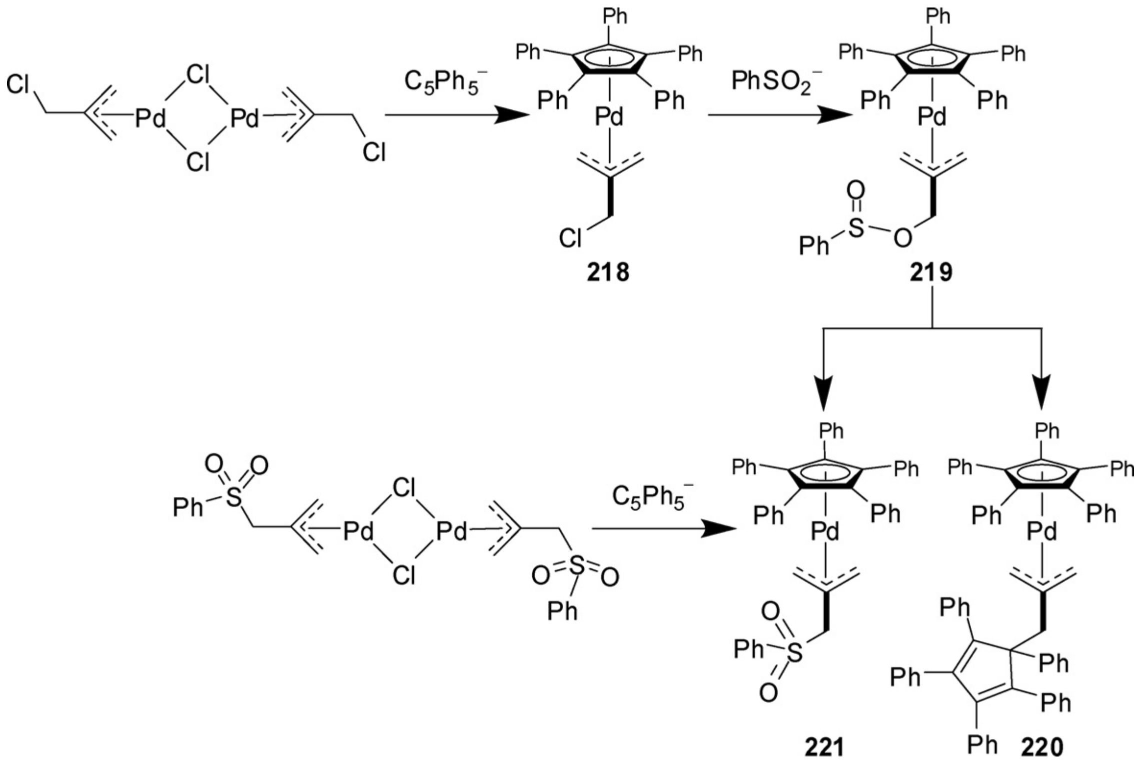

Scheme 76.

which was structurally characterized (Fig. 61) as a pair of enantiomers, which arise as a consequence of the configuration of the unbound oxygen atom. When this material is warmed in a polar solvent, or eluted over alumina, partial conversion to purple crystals of [Pd(η^5-C_5Ph_5){η^3-$CH_2C(CH_2C_5Ph_5)CH_2$}] (**220**), and the *S*-alkylated, [Pd(η^5-C_5Ph_5){η^3-$CH_2C(CH_2S(=O)_2Ph)CH_2$}] (**221**) results. The latter can also be prepared by treatment of [Pd{η^3-$CH_2C(CH_2S(=O)_2Ph)CH_2$}]$_2$(μ-Cl)$_2$ with $C_5Ph_5^-$ (Scheme 76).

Univalent palladium $C_5Ph_5^-$ complexes, such as [Pd(η^5-C_5Ph_5)]$_2$(μ-PhC≡CPh) (**31**), have also been recognized as important gasoline and diesel fuel additives [169].

2.8.3. *Platinum complexes*

Tetrameric [Pt(η^3-allyl)Cl]$_4$, reacts with NaC_5Ph_5 (**39**) in THF to give [Pt(η^5-C_5Ph_5)(η^3-allyl)] as an orange solid in 20% yield [166].

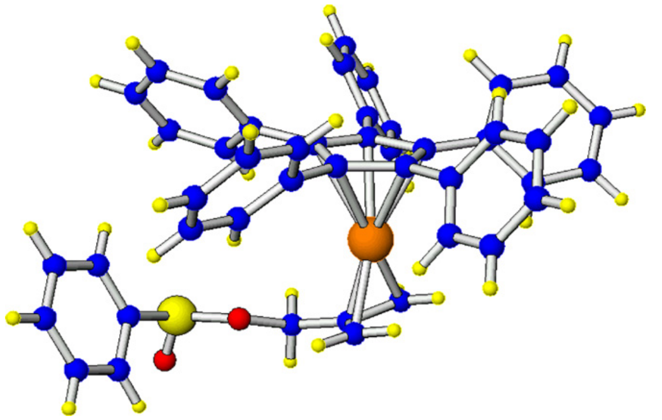

Fig. 61. Structure of [Pd(η^5-C_5Ph_5){η^3-$CH_2C(CH_2OS(=O)Ph)CH_2$}] (**219**) [23ag].

2.9. *Complexes of Group 11*

2.9.1. *Copper complexes*

Colourless needles of the first copper pentaphenylcyclopentadienyl complex, [Cu(η^5-C_5Ph_5)PPh_3] (**222**) are prepared in 40% yield (Scheme 77) by the reaction of [CuCl(PPh_3)]$_4$ with NaC_5Ph_5 (**39**) [23ad].

[Cu(η^5-C_5Ph_5)PPh_3] (**222**), which is somewhat air sensitive in solution, but stable in air for several days, is a rare example of a structurally characterized, π-bound copper cyclopentadienyl derivative. The molecule is chiral, because of the canted orientation of the phenyl groups, and has a near linear P–Cu–(C_5-ring centroid) vector (Fig. 62); the Cu–(C_5-ring centroid) distance is 1.876(5) Å. The spectroscopic data are unremarkable, except that the ^{31}P NMR resonance is unusually far downfield from free PPh_3 (28.8 ppm, rather than the more common ~15 ppm) for a Cu(I)(PPh_3) complex, an effect attributed to the influence of the $C_5Ph_5^-$ phenyl rings. White crystals of the triethylphosphine analogue (**223**) can be prepared similarly from NaC_5Ph_5 (**39**) and [CuCl(PEt_3)]$_4$ in 44% yield, and are less thermally and air-stable than the PPh_3 complex [170]. The ^{31}P NMR resonance of **226** is observed as a broad singlet at δ 11.8 ppm.

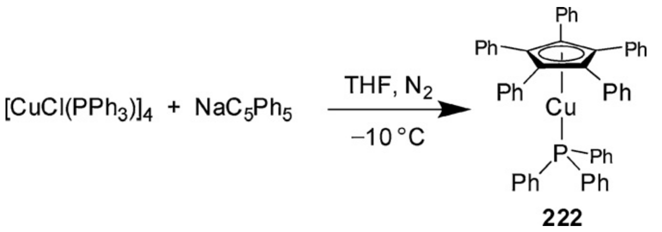

Scheme 77.

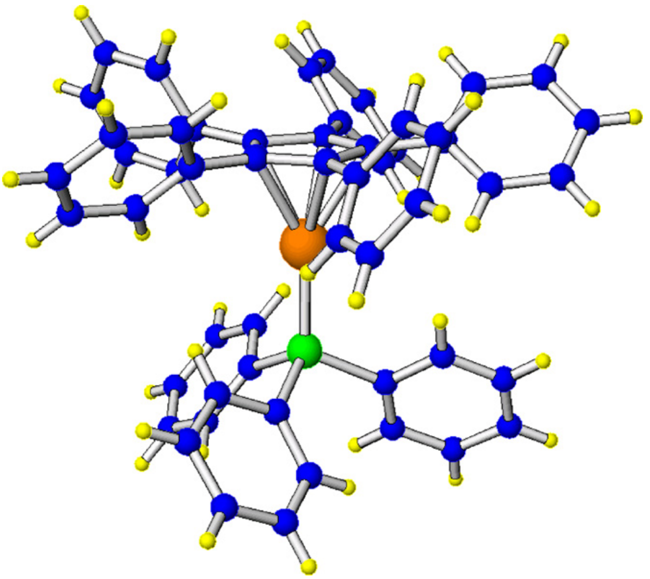

Fig. 62. Structure of [Cu(η^5-C_5Ph_5)PPh_3] (**222**) [23ad].

2.9.2. Silver complexes

The only reported silver complex is [Ag(C_5Ph_5)PR_3] (**224**), which is prepared as an impure, purple solid from NaC_5Ph_5 (**39**) and [$AgCl(PR_3)$]$_4$ in THF under argon at 0 °C [170]. The purple colouration indicates that the presence of the $C_5Ph_5^\bullet$ radical (**4**) in the impure solid is likely.

2.10. Lanthanide and Group 3 metal complexes

Whilst the utility of suitably modified cyclopentadienyl ligands with the chemistry of Group 3 and *f*-element metals is well-established [171], the solubility of complexes incorporating the $C_5Ph_5^-$ ligand has left the application of this ligand to *f*-element metal chemistry underdeveloped. The reactions of NaC_5Ph_5 (**39**) with $LuCl_3$ in the molar ratios 1:1 and 2:1 are claimed to produce [Lu(C_5Ph_5)Cl_2(THF)$_n$] (**225**) or [Lu(C_5Ph_5)$_2$Cl] (**226**), respectively [10a]. [Pr(C_8H_8)(THF)$_2$]$_2$(μ-Cl)$_2$ reacts with NaC_5Ph_5 (**39**) to produce a 27% yield of yellow crystals of the Pr(III) complex, [Pr(C_5Ph_5)(C_8H_8)] (**227**) [172].

The first structurally characterized lanthanoid complex of $C_5Ph_5^-$ is red, crystalline, binuclear [Yb(η^5-C_5Ph_5)(THF)]$_2$(μ-C≡CPh)$_2$ (**228**, Fig. 63), which is produced in 70% yield from the reaction of ytterbium metal with PhHgC≡CPh and C_5Ph_5H (**1**) in THF [173].

The $C_5Ph_5^-$ ligand is unremarkable, and presents all cyclopentadienyl carbon atoms equidistant from the ytterbium with the usual propeller orientation of the phenyl substituents. The Yb–(C_5-ring centroid) distance is 2.440(3) Å, and the symmetry-related Yb centres are separated by 3.606(1) Å.

The reaction of excess ytterbium metal with two equivalents of C_5Ph_5H (**1**) and one equivalent of $HgPh_2$ gives a green solid, which, when recrystallized from THF, yields green crystals of "Yb(C_5Ph_5)$_2$(THF)$_6$". These were structurally characterized as [Yb(THF)$_6$][C_5Ph_5]$_2$ (**7**), containing isolated $C_5Ph_5^-$ anions and [Yb(THF)$_6$]$^{2+}$ cations. The solvent-free, homoleptic, sandwich compound, [Yb(η^5-C_5Ph_5)$_2$] (**229**), can be accessed in low yield by the reaction between equimolar amounts of [Yb(C≡CBu^t)$_2$] and C_5Ph_5H (**1**) in toluene at 60 °C (Fig. 64) [38b].

The Yb–(C_5-ring centroid) distance of the sandwich compound **229** is 2.371(4) Å. This is slightly shorter than the corresponding distance in half-sandwich **228** (2.440(3) Å), and the decrease is typical for a sandwich compound in relation to a comparable half-sandwich, which has a greater degree of coordination around the metal nucleus [23g]. Of particular note in the structure of **229** are the relatively short distances (2.79 Å average) between the *ortho*-C–H of the phenyl substituents and the *ortho*-C of the phenyl group attached to the adjoining carbocycle [38b]; this resembles the structure of [{C_5(4-Bu^nC_6H_4)$_5$}K] (**14**) and the barium analogue, [Ba{C_5(4-Bu^nC_6H_4)$_5$}$_2$] (**48**), where such interactions were inter- as well as intramolecular [41]. The short distances observed, which are well within the sum of the van der Waals radii for C and H (2.90 Å), have been interpreted in terms of a non-classical *ortho*-C–H···C(π) interaction [38b,41,43,101], that adds to the sta-

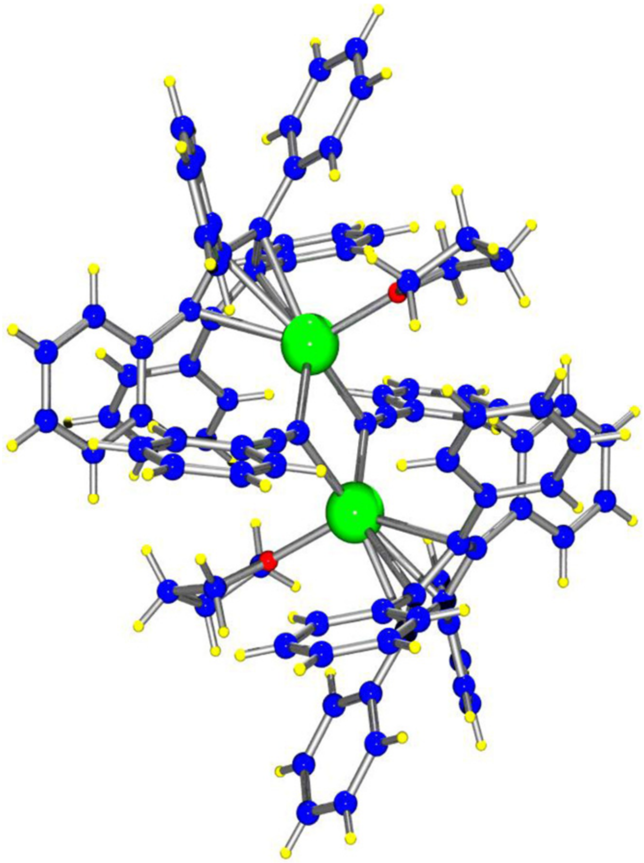

Fig. 63. Structure of [Yb(η^5-C_5Ph_5)(THF)]$_2$(μ-C≡CPh)$_2$ (**228**) [38b].

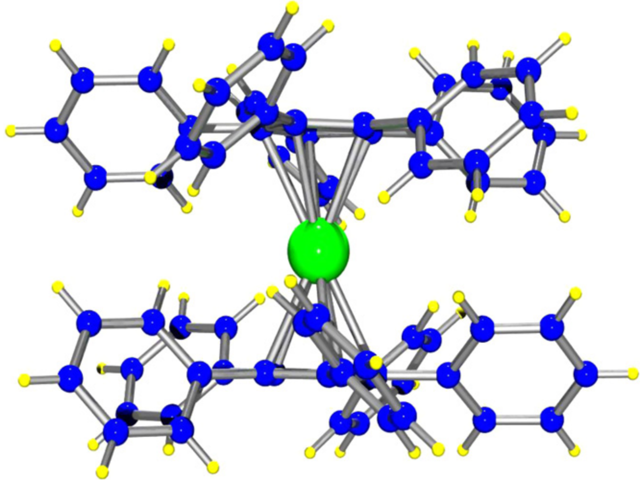

Fig. 64. Structure of base-free [Yb(η^5-C_5Ph_5)$_2$] (**229**) [38b].

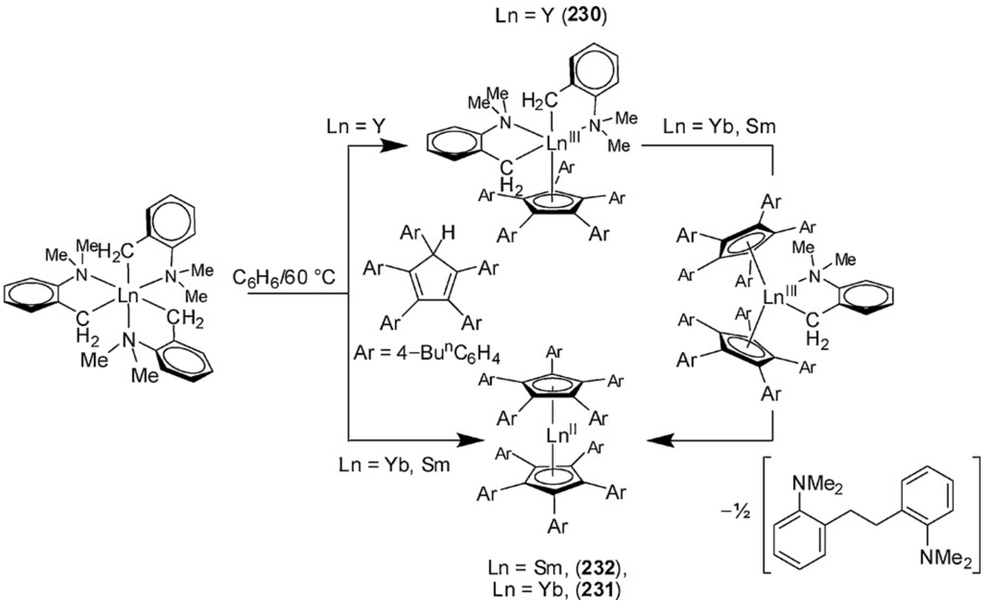

Scheme 78.

bility of the sandwich structure, and predisposes the sandwich to S_{10} molecular symmetry, which maximizes such interactions. Such C–H(δ^+)···(δ^-)C(π) interactions are reasonably well-established [43], and manifest in the solid state structure of benzene. Here again the steric demand of the penta-arylcyclopentadienyl ligand distinguishes the geometry of the base-free sandwich compound; parallel carbocycles are observed, and not the bent geometries as seen in the Ln(II) series, Ln(η^5-C_5Me_5)$_2$ [104a–d].

The problems associated with the insolubility of lanthanoid sandwich complexes bearing the conventional $C_5Ph_5{}^-$ ligand can be greatly alleviated by the use of C_5(4-Bu^nC_6H_4)$_5$H (**11**), whose alkaline earth and *f*-element metal complexes display much greater solubility in suitable solvents [101]. When C_5(4-Bu^nC_6H_4)$_5$H (**11**) is added to the *tris*chelate lanthanoid, [Y(*o*-$CH_2C_6H_4NMe_2$)$_3$], the half-sandwich, [Y(C_5Ar_5)(*o*-$CH_2C_6H_4NMe_2$)$_2$] (**230**) (Ar = 4-Bu^nC_6H_4), is isolated by σ-bond metathesis. However, for the analogous reaction with [Ln(*o*-$CH_2C_6H_4NMe_2$)$_3$] (Ln = Yb, Sm, *f*-element metals with an easily accessible bivalent oxidation state) spontaneous reduction of the Ln(III) ion occurs to give the sandwich complexes, [Ln{C_5(4-Bu^nC_6H_4)$_5$}$_2$] (Ln = Yb (**231**), Sm (**232**)) (Scheme 78) [101a]. The Yb–(C_5-ring centroid) distance of the sandwich compound **231** (2.382(1) Å) is quite comparable to the corresponding distance in **232**, and again provides an example of perfectly parallel η^5-coordination to give S_{10} molecular symmetry. The reduction of Ln(III) to Ln(II) is supposed to be driven by steric congestion of the presumed Ln(III) sandwich intermediate, [Ln(C_5Ar_5)$_2$(*o*-$CH_2C_6H_4NMe_2$)], which eliminates half an equivalent of 1,2-(2-(Me_2N)C_6H_4)ethane to supply the electrons necessary to reduce the metal centre. This process is touted as an example of the so-called sterically induced reduction that is presumed to operate for [Sm(C_5Me_5)$_3$] complexes [174].

2.11. Complexes of Group 12

No complexes of these metals have been reported.

2.12. Complexes of Group 13

No complexes of boron, aluminum or gallium have been reported.

2.12.1. Complexes of Indium and Thallium

The "traditional" methods of syntheses of thallium cyclopentadienyl complexes, reaction with TlX (X = OH, 1/2(SO_4)) in the presence of KOH, or the reaction of a Li cyclopentadienyl with Tl_2SO_4, produced only low yields of materials that were difficult to purify. However, reaction of C_5Ph_5H (**1**) with thallium ethoxide was quantitative (98%), driven by the insolubility of the TlC_5Ph_5 (**233**), which can be conveniently prepared as a yellow powder on the 5–10 g scale. Because of the insolubility, characterization was by infrared absorptions (3075w, 3052m, 3025m, 2960m to s, 2900w, 2865w, 1950–1660vw, 1597m to s, 1574w, 1520w, 1500s, 1462vw, 1442m, 1394w, 1363w to m, 1325w, 1312vw, 1269w to m, 1200w, 1179w, 1155w, 1143w to m, 1118w, 1110sh, 1073m, 1059sh, 1025m, 1015sh, 1001vw, 978vw(br), 920sh, 912w to m, 840 m to s, 789m, 780m, 775w, 754w, 745m, 735w, 705sh, 696vs, 678w, 590vw, 568m, 540w, 498w, 455w, 368w to m, 347w, 330w cm^{-1}) and mass spectroscopy, the electron impact spectrum of the latter exhibited a molecular ion ($^{205}TlC_5Ph_5$, *m*/*z* 650)$^+$, in 25% abundance [175].

A series of indium and thallium complexes of formula M{C_5(4-RC_6H_4)$_5$} (M = In, Tl) has been prepared by the methodology of Scheme 79, starting from C_5Ph_5H (**1**). The complexes were characterized by ^{1}H and ^{13}C NMR spectroscopy [34a,126c].

2.13. Complexes of Group 14

2.13.1. Complexes of silicon, germanium, and lead

A notable absence from the family of neutral pentaphenylcyclopentadienes is the trimethylsilyl derivative, $C_5Ph_5SiMe_3$. Just as with C_5H_5($SiMe_3$), for which extrusion of trimethylchlorosilane is an effective strategy for the formation of mono-substituted Ti(η^5-C_5H_5)X_3, or M(η^5-C_5H_5)Cl_4 (X = Cl, Br, I; M = Nb, Ta) [176], addition of $C_5Ph_5SiMe_3$ or its more soluble derivatives to a metal–halide precursor, might lead to facile formation of M–C_5Ar_5 bonds. Whilst the absence of trimethylsilyl derivatives of pentaphenylcyclopentadiene is surprising, germanium, tin, and lead were amongst the earliest metals to be coordinated to the ligand, to form a [M(η^5-C_5Ph_5)$_2$] series (M = Ge (**234**), Sn (**235**), Pb (**41**)) [23f,177]. The anti-tumour properties of the tin (**235**) and germanium (**234**) derivatives have been briefly reported [178].

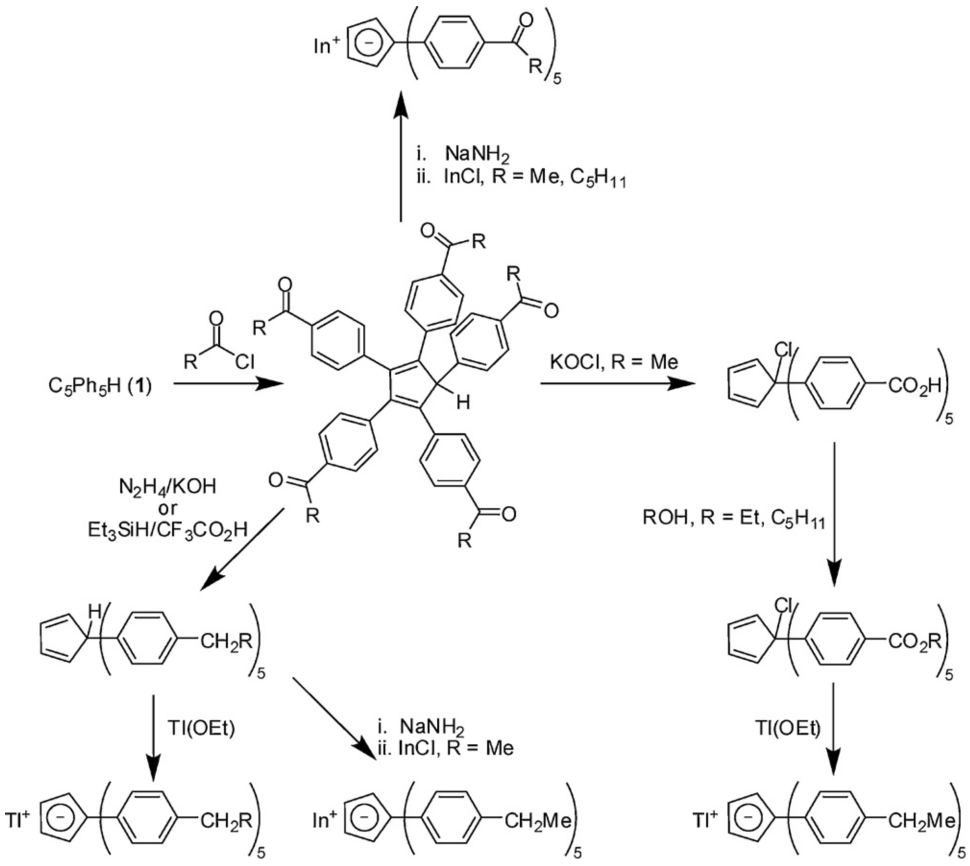

Scheme 79.

2.13.2. Tin complexes

[Sn(η^5-C_5Ph_5)$_2$] (**235**) was the first decaphenylmetallocene structurally characterized and its high symmetry is noteworthy (Fig. 65) [23c], with S_{10} molecular geometry again featured. The Sn–(C_5-ring centroid) distance is 2.401(6) Å, and at twice this distance, the *trans*-annular separation is sufficient to impose no significant inward or outward bending of the substituent phenyl groups ($-\alpha_{\text{average}} = 1.2^\circ$, Fig. 16) [101a]. The probable existence of C–H···C(π) interactions (average distance = 2.68 Å), combined with steric bulk of the ligands, is sufficient to override the stereochemically active tin lone pair that generally imposes a bent structure on Sn(II) metallocenes, to result in parallel alignment of the C_5 cores. Interestingly, the Sn–(C_5-ring centroid) in stannocene, [Sn(η^5-C_5H_5)$_2$], is at 2.401(1) Å identical to that in [Sn(η^5-C_5Ph_5)$_2$] (**235**); whilst stannocene is not isostructural with [Sn(η^5-C_5Ph_5)$_2$] (**235**), non-classical C–H···C(π) interactions in the latter are evidently sufficient to overcome significant steric interaction.

The sandwich structure of [Sn(η^5-C_5Ph_5)$_2$] (**235**) is to be compared with the conventional bent structure of [Sn(η^5-C_5Ph_5)(η^5-C_5H_5)] (**236**, Fig. 66) [23f]. Here the Sn–(C_5H_5-ring centroid) distance is 2.3724(4) Å, whereas the Sn–(C_5Ph_5-ring centroid) distance is 2.4620(3) Å [102a,179]; the lone pair on the tin centre, however, gives rise to an angle between the metal-centroid vectors of 151.1(1)°, similar to the angle of 143(2)° observed for stannocene [23f].

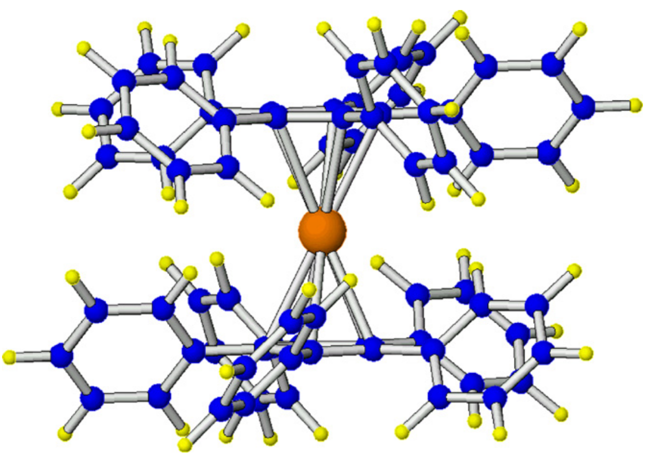

Fig. 65. Structure of [Sn(η^5-C_5Ph_5)$_2$] (**235**) [23c].

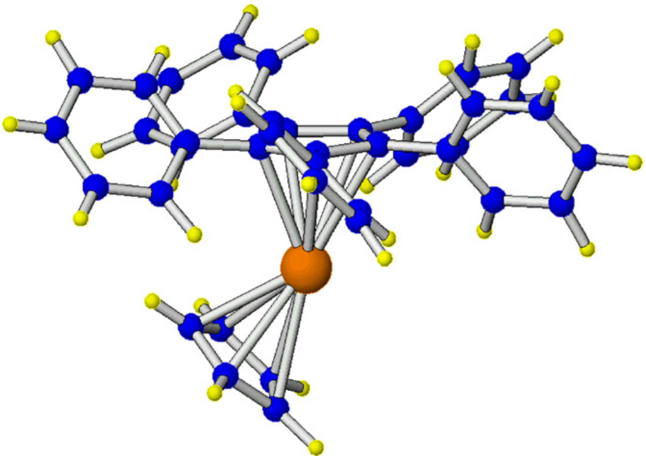

Fig. 66. Structure of [Sn(η^5-C_5Ph_5)(η^5-C_5H_5)] (**236**) [23f].

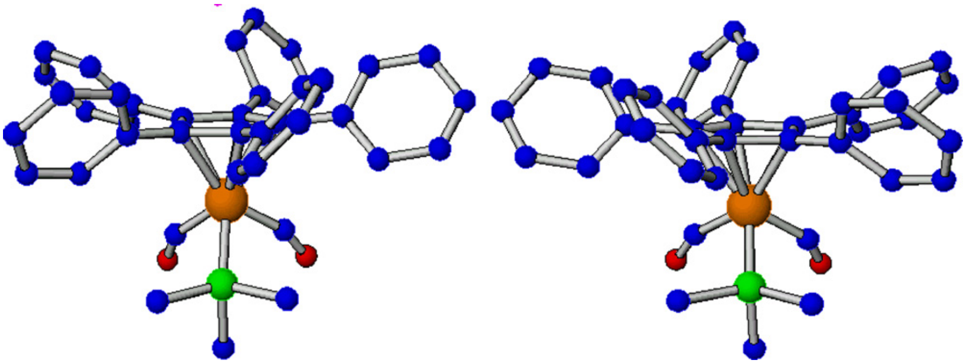

Fig. 67. Two molecules in the unit cell of [Fe(η^5-C_5Ph_5)(CO){C(=O)H}PMe_3] (**100**) with clockwise and anticlockwise canting of the phenyl rings (hydrogen atoms omitted) [23r].

Whereas C_5Ph_5Cl (**19**) reacts with stannous chloride to give intensely dark red Sn(η^1-C_5Ph_5)Cl_3 (**237**) in the expected oxidative addition reaction (Eq. (18)), the corresponding reaction with $SnBr_2$ or $SnCl_2$ and C_5Ph_5Br (**3**) afforded the $C_5Ph_5^{\bullet}$ radical (**4**), and a presumably transient "SnX_3", which metathesizes to Sn(II) and Sn(IV) products (Eq. (2)) [23h,aa]:

$$\underset{E=Sn,\,Ge}{C_5Ph_5Cl + ECl_2} \xrightarrow{THF} E(C_5Ph_5)Cl_3 \tag{18}$$

The hapticity of the pentaphenylcyclopentadienyl unit of Sn(η^1-C_5Ph_5)Cl_3 (**237**) was confirmed by the X-ray crystal structure [23aa]. Both Sn(η^1-C_5Ph_5)Cl_3 (**237**) and its germanium analogue, Ge(η^1-C_5Ph_5)Cl_3 (**238**), resisted reduction with potassium anthracenide, and only C_5Ph_5H (**1**) was isolated.

2.13.3. *Complexes of lead*

[Pb(C_5Ph_5)$_2$] (**41**), prepared from Pb(OAc)$_2$ and $C_5Ph_5^-$ in an ethereal solvent, remains the only lead derivative of pentaarylcyclopentadiene. It was recrystallized from toluene in 54% yield, and is air- and water-stable [23f]. The lead sandwich has been used as a substrate for the deposition of thin films of the $C_5Ph_5^{\bullet}$ (**4**) radical [11].

3. Applications

3.1. *Asymmetry*

The staggered conformation of the phenyl rings in the solid state confers chirality on the pentaphenylcyclopentadienyl ligand. This chirality can be seen in the structure of the formyl complex, [Fe(η^5-C_5Ph_5)(CO){C(=O)H}PMe_3] (**100**) [23r,126a,b]. Fig. 67 illustrates two molecules with clockwise and anticlockwise helices in the unit cell. In these [Fe(η^5-C_5Ar_5)(CO){C(=O)R}PR_3] derivatives, the combination of the stereogenic iron centre and the clockwise or anticlockwise canting of the aryl rings generate a diastereomeric mixture, which can be distinguished by NMR spectroscopy at low temperatures. For the derivative, [Fe(η^5-C_5Ph_5)(CO){C(=O)Et}PMe_2Ph] (**239**), the activation energies for the rotations of the [Fe(CO){C(=O)Et}PMe_2Ph] tripod and the phenyl rings, have been determined to be 36.4 and 49.0 kJ mol^{-1}, respectively; the difference in the two values suggests that the two fluxional processes occur independently [23r].

A practical application of the asymmetry possessed by half sandwich pentaphenylcyclopentadienyl complexes is provided by the dynamic kinetic resolution of secondary alcohols achieved by combination of an enzyme with a catalytic amount of metal complex [103], for which the half sandwich Ru complexes, for instance [Ru(C_5Ph_5)(CO)$_2$X] and analogues (X = Br (**130**)), serve as very efficient catalysts [180]. The proposed mechanism involves (i) metathesis of the halide ligand with Bu^{t}OK, followed by (ii) exchange of the butoxide with a secondary alkoxide from the substrate, and (iii) β-hydride elimination from an unsaturated Ru species that racemizes the alcohol. Both the first two processes seem to be assisted by the bound carbonyl ligands, which allow formation of an acyl group that facilitates alkoxide exchange [180g]. As shown in Scheme 80, which depicts the racemization of homochiral 1-phenylethanol, the acyl intermediate (boxed), which is confirmed experimentally for addition of KOBu^t [180g], and inferred for the rapid exchange of the alkoxides [180g,h], efficiently mediates alkoxide metathesis or exchange. The bound secondary alkoxide undergoes rapid racemization by β-hydride elimination, and in combination with an added acyl donor and an immoblized lipase affords excellent yields of enantiopure acetates in dynamic kinetic resolutions. The β-hydride elimination can occur only with the creation of a vacant coordination site as shown, which can be achieved by either loss of a carbonyl ligand or the depicted η^5–η^3 ring slippage [180f].

3.2. *Miscellaneous*

Compounds such as **240** (pictured), in combination with an olefinic group have been patented as chargeable, laminated, electrophotographic photoreceptors [181].

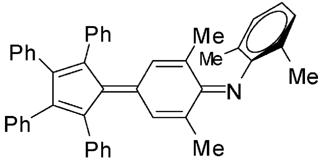

240

The activation barriers for the 3,3-sigmatropic shifts of the acyloxy groups in the pictured compounds (**241**) were estimated to be 26.0–34.8 kJ mol^{-1} [182].

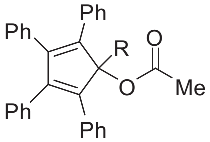

241

The mass spectroscopic fragmentation pathway of C_5Ar_5OH species, in which Ar is substituted in the *para* position of the 1- or 3- and 4-Ph rings, is determined by the electron-donating or -withdrawing ability of the substituents [183].

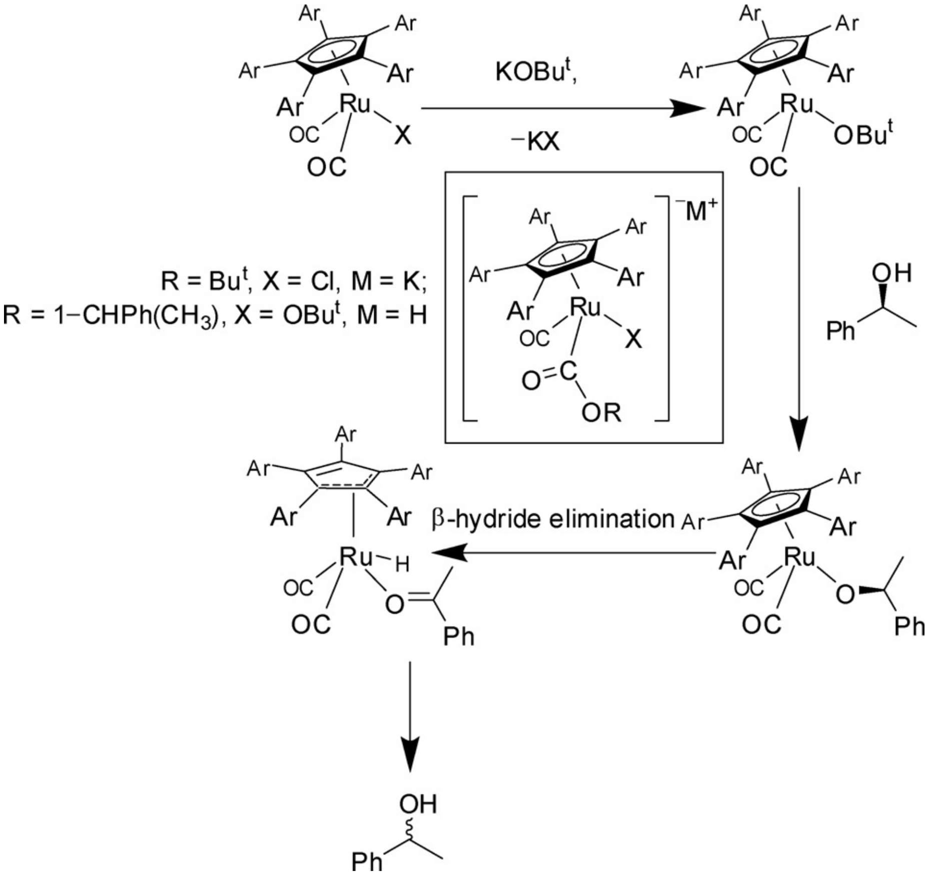

Scheme 80.

4. Conclusions

Complexes incorporating penta-arylcyclopentadienyl ligands feature across the periodic table. Aryl loading of the cyclopentadienyl platform confers the advantages of (i) structural rigidity and steric saturation; and (ii) the chirality engendered by the propeller-like array of the phenyl groups canted clockwise or anticlockwise. With respect to the structural rigidity, the S_{10} molecular geometries of all structurally characterized sandwich compounds that incorporate a pair of penta-arylcyclopentadienyl ligands exhibit significant *ortho*-C–H···*ortho*-C(π) interactions between the aryl substituents of proximate carbocycles, which have been convincingly argued as a rationale for the observed geometries [43]. With respect to asymmetry, the archetypal ruthenium half-sandwich complex, [Ru(η^5-C_5Ph_5)(CO)$_2$Br] (**130**), has been used in dynamic kinetic resolution of secondary alcohols [180d,f], and work into the mechanism is ongoing [180h].

The major Achilles' heel of the C_5Ph_5H (**1**) system is undoubtedly the insolubility that the phenyl rings confer upon its metal complexes. Nevertheless, substitution of at least one of the phenyl groups by *p*-tolyl, 4-Bu^{n}C$_6$H$_4$, 3,5-R$_2$C$_6$H$_4$ (R = Me, Bu^t) rings, gives rise to complexes that can be deployed in apolar media such as toluene and even pentane and hexanes. Such substitution on the cyclopentadienyl ring can be usually performed as a one pot procedure by the use of a suitable aryl bromide, and palladium catalysis [40,75a,c]. Selection of a suitable aryl group for substitution on the C_5 carbocycle have thus lead to complexes with improved solubility and spectroscopic simplicity, and much more amenable to solution spectroscopy.

With respect to the transition metals, penta-arylcyclopentadienyl chemistry is relatively mature. Penta-arylcyclopentadienyl complexes as half or sandwich complexes exist for most transition metal centres, and their chemistry has begun to be utilized in several applications, of which asymmetric synthesis is the most obvious and important example [132]. Greater opportunities for new chemistry of penta-arylcyclopentadienyl ligands exist with respect to the *f*-element metals, which so far have only the eight complexes that incorporate these bulky ligands. Nevertheless, such *f*-element metal sandwich complexes and the equally few such alkaline earth metal sandwiches have demonstrated: (i) unusual, non-bent metallocene structures in which the (C_5-ring centroid)–M–(C_5-ring centroid) vector is perfectly linear; (ii) the existence of non-classical C–H···C(π) interactions that have definite structural consequences; and (iii) two excellent examples of sterically induced reduction that results in the samarium and ytterbium sandwich complexes. Given that the problem of insolubility may be overcome by utilization of solubilizing aryl groups, and that cyclopentadienyl complexes of the *f*-element metals are especially numerous, a wide variety of lanthanide and actinide complexes that incorporate penta-arylcyclopentadienyl ligands await isolation. Bivalent chemistry of the *f*-element (and also of the Group 3) [184] metals is also an area of active research interest [38b,174,185]. The steric requirements of penta-arylcyclopentadienyl ligands, and also their ability to stabilize lower oxidation states, might yet play an important role in this chemistry.

References

[1] (a) T.J. Kealy, P.L. Pauson, Nature 168 (1951) 1039;
(b) E.O. Fischer, W. Pfab, Z. Naturforsch. B: Chem. Sci. 7 (1952) 377;
(c) S.A. Miller, J.A. Tebboth, J.F. Tremaine, J. Chem. Soc. (1952) 632;
(d) G. Wilkinson, M. Rosenblum, M.C. Whiting, R.B. Woodward, J. Am. Chem. Soc. 74 (1952) 2125;
(e) G. Wilkinson, J. Organomet. Chem. 100 (1975) 273;

(f) P.L. Pauson, J. Organomet. Chem. 637 (2001) 3.

[2] C. Janiak, H. Schumann, Adv. Organomet. Chem. 33 (1991) 291.

[3] K. Ziegler, B. Schnell, Justus Liebigs Ann. Chem. 445 (1925) 266.

[4] W. Hübel, R. Merényi, J. Organomet. Chem. 2 (1964) 213.

[5] L.D. Field, T.W. Hambley, C.M. Lindall, A.F. Masters, Inorg. Chem. 31 (1992) 2366.

[6] G. Vives, A. Carella, J.-P. Launay, G. Rapenne, Coord. Chem. Rev. 252 (2008) 1451.

[7] M. Saunders, R. Berger, A. Jaffe, J.M. Mcbride, J. O'Neill, R. Breslow, J.M. Hoffman, C. Perchonock, E. Wasserman, R.S. Hutton, V.J. Kuck, J. Am. Chem. Soc. 95 (1973) 3017.

[8] (a) H. Adams, N.A. Bailey, A.F. Browning, J.A. Ramsden, C. White, J. Organomet. Chem. 387 (1990) 305;
(b) T. Niem, M.D. Rausch, J. Org. Chem. 42 (1977) 275.

[9] T.R. Jack, C.J. May, J. Powell, J. Am. Chem. Soc. 99 (1977) 4707.

[10] (a) R. Zhang, M. Tsutsui, Youji Huaxue (1982) 435;
(b) M. Matusz, Ph.D. thesis, University of Southern Illinois, Carbondale, Illinois, 1984.

[11] S. Lamansky, M.E. Thompson, Chem. Mater. 14 (2002) 109.

[12] J.J. Eisch, Y. Qian, M. Singh, J. Organomet. Chem. 512 (1996) 207.

[13] L.D. Field, K.M. Ho, C.M. Lindall, A.F. Masters, A.G. Webb, Aust. J. Chem. 43 (1990) 281.

[14] R. Zhang, M. Tsutsui, D.E. Bergbreiter, J. Organomet. Chem. 229 (1982) 109.

[15] C.M. Lindall, Ph.D. thesis, The University of Sydney, Sydney, 1992.

[16] K.N. Brown, L.D. Field, P.A. Lay, C.M. Lindall, A.F. Masters, J. Chem. Soc., Chem. Commun. (1990) 408.

[17] (a) W.Y. Yeh, S.M. Peng, G.H. Lee, J. Chem. Soc., Chem. Commun. (1993) 1056;
(b) W.Y. Yeh, C.L. Ho, M.Y. Chiang, I.T. Chen, Organometallics 16 (1997) 2698.

[18] D.R. Latimer, M.Sc. thesis, University of Sydney, Sydney, 1992.

[19] R. Breslow, H.W. Chang, J. Am. Chem. Soc. 83 (1961) 3727.

[20] F.G. Bordwell, M.J. Bausch, J. Am. Chem. Soc. 105 (1983) 6188.

[21] (a) F.G. Bordwell, J.P. Cheng, M.J. Bausch, J. Am. Chem. Soc. 110 (1988) 2872;
(b) F.G. Bordwell, J.A. Harrelson Jr., A.V. Satish, J. Org. Chem. 54 (1989) 3101.

[22] J. Baghdadi, N.A. Bailey, A.S. Dowding, C. White, J. Chem. Soc., Chem. Commun. (1992) 170.

[23] (a) E. Ban, P.T. Cheng, T. Jack, S.C. Nyburg, J. Powell, J. Chem. Soc., Chem. Commun. (1973) 368;
(b) H. Hoberg, R. Krause-Göing, C. Krüger, J.C. Sekutowski, Angew. Chem., Int. Ed. Engl. 16 (1977) 183;
(c) M.J. Heeg, C. Janiak, J.J. Zuckerman, J. Am. Chem. Soc. 106 (1984) 4259;
(d) U. Behrens, F. Edelmann, Z. Naturforsch. B: Chem. Sci. 41 (1986) 1426;
(e) J.W. Chambers, A.J. Baskar, S.G. Bott, J.L. Atwood, M.D. Rausch, Organometallics 5 (1986) 1635;
(f) M.J. Heeg, R.H. Herber, C. Janiak, J.J. Zuckerman, H. Schumann, W.F. Manders, J. Organomet. Chem. 346 (1988) 321;
(g) L.D. Field, T.W. Hambley, C.M. Lindall, A.F. Masters, Polyhedron 8 (1989) 2425;
(h) C. Janiak, M. Schwichtenberg, F.E. Hahn, J. Organomet. Chem. 365 (1989) 37;
(i) M. Huhn, W. Kläui, L. Ramacher, R. Herbst-Irmer, E. Egert, J. Organomet. Chem. 398 (1990) 339;
(j) D.W. Slocum, M. Matusz, A. Clearfield, R. Peascoe, S.A. Duraj, J. Macromol. Sci., Pure Appl. Chem. 27 (1990) 1405;
(k) N.G. Connelly, W.E. Geiger, A.G. Orpen, J.J. Orsini, K.E. Richardson, J. Chem. Soc., Dalton Trans. (1991) 2967;
(l) L.D. Field, T.W. Hambley, P.A. Lay, C.M. Lindall, A.F. Masters, J. Chem. Soc., Dalton Trans. (1991) 1499;
(m) W. Kläui, M. Huhn, R. Herbst-Irmer, J. Organomet. Chem. 415 (1991) 133;
(n) U. Thewalt, G. Schmid, J. Organomet. Chem. 412 (1991) 343;
(o) M.J. Aroney, I.E. Buys, G.D. Dennis, L.D. Field, T.W. Hambley, P.A. Lay, A.F. Masters, Polyhedron 12 (1993) 2051;
(p) R.J. Hoobler, M.A. Hutton, M.M. Dillard, M.P. Castellani, A.L. Rheingold, A.L. Rieger, P.H. Rieger, T.C. Richards, W.E. Geiger, Organometallics 12 (1993) 116;
(q) D. Matt, M. Huhn, J. Fischer, A. Decian, W. Kläui, I. Tkatchenko, M.C. Bonnet, J. Chem. Soc., Dalton Trans. (1993) 1173;
(r) L.J. Li, A. Decken, B.G. Sayer, M.J. McGlinchey, P. Brégaint, J.Y. Thépot, L. Toupet, J.-R. Hamon, C. Lapinte, Organometallics 13 (1994) 682;
(s) H. Schumann, A. Lentz, R. Weimann, J. Pickardt, Angew. Chem., Int. Ed. Engl. 33 (1994) 1731;
(t) T. Tanase, T. Fukushima, T. Nomura, Y. Yamamoto, K. Kobayashi, Inorg. Chem. 33 (1994) 32;
(u) D. Matt, M. Huhn, M. Bonnet, I. Tkatchenko, U. Englert, W. Kläui, Inorg. Chem. 34 (1995) 1288;
(v) R. Ficker, W. Hiller, S. Drobnik, I.P. Lorenz, Z. Kristallgr. 211 (1996) 845;
(w) L.D. Field, T.W. Hambley, T. He, P.A. Humphrey, C.M. Lindall, A.F. Masters, Aust. J. Chem. 49 (1996) 889;
(x) D.J. Hammack, M.M. Dillard, M.P. Castellani, A.L. Rheingold, A.L. Rieger, P.H. Rieger, Organometallics 15 (1996) 4791;
(y) L.C. Song, Q.M. Hu, J.S. Yang, X.C. Cao, R.J. Wang, T.C.W. Mak, Inorg. Chim. Acta 245 (1996) 109;
(z) L.D. Field, T.W. Hambley, T. He, A.F. Masters, P. Turner, Aust. J. Chem. 50 (1997) 1035;
(aa) C. Janiak, R. Weimann, F. Görlitz, Organometallics 16 (1997) 4933;
(ab) M. Scheer, U. Becker, J. Organomet. Chem. 545 (1997) 451;
(ac) H. Schumann, A. Lentz, R. Weimann, Z. Naturforsch. B: Chem. Sci. 52 (1997) 573;
(ad) Q.T. Anderson, E. Erkizia, R.R. Conry, Organometallics 17 (1998) 4917;
(ae) C.U. Beck, L.D. Field, T.W. Hambley, P.A. Humphrey, A.F. Masters, P. Turner, J. Organomet. Chem. 565 (1998) 283;
(af) L.D. Field, T.W. Hambley, P.A. Humphrey, A.F. Masters, P. Turner, Polyhedron 17 (1998) 2587;
(ag) S. Watanabe, H. Kurosawa, Organometallics 17 (1998) 479;
(ah) D.L. Greene, O.A. Villalta, D.M. Macias, A. Gonzalez, W. Tikkanen, B. Schick, K. Kantardjieff, Inorg. Chem. Commun. 2 (1999) 311;
(ai) T.H. He, Ph.D. thesis, The University of Sydney, Sydney, 1999;
(aj) B.L. Hodous, J.C. Ruble, G.C. Fu, J. Am. Chem. Soc. 121 (1999) 2637;
(ak) B. Tao, J.C. Ruble, D.A. Hoic, G.C. Fu, J. Am. Chem. Soc. 121 (1999) 10452;
(al) B.T. Tao, J.C. Ruble, D.A. Hoic, G.C. Fu, J. Am. Chem. Soc. 121 (1999) 5091;
(am) W.Y. Yeh, S.M. Peng, G.H. Lee, J. Organomet. Chem. 572 (1999) 125;
(an) M.A. Hutton, J.C. Durham, R.W. Grady, B.E. Harris, C.S. Jarrell, J.M. Mooney, M.P. Castellani, A.L. Rheingold, U. Kolle, B.J. Korte, R.D. Sommer, G.T. Yee, J.M. Boggess, R.S. Czernuszewicz, Organometallics 20 (2001) 734;
(ao) C.I. Li, W.Y. Yeh, S.M. Peng, G.H. Lee, J. Organomet. Chem. 620 (2001) 106;
(ap) B. Tao, M.-M.C. Lo, G.C. Fu, J. Am. Chem. Soc. 123 (2001) 353;
(aq) B.T. Carter, M.P. Castellani, A.L. Rheingold, S. Hwang, S.E. Longacre, M.G. Richmond, Organometallics 21 (2002) 373;
(ar) L.D. Field, T.W. Hambley, P.A. Humphrey, A.F. Masters, P. Turner, Inorg. Chem. 41 (2002) 4618;
(as) D.L. Greene, A. Chau, M. Monreal, C. Mendez, I. Cruz, T. Wenj, W. Tikkanen, B. Schick, K. Kantardjieff, J. Organomet. Chem. 682 (2003) 8.

[24] (a) D.C. Reitz, J. Chem. Phys. 34 (1961) 701;
(b) K. Möebius, H. Haustein, M. Plato, Z. Naturforsch. A: Phys. Sci. 23 (1968) 1626;
(c) K. Möebius, H. Van Willigen, A.H. Maki, Solution ENDOR [electron nuclear double resonance] study of the lifting of orbital degeneracy by methyl substituents in five-membered ring systems, in: 16th Magn. Resonance Relat. Phenomena, Proc. Congr. (AMPERE), Publ. House Acad. Soc. Repub. Rom., Bucharest, Rumania, 1971, p. 1114;
(d) K. Möebius, H. Van Willigen, A.H. Maki, Mol. Phys. 20 (1971) 289.

[25] P.G. Gassman, D.W. Macomber, J.W. Hershberger, Organometallics 2 (1983) 1470.

[26] A.M. Bond, R. Colton, D.A. Fiedler, L.D. Field, T.A. He, P.A. Humphrey, C.M. Lindall, F. Marken, A.F. Masters, H. Schumann, K. Sühring, V. Tedesco, Organometallics 16 (1997) 2787.

[27] (a) K. Broadley, G.A. Lane, N.G. Connelly, W.E. Geiger, J. Am. Chem. Soc. 105 (1983) 2486;
(b) N.G. Connelly, S.J. Raven, J. Chem. Soc., Dalton Trans. (1986) 1613.

[28] K. Broadley, N.G. Connelly, G.A. Lane, W.E. Geiger, J. Chem. Soc., Dalton Trans. (1986) 373.

[29] (a) H. Kurreck, W. Broser, Chem. Ber. 98 (1965) 11;
(b) J.Y. Thépot, C. Lapinte, J. Organomet. Chem. 656 (2002) 146.

[30] A.E. Shilov, Activation of Saturated Hydrocarbons by Transition Metal Complexes, Kluwer Academic Publishers, Boston, Hingham, MA, USA, 1984.

[31] A.A. Bumber, G.A. Dushenko, I.A. Profatilova, A.A. Arutyunyants, I.E. Mikhailov, Russ. J. Electrochem. 36 (2000) 553.

[32] L.D. Field, T.W. Hambley, T.H. He, M.G. Humphrey, R. Hundal, P. Turner, A.F. Masters, unpublished results.

[33] (a) S.A. Bourne, L.R. Nassimbeni, M.L. Niven, J. Phys. Org. Chem. 5 (1992) 769;
(b) S.A. Bourne, L.R. Nassimbeni, M.L. Niven, A.M. Modro, J. Inclusion Phenom. Mol. Recognit. Chem. 13 (1992) 301.

[34] (a) H. Schumann, A. Lentz, Z. Naturforsch. B: Chem. Sci. 49 (1994) 1717;
(b) L.D. Field, T. He, A.F. Masters, P. Turner, Polyhedron 21 (2002) 1707.

[35] G. Evrard, P. Piret, G. Germain, M. Van Meerssche, Acta Crystallogr., Sect. B: Struct. Sci. 27 (1971) 661.

[36] W. Broser, P. Siegle, H. Kurreck, Chem. Ber. 101 (1968) 69.

[37] (a) H. Sitzmann, R. Boese, Angew. Chem., Int. Ed. Engl. 30 (1991) 971;
(b) H. Sitzmann, H. Bock, R. Boese, T. Dezember, Z. Havlas, W. Kaim, M. Moscherosch, L. Zanathy, J. Am. Chem. Soc. 115 (1993) 12003.

[38] (a) S. Holl, H. Bock, K. Gharagozloo-Hubmann, Acta Crystallogr., Sect. E: Struct. Rep. Online 57 (2001) M31;
(b) G.B. Deacon, C.M. Forsyth, F. Jaroschik, P.C. Junk, D.L. Kay, T. Maschmeyer, A.F. Masters, J. Wang, L.D. Field, Organometallics 27 (2008) 4772.

[39] G.R. Giesbrecht, J.C. Gordon, D.L. Clark, B.L. Scott, Dalton Trans. (2003) 2658.

[40] G. Dyker, J. Heiermann, M. Miura, J.-I. Inoh, S. Pivsa-Art, T. Satoh, M. Nomura, Chem. Eur. J. 6 (2000) 3426.

[41] S. Harder, C. Ruspic, J. Organomet. Chem. 694 (2009) 1180.

[42] C. Dohmeier, E. Baum, A. Ecker, R. Köppe, H. Schnöckel, Organometallics 15 (1996) 4702.

[43] D. Kuchenbecker, S. Harder, G. Jansen, Z. Anorg, Allg. Chem. 636 (2010) 2257.

[44] G. Rio, A. Ranjon, C.R. Seances, Acad. Sci. 254 (1962) 2997.

[45] (a) D.W. Slocum, S. Duraj, M. Matusz, J.L. Cmarik, K.M. Simpson, D.A. Owen, in: J.E. Sheats, C.E.J. Carraher, C.U. Pittman (Eds.), Metal Containing Polymeric Systems, Plenum, New York, 1985, p. 59;
(b) H. Schumann, C. Janiak, J.J. Zuckerman, Chem. Ber. 121 (1988) 207.

[46] A.K. Youssef, M.A. Ogliarus, J. Org. Chem. 37 (1972) 2601.

[47] C. Dufraisse, G. Rio, A. Ranjon, C.R. Seances, Acad. Sci. 253 (1961) 2441.

[48] C.F.H. Allen, J.A. VanAllan, J. Am. Chem. Soc. 65 (1943) 1384.

[49] R.A. Brand, J.E. Mulvaney, J. Org. Chem. 45 (1980) 633.

[50] L.J. Bartal, H.J. Ache, J. Phys. Chem. 77 (1973) 2060.

[51] G. Rio, G. Sanz, Bull. Soc. Chim. Fr. (1966) 3775.

[52] (a) W. Schlenk, E. Bergmann, Justus Liebigs Ann. Chem. 463 (1928) 2;
(b) E. Bergmann, O. Zwecker, Justus Liebigs Ann. Chem. 487 (1931) 155;

(c) E. Bergmann, W. Schreiber, Justus Liebigs Ann. Chem. 500 (1933) 118;
(d) L.I. Smith, H.H. Hoehn, J. Am. Chem. Soc. 63 (1941) 1184;
(e) F.C. Leavitt, T.A. Manuel, F. Johnson, J. Am. Chem. Soc. 81 (1959) 3163;
(f) F.C. Leavitt, T.A. Manuel, F. Johnson, L.U. Matternas, D.S. Lehman, J. Am. Chem. Soc. 82 (1960) 5099;
(g) E.H. Braye, I. Caplier, W. Hübel, J. Am. Chem. Soc. 83 (1961) 4406.
[53] W. Priebsch, M. Hoch, D. Rehder, Chem. Ber. 121 (1988) 1971.
[54] R. Breslow, H.W. Chang, J. Am. Chem. Soc. 87 (1965) 2200.
[55] M.A. Battiste, Chem. Ind. (1961) 550.
[56] M.A. Battiste, J. Am. Chem. Soc. 83 (1961) 4101.
[57] D.J. Anderson, A. Hassner, J. Am. Chem. Soc. 93 (1971) 4339.
[58] (a) H. Dürr, G. Schepper, Chem. Ber. 100 (1967) 3236;
(b) H. Dürr, G. Schepper, Angew. Chem., Int. Ed. Engl. 7 (1968) 371;
(c) H. Dürr, H. Kober, I. Halberst, U. Neu, T.T. Coburn, T. Mitsuhas, W.M. Jones, J. Am. Chem. Soc. 95 (1973) 3818.
[59] H. Dürr, A. Hackenberger, Synthesis (1978) 594.
[60] (a) P.L. Pauson, B.J. Williams, J. Chem. Soc. (1961) 4162;
(b) D. Lloyd, F.I. Wasson, J. Chem. Soc. C (1966) 408;
(c) M. Regitz, A. Liedhege, Tetrahedron 23 (1967) 2701.
[61] A. Efraty, J.A. Potenza, L. Zyontz, J. Daily, M.H.A. Huang, B. Toby, J. Organomet. Chem. 145 (1978) 315.
[62] J.A. Potenza, R.J. Johnson, R. Chirico, A. Efraty, Inorg. Chem. 16 (1977) 2354.
[63] G.M. Holtzapple, P.S. Woon, M.F. Farona, Inorg. Nucl. Chem. Lett. 12 (1976) 623.
[64] (a) E.R.H. Jones, P.C. Wailes, M.C. Whiting, J. Chem. Soc. (1955) 4021;
(b) G.N. Schrauzer, Chem. Ind. (1958) 1404;
(c) G.N. Schrauzer, J. Am. Chem. Soc. 81 (1959) 5307.
[65] G.A. Carriedo, J.A.K. Howard, D.B. Lewis, G.E. Lewis, F.G.A. Stone, J. Chem. Soc., Dalton Trans. (1985) 905.
[66] (a) R. Breslow, W.A. Yager, H.W. Chang, J. Am. Chem. Soc. 85 (1963) 2033;
(b) J.J. Eisch, J.E. Galle, B. Shafii, A.L. Rheingold, Organometallics 9 (1990) 2342.
[67] (a) M. Kotora, C.J. Xi, T. Takahashi, Tetrahedron Lett. 39 (1998) 4321;
(b) C.J. Xi, M. Kotora, K. Nakajima, T. Takahashi, J. Org. Chem. 65 (2000) 945.
[68] P.-T. Cheng, T.R. Jack, C.J. May, S.C. Nyburg, J. Powell, J. Chem. Soc., Chem. Commun. (1975) 369.
[69] T.A. Stephenson, S.M. Morehouse, A.R. Powell, J.P. Heffer, G. Wilkinson, J. Chem. Soc. (1965) 3632.
[70] P.M. Maitlis, Acc. Chem. Res. 9 (1976) 93.
[71] P.M. Maitlis, The Organic Chemistry of Palladium, Academic Press, New York, NY, 1971.
[72] A.T. Blomquist, P.M. Maitlis, J. Am. Chem. Soc. 84 (1962) 2329.
[73] (a) L. Malatesta, G. Santarella, L. Vallarino, F. Zingales, Angew. Chem. 72 (1960) 34;
(b) L.M. Vallerino, G. Santarella, Gazz. Chim. Ital. 94 (1964) 252.
[74] J.J. Eisch, A.A. Aradi, M.A. Lucarelli, Y. Qian, Tetrahedron 54 (1998) 1169.
[75] (a) M. Miura, S. Pivsa-Art, G. Dyker, J. Heiermann, T. Satoh, M. Nomura, Chem. Commun. (1998) 1889;
(b) M. Miura, S. Pibusaaht, G. Decker, J. Heilemann, T. Sato, J. Inao, M. Nomura, JP 2000053599 A 20000222, Kokai Tokkyo Koho, Japan, 2000;
(c) G. Dyker, J. Heiermann, M. Miura, Adv. Synth. Catal. 345 (2003) 1127.
[76] O. Oms, T. Jarrosson, L.H. Tong, A. Vaccaro, G. Bernardinelli, A.F. Williams, Chem. Eur. J. 15 (2009) 5012.
[77] Q. Shelby, N. Kataoka, G. Mann, J. Hartwig, J. Am. Chem. Soc. 122 (2000) 10718.
[78] F. Maassarani, M. Pfeffer, G. Leborgne, Organometallics 6 (1987) 2029.
[79] M. Pfeffer, J.P. Sutter, A. DeCian, J. Fischer, Organometallics 12 (1993) 1167.
[80] S.M. Bloom, A.P. Krapcho, Chem. Ind. (1959) 882.
[81] R. Breslow, P. Dowd, J. Am. Chem. Soc. 85 (1963) 2729.
[82] G. Montaudo, G. Purrello, Ann. Chim. 51 (1961) 865.
[83] H. Volz, Tetrahedron Lett. 5 (1964) 1899.
[84] S. Li, J. Ma, Y. Jiang, J. Phys. Chem. A 101 (1997) 5587.
[85] (a) R. Breslow, H.W. Chang, R. Hill, E. Wasserman, J. Am. Chem. Soc. 89 (1967) 1112;
(b) W. Broser, H. Kurreck, P. Siegle, Chem. Ber. 100 (1967) 788.
[86] A. Louati, M. Huhn, Inorg. Chem. 32 (1993) 3601.
[87] (a) N.G. Connelly, W.E. Geiger, G.A. Lane, S.J. Raven, P.H. Rieger, J. Am. Chem. Soc. 108 (1986) 6219;
(b) G.A. Lane, W.E. Geiger, N.G. Connelly, J. Am. Chem. Soc. 109 (1987) 402;
(c) M.J. Shaw, W.E. Geiger, J. Hyde, C. White, Organometallics 17 (1998) 5486.
[88] M.M. Kreevoy, Tetrahedron 2 (1958) 354.
[89] J.E. Wertz, C.F. Koelsch, J.L. Vivo, J. Chem. Phys. 23 (1955) 2194.
[90] (a) K. Möebius, Z. Naturforsch. A: Phys. Sci. 20 (1965) 1102;
(b) W. Broser, H. Kurreck, P. Siegle, Chem. Ber. 99 (1966) 2246;
(c) W. Broser, J. Reusch, H. Kurreck, P. Siegle, Chem. Ber. 102 (1969) 1715;
(d) H. Kurreck, W. Broser, Z. Naturforsch. B: Chem. Sci. 24 (1969) 1199;
(e) S. Oestreich, W. Broser, H. Kurreck, Z. Naturforsch. B: Chem. Sci. 32 (1977) 686;
(f) W. Kieslich, H. Kurreck, J. Am. Chem. Soc. 106 (1984) 4328.
[91] S.B. Colbran, D.C. Craig, W.M. Harrison, A.E. Grimley, J. Organomet. Chem. 408 (1991) C33.
[92] J.J. Basselier, J.P. Leroux, Bull. Soc. Chim. Fr. (1971) 4448.
[93] M.A. Ogliaruso, M.G. Romanelli, E.I. Becker, Chem. Rev. 65 (1965) 261.
[94] (a) W. Dilthey, F. Quint, J. Prakt. Chem. 128 (1930) 139;
(b) B.S. Furniss, A.J. Hannaford, V. Rogers, P.W.G. Smith, A.R. Tatchell, Vogel's Textbook of Practical Organic Chemistry, Including Qualitative Organic Analysis, 4th ed., Longmans, New York, 1978.
[95] M.S. Kharasch, O. Reinmuth, Grignard Reactions of Nonmetallic Substances, Prentice-Hall, New York, NY, 1954.
[96] Y. Kimura, Y. Tomita, S. Nakanishi, Y. Otsuji, Chem. Lett. (1979) 321.
[97] L.D. Field, A.F. Masters, M. Gibson, D.R. Latimer, T.W. Hambley, I.E. Buys, Inorg. Chem. 32 (1993) 211.
[98] (a) D. Janzen, H. Kurreck, Tetrahedron Lett. 13 (1972) 5231;
(b) H. Kurreck, S. Oestreich, Tetrahedron 30 (1974) 3199.
[99] W. Broser, D. Janzen, H. Kurreck, D. Braasch, S. Oestreich, M. Plato, Tetrahedron 32 (1976) 1819.
[100] P.S. Tanner, T.P. Hanusa, Polyhedron 13 (1994) 2417.
[101] (a) C. Ruspic, J.R. Moss, M. Schürmann, S. Harder, Angew. Chem., Int. Ed. 47 (2008) 2121;
(b) L. Orzechowski, D.F.J. Piesik, C. Ruspic, S. Harder, Dalton Trans. (2008) 4742.
[102] (a) P. Jützi, N. Burford, Chem. Rev. 99 (1999) 969;
(b) M.J. Harvey, K.T. Quisenberry, T.P. Hanusa, V.G. Young, Eur. J. Inorg. Chem. (2003) 3383.
[103] M. del Mar Conejo, R. Fernández, D. del Río, E. Carmona, A. Monge, C. Ruiz, A.M. Márquez, J. Fernández Sanz, Chem. Eur. J. 9 (2003) 4452.
[104] (a) R.A. Andersen, J.M. Boncella, C.J. Burns, R. Blom, A. Haaland, H.V. Volden, J. Organomet. Chem. 312 (1986) C49;
(b) R.A. Williams, T.P. Hanusa, J.C. Huffman, Organometallics 9 (1990) 1128;
(c) M. Kaupp, P. von Rague Schleyer, M. Dolg, H. Stoll, J. Am. Chem. Soc. 114 (1992) 8202;
(d) T.K. Hollis, J.K. Burdett, B. Bosnich, Organometallics 12 (1993) 3385;
(e) D.J. Burkey, T.P. Hanusa, Comments Inorg. Chem. 17 (1995) 41;
(f) T.P. Hanusa, Organometallics 21 (2002) 2559.
[105] D.W. Slocum, S. Johnson, M. Matusz, S. Duraj, J.L. Cmarik, K.M. Simpson, D.A. Owen, Polym. Mater. Sci. Eng. 49 (1983) 353.
[106] L.D. Field, C.M. Lindall, T. Maschmeyer, A.F. Masters, Aust. J. Chem. 47 (1994) 1127.
[107] S. Barry, A. Kucht, H. Kucht, M.D. Rausch, J. Organomet. Chem. 489 (1995) 195.
[108] J.L. Robbins, N. Edelstein, B. Spencer, J.C. Smart, J. Am. Chem. Soc. 104 (1982) 1882.
[109] V.V. Strelets, S.V. Kukharenko, Nouv. J. Chim. 8 (1984) 785.
[110] (a) H.J. Keller, Z. Naturforsch. A: Phys. Sci. 23 (1968) 131;
(b) J.T. Landrum, C.D. Hoff, J. Organomet. Chem. 282 (1985) 215;
(c) T.J. Jaeger, M.C. Baird, Organometallics 7 (1988) 2074;
(d) S.J. McLain, J. Am. Chem. Soc. 110 (1988) 643;
(e) L.Y. Goh, T.W. Hambley, D.J. Darensbourg, J. Reibenspies, J. Organomet. Chem. 381 (1990) 349;
(f) W.C. Watkins, T. Jaeger, C.E. Kidd, S. Fortier, M.C. Baird, G. Kiss, G.C. Roper, C.D. Hoff, J. Am. Chem. Soc. 114 (1992) 907.
[111] M. Fei, S.K. Sur, D.R. Tyler, Organometallics 10 (1991) 419.
[112] C.G. Atwood, W.E. Geiger, J. Am. Chem. Soc. 116 (1994) 10849.
[113] (a) G.P. Abramo, J.R. Norton, Macromolecules 33 (2000) 2790;
(b) J.J.C. Grove, H.A. Mahomed, L. Griesel, WO 2003004158 A2 20030116, Sasol Technology Pty Ltd., South Africa, 2003.
[114] H. Mahomed, A. Bollmann, J.T. Dixon, V. Gokul, L. Griesel, C. Grove, F. Hess, H. Maumela, L. Pepler, Appl. Catal. A 255 (2003) 355.
[115] D. Edwards-Davies, L.D. Field, A.F. Masters, P. Turner, unpublished results.
[116] S.-C. Chang, W.-Y. Yeh, G.-H. Lee, S.-M. Peng, J. Chin. Chem. Soc. (Taipei, Taiwan) 49 (2002) 325.
[117] (a) F. Mao, S.K. Sur, D.R. Tyler, J. Am. Chem. Soc. 111 (1989) 7627;
(b) F. Mao, C.E. Philbin, T.J.R. Weakley, D.R. Tyler, Organometallics 9 (1990) 1510.
[118] W.-Y. Yeh, S.-M. Peng, G.-H. Lee, Organometallics 21 (2002) 3058.
[119] P.A. Cox, P. Grebenik, R.N. Perutz, M.D. Robinson, R. Grinter, D.R. Stern, Inorg. Chem. 22 (1983) 3614.
[120] S.B. Colbran, W.M. Harrison, C. Saadeh, Organometallics 13 (1994) 1061.
[121] L.D. Field, T. He, P. Humphrey, A.F. Masters, P. Turner, Polyhedron 25 (2006) 1498.
[122] C. Löwe, V. Shklover, H.W. Bosch, H. Berke, Chem. Ber. 126 (1993) 1769.
[123] G.I. Childs, C.S. Colley, J. Dyer, D.C. Grills, X.-Z. Sun, J.X. Yang, M.W. George, J. Chem. Soc., Dalton Trans. (2000) 1901.
[124] D.J. Lawes, S. Geftakis, G.E. Ball, J. Am. Chem. Soc. 127 (2005) 4134.
[125] S. McVey, P.L. Pauson, J. Chem. Soc. (1965) 4312.
[126] (a) P. Brégaint, J.-R. Hamon, C. Lapinte, J. Organomet. Chem. 398 (1990) C25;
(b) P. Brégaint, J.-R. Hamon, C. Lapinte, Organometallics 11 (1992) 1417;
(c) H. Schumann, H. Kucht, A. Kucht, Z. Naturforsch. B: Chem. Sci. 47 (1992) 1281;
(d) L.D. Field, T.W. Hambley, P.A. Humphrey, C.M. Lindall, G.J. Gainsford, A.F. Masters, T.G. St. Pierre, J. Webb, Aust. J. Chem. 48 (1995) 851.
[127] M.A. Guillevic, P. Bregaint, C. Lapinte, J. Organomet. Chem. 514 (1996) 157.
[128] (a) I. Kuksis, M.C. Baird, J. Organomet. Chem. 512 (1996) 253;
(b) I. Kuksis, I. Kovács, M.C. Baird, K.F. Preston, Organometallics 15 (1996) 4991.
[129] C.U. Beck, The University of Sydney, Sydney, 2002.
[130] (a) J.C. Ruble, H.A. Latham, G.C. Fu, J. Am. Chem. Soc. 119 (1997) 1492;
(b) G.C. Fu, Acc. Chem. Res. 33 (2000) 412;
(c) G.C. Fu, Acc. Chem. Res. 37 (2004) 542;
(d) R.P. Wurz, E.C. Lee, J.C. Ruble, G.C. Fu, Adv. Synth. Catal. 349 (2007) 2345.
[131] S. Bellemin-Laponnaz, J. Tweddell, J.C. Ruble, F.M. Breitling, G.C. Fu, Chem. Commun. (2000) 1009.
[132] (a) I.D. Hills, G.C. Fu, Angew. Chem., Int. Ed. 42 (2003) 3921;
(b) A.H. Mermerian, G.C. Fu, J. Am. Chem. Soc. 125 (2003) 4050.

[133] D.W. Slocum, S. Johnson, M. Matusz, S. Duraj, J.L. Cmarik, K.M. Simpson, D.A. Owen, Models for highly phenylated transition metal-containing polymers—derivatives of the pentaphenylcyclopentadienyl ligand, in: Abstr. Pap. Am. Chem. Soc., 1983, 186th PMSE75, 1983.
[134] V.V. Strelets, Coord. Chem. Rev. 114 (1992) 1.
[135] F. Coat, M.-A. Guillevic, L. Toupet, F. Paul, C. Lapinte, Organometallics 16 (1997) 5988.
[136] N.G. Connelly, W.E. Geiger, The Fc +/0 couple is taken as +0.460 V vs. SCE, Chem. Rev. 96 (1996) 877.
[137] J.G. Bullitt, F.A. Cotton, T.J. Marks, Inorg. Chem. 11 (1972) 671.
[138] I. Kuksis, M.C. Baird, Organometallics 13 (1994) 1551.
[139] J.V. Caspar, T.J. Meyer, J. Am. Chem. Soc. 102 (1980) 7794.
[140] I. Kuksis, M.C. Baird, Organometallics 15 (1996) 4755.
[141] E.V. Salo, Z.B. Guan, Organometallics 22 (2003) 5033.
[142] M. Watanabe, T. Okada, M. Sato, S. Hamura, M. Tanabiki, US 20020120160 A1 20020829, 2002.
[143] M. Watanabe, Macromol. Rapid Commun. 26 (2005) 34.
[144] J.G. Hansen, M. Johannsen, J. Org. Chem. 68 (2002) 1266.
[145] N.G. Connelly, I. Manners, J. Chem. Soc., Dalton Trans. (1989) 283.
[146] N.G. Connelly, A.C. Loyns, I. Manners, D.L. Mercer, K.E. Richardson, P.H. Rieger, J. Chem. Soc., Dalton Trans. (1990) 2451.
[147] P.A. Humphrey, P. Turner, A.F. Masters, L.D. Field, M.P. Cifuentes, M.G. Humphrey, I. Asselberghs, A. Persoons, M. Samoc, Inorg. Chim. Acta 358 (2005) 1663.
[148] P.A. Humphrey, P. Turner, A.F. Masters, L.D. Field, unpublished results.
[149] W. Kläui, L. Ramacher, Angew. Chem., Int. Ed. Engl. 25 (1986) 97.
[150] N.G. Connelly, S.J. Raven, W.E. Geiger, J. Chem. Soc., Dalton Trans. (1987) 467.
[151] M.C.R. Symons, S.W. Bratt, J. Chem. Soc., Dalton Trans. (1979) 1739.
[152] D.A. Braden, D.R. Tyler, J. Am. Chem. Soc. 120 (1998) 942.
[153] W. Liu, B. Shi, G. Li, Jiangsu Shiyou Huagong Xueyuan Xuebao 11 (1999) 20.
[154] P. Seiler, J.D. Dunitz, Acta Crystallogr., Sect. B: Struct. Sci. 35 (1979) 1068.
[155] M.P. Castellani, S.J. Geib, A.L. Rheingold, W.C. Trogler, Organometallics 6 (1987) 1703.
[156] A. Schott, H. Schott, G. Wilke, J. Brandt, H. Hoberg, E.G. Hoffmann, Justus Liebigs Ann. Chem. (1973) 508.
[157] H.P. Fritz, K.E. Schwarzhans, Chem. Ber. 97 (1964) 1390.
[158] A.J. Bard, E. Garcia, S. Kukharenko, V.V. Strelets, Inorg. Chem. 32 (1993) 3528.
[159] H. Lehmkuhl, J. Näser, G. Mehler, T. Keil, F. Danowski, R. Benn, R. Mynott, G. Schroth, C. Krüger, P. Betz, Chem. Ber. 124 (1991) 441.
[160] M. Huhn, M. Burgard, D. Matt, J. Steiner, DE 4415725 A1 19941110, Ecole Europeene des Hautes Etudes des Industries Chimiques et de Strasbourg, 1994.
[161] D. Soulivong, C. Wieser, M. Marcellin, D. Matt, A. Harriman, L. Toupet, J. Chem. Soc., Dalton Trans. (1997) 2257.
[162] T.R. Jack, J. Powell, Ring opening and insertion reactions of endo-alkoxycyclobutenylpalladium(II) compounds: formation of cyclopentadienylpalladium(I) derivatives, in: Proc. 16th Int. Conf. Coord. Chem., Univ. Coll., Dublin, Dep. Chem., 1974, p. 3.
[163] W.E. Geiger, P.H. Rieger, C. Corbato, J. Edwin, E. Fonseca, G.A. Lane, J.M. Mevs, J. Am. Chem. Soc. 115 (1993) 2314.
[164] J.A. DeGray, W.E. Geiger, G.A. Lane, P.H. Rieger, Inorg. Chem. 30 (1991) 4100.
[165] M. Herberhold, T. Schmalz, W. Milius, B. Wrackmeyer, Inorg. Chim. Acta 334 (2002) 10.
[166] J. Powell, N.I. Dowling, Organometallics 2 (1983) 1742.
[167] (a) T. Tanase, T. Nomura, Y. Yamamoto, K. Kobayashi, J. Organomet. Chem. 410 (1991) C25;
(b) T. Tanase, T. Nomura, T. Fukushima, Y. Yamamoto, K. Kobayashi, Inorg. Chem. 32 (1993) 4578.
[168] H. Werner, H.J. Kraus, U. Schubert, K. Ackermann, Chem. Ber. 115 (1982) 2905.
[169] (a) W.E. Bowers, B.N. Sprague, US 4892562 A 19900109, Fuel Tech, Inc., USA, 1990.;
(b) W.E. Bowers, B.N. Sprague, US 4891050 A 19900102, Fuel Tech, Inc., USA, 1990.
[170] L. Lettko, M.D. Rausch, Organometallics 19 (2000) 4060.
[171] T.J. Marks, R.D. Ernst, in: G. Wilkinson, F.G.A. Stone, E.W. Abel (Eds.), Comprehensive Organometallic Chemistry, Pergamon, Oxford, UK, 1982 (Chapter 2).
[172] H. Schumann, J. Winterfeld, M. Glanz, R.D. Köhn, H. Hemling, J. Organomet. Chem. 481 (1994) 275.
[173] C.M. Forsyth, G.B. Deacon, L.D. Field, C. Jones, P.C. Junk, D.L. Kay, A.F. Masters, A.F. Richards, Chem. Commun. (2006) 1003.
[174] W.J. Evans, Inorg. Chem. 46 (2007) 3435.
[175] H. Schumann, C. Janiak, H. Khani, J. Organomet. Chem. 330 (1987) 347.
[176] (a) A.M. Cardoso, R.J.H. Clark, S. Moorhouse, J. Chem. Soc., Dalton Trans. (1980) 1156;
(b) A.M. Cardoso, R.J.H. Clark, S. Moorhouse, J. Organomet. Chem. 186 (1980) 237.
[177] C. Janiak, H. Schumann, C. Stader, B. Wrackmeyer, J.J. Zuckerman, Chem. Ber. 121 (1988) 1745.
[178] (a) P. Köpf-Maier, C. Janiak, H. Schumann, Inorg. Chim. Acta 152 (1988) 75;
(b) P. Köpf-Maier, Prog. Clin. Biochem. Med. 10 (1989) 151.
[179] C.E. Holloway, M. Melnik, Main Group Met. Chem. 23 (2000) 1.
[180] (a) J.H. Choi, Y.H. Kim, S.H. Nam, S.T. Shin, M.J. Kim, J. Park, Angew. Chem., Int. Ed. 41 (2002) 2373;
(b) J.H. Choi, Y.K. Choi, Y.H. Kim, E.S. Park, E.J. Kim, M.J. Kim, J.W. Park, J. Org. Chem. 69 (2004) 1972;
(c) B. Martín-Matute, M. Edin, K. Bogár, J.-E. Bäckvall, Angew. Chem., Int. Ed. 43 (2004) 6535;
(d) B. Martín-Matute, M. Edin, K. Bogár, F.B. Kaynak, J.-E. Bäckvall, J. Am. Chem. Soc. 127 (2005) 8817;
(e) S.B. Ko, B. Baburaj, M.J. Kim, J. Park, J. Org. Chem. 72 (2007) 6860;
(f) B. Martín-Matute, J.B. Åberg, M. Edin, J.-E. Bäckvall, Chem. Eur. J. 13 (2007) 6063;
(g) J.B. Åberg, J. Nyhlén, B. Martín-Matute, T. Privalov, J.-E. Bäckvall, J. Am. Chem. Soc. 131 (2009) 9500;
(h) J. Nyhlén, T. Privalov, J.-E. Bäckvall, Chem. Eur. J. 15 (2009) 5220.
[181] H. Hayata, JP 07160022 A 19950623, Konishiroku Photo Ind., Japan, 1995.
[182] G.A. Dushenko, I.E. Mikhailov, I.A. Kamenetskaya, R.V. Skachkov, A. Zwchunke, K. Muegge, V.I. Minkin, Zh. Org. Khim. 30 (1994) 1481.
[183] T.A. Perfetti, M.A. Ogliaruso, J. Org. Chem. 43 (1978) 884.
[184] (a) P.L. Arnold, F.G.N. Cloke, J.F. Nixon, Chem. Commun. (1998) 797;
(b) G.K.B. Clentsmith, F.G.N. Cloke, J.C. Green, J. Hanks, P.B. Hitchcock, J.F. Nixon, Angew. Chem., Int. Ed. 42 (2003) 1038.
[185] (a) M.N. Bochkarev, I.L. Fedushkin, A.A. Fagin, T.V. Petrovskaya, J.W. Ziller, R.N.R. Broomhall-Dillard, W.J. Evans, Angew. Chem., Int. Ed. Engl. 36 (1997) 133;
(b) W.J. Evans, N.T. Allen, J.W. Ziller, J. Am. Chem. Soc. 122 (2000) 11749;
(c) M.N. Bochkarev, I.L. Fedushkin, S. Dechert, A.A. Fagin, H. Schumann, Angew. Chem., Int. Ed. 40 (2001) 3176;
(d) W.J. Evans, N.T. Allen, J.W. Ziller, J. Am. Chem. Soc. 123 (2001) 7927;
(e) M.C. Cassani, Y.K. Gunǐko, P.B. Hitchcock, A.G. Hulkes, A.V. Khvostov, M.F. Lappert, A.V. Protchenko, J. Organomet. Chem. 647 (2002) 71;
(f) W.J. Evans, N.T. Allen, J.W. Ziller, Angew. Chem., Int. Ed. 41 (2002) 359;
(g) K. Izod, Angew. Chem., Int. Ed. 41 (2002) 743;
(h) M.N. Bochkarev, Coord. Chem. Rev. 248 (2004) 835;
(i) W.J. Evans, J.M. Perotti, S.A. Kozimor, T.M. Champagne, B.L. Davis, G.W. Nyce, C.H. Fujimoto, R.D. Clark, M.A. Johnston, J.W. Ziller, Organometallics 24 (2005) 3916;
(j) W.J. Evans, S.E. Lorenz, J.W. Ziller, Inorg. Chem. 48 (2009) 2001;
(k) F. Jaroschik, A. Momin, F. Nief, G.X.-F. Le, G.B. Deacon, P.C. Junk, Angew. Chem., Int. Ed. 48 (2009) 1117.